

2789

FUEL CONTAINMENT AND DAMAGE TOLERANCE IN LARGE COMPOSITE PRIMARY AIRCRAFT STRUCTURES PHASE II -- TESTING

J.P. SANDIFER, A. DENNY, M.A. HOOD

STRUCTURES AND MATERIALS LABORATORY
KELLY JOHNSON RESEARCH AND DEVELOPMENT CENTER AT RYE CANYON
LOCKHEED-CALIFORNIA COMPANY
BURBANK, CALIFORNIA 91520

NASA Contract No. NAS 1-16856

April, 1985

(NASA-CR-172519) FUEL CONTAINMENT AND
DAMAGE TOLERANCE IN LARGE COMPOSITE PRIMARY
AIRCRAFT STRUCTURES. PHASE 2: TESTING
(Lockheed-California Co.) 278 p CSCL 01C

N88-25452

Unclas
G3/05 0146419

Date for general release will be three (3)
years from date indicated on the document.



National Aeronautics and
Space Administration

Langley Research Center
Hampton, Virginia 23665



NASA CONTRACTOR REPORT 172519

FUEL CONTAINMENT AND DAMAGE TOLERANCE IN LARGE COMPOSITE PRIMARY AIRCRAFT STRUCTURES PHASE II -- TESTING

J.P. SANDIFER, A. DENNY, M.A. WOOD

STRUCTURES AND MATERIALS LABORATORY
KELLY JOHNSON RESEARCH AND DEVELOPMENT CENTER AT RYE CANYON
LOCKHEED-CALIFORNIA COMPANY
BURBANK, CALIFORNIA 91520

NASA Contract No. NAS 1-16856

April, 1985

██████ Date for general release will be three (3)
years from date indicated on the document.



National Aeronautics and
Space Administration

Langley Research Center
Hampton, Virginia 23665



INTRODUCTION

The objective of this program was to identify and resolve technical issues associated with fuel containment and damage tolerance of composite wing structure for transport aircraft. This two-phased program focused on the structural and manufacturing technologies associated with composite material wing surface and the surface-to-substructure interfaces.

The first phase of the program encompassed the development of generic technology, including preliminary design of damage tolerant composite wing surfaces, and evaluation of fuel sealing methods and lightning protection techniques. Design and manufacturing development tests were conducted to establish an engineering data base and reliable manufacturing process. Results of this phase were reported in Reference 1.

In the second phase of the program, the technical effort was focused on the following: alternate toughened resin composites, fuel leakage after impact damage, and lightning strike protection techniques. The technology developed was demonstrated by the fabrication and test of a technology demonstration panel. The results of this phase of the program are presented in the following sections of this report.

~~1.1~~

Use of commercial products or names or manufacturers in this report does not constitute official endorsement of such products or manufacturers, either expressed or implied, by the National Aeronautics and Space Administration.

PRECEDING PAGE BLANK NOT FILMED

TABLE OF CONTENTS

<u>Section</u>	<u>Page No.</u>
1 FUEL SEALING TESTS	
1.1 INTRODUCTION	1-1
1.2 BOX BEAM FABRICATION	1-1
1.2.1 Laminates	1-1
1.2.2 Machining and Assembly	1-1
1.3 TEST PROCEDURES	1-5
1.4 RESULTS 1-7	1-7
2 MATERIALS EVALUATION TESTS	
2.1 INTRODUCTION	2-1
2.2 TRIAL IMPACT TESTS	2-1
2.3 QUASI-ISOTROPIC COMPRESSION TESTS	2-34
2.4 QUASI-ISOTROPIC TENSION TESTS	2-48
2.5 0° TENSION TESTS	2-55
2.6 90° TENSION TESTS	2-55
2.7 +45° TENSILE TESTS	2-65
2.8 EDGE DELAMINATION TENSION TESTS	2-65
2.9 DOUBLE CANTILEVER BEAM (DCB) TESTS	2-68
2.10 SUMMARY	2-77
3 POST IMPACT FUEL LEAK	
3.1 INTRODUCTION	3-1
3.2 TEST LAMINATES	3-1
3.3 TRIAL IMPACT TESTS	3-4
3.4 LEAK TESTING	3-4
4 DESIGN DEVELOPMENT TESTS	
4.1 INTRODUCTION	4-1
4.2 TRIAL IMPACT TESTS	4-7
4.3 STIFFENER PULL-OFF TESTS	4-10
4.4 STIFFENER SIDE LOAD TESTS	4-23
4.5 FAIL SAFE TESTS	4-34
4.6 UNDAMAGED STIFFENER COMPRESSION TESTS	4-41
4.7 IMPACTED STIFFENER COMPRESSION TEST	4-47
4.8 IMPACTED STIFFENED PANEL COMPRESSION TEST	4-75
4.9 CONCLUSIONS	4-89

TABLE OF CONTENTS - CONTINUED

<u>Section</u>		<u>Page No.</u>
5	LIGHTNING STRIKE AND UNDAMAGED COMPRESSION TESTS	
	5.1 INTRODUCTION	5-1
	5.2 COMPRESSION TEST PROCEDURES	5-1
	5.3 COMPRESSION TEST RESULTS	5-6
6	TECHNOLOGY DEMONSTRATION ARTICLE	
	6.1 INTRODUCTION	6-1
	6.2 SUMMARY OF RESULTS	6-1
	6.3 TEST ARTICLE	6-2
	6.4 TEST PROCEDURE	6-8
	6.5 TEST LOADS, MONITORING, AND DAT ACQUISITION	6-16
	6.5.1 Fuel Pressure Tests	6-16
	6.5.2 Impact Tests	6-16
	6.5.3 Fatigue Loading Test	6-18
	6.5.4 Residual Static Strength Test	6-18
	6-6 TEST AND INSPECTION RESULTS	6-18
	REFERENCES	R-1

LIST OF TABLES

<u>Table No.</u>		<u>Page No.</u>
1.1	Maximum, Minimum and Peak-Peak Values For Beam 270-1	1-8
1.2	Maximum, Minimum and Peak-Peak Values For Beam 270-2	1-9
1.3	Maximum, Minimum and Peak-Peak Values For Beam 270-3	1-10
1.4	Residual Strength Failure Conditions	1-12
1.5	Summary of Residual Strength Test Failure Locations	1-13
2.1	Static Test Program for High Strain Celion/HX1504 and High Strain Celion/5245	2-2
2.2	Laminate Properties	2-3
2.3	Trial Impact Test Results for High Strain Celion/HX1504	2-7
2.4	Trial Impact Test Results for High Strain Celion/5245	2-8
2.5	Comparison of C-Scan and Microscope Delamination Measurements	2-33
2.6	Impact Test Results for High Strain Celion/HX1504	2-40
2.7	Impact Test Results for High Strain Celion/5245	2-41
2.8	High Strain Celion/HX1504 Compression Test Data	2-42
2.9	High Strain Celion/5245 Compression Test Data	2-43

LIST OF TABLES - Continued

<u>Table No.</u>		<u>Page No.</u>
2.10	High Strain Celion/HX1504 Quasi-Isotropic Tension Test Data	2-51
2.11	High Strain Celion/5245 Quasi-Isotropic Tension Test Data	2-52
2.12	High Strain Celion/HX1504 0° Tension Test Data	2-58
2.13	High Strain Celion/5245 0° Tension Test Data	2-58
2.14	Sandwich Beam Geometry	2-60
2.15	High Strain Celion/HX1504 90° Tension Test Data	2-63
2.16	High Strain Celion/5245 90° Tension Data	2-64
2.17	High Strain Celion/HX1504 +45° Tension Test Data	2-66
2.18	High Strain Celion/5245 +45° Tension Test Data	2-66
2.19	8 Ply High Strain Celion/HX1504 Edge Delamination Test Data	2-71
2.20	11 Ply High Strain Celion/HX1505 Edge Delamination Test Data	2-71
2.21	8 Ply High Strain Celion/5245 Edge Delamination Test	2-72
2.22	11 Ply High Strain Celion/5245 Edge Delamination Test	2-72
2.23	High Strain Celion/5245 Double Cantilever Beam Test Data Modified Direct Beam Equation Method	2-79

LIST OF TABLES - Continued

<u>Table No.</u>		<u>Page No.</u>
2.24	High Strain Celion/5245 Double Cantilever Beam Test Data Summary	2-79
2.25	Compression Test Data Comparison, (45/0/135/90) _{6s} Quasi-Isotropic Laminate	2-80
2.26	Quasi-Isotropic Tension Test Data Comparison	2-82
2.27	Tension Test Data Comparison	2-83
2.28	8 and 11 Ply Edge Delamination Test Data Comparison	2-83
3.1	Panel Coating	3-2
3.2	Weights of Post-Impact Fuel Leak Coatings	3-3
3.3	Trial Panel Impact Energy	3-5
3.4	Visual Observations of Trial Impact Test Damage	3-7
3.5	Trial Impact Ultrasonic Inspection Damage Areas	3-11
3.6	Summary of Time of Leak	3-12
4.1	Design Development Tests	4-3
4.2	Stiffener Pull-Off and Stiffener Side Load Specimen Dimensions	4-11
4.3	Stiffener Pull-Off and Side Load Test Results	4-14
4.4	Undamaged Stiffener Panel Dimensions	4-48
4.5	Impacted Stiffener Panel Dimensions	4-59
4.6	Impacted Stiffened Panel G Thickness Dimensions (in.)	4-78

LIST OF TABLES - Continued

<u>Table No.</u>		<u>Page No.</u>
5.1	Compression Test Results for Lightning Strike Damaged and Undamaged Compression Tests	5-7
6.1	Strain Gage Readings During a Typical Interval of Fatigue Loading	6-21
6.2	Strain Gage Readings for the First and Last Application of the 80% Design Limit Compressive Load Cycle During Fatigue Testing	6-22
6.3	Strain Gage Readings for the Static Tests to Design Ultimate Compressive Load and Residual Strength Failure Load	6-23

LIST OF ILLUSTRATIONS

<u>Figure No.</u>		<u>Page No.</u>
1-1	Fastener callout and spacing for Panels 270-1 and 270-2	1-2
1-2	Fastener callout and spacing for Panels 270-3	1-3
1-3	Fixed attachment and strain gage locations	1-4
1-4	Overall view of test set-up	1-6
1-5	Close-up of test set-up	1-6
1-6	Top view of beam 270-1 with two types of fastener heads	1-14
1-7	Side view of beam 270-1 showing method of attachment and fractures as indicated	1-14
1-8	Bottom view of 270-1 showing ports for adding oil (2) and hydraulic fitting for pressurizing tank	1-15
1-9	Top view of beam 270-2 showing failure locations	1-15
1-10	Side view of beam 270-2	1-16
1-11	Bottom view of beam 270-2 showing by-pass fittings	1-16
1-12	Top view of beam 270-3 showing failure locations	1-17
1-13	Side view of beam 270-3	1-17
1-14	Bottom view of 270-3	1-18
1-15	Close-up view of skin and Z shaped web: Side A-C, beam 270-1	1-19

LIST OF ILLUSTRATIONS - CONTINUED

<u>Figure No.</u>		<u>Page No.</u>
1-16	Close-up view of skin and z shaped web: Side B-D, beam 270-1	1-19
1-17	Close-up view of beam 270-2 A-C side	1-20
1-18	Close-up view of beam 270-2 B-D side	1-20
1-19	Close-up of beam 270-3 failure AC side	1-21
1-20	Close-up of beam 270-3 failure BC side	1-21
2-1	Detail View of Impactor Mass, Panel Tie- down Fixture and Panel	2-4
2-2	Impactor Assembly	2-5
2-3a	Celion/HX1504 Trial Impact Panel 210-1, Front Surface	2-9
2-3b	Celion/HX1504 Trial Impact Panel 210-1, Back Surface	2-10
2-4a	Celion/HX1504 Trial Impact Panel 210-2, Front Surface	2-11
2-4b	Celion/HX1504 Trial Impact Panel 210-2, Back Surface	2-12
2-5	10 ft-lb Impact of Celion/HX1504	2-13
2-6	20 ft-lb Impact of Celion/HX1504	2-14
2-7	30 ft-lb Impact of Celion/HX1504	2-15
2-8	30 ft-lb Impact of Celion/HX1504	2-16
2-9	40 ft-lb Impact of Celion/HX1504	2-17
2-10	40 ft-lb Impact of Celion/HX1504	2-18

LIST OF ILLUSTRATIONS - CONTINUED

<u>Figure No.</u>		<u>Page No.</u>
2-11	60 ft-lb Impact of Celion/HX1504	2-19
2-12	80 ft-lb Impact of Celion/HX1504	2-20
2-13a	Celion/5245 Trial Impact Panel 243-1	2-21
2-13b	Celion/5245 Trial Impact Panel 243-1	2-22
2-14a	Celion/5245 Trial Impact Panel 243-2	2-23
2-14b	Celion/5245 Trial Impact Panel 243-2	2-24
2-15	Typical 20 ft-lb Impact of Celion/5245	2-25
2-16	Typical 30 ft-lb Impact of Celion/5245	2-26
2-17	Photomicrographs of a Cross-Section Through the Center of Impacted Damage Regions of Celion/HX1504	2-27
2-18	Photomicrographs of a Cross-Section Through the Center of Impacted Damage Regions of Celion/HX5245	2-28
2-19	Center of Impact Area of High Strain Celion/ HX1504 at 20 ft-lbs	2-29
2-20	Center of Impact Area of High Strain Celion/ HX1504 at 30 ft-lbs	2-30
2-21	Center of Impact Area of High Strain Celion/ 5245 at 20 ft-lbs	2-31
2-22	Center of Impact Area of High Strain Celion/ 5245 at 30 ft-lbs Impact	2-32
2-23	Compression Coupon	2-35
2-24	Compression Coupon	2-36

LIST OF ILLUSTRATIONS - CONTINUED

<u>Figure No.</u>		<u>Page No.</u>
2-25	Percentage of Weight Gain of Celion/HX1504 During Immersion in 160°F Water for 45 Days	2-37
2-26	Compression Test Fixture	2-38
2-27a	Typical Failures of Unnotched Compression Specimens Tested at Room Temperature: Front View	2-44
2-27b	Typical Failures of Unnotched Compression Specimens Tested at Room Temperature: Edge View	2-45
2-28	Typical Failures of 1.00 in. Diameter Hole Compression Specimens	2-46
2-29	Typical Failures of Compression Specimens Impacted at 20 ft-lbs	2-47
2-30	Inplane Tension Specimen Geometry	2-49
2-31	Inplane Tension Specimen Geometry	2-49
2-32	Tension Test Set-Up	2-50
2-33	Typical Failures of Unnotched Tension Tests	2-53
2-34	Typical Failure of Notched Tension Tests	2-54
2-35	<u>+45°</u> and 0° Tensile Test Specimen Geometry	2-56
2-36	Typical Failure of 0° Tension Tests	2-57
2-37	90° Tension Test Setup Geometry	2-59
2-38	90° Tension Test Setup	2-61
2-39	Typical Failure of 90° Sandwich Beam Tests	2-62
2-40	Typical <u>+45°</u> Tension Test Failures	2-67
2-41	Edge Delamination Tension Test Specimen	2-69

LIST OF ILLUSTRATIONS - CONTINUED

<u>Figure No.</u>		<u>Page No.</u>
2-42a	Edge Delamination Test Specimen in Test Machine with Extensometer Attached	2-70
2-42b	Close-up of Extensometer Attachment to Edge Delamination Specimen	2-70
2-43	Edge of 8-Ply, +35 ⁰ Celion/5245 Edge Delamination Specimens	2-73
2-44	Edges of 11-Ply, +30 ⁰ Celion/5245 Edge Delamination Specimens	2-73
2-45	Hinged Double Cantilever Beam Specimen	2-75
2-46	Hinge Attachment Details	2-75
2-47	Double Cantilever Beam Test Setup	2-76
2-48	Energy-Area Integration Method for Calculating G_{IC}	2-78
3-1	Trial Impact Panel Layout	3-6
3-2	Test Panel Layout	3-6
3-3	Overall View of Test Set-up	3-9
3-4	A Close-up of the Test Showing Where Fuel Has Leaked and Flowed Over the Black Paint	3-10
4-1	Skin and Stiffener Side View of Process Development Panel	4-2
4-2	Process Development Test Specimen Configurations and Loading Directions	4-4
4-3	Stiffened Panel Process Development Test Specimens	4-5
4-4	Stiffened Panel Process Development Test Specimens	4-6

LIST OF ILLUSTRATIONS - CONTINUED

<u>Figure No.</u>		<u>Page No.</u>
4-5	Trial Impact Panel Impact Locations and Energies in ft-lbs	4-8
4-6	C-Scan of Trial Impact Panel	4-9
4-7	Stiffener Pull-off Test Setup	4-12
4-8	Typical Failure of Stiffener Pull-off Specimen (C3)	4-13
4-9	Load-Deflection Curve for Stiffener Pull-Off Specimen C1	4-15
4-10	Load-Deflection Curve for Stiffener Pull-Off Specimen C2	4-16
4-11	Load-Deflection Curve for Stiffener Pull-off Specimen C3	4-17
4-12	Load-Deflection Curve for Stiffener Pull-off Specimen C4	4-18
4-13	Stiffener Pull-off Specimen C1 Failure	4-19
4-14	Stiffener Pull-off Specimen C2 Failure	4-20
4-15	Stiffener Pull-off Specimen C3 Failure	4-21
4-16	Stiffener Pull-off Specimen C4 Failure	4-22
4-17	Stiffener Side Load Test Set-up	4-24
4-18	Load-Deflection Curve for Stiffener Side Load Specimen D1	4-25
4-19	Load-Deflection Curve for Stiffener Side Load Specimen D2.	4-26
4-20	Load-Deflection Curve for Stiffener Side Load Specimen D3	4-27

LIST OF ILLUSTRATIONS - CONTINUED

<u>Figure No.</u>		<u>Page No.</u>
4-21	Load-Deflection Curve for Stiffener Side Load Specimen D4	4-28
4-22	Stiffener Side Load Specimen D1 Failure	4-29
4-23	Stiffener Side Load Specimen D2 Failure	4-30
4-24	Stiffener Side Load Specimen D3 Failure	4-31
4-25	Stiffener Side Load Specimen D4 Failure	4-32
4-26	Sequence of Damage Progression in Stiffener Side Load Test	4-33
4-27	Stiffener Failsafe Test Setup	4-35
4-28	Fail Safe Specimen Strain Gage Locations	4-36
4-29	Failure of Fail-safe Specimen	4-37
4-30	Failure Showing Fastener Head Tearout	4-38
4-31	Closeup of Skin Side of Failed Fail-safe Specimens	4-39
4-32	Fail Safe Specimen Failure Showing Delamination Above the Secondary Bond Line	4-40
4-33	Load-Deflection Curve for Fail-Safe Specimen E1	4-42
4-34	Load-Strain Curve for Fail-Safe Specimen E1	4-43
4-35	Load-Deflection Curve for Fail-Safe Specimen E1	4-44
4-36	Load-Deflection Curve for Fail-Safe Specimen E1	4-45
4-37	Undamaged Stiffener Panel Test Configuration and Strain Gage Layout	4-46

LIST OF ILLUSTRATIONS - CONTINUED

<u>Figure No.</u>		<u>Page No.</u>
4-38	Stiffened Compression Panel A Ready for Test	4-49
4-39	Overall View of Failed Stiffened Panel A	4-50
4-40	Failure of Stiffener of Panel A	4-51
4-41	Skin Failure of Stiffened Panel A	4-52
4-42	Load-Deflection Plot for Undamaged Stiffened Compression Panel A	4-53
4-43	Load-Strain Plot of Strain Gages 1A and 1B on Panel A	4-54
4-44	Load-Strain Plot of Strain Gages 2A and 2B on Panel A	2-55
4-45	Load-Strain Plot of Strain Gages 3A and 3B on Panel A	4-56
4-46	Impacted Stiffener Compression Test B Setup	4-58
4-47	Overall View of Failure of Impacted Stiffened Panel B	4-60
4-48	Closeup of Stiffener Buckle in Test of Impacted Stiffened Panel B	4-61
4-49	Load-Deflection Plot for Impacted Stiffened Compression Panel B	4-63
4-50	Load-Strain Plot of Strain Gages 1A and 1B on Panel B	4-64
4-51	Load-Strain Plot of Strain Gages 2A and 2B on Panel B	4-65
4-52	Load-Strain Plot of Strain Gages 3A and 3B on Panel B	4-66

LIST OF ILLUSTRATIONS - CONTINUED

<u>Figure No.</u>		<u>Page No.</u>
4-53	View of Skin and Stiffener Failure Modes of Retest of Impacted Stiffener Specimen	4-67
4-54	Stiffener Failure Detail View of Impacted Stiffener Retest	4-68
4-55	Side View of Retest of Impacted Stiffener Showing Location of Impact Relative to Failure	4-69
4-56	View of Skin and Stiffener of Failure of Retest of Impacted Stiffener	4-70
4-57	Load-Deflection Plot of Retest of Impacted Stiffened Panel B	4-71
4-58	Load-Strain Plot of Strain Gages 1A and 1B on Retest of Panel B	4-72
4-59	Load-Strain Plot of Gages 2A and 2B on Retest of Panel B	4-73
4-60	Load-Strain Plot of Strain Gages 3A and 3B on Retest of Panel B	4-74
4-61	Potted End of Impacted Stiffened Compression Retest	4-76
4-62	Impacted Compression Test Setup	4-77
4-63	Front Side of Failed Impacted Stiffened Panel	4-80
4-64	Back Side of Failed Impacted Stiffened Panel	4-81
4-65	Closeup of Skin Side Failure Zone	4-82
4-66	Closeup of Failure Zone	4-83
4-67	Sections of Failed Impacted Panel	4-84

LIST OF ILLUSTRATIONS - CONTINUED

<u>Figure No.</u>		<u>Page No.</u>
4-68	Load-Deflection Curve for Impacted Compression Panel G	4-85
4-69	Load-Strain Plot of Strain Gages 1A and 1B on Panel G	4-86
4-70	Load-Strain Plot of Strain Gages 3A, 3B, 4A, 4B, 6A and 6B on Panel G	4-87
4-71	Load-Strain Plot of Strain Gages 2A, 5A, and 5B on Panel G	4-88
5-1	Compression Coupon	5-2
5-2	Compression Test Specimen Locations on Lightning Strike Panels	5-3
5-3	Damaged and Undamaged Compression Test Coupon Locations from Panel 261	5-4
5-4	Damaged and Undamaged Compression Test Coupon Locations from Panel 263	5-5
5-5	Simple Supported Composite Compression Test Fixture #4	5-8
5-6	Simple Supported Composite Compression Test Fixture #4	5-9
6-1	Interior Surface of the Test Article	6-3
6-2	Exterior surface of the Test Article	6-4
6-3	End View of Test Article	6-5
6-4	Test Article with Graphite/Epoxy and Doublers	6-6
6-5	Aluminum End Doublers Installed on Interior Surface of Test Article	6-7

LIST OF ILLUSTRATIONS - CONTINUED

<u>Figure No.</u>		<u>Page No.</u>
6-6	Appearance of Test Article Exterior Surface After Doubler Installations	6-7
6-7	Fuel Containment Pressure Enclosure	6-9
6-8	Fuel Containment Pressure Test Set-up	6-9
6-9	Impact Support Frame Installed on Test Article	6-11
6-10	Impact Test Set-up Showing Panel With Support Frame	6-11
6-11	Impact Locations on Test Article	6-12
6-12	Extent of Internal Damage from Impact	6-13
6-13	Strain Gage Locations on Test Article	6-14
6-14	Fatigue Test Set-up Showing Test Article with Bending Restraint Flexure	6-15
6-15	Residual Static Compressive Strength Test Set-up	6-17
6-16	Typical Fatigue Test Loading Cycle	6-19
6-17	Deflection During Fatigue Test Application of the First Load Cycle	6-24
6-18	Deflection During Fatigue Test Application of the Last Load Cycle	6-25
6-19	Exterior Surface of the Test Article After Failure in the Residual Static Compressive Strength Test	6-27
6-20	Exterior Surface Damage in Failed Test Article	6-28
6-21	Interior Surface of the Test Article After Failure in the Residual Static Compressive Strength Test	6-29

LIST OF ILLUSTRATIONS - CONTINUED

<u>Figure No.</u>		<u>Page No.</u>
6-22	Interior Damage in Failed Test Article	6-30
6-23	Edge View of Failed Test Article with Secondary Damage to the Edge-Closure Angle	6-31
6-24	Deflection During Residual Static Compressive Strength Test	6-32
6-25	Strains at Gage Locations 1A and 1B During Residual Static Compressive Strength Test	6-33
6-26	Strains at Gage Locations 2A and 2B During Residual Static Compressive Strength Test	6-34
6-27	Strains at Gage Locations 3A and 3B During Residual Static Compressive Strength Test	6-35
6-28	Strains at Gage Locations 4A and 4B During Residual Static Compressive Strength Test	6-36
6-29	Strains at Gage Locations 5A and 5B During Residual Static Compressive Strength Test	6-37
6-30	Strains at Gage Locations 6A and 6B During Residual Static Compressive Strength Test	6-38
6-31	Strains at Gage Locations 7A and 7B During Residual Static Compressive Strength Test	6-39
6-32	Strains at Gage Locations 8A and 8B During Residual Static Compressive Strength Test	6-40
6-33	Strains at Gage Locations 9A and 9B During Residual Static Compressive Strength Test	6-41

SECTION 1

FUEL SEALING TESTS

1.1 INTRODUCTION

Tests were conducted on three graphite/epoxy box beams simulating a wing cover to spar cap joint configuration of a pressurized fuel tank. The test objectives were to evaluate the effectiveness of sealing methods with various fastener types and spacings under fatigue loading with fuel under pressure, and to determine the mode(s) of failure of the simulated pressurized fuel tank.

1.2 BOX BEAM FABRICATION

1.2.1 Laminates

One 32-ply graphite/epoxy flat laminate and three 32-ply graphite/epoxy Z-stiffener laminates were fabricated from AS4/3502 prepreg material. All laminates consisted of 25% 0° plies, 50% \pm 45° plies and 25% 90° plies with an orientation of (45/0/135/90)_{4s}.

Each laminate contained 1/4 in. and 1/2 in. diameter Teflon ultrasonic test standards placed at the laminate midplane. After curing each was inspected for voids or defects. Resin content, specific gravity, thickness, and grind-down checks were also made. Results are given in Reference 1.

1.2.2 Machining and Assembly

Caps and Z-webs were machined and holes match drilled as shown in Figures 1-1 through 1-3. All holes were drilled 0.249/0.252 in. diameter. After drilling, parts were disassembled and cleaned with methylethylketone and air dried.

PANEL 270-1 (1 1/8" Spacing)

ID FASTENER

A	NAS 4604U-() * HL94LP-8	SCREW COLLAR
B		
C		
D		

PANEL 270-2 (1 1/8" Spacing)

ID FASTENER

A	NAS 4604U-() * HL87DU-8	SCREW COLLAR
B	NAS 4604U-() * HL87DU-8 NAS 1070-416	SCREW COLLAR WASHER
C	LGPL8SC-V08B SLFC-MV08	SCREW COLLAR
D	LGPL8SC-V08B SLFC-MV08 (INSTALL DRY- WITHOUT SEALANT)	SCREW COLLAR

* Appropriate length

45° Fillet Seal Not Applied

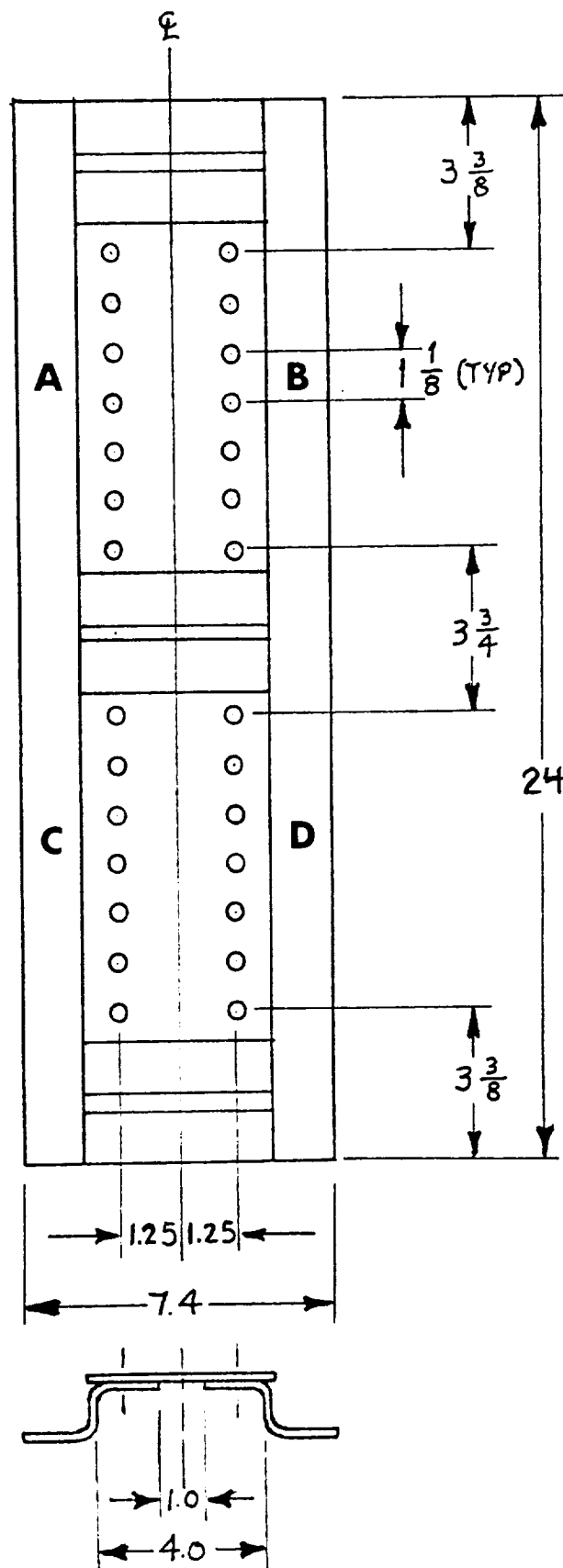


FIGURE 1-1

Fastener callout and spacing for Panels 270-1 and 270-2.

PANEL 270-3 (1 1/2" Spacing)

ID FASTENER

A }
B }
C }
D }

NAS 4604U-()*

SCREW

HL94LP-8

COLLAR

* Appropriate length

45° Fillet Seal Not Applied

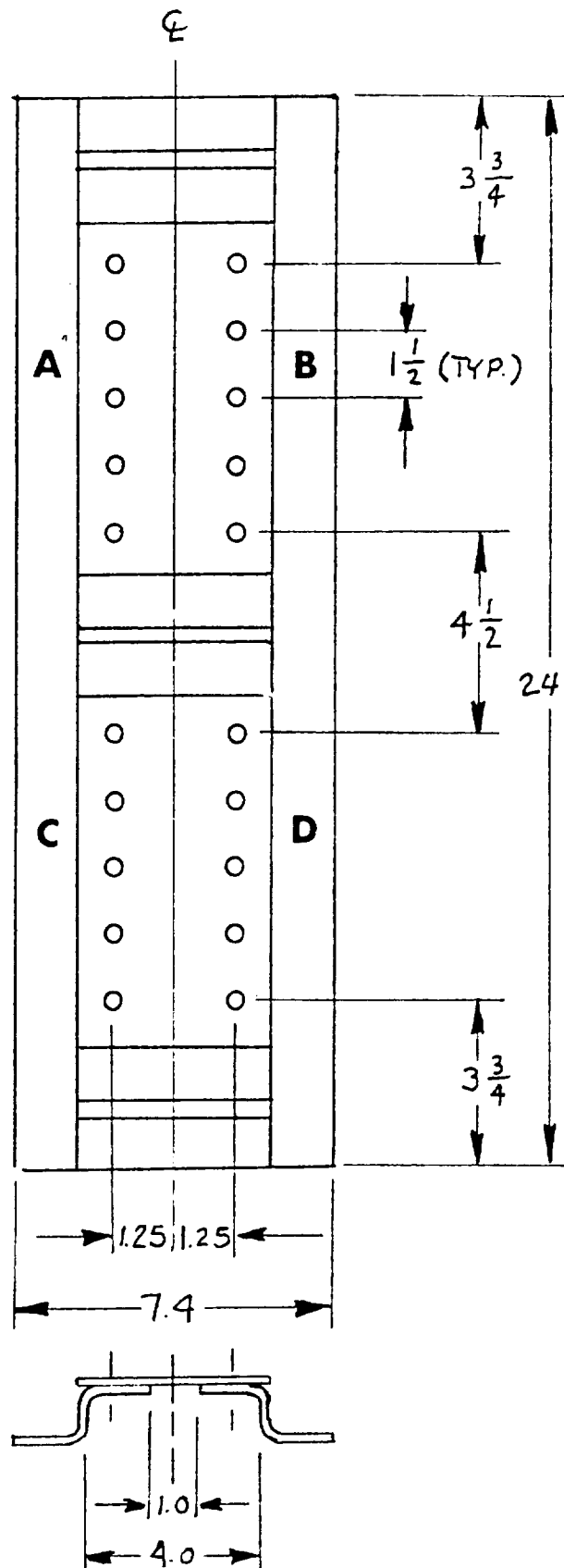
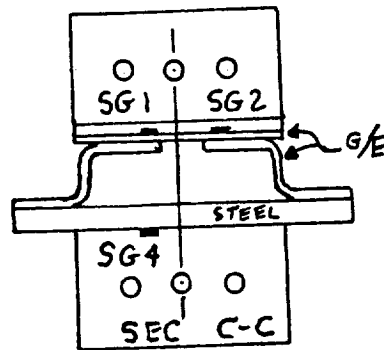
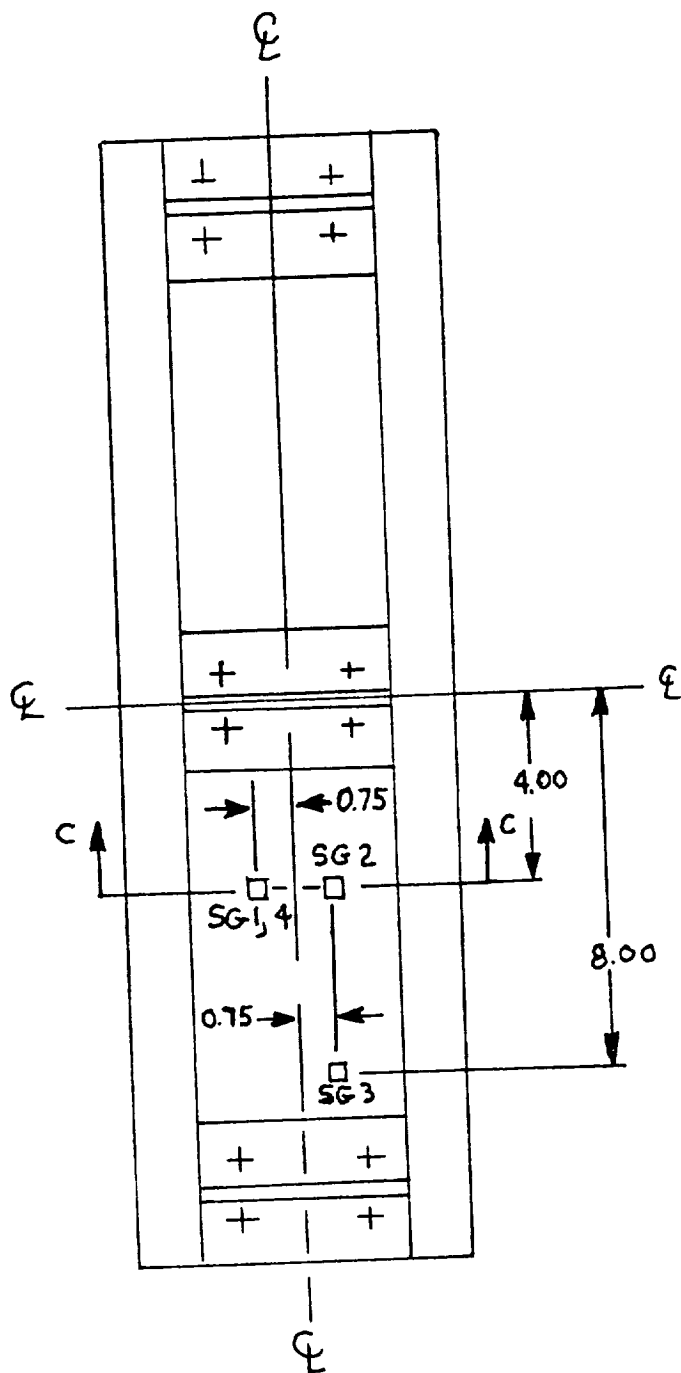


FIGURE 1-2

Fastener callout and spacing for Panels 270-3.



Strain Gage #1 = Ch. #52
 " " #2 = #53
 " " #3 = #54
 " " #4 = #55 (Steel)
 Stroke = #51

FIGURE 1-3

Fixed Attachment and Strain Gage Locations.

Faying surface sealant was then applied to the mating surfaces and the sections clamped together. Fasteners were installed wet (except as noted on beam specimen 270-2D in Figure 1-1) and collars were brushed with sealant. End and center ribs were installed with sealant on all surfaces plus a 45° fillet seal on the upper cap-to-web flange joint inside the box. The T fittings were also drilled, cleaned, and sealed.

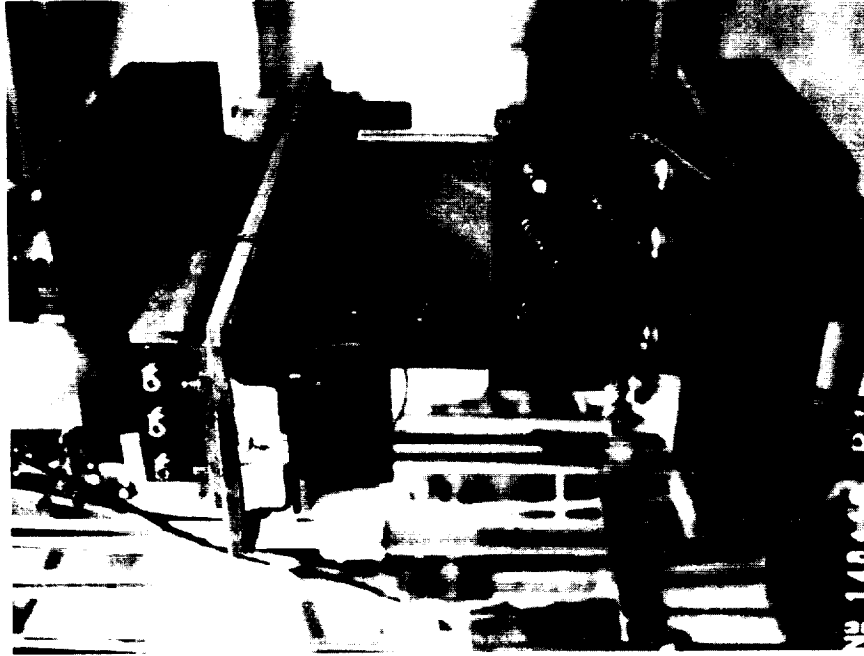
After assembly hydraulic fittings were installed in the steel base plate for fuel injection and pressurization. Each box was then drilled to mate with fixtures in the MTS hydraulic test machine as shown in Figures 1-4 and 1-5.

1.3 TEST PROCEDURES

After mating, the box beams were instrumented with four strain gages located as shown in Figure 1-3. Beams were then reinstalled in the test machine for fatigue testing. For each test the box beam was air pressurized to 6 psig to check for major leaks, then installed in the test machine and filled with fuel simulant Shell Pella "A" with fluorescent dye added. A flex hose was attached to the tank hydraulic fitting, and put at a higher elevation with more fuel added so extra liquid fuel was available in case of leaks or absorption. The end of the flex hose not attached to the box beam went to a cylinder of nitrogen gas to pressurize the fluid. The output of the pressure transducer went to a strip chart recorder for continuously monitoring tank pressure. For beam I.D. number 270-1, 40 cc of fluid was added (including the flex tube) at the end of the fatigue test. This was probably due to the beam appearing full, but still containing air bubbles. For beams 270-2 and 270-3, a sight gage was added to the top of the flex tube, and after all bubbles were removed, the level did not go down between the start and the end of the fatigue spectrum for either panel.

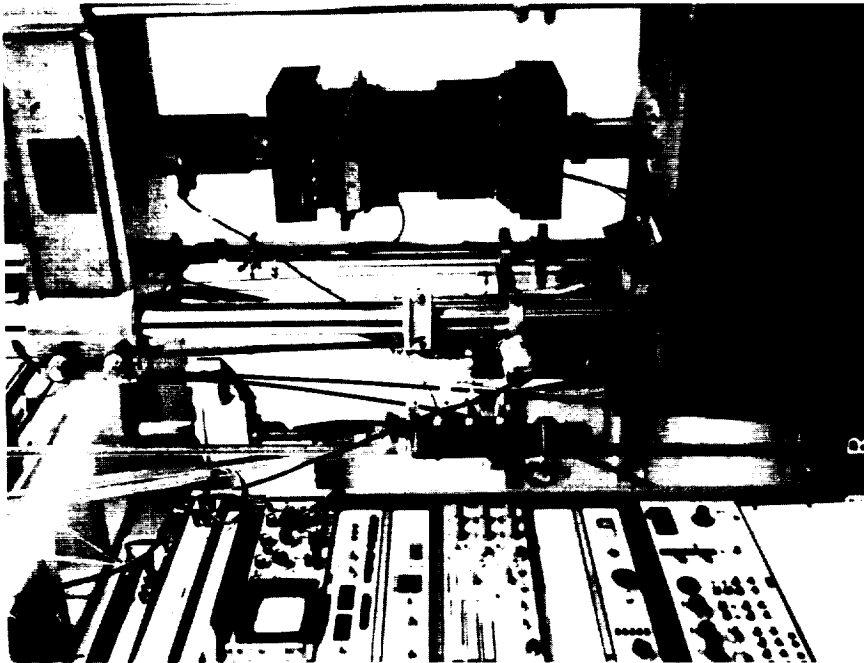
After pressurizing at 6 psig with the strip chart turned on, an initial static survey to 6000 lbs and back to 0 was done, then the fatigue spectrum was applied for one lifetime. The spectrum consisted of a block containing of 1000 cycles of 6000 lbs maximum ($R = -1/2$) followed by one cycle of 9600 lbs maximum ($R = -1/2$) for 36 blocks or a total of 36,036 cycles, all at 2.5 Hz. Load vs strain for each of the four strain gages and load vs stroke

ORIGINAL PAGE IS
OF POOR QUALITY



148409R

Figure 1.5: Close-up of test set-up.



148410R

Figure 1-4: Overall view of test set-up.

data were taken on selected overload cycles as well as the three normal cycles proceeding and following the overload cycle. The beam was also visually checked for leaks after each overload using a ultraviolet lamp to detect fluorescence of the dye in the Shell Pella "A" fuel simulant.

1.4 RESULTS

The load, strain, and deflection recorded for each beam are as follows:

1. An initial static survey to 6000 lbs.
2. Dynamic overload cycle @ 1/4 lifetimes.
3. Dynamic overload cycle @ 1/2 lifetimes.
4. Dynamic overload cycle @ 3/4 lifetimes.
5. Dynamic overload cycle @ 1 lifetime.
6. Static survey to failure.

For each of the above data sets, plots of load vs strain for each of the four gages and plots of load vs stroke were recorded and reported in Reference 2. Tabulated results of maximum-minimum and peak-to-peak values of these plots are presented in Tables 1.1, 1.2, and 1.3. For the overload cycle, variations in load, strain, or stroke during the fatigue life of the test were minor, with strain (channels 54 and 55) showing the largest difference. For each panel no leaks were found at any of the graphite-graphite interfaces, or between the graphite and any of the fasteners at the completion of the fatigue testing.

Upon completion of the fatigue testing static residual strength tests were performed to determine failure and leak mode. For residual strength testing, the testing mode of the MTS fatigue machine was changed from load control to stroke control. The period of the ramp was adjusted such that the stroke rate was 0.04 inch/minute. The beam was loaded until a noticeable loss of fluid occurred, as indicated by either a pressure drop or visible leakage, at which time the nitrogen gas above the fluid was shut off with loading continuing until failure. Fluid loss occurred immediately preceeding failure for all three tests.

TABLE 1.1
MAXIMUM, MINIMUM AND PEAK-PEAK VALUES FOR BEAM 270-1

Cycles	Load In Pounds Maximum Minimum (Peak-Peak)	Stroke In Inches Maximum Minimum (Peak-Peak)	Ch 52 in Microstrain Maximum Minimum (Peak-Peak)	Ch. 53 in Microstrain Maximum Minimum (Peak-Peak)	Ch. 54 in Microstrain Maximum Minimum (Peak-Peak)	Ch. 55 in Microstrain Maximum Minimum (Peak-Peak)
3000	9558 -4754 (14312)	.1630 -.0268 (.1898)	1563 -495.5 (2058.5)	1572 -522.2 (2094.2)	810.5 -134.8 (945.3)	164.1 -463.2 (627.3)
9000	9696 -4826 (14522)	.1739 -.0158 (.1897)	1586 -486.3 (2072.3)	1597 -507 (2104)	829.9 -120.7 (950.6)	159.9 -471.8 (631.7)
19000	9725 -4836 (14561)	.1761 -.0137 (.1898)	1580 -493.3 (2073.3)	1594 -509.8 (2103.8)	826.4 -124.5 (950.9)	156.8 -478.2 (635)
27000	9719 -4835 (14554)	.1766 -.0135 (.1901)	1575 -499.7 (2074.7)	1589 -515.1 (2104.1)	824 -128.8 (952.8)	153.7 -482.0 (635.7)
36000	9717 -4838 (14555)	.1774 -.0128 (.1902)	1565 -512 (2077)	1580 -525.7 (2105.7)	817.8 -136.7 (954.5)	148.9 -488.3 (637.2)

TABLE 1.2
MAXIMUM, MINIMUM AND PEAK-PEAK VALUES FOR BEAM 270-2

Cycles	Load In Pounds Maximum Minimum (Peak-Peak)	Stroke In Inches Maximum Minimum (Peak-Peak)	Ch 52 in Microstrain Maximum Minimum (Peak-Peak)	Ch. 53 in Microstrain Maximum Minimum (Peak-Peak)	Ch. 54 in Microstrain Maximum Minimum (Peak-Peak)	Ch. 55 in Microstrain Maximum Minimum (Peak-Peak)
1000	9758 -4699 (14457)	.1624 -.0408 (.2032)	1612 -548.5 (2160.5)	1649 -563.5 (2212.5)	850.2 -153.5 (1003.1)	167.6 -441.7 (609.3)
9000	9710 -4484 (14194)	.1632 -.0382 (.2014)	1599 -492 (2091)	1633 -487.6 (2120.6)	867.3 -121.4 (988.7)	151.2 -447.5 (598.7)
1800	9729 -4431 (14160)	.1650 -.0373 (.2023)	1591 -495 (2086)	1620 -493.2 (2113.2)	854.5 -125.5 (980)	141.5 -452.3 (593.8)
27000	9730 -4420 (14150)	.1656 -.0377 (.2033)	1582 -486.5 (2068.5)	1623 -487.8 (2110.8)	854.5 -123.2 (977.7)	141.5 -458.9 (600.4)
36000	9720 -4405 (14125)	.1658 -.0372 (.2030)	1581 -477.7 (2058.7)	1628 -478.5 (2106.5)	856.3 -120.2 (976.5)	142 -454 (596)

TABLE 1.3
MAXIMUM, MINIMUM AND PEAK-PEAK VALUES FOR BEAM 270-3

Cycles	Load In Pounds		Stroke In Inches		Ch 52 in Microstrain		Ch. 53 in Microstrain		Ch. 54 in Microstrain		Ch. 55 in Microstrain	
	Maximum	Minimum	Maximum	Minimum	Maximum	Minimum	Maximum	Minimum	Maximum	Minimum	Maximum	Minimum
	(Peak-Peak)	(Peak-Peak)	(Peak-Peak)	(Peak-Peak)	(Peak-Peak)	(Peak-Peak)	(Peak-Peak)	(Peak-Peak)	(Peak-Peak)	(Peak-Peak)	(Peak-Peak)	(Peak-Peak)
1000	9640	-4472 (14112)	.1365 -.0823 (.2188)		1850 -634.2 (2484.2)		1863 -691.2 (2554.2)		784.5 -165.9 (950.4)		194.7 -483.1 (677.8)	
9000	9640	-4477 (14112)	.1417 -.0805 (.2222)		1833 -620.1 (2453.1)		1842 -681.7 (2523.7)		758.9 -155.6 (914.5)		189.5 -482.8 (672.3)	
19000	9654 -4524 (14178)		.1424 -.0739 (.2163)		1805 -596.9 (2401.9)		1846 -631.1 (2477.1)		751.3 -107.9 (859.2)		182.1 -472.9 (655)	
27000	9633 -4540 (14173)		.1427 -.0693 (.2120)		1794 -604.8 (2398.8)		1835 -638.3 (2473.3)		741.0 -111.6 (852.6)		175.1 -477.7 (652.8)	
36000	9645 -4592 (14237)		.1446 -.0663 (.2109)		1782 -632.1 (2414.1)		1822 -699.7 (2491.7)		731.6 -131.8 (863.4)		174.4 -485.2 (659.6)	

In residual strength, beam 270-3 failed at the lowest load of the three with 270-1 and 270-2 having essentially the same value for failure load, delta strain and delta stroke as shown in Table 1.4. For each beam, failure during residual strength testing occurred in the graphite/epoxy skin at the first fastener outside the mid span attachment of the steel tee to the box beam. Top, side and bottom views of the three failed beams are shown in Figures 1-6 - 1-14. Failure occurred in the graphite/epoxy Z shaped web and skin in all cases. A summary of failure locations in the skin and Z is given in Table 1.5. Close-up photographs of the failure regions are presented in Figures 1-15 - 1-20. Of the load-strain plots, channels 54 and 55 showed the greatest deviation from linearity of the strain gages.

TABLE 1.4
RESIDUAL STRENGTH FAILURE CONDITIONS

Specimen	Max. Load (lbs.)	Stroke (in.)	Strain Ch. 52 ($\mu\epsilon$)	Strain Ch. 53 ($\mu\epsilon$)	Strain Ch. 54 ($\mu\epsilon$)	Strain Ch. 55 ($\mu\epsilon$)
270-1	23850	.475	3826	3838	2168	-1184
270-2	23510	.452	3709	3831	2033	-1090
270-3	20000	.317	3488	3600	1564	-1060

TABLE 1-5

SUMMARY OF RESIDUAL STRENGTH TEST FAILURE LOCATIONS

BOX 270-1

AC side Z web:	Failed in region C through first fastener hole, normal to long axis, (Figure 15).
Skin:	Failure in CD side through first row of fastener holes (Figures 15 & 16).
BD side Z web:	Failed in region D through the attachment bolt hole (Figure 16).

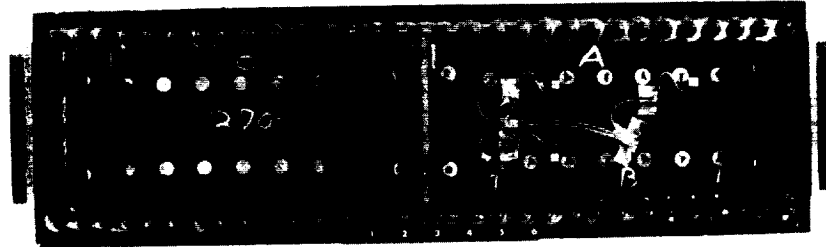
BOX 270-2

AC side Z web:	Failed in region A through first fastener hole, normal to long axis (Figure 17).
Skin:	Failure in AB side through first row of fastener holes (Figures 17 & 18).
BD side Z web:	Failed in region B through tee attachment bolt holes (Figure 18).

BOX 270-3

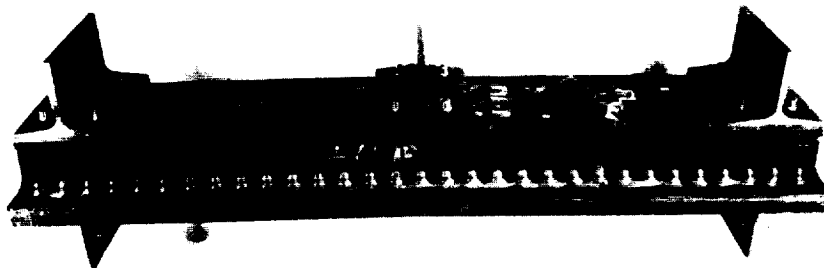
AC side Z web:	Failed in region C through tee attachment bolt hole (Figure 19).
Skin:	Failure in CD side through first row of fastener holes (Figures 19 & 20).
BD side Z web:	Failed in region D through tee attachment bolt hole. Some delamination along fastener at Z to steel bonding plate also observed.

* Locations are shown in Figures 1-1 through 1-3.



148541R

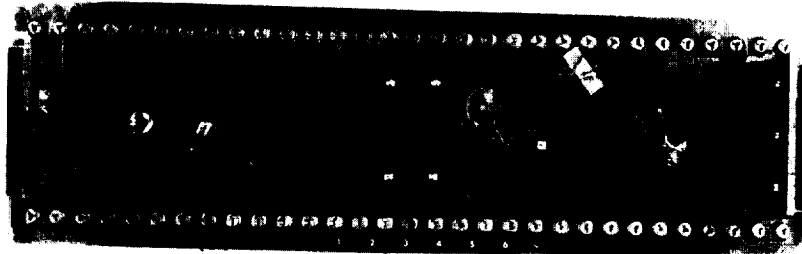
Figure 1-6: Top view of beam 270-1 with two types of fastener heads.



148543R

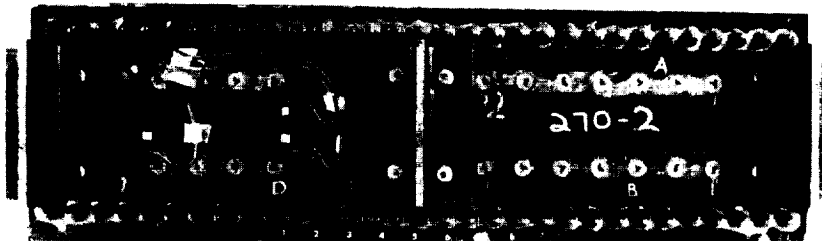
Figure 1-7: Side view of beam 270-1 showing method of attachment and fractures as indicated.

ORIGINAL PAGE IS
OF POOR QUALITY



148542R

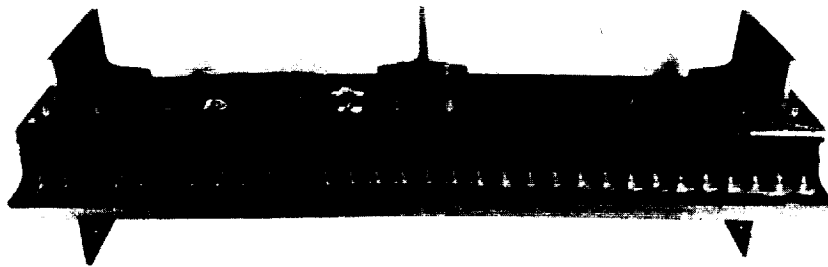
Figure 1-8: Bottom view of 270-1 showing ports for adding oil (2) and hydraulic fitting for pressurizing tank.



148536R

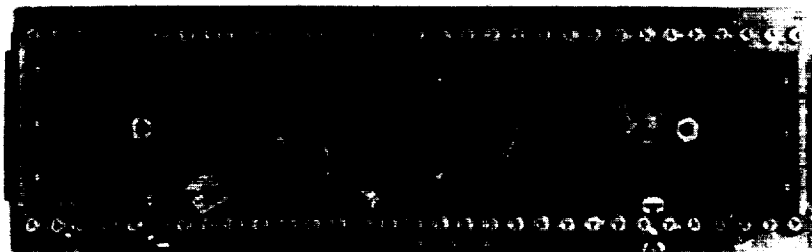
Figure 1-9: Top view of beam 270-2 showing failure locations.

ORIGINAL PAGE IS
OF POOR QUALITY



148538R

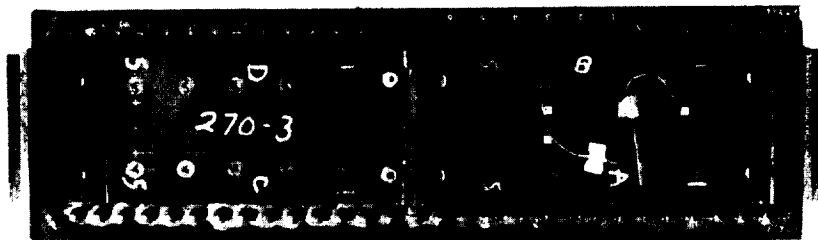
Figure 1-10: Side view of beam 270-2.



148537R

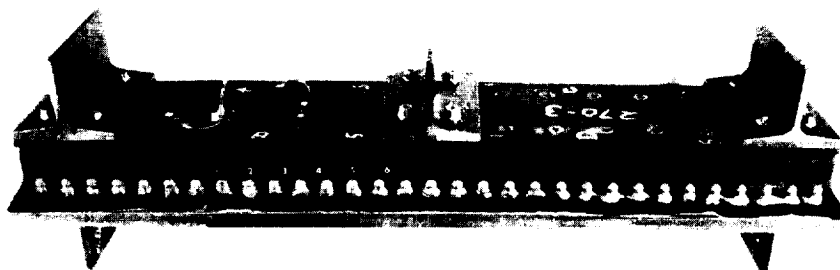
Figure 1-11: Bottom view of beam 270-2 showing by-pass fittings.

ORIGINAL PAGE
OF POOR QUALITY



148531R

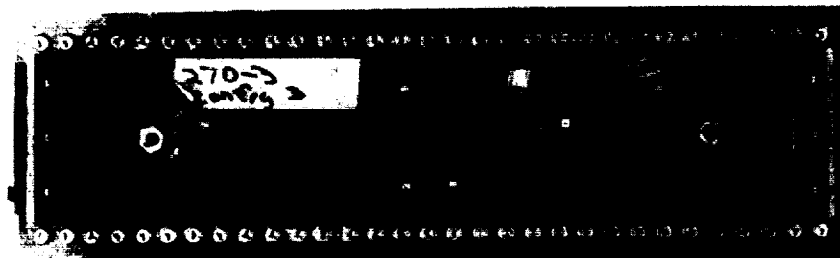
Figure 1-12: Top view of beam 270-3 showing failure locations.



148533R

Figure 1-13: Side view of beam 270-3.

ORIGINAL SOURCE
OF POOR QUALITY



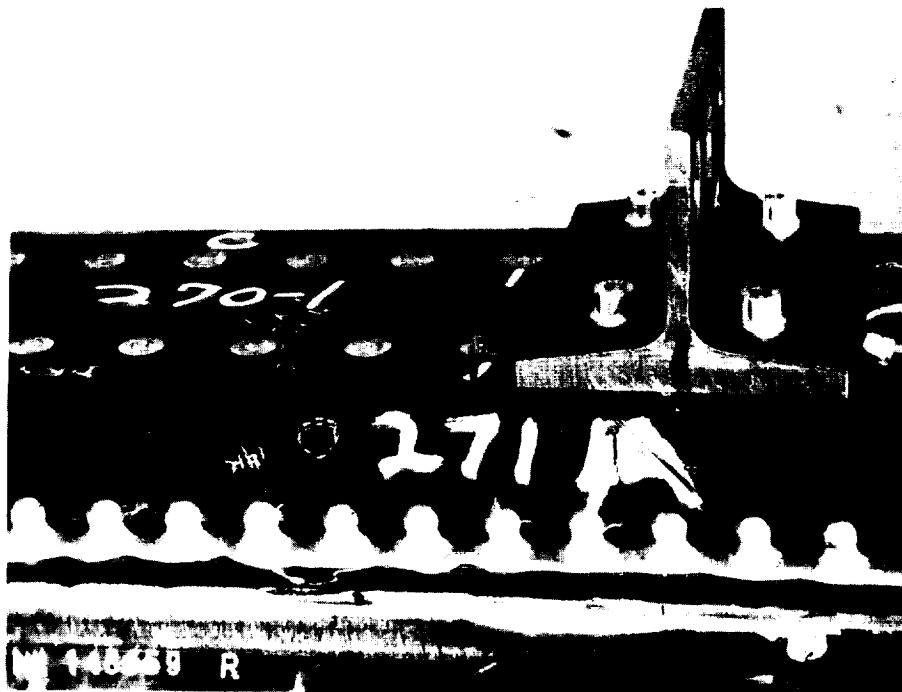
148532R

Figure 1-14: Bottom view of 270-3.



148545R

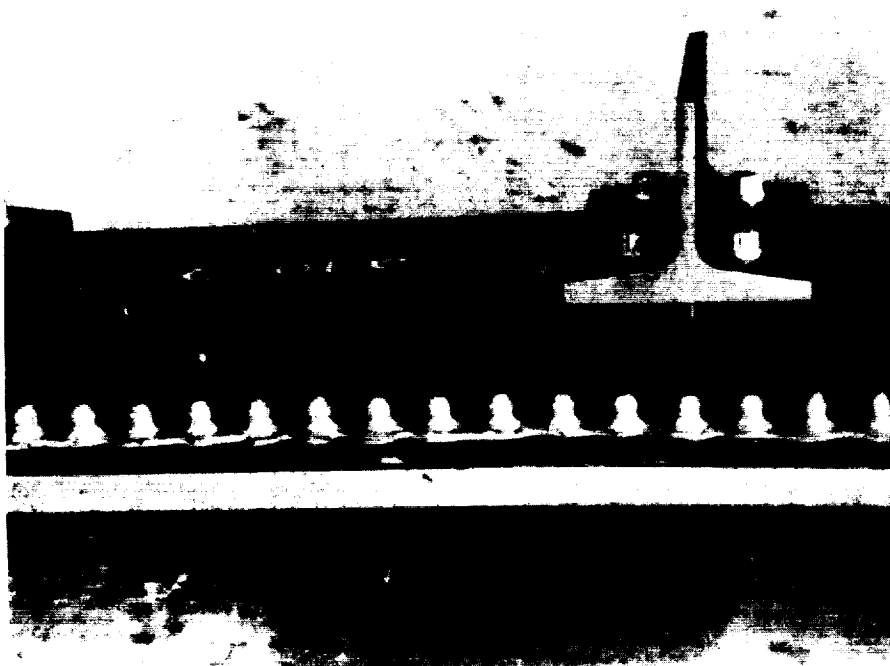
Figure 1-15: Close-up view of skin and Z shaped web:
Side A-C, beam 270-1.



148559R

Figure 1-16: Close-up view of skin and Z shaped web:
Side B-D, beam 270-1.

ORIGINAL FILED IN
OF POOR QUALITY



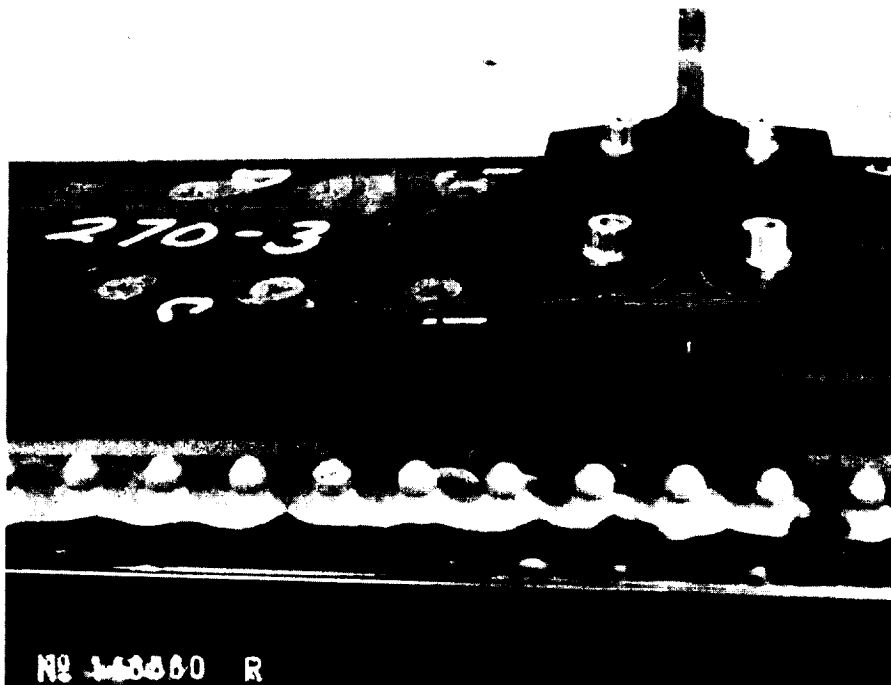
148658R

Figure 1-17: Close-up view of beam 270-2 A-C side.



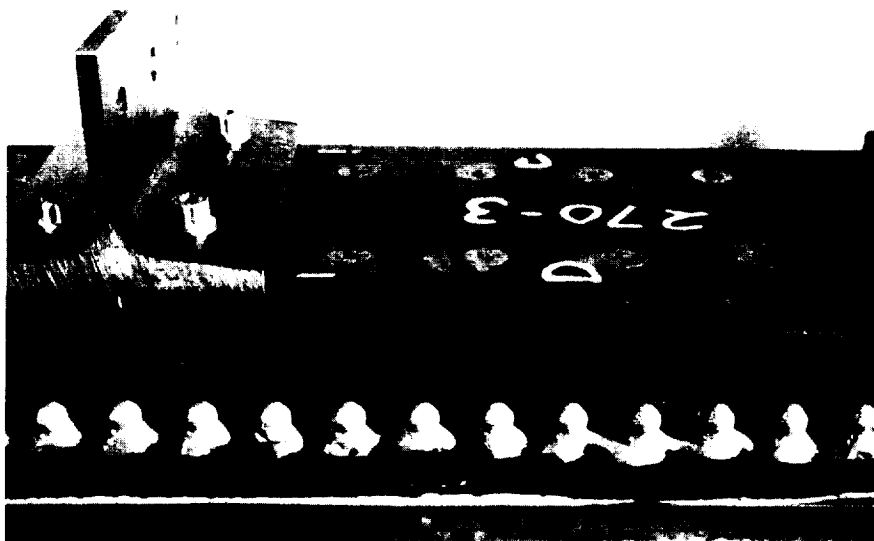
148540R

Figure 1-18: Close-up view of beam 270-2 B-D side.



148560R

Figure 1-19: Close-up of Beam 270-3 failure
AC side.



148535R

Figure 1-20: Close-up of Beam 270-3 failure,
BD side.

SECTION 2

MATERIALS EVALUATION TESTS

2.1 INTRODUCTION

This test series consisted of evaluating two toughened resin composites: Celion/HX1504 and Celion/5245. Table 2-1 contains an outline of the work performed. Table 2-2 contains the resin content, specific gravity, and thickness values for each of the laminate panels. The impact, quasi-isotropic tension and compression, edge delamination, and double cantilever beam tests were performed according to specifications set forth in the "Standard Tests for Toughened Resin Composites", revised edition, NASA Reference Publication 1092, 1983.

2.2 TRIAL IMPACT TESTS

Trial impact tests were conducted to determine the amount of damage done to a laminate at various impact energies. Two quasi-isotropic, $(45/0/-45/90)_{6S}$ 48-ply panels of Celion/HX1504 and Celion/5245 were impacted four times each at energies ranging from 10 to 80 ft-lbs. The impact tests were conducted according to the impact procedure specified in NASA Standard Test "ST-1: Specification for Compression After Impact Test". The impact test fixture is shown in Figures 2-1 and 2-2. The panels were placed in a tie-down fixture described in NASA ST-1 and a 12 lb., 0.5 in. diameter spherical head impactor was used.

TABLE 2 1

STATIC TEST PROGRAM FOR HIGH STRAIN CELION/HX1504 AND HIGH STRAIN
CELION/5245

Laminate Orientation	Type of Test	Condition	No. of plies	Size L x W, in.	Impact Energy	Hole Dia., in.	No. of Tests			Instrumentation
							-65°F D ^a	75°F D ^a	180°F W ^a	
(45/0/-45/90) _{4s}	Tension	UN	32	1 x 8				3		1 Axial Gage
(45/0/-45/90) _{6s}	Tension	UN	48	1 x 8			3			1 Axial Gage
(45/0/-45/90) _{6s}	Tension	N	48	2 x 14		0.25		3		1 Axial Gage
(45/0/-45/90) _{6s}	Tension	UN	48	2 x 14				3		1 Axial Gage
(45/0/-45/90) _{6s}	Tension	N	48	2 x 14		0.25	3			1 Axial Gage
(45/0/-45/90) _{6s}	Compression	UN	48	3 x 10					3	2 Axial Gages, B/B ^d
(45/0/-45/90) _{6s}	Compression	N	48	5 x 10		1.0		3		2 Axial Gages, B/B ^d
(45/0/-45/90) _{6s}	Trial Impact	I	48	7 x 25				8		None
(45/0/-45/90) _{6s}	Compression	I	48	5 x 10	20, 30 ft-lbs.			3, 3		2 Axial Gages, B/B ^d
0° 12	Tension	UN	12	0.5 x 10.5				5		1 T Gage
90° 20	Sand. Beam	UN	20	1 x 22				5		1 Axial Gage
(±45) _{3s}	Tension	UN	6	1 x 10.5				5		1 T Gage
0° 24	DC Beam	UN	24	1.5 x 9						Head Deflection
(±30 ₂ /90/90) _s	Edge Delam.	UN	12	1.5 x 10				5		Extensometer
(±35/0/90) _s	Edge Delam.	UN	8	1.5 x 10				5		Extensometer

a) D = Dry; W = Wet, 45 day immersion in water @ 160°F.

b) Celion/HX1504 quasi-isotropic tension tests.

c) Celion/5245 quasi-isotropic tension tests.

d) B/B = Back-to-back gages

NOTE: Under "Condition": N = Notched; UN = Unnotched; I = Impacted.

TABLE 2.2
LAMINATE PROPERTIES (1)

Material	Panel	Resin Content, %	Specific Gravity	Thickness, in.
Celion/HX1504	(2)			
	202	32.0	1.53	0.183
	210	33.7	1.52	0.270
	211	32.6	1.54	0.271
	212	28.4	1.57	0.066
	213	31.7	1.54	0.110
	214	30.5	1.55	0.072
	215	30.6	1.55	0.062
	216	31.7	1.54	0.046
Celion/5245	233	29.6	1.57 (3)	0.114
	239	33.0	---	0.067
	243	33.0	1.54	0.260
	245	31.2	1.52	0.070
	246	29.1	1.56	0.060
	247	28.3	1.56	0.043
	248	31.3	1.55	0.257
	249	26.9	1.58	0.128

(1) Reference Periodic Technical Progress Report No. 22, July 1983.

(2) 32-Ply quasi-isotropic laminate.

(3) Data not available.



Figure 2-1: Detail View of Impactor Mass, Panel Tie-down Fixture and Panel.

ORIGINAL PAGE IS
OF POOR QUALITY

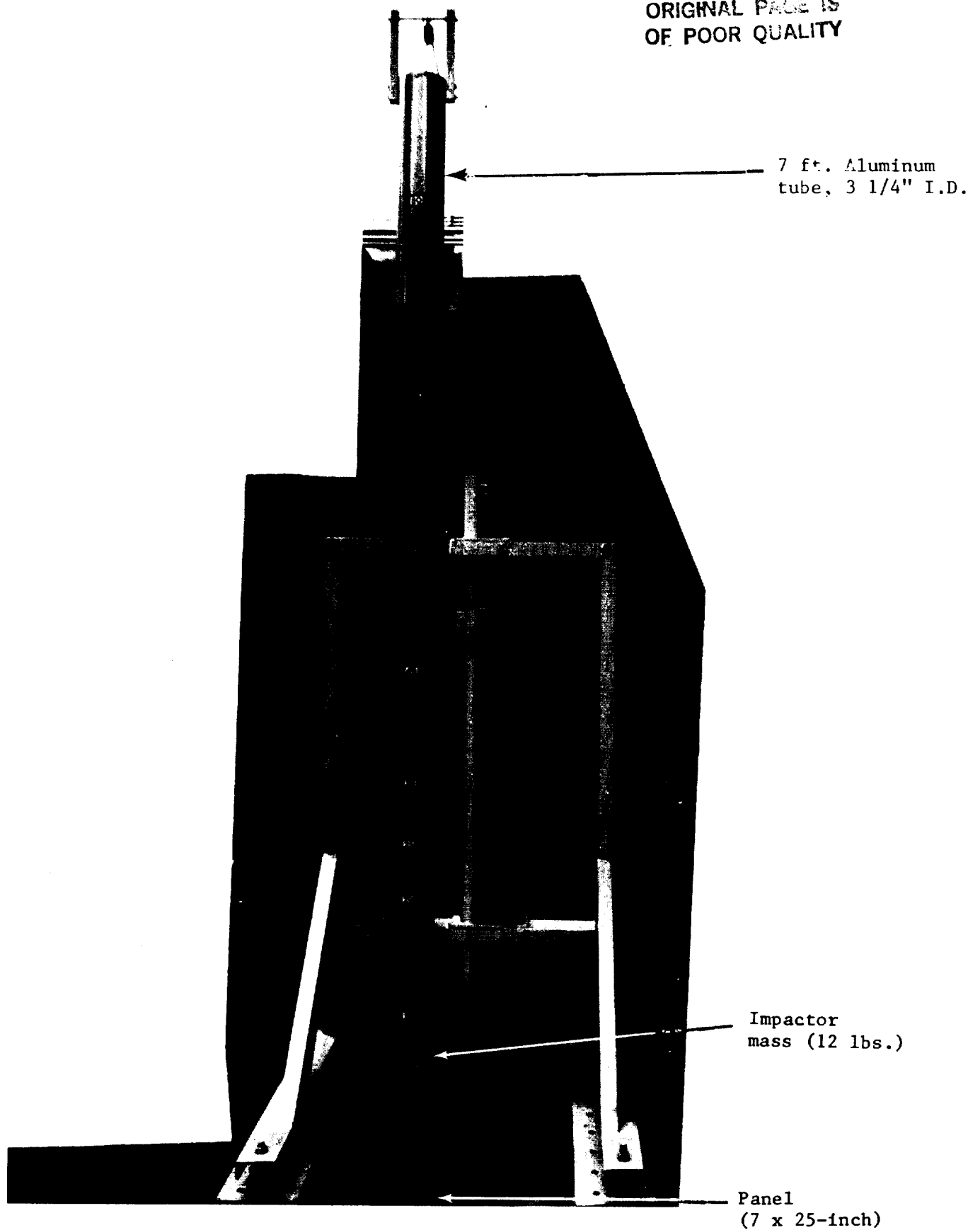


Figure 2-2:

Impactor Assembly

After impact the panels were visually inspected for front and back surface damage, and then ultrasonically C-scanned to determine the extent of internal damage. Visible front and back surface damage and internal damage dimensions are listed in Tables 2-3 and 2-4. Photographs of the front and back surfaces of the impacted Celion/HX1504 and Celion/5245 panels are shown in Figures 2-3 through 2-16. Close up photos of typical Celion/5245 20 and 30 ft-lb impacts from the later tested compression impact specimens are also included, but close-up photos of the Celion/5245 trial impacts were not taken. The impact damage areas of the Celion/HX1504 are, for the most part, greater than those of Celion/5245 by 10 to 50%. The exceptions are at 20 ft-lbs, where the damage areas are comparable, and at 80 ft-lbs where the damage area of the fully penetrated Celion/HX1504 is 65% that of the partially penetrated Celion/5245. The front surface damage of the Celion/HX1504 was slightly more visible than that of Celion/5245. The Celion/5245 first had back surface delaminations at 30 ft-lb impacts and the Celion/5245 showed them at 40 ft-lbs. The Celion/5245 delaminations were always larger than those of Celion/HX1504, except at full penetration.

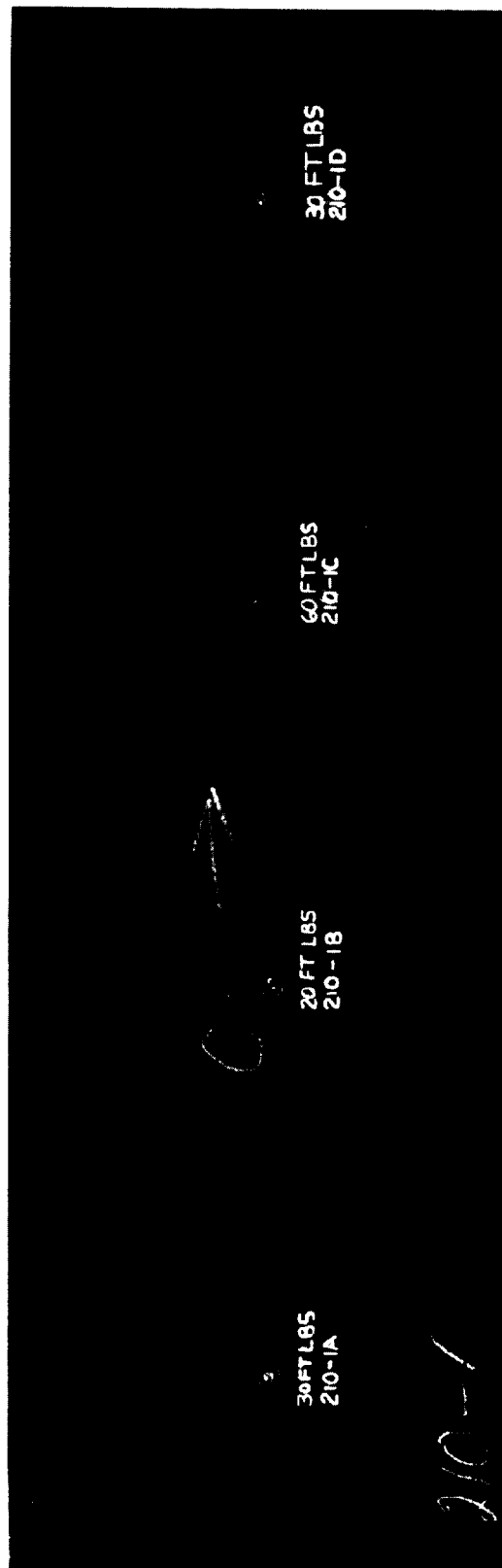
Photomicrographs were made of the 10, 20, 30 and 60 ft-lb impacts of both Celion/HX1504 and Celion/5245. Figures 2-17 and 2-18 show composite photomicrographs of the damaged regions for Celion/HX1504 and Celion/5245, respectively. The damage consisted of extensive matrix cracking in the central impacted region. The horizontal arrows outline the outer extent of the matrix cracking region. Delaminations occurred throughout the matrix cracked region and extended out to the vertical arrows. The outermost delaminations occurred at the second to fourth, mainly third, 90/+45 interfaces from the back side of the panel. Figures 2-19 through 2-22 show the damage in the central impact region resulting from 20 and 30 ft-lb impacts of the Celion/HX1504 and Celion/5245. The 20 and 30 ft-lb impact energy levels were selected for impact compression tests described in Section 2.3. As can be seen from Table 2-5, the length of the longest

TABLE 2.3
TRIAL IMPACT TEST RESULTS FOR HIGH STRAIN CELION/HX1504

Laminate Orientation: (45/0/-45/90) _{6s} Laminate Resin Content: 33.7% Laminate Thickness: 0.274						
Energy, ft-lbs	Location, ID	Ultrasonic Damage Measurements			Visual Indications	
		Width, in.	Length, in.	Area, in. ²	Front	Back
10	210-2B	1.68	1.70	2.20	Small dent	None
20	210-1B	2.00	1.90	2.70	Small dent	None
30	210-1A	2.74	2.36	4.95	Dent	0.6" Delam.
30	210-1D	2.64	2.31	4.65	Dent	0.6" Delam.
40	210-2A	3.20	2.97	7.20	Dent	1.5" Delam.
40	210-2D	3.06	2.94	7.10	Dent	1.0" Delam.
60	210-1C	4.64	4.32	15.50	Broken fibers, large dent	1.8" Delam.
80	210-2C	2.90	2.55	5.95	Full Penetration	Full Penetration 7.1" Delam.

TABLE 2.4
TRIAL IMPACT TEST RESULTS FOR HIGH STRAIN CELION/5245

Laminate Orientation: (45/0/-45/90) _{6s}						
Laminate Resin Content: 33.0%						
Laminate Thickness: 0.260						
Energy, ft-lbs	Location, ID	Ultrasonic Damage Measurements			Visual Indications	
		Width, in.	Length, in.	Area, in. ²	Front	Back
10	243-2B	1.50	1.50	1.65	Slight dent	None
20	243-1B	2.02	2.02	2.60	Slight dent	None
30	243-1A	2.46	2.14	4.00	Slight dent	None
30	243-1D	2.44	2.38	4.40	Slight dent	None
40	243-2A	2.80	2.83	5.90	Dent	3.1" Delam.
40	243-2D	2.70	2.74	5.20	Dent	1.4" Delam.
60	243-1C	3.42	3.90	10.35	Broken fibers	5.1" Delam.
80	243-2C	3.55	3.73	9.10	Partial penetration	6.9" Delam.



ORIGINAL PAGE IS
OF POOR QUALITY.

Photo No. 147853

Figure 2-3a: Celion/HX1504 trial impact panel 210-1, front surface.

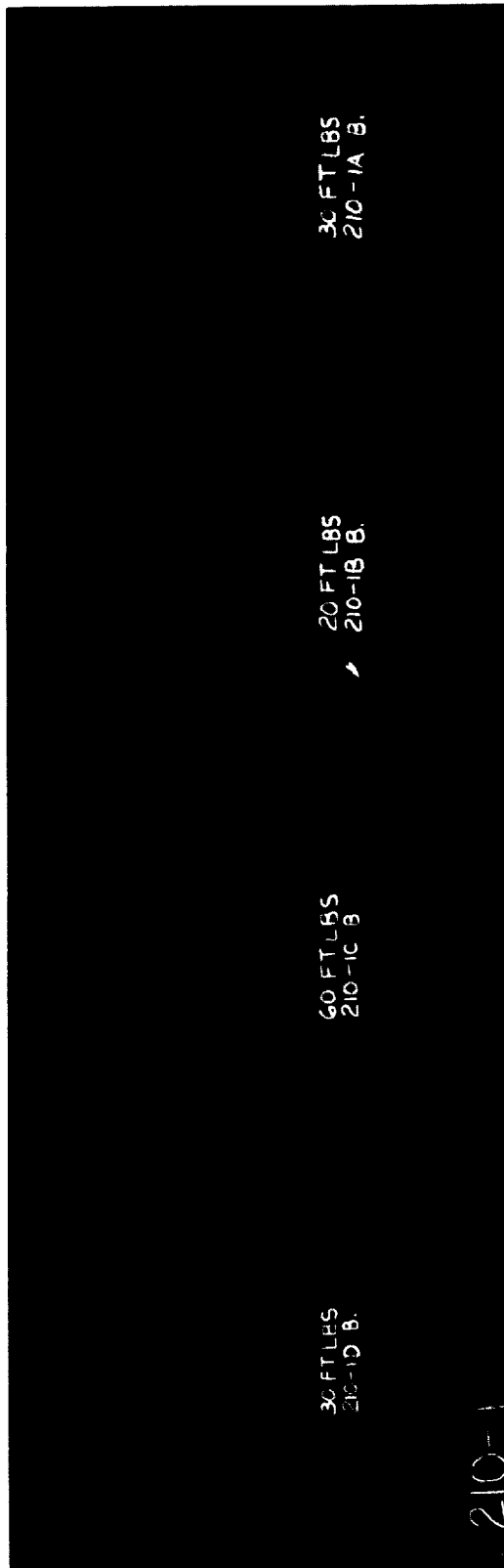


Photo No. 147852

Figure 2-3b: Celion/HX1504 trial impact panel 210-1, back surface.

ORIGINAL PAGE IS
OF POOR QUALITY

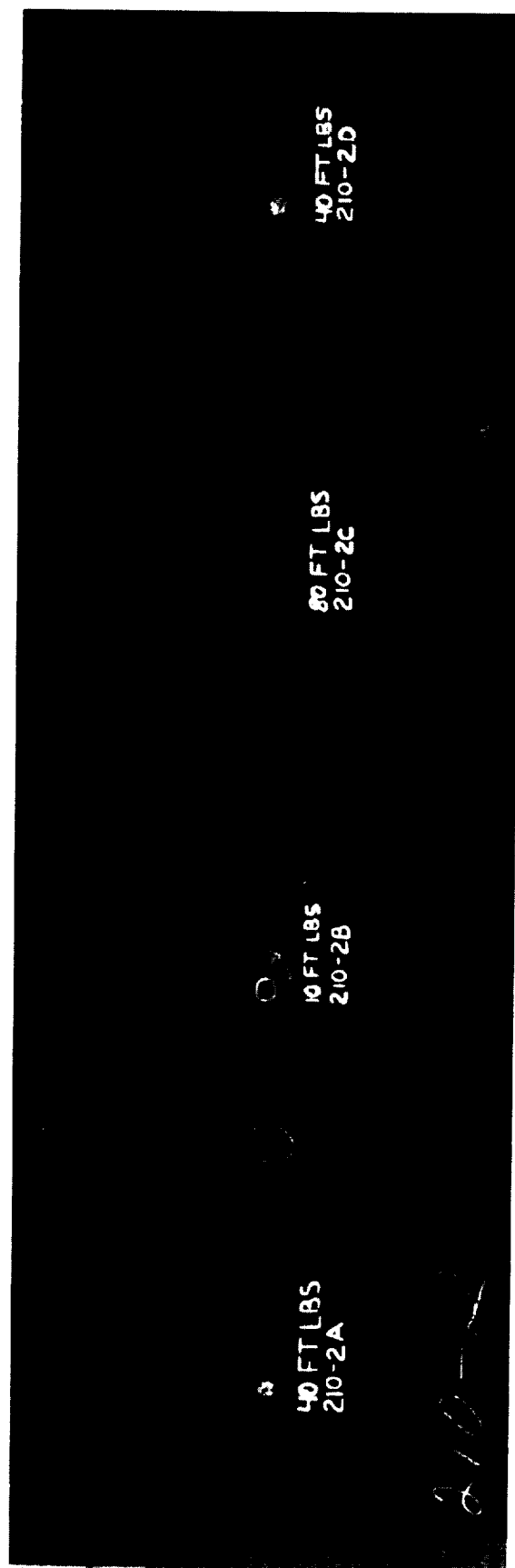


Photo No. 147866

Figure 2-4a: Celion/HX1504 trial impact panel 210-2, front surface.

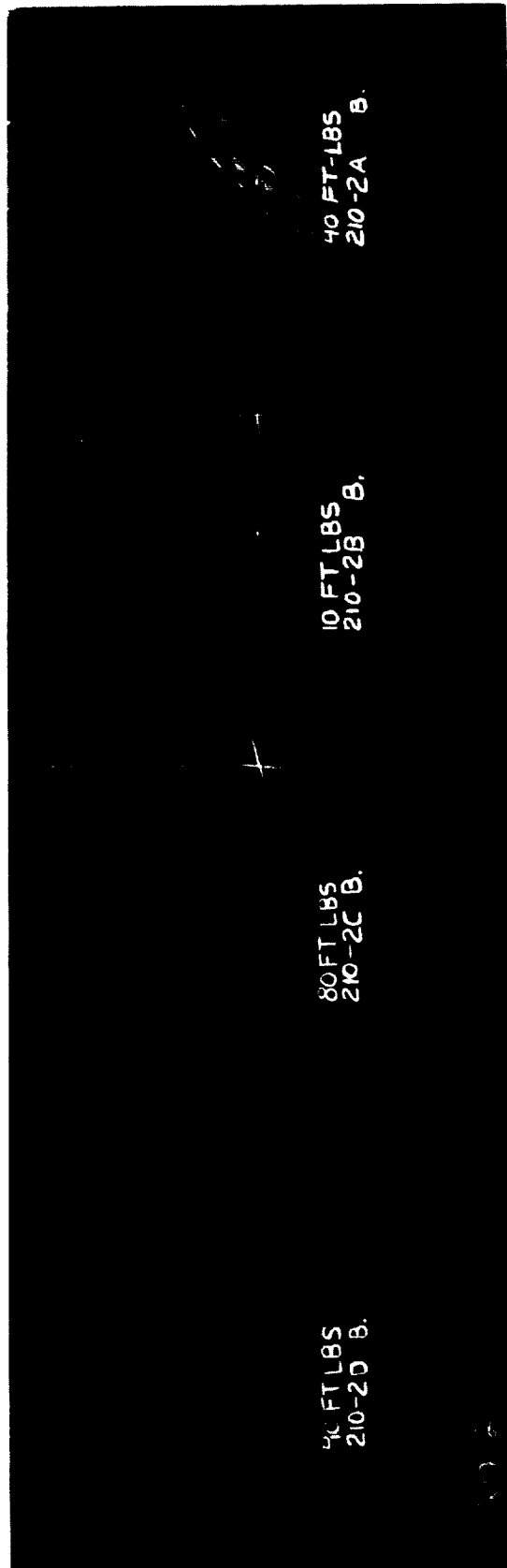
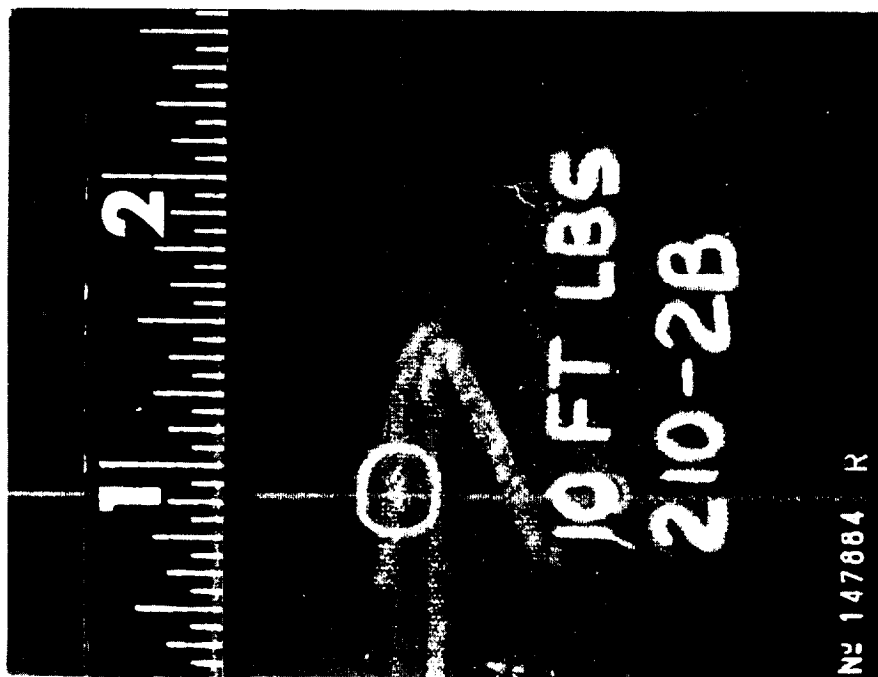


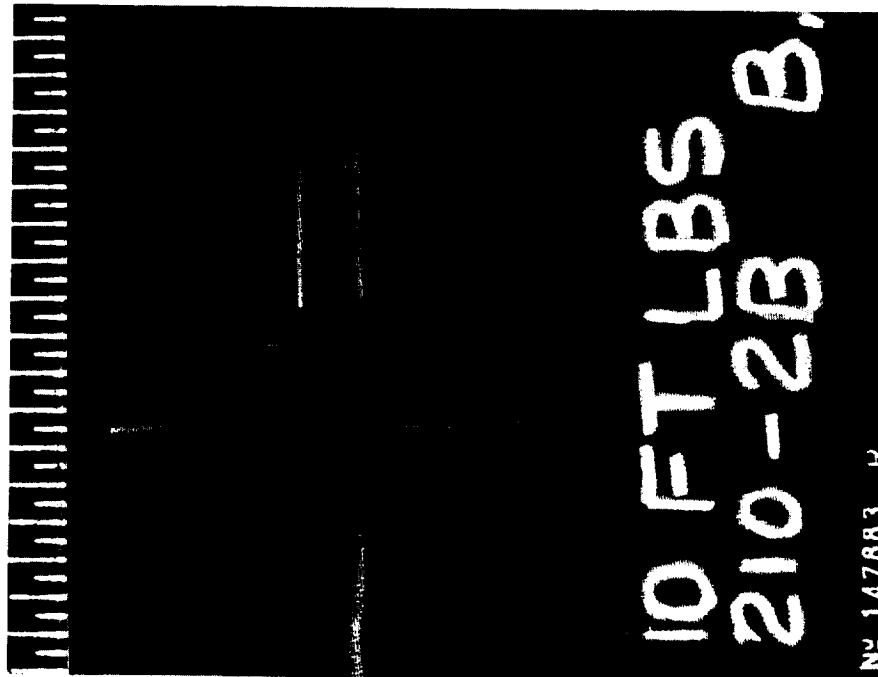
Photo No. 148223

Figure 2-4b: Celion/HX1504 trial impact panel 210-2, back surface.

ORIGINAL PAGE IS
OF POOR QUALITY



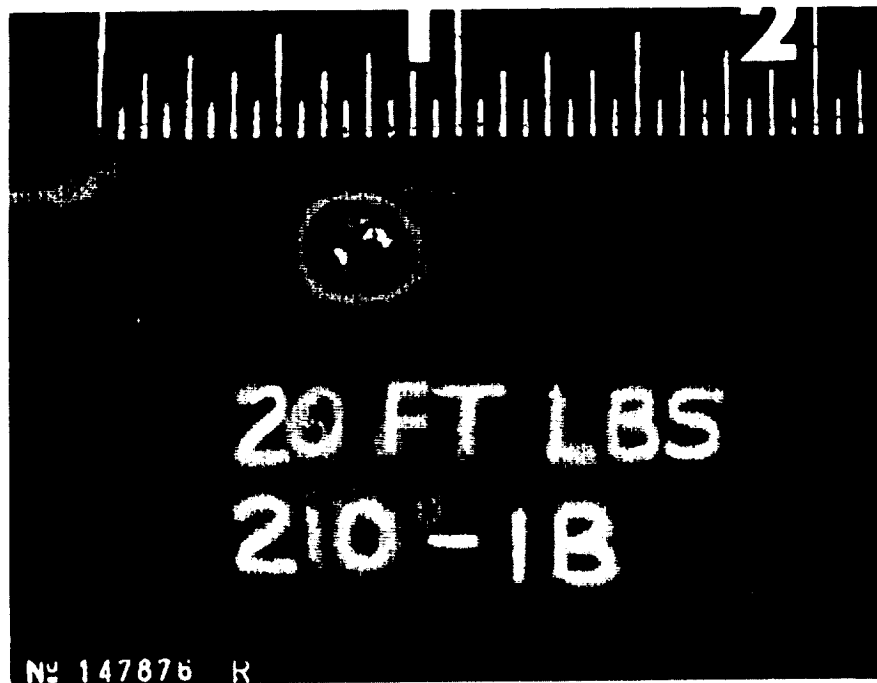
(a)



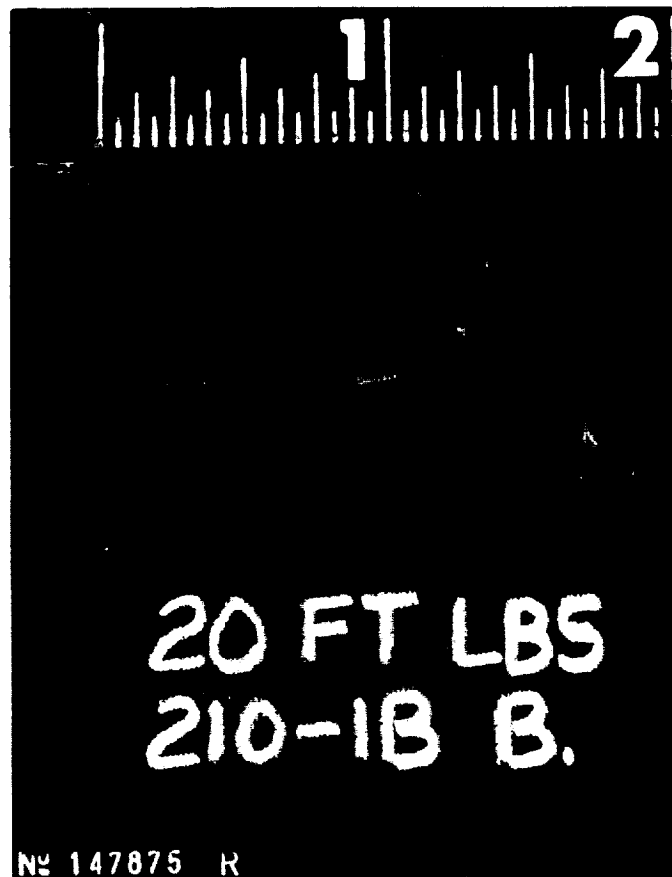
(b)

ORIGINAL PAGE IS
OF POOR QUALITY

Figure 2-5: 10 ft-lb impact of Celion/HX1504: a) front surface, b) back surface.

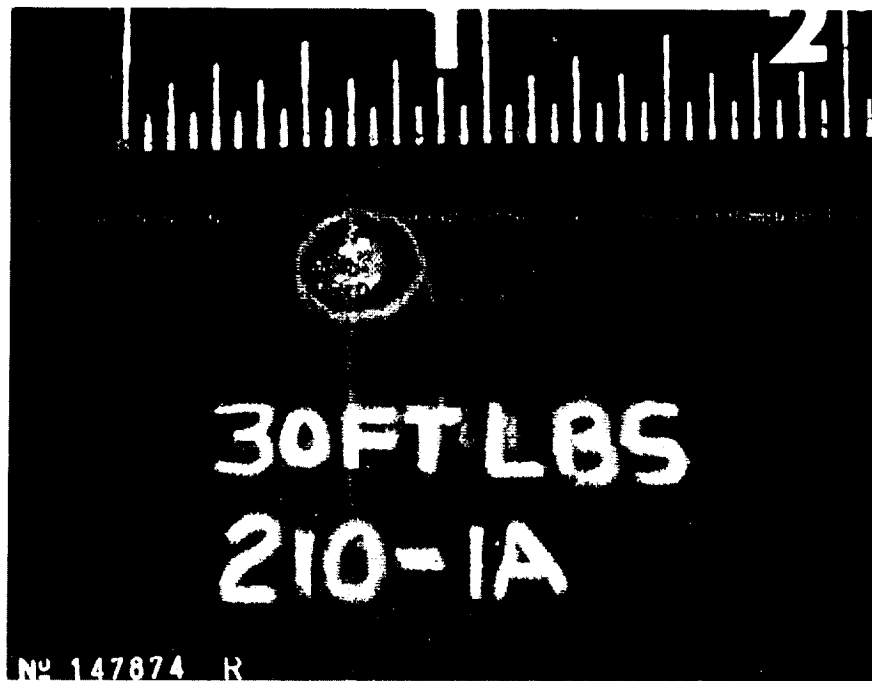


(a)

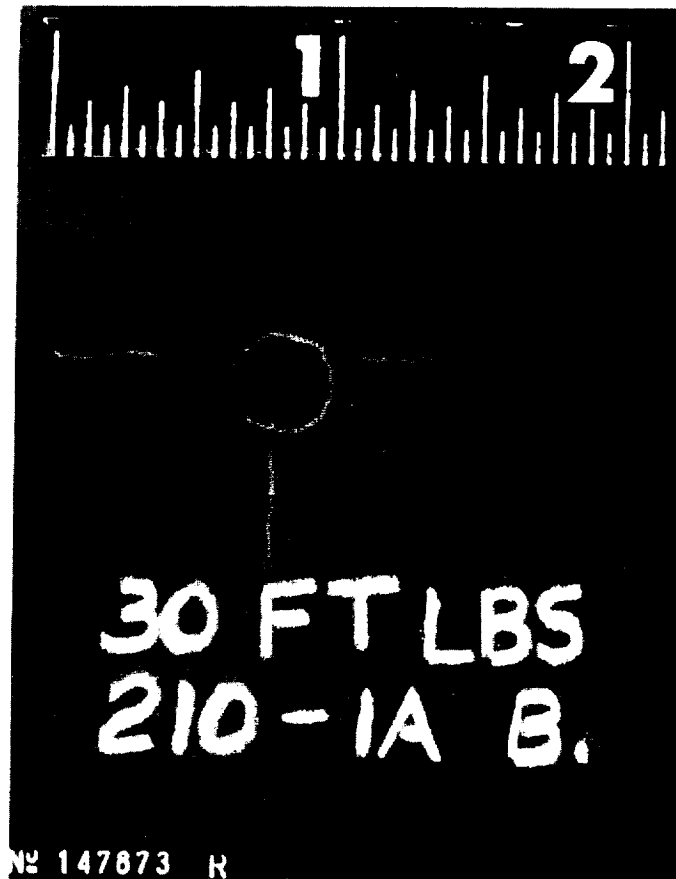


(b)

Figure 2-6: 20 ft-lb impact of Celion/HX1504: a) front surface, b) back surface.

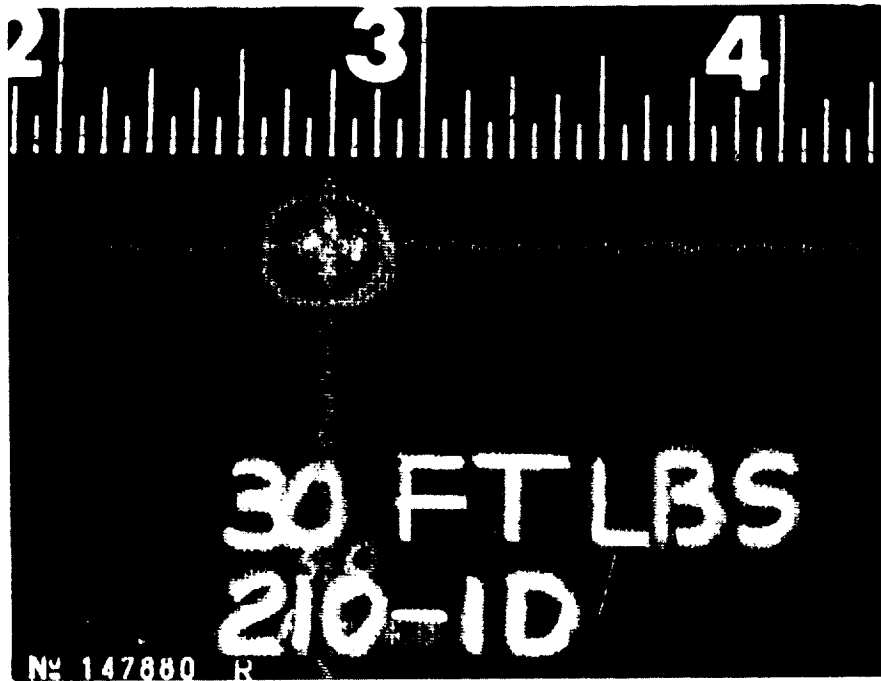


(a)

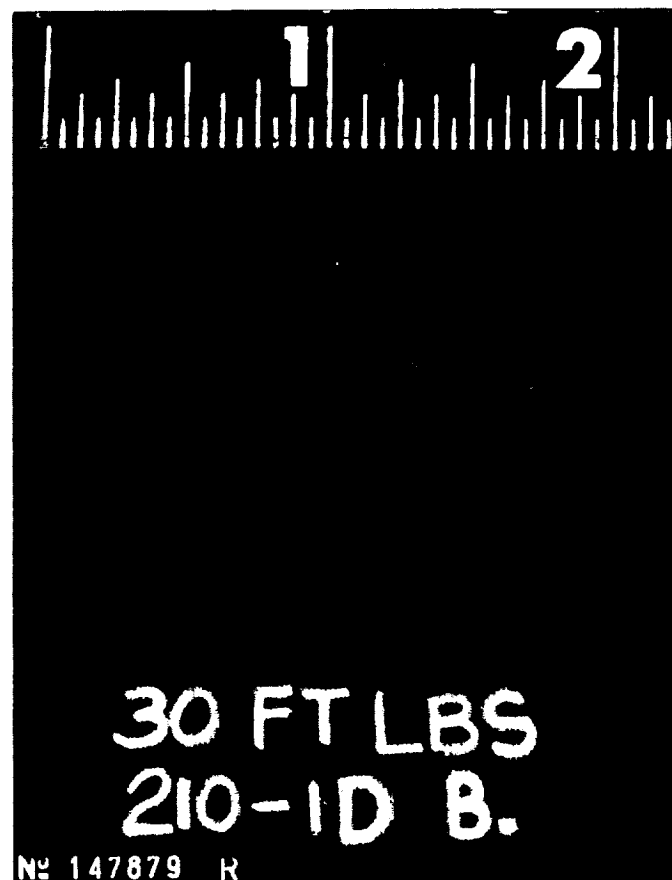


(b)

Figure 2-7: 30 ft-lb impact of Celion/HX1504: a) front surface, b) back surface.

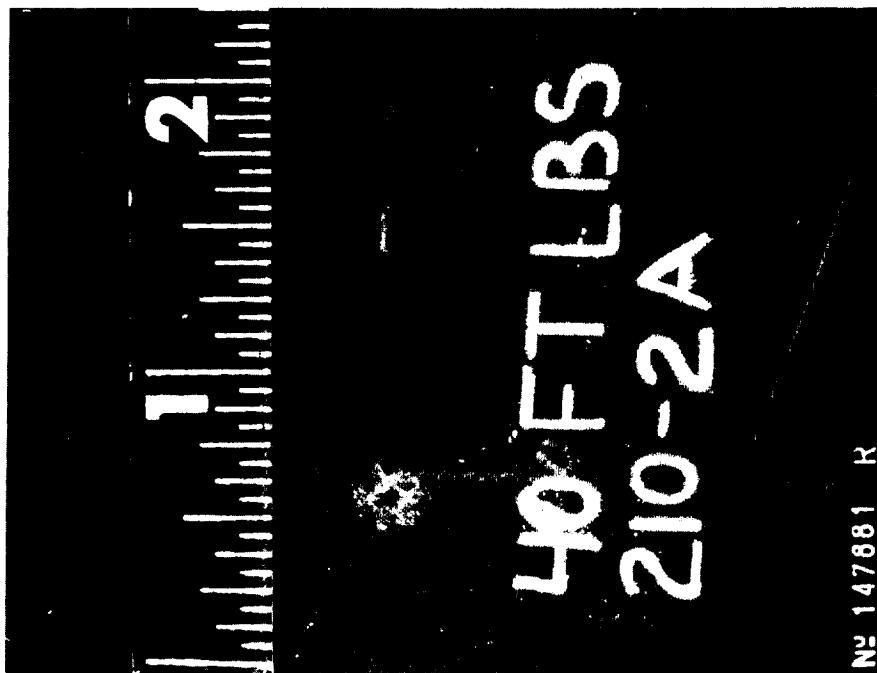


(a)

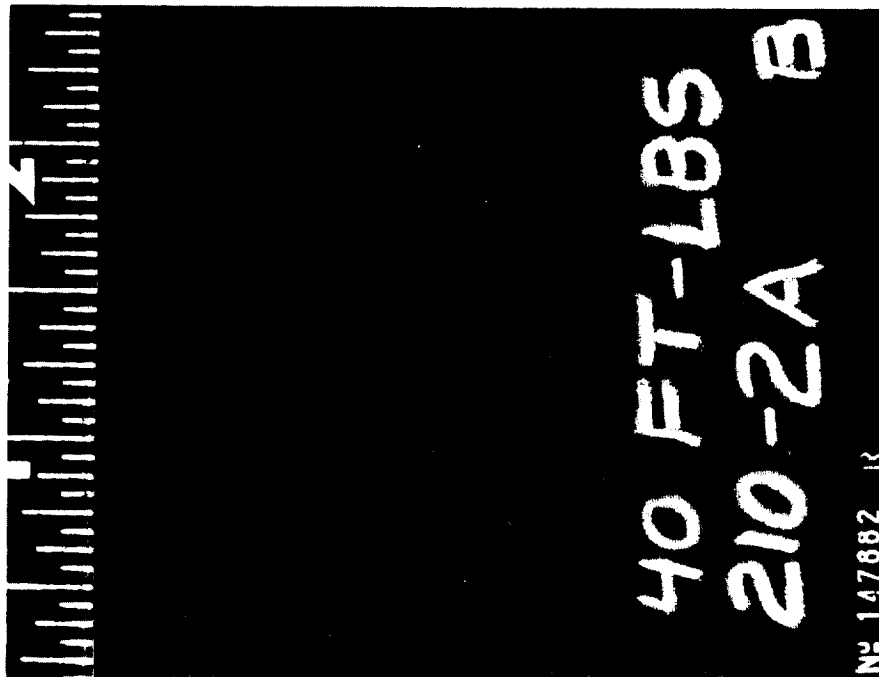


(b)

Figure 2-8: 30 ft-lb impact of Celion/HX1504: a) front surface, b) back surface



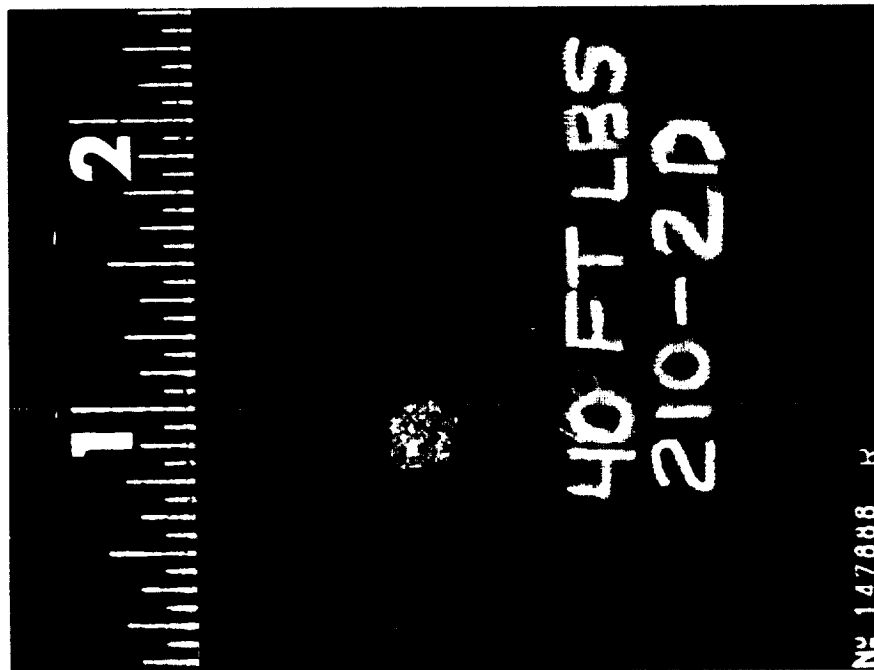
(a)



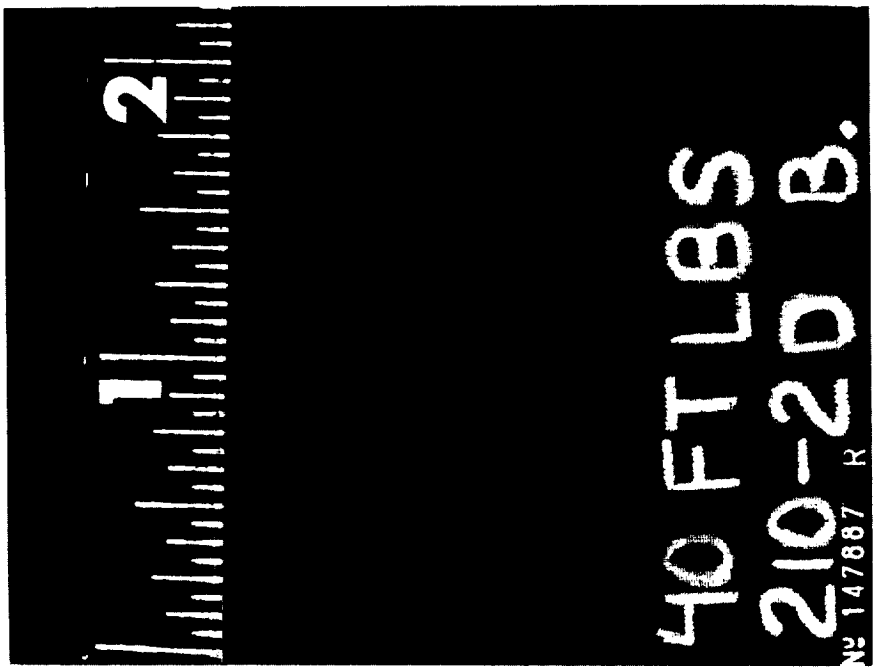
(b)

ORIGINAL OF POOR QUALITY

Figure 2-9: 40 ft-lb impact of Celion/HX1504: a) front surface, b) back surface.

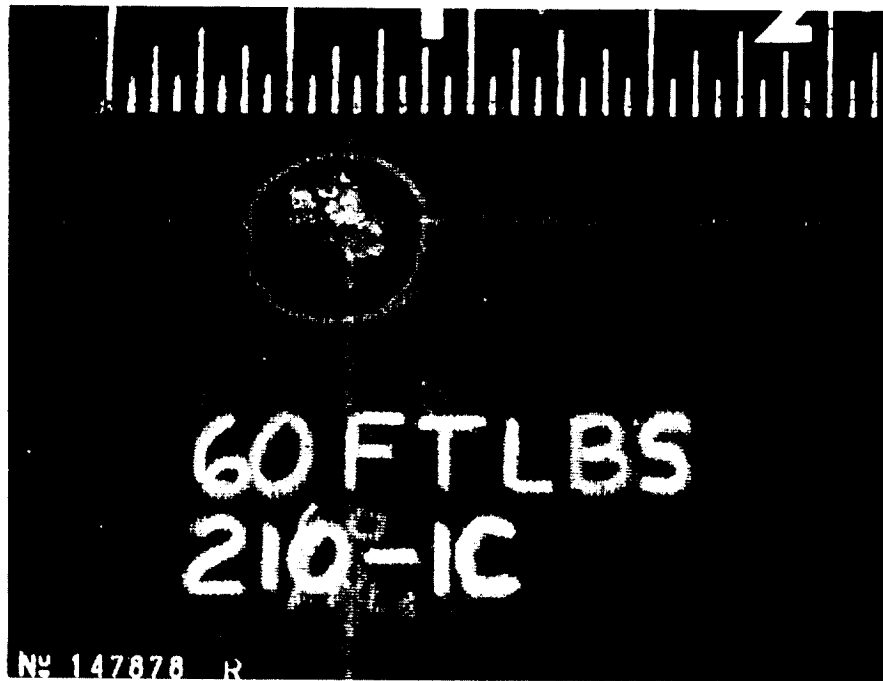


(a)

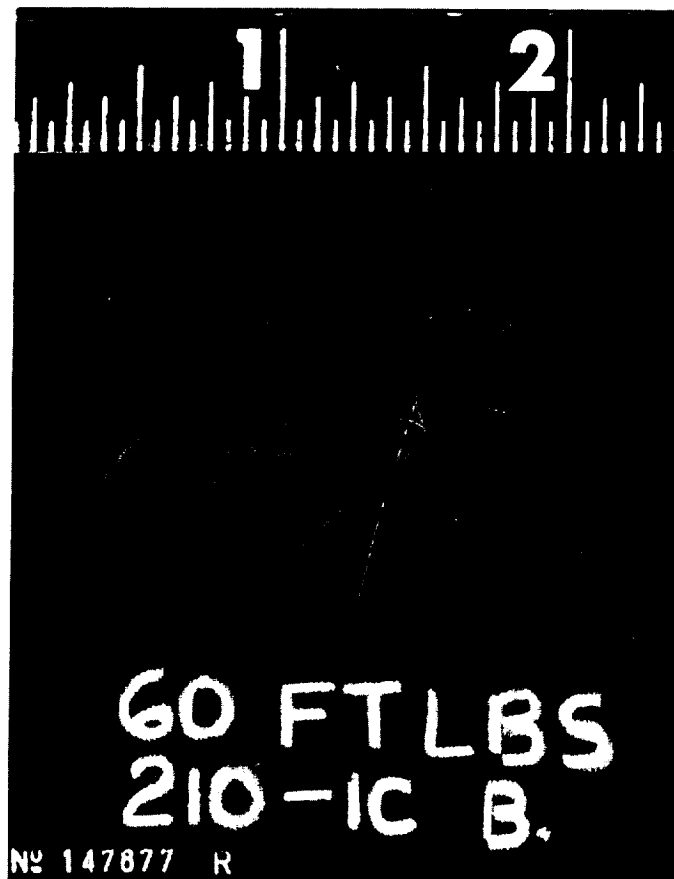


(b) **CELION/HX1504**
OF POOR QUALITY

Figure 2-10: 40 ft-lb impact of Celion/HX1504: a) front surface, b) back surface.



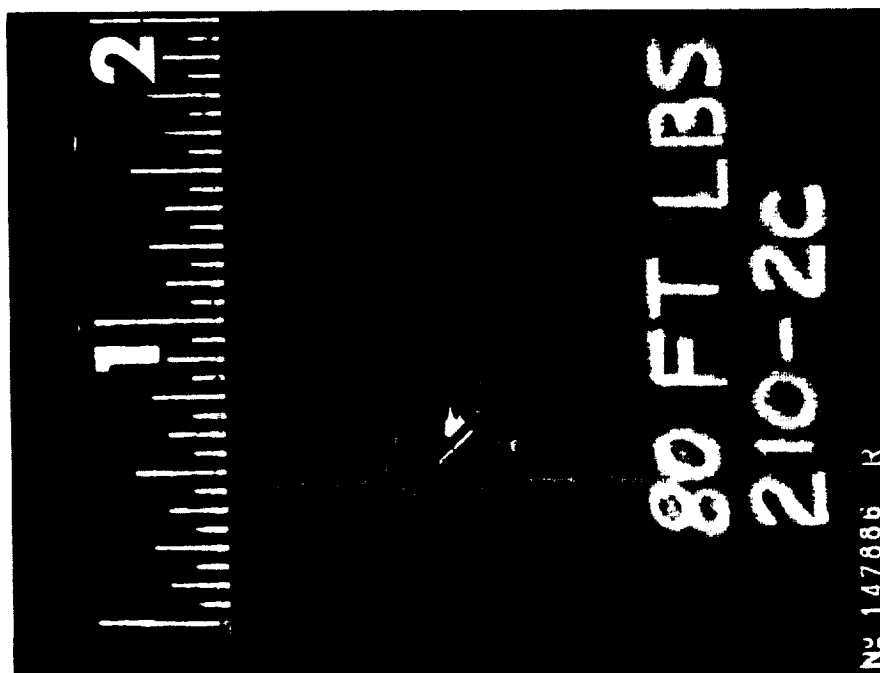
(a)



(b)

Figure 2-11: 60 ft-lb impact of Celion/HX1504: a) front surface, b) back surface.

(a)



(b)

CELLION
OF PCOR QUALITY

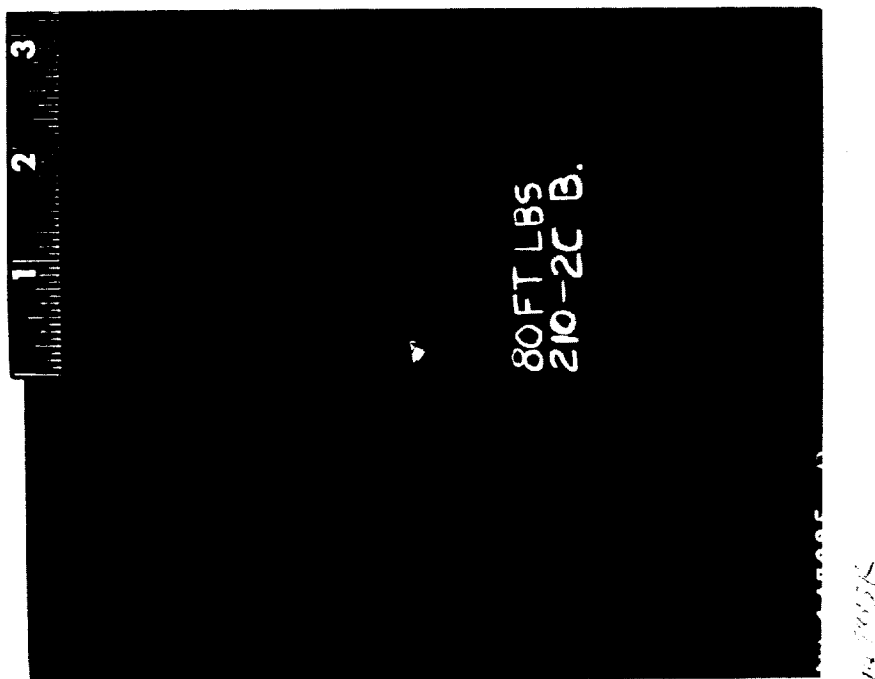


Figure 2-12: 80 ft-lb impact of Celion/HX1504: a) front surface, b) back surface.

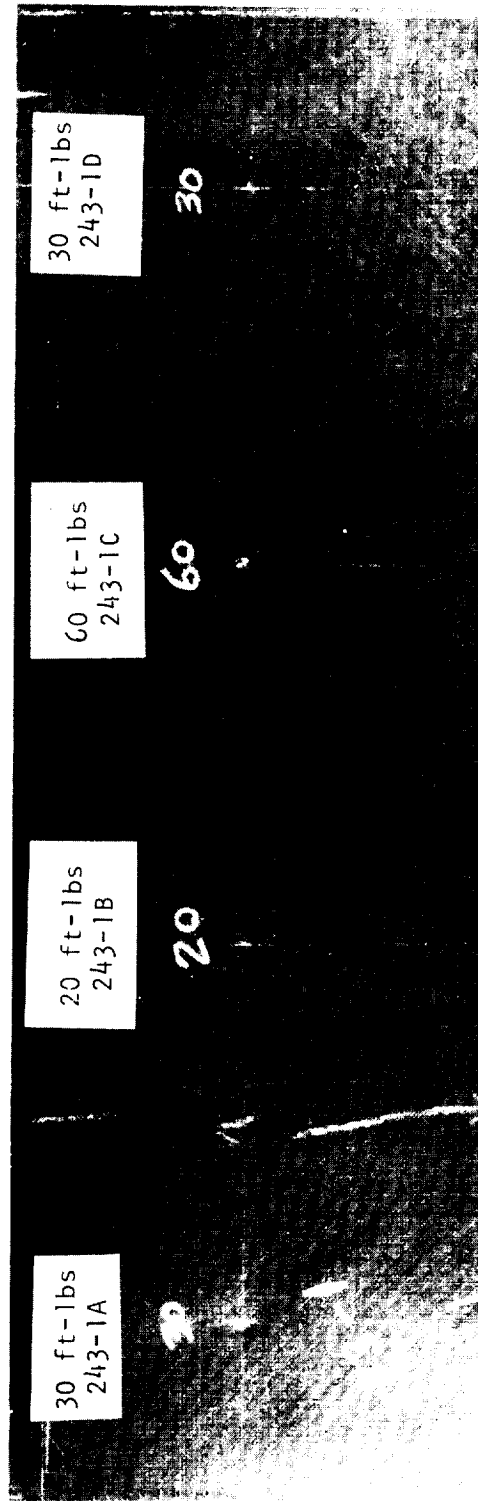


Photo No. 1482/1

Figure 2-13a: Celion/5245 trial impact panel 243-1: front surface.

ORIGINAL PHOTOGRAPH
OF POOR QUALITY

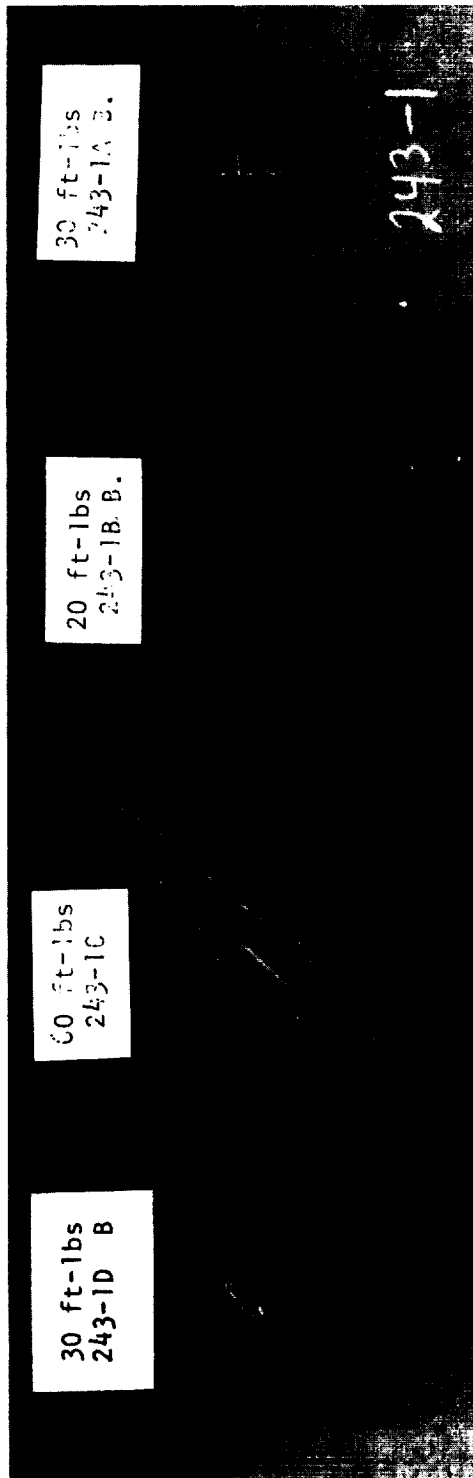


Photo No. 147282

Figure 2-13b: Celion/5245 trial impact panel 243-1, back surface.

OR
OF POOR QUALITY

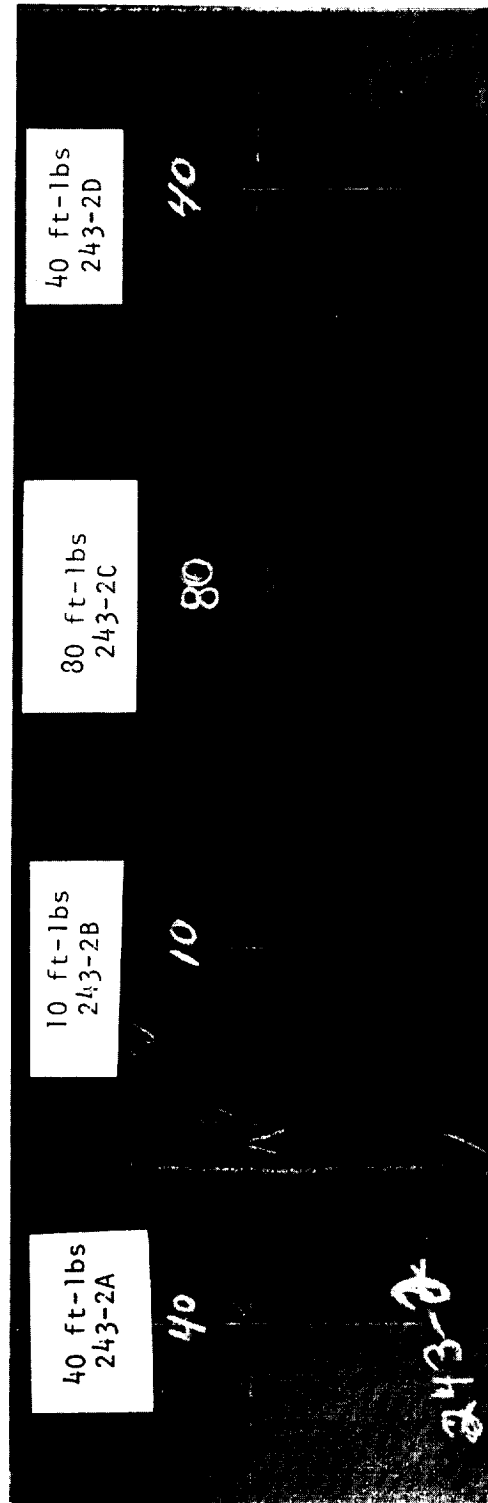


Photo No. 148275

Figure 2-14a: Celion/5245 trial impact panel 243-2: front surface.

ORIGINAL FACED
OF POOR QUALITY

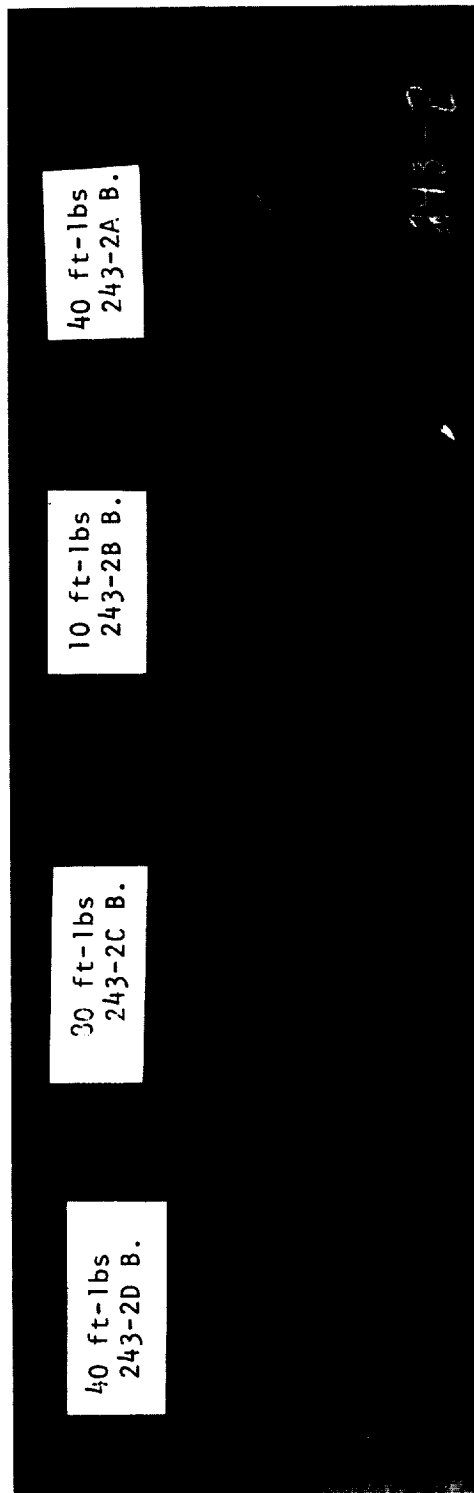


Photo No. 148276

Figure 2-14b: Celion/5245 trial impact panel 243-2: back surface.

ORIGINAL
OF POOR QUALITY

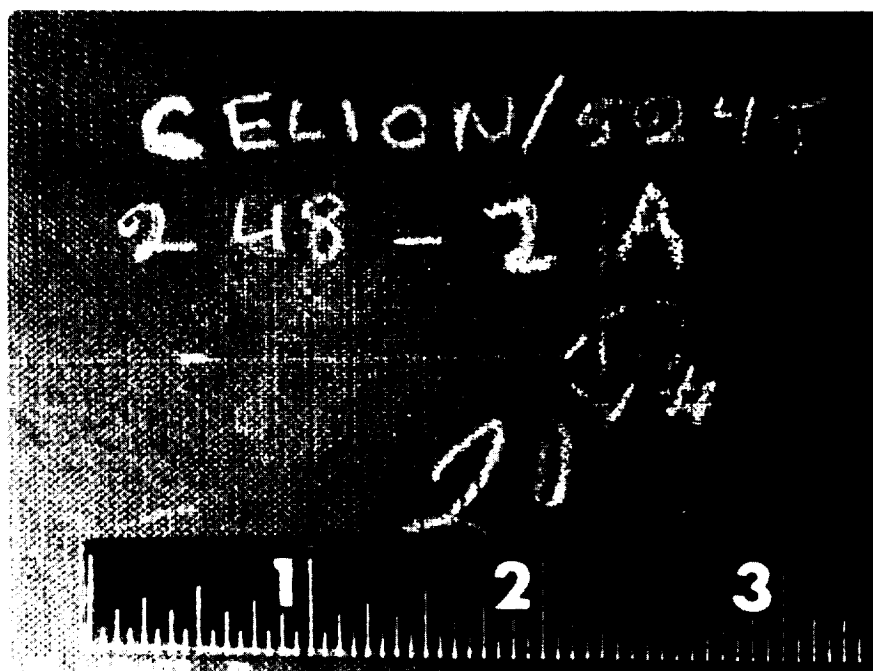


Photo No.
148402

(a)

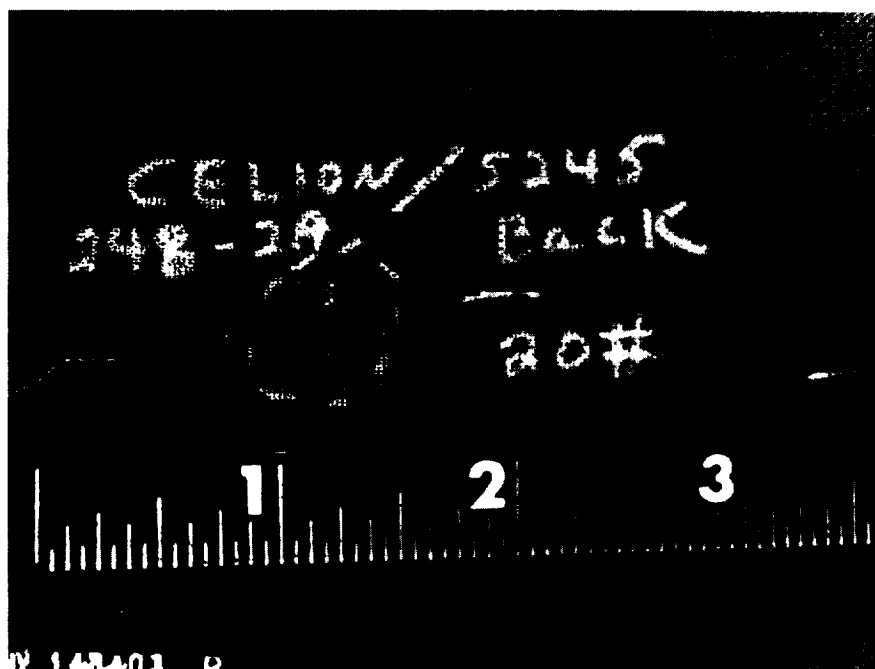


Photo No.
148401

(b)

Figure 2-15: Typical 20 ft-lb impact of Celion/5245: a) front surface, b) back surface.

ORIGINAL COPY
OF POOR QUALITY

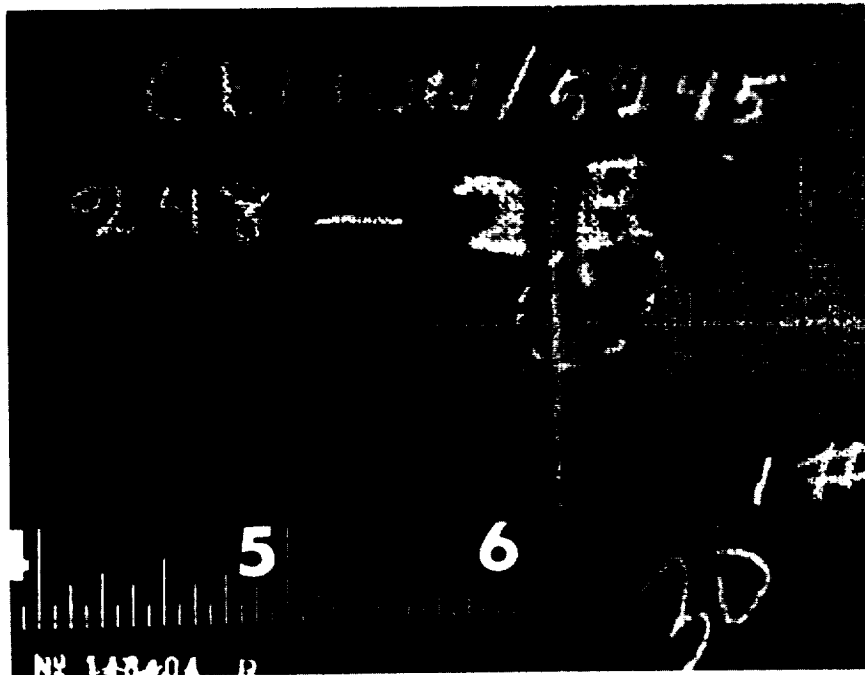


Photo No.
148404

(a)

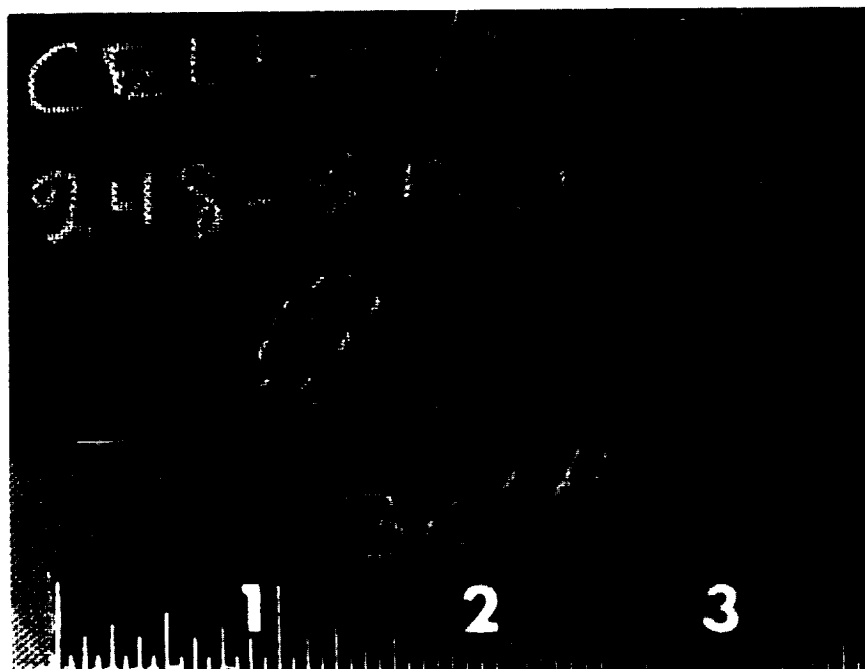


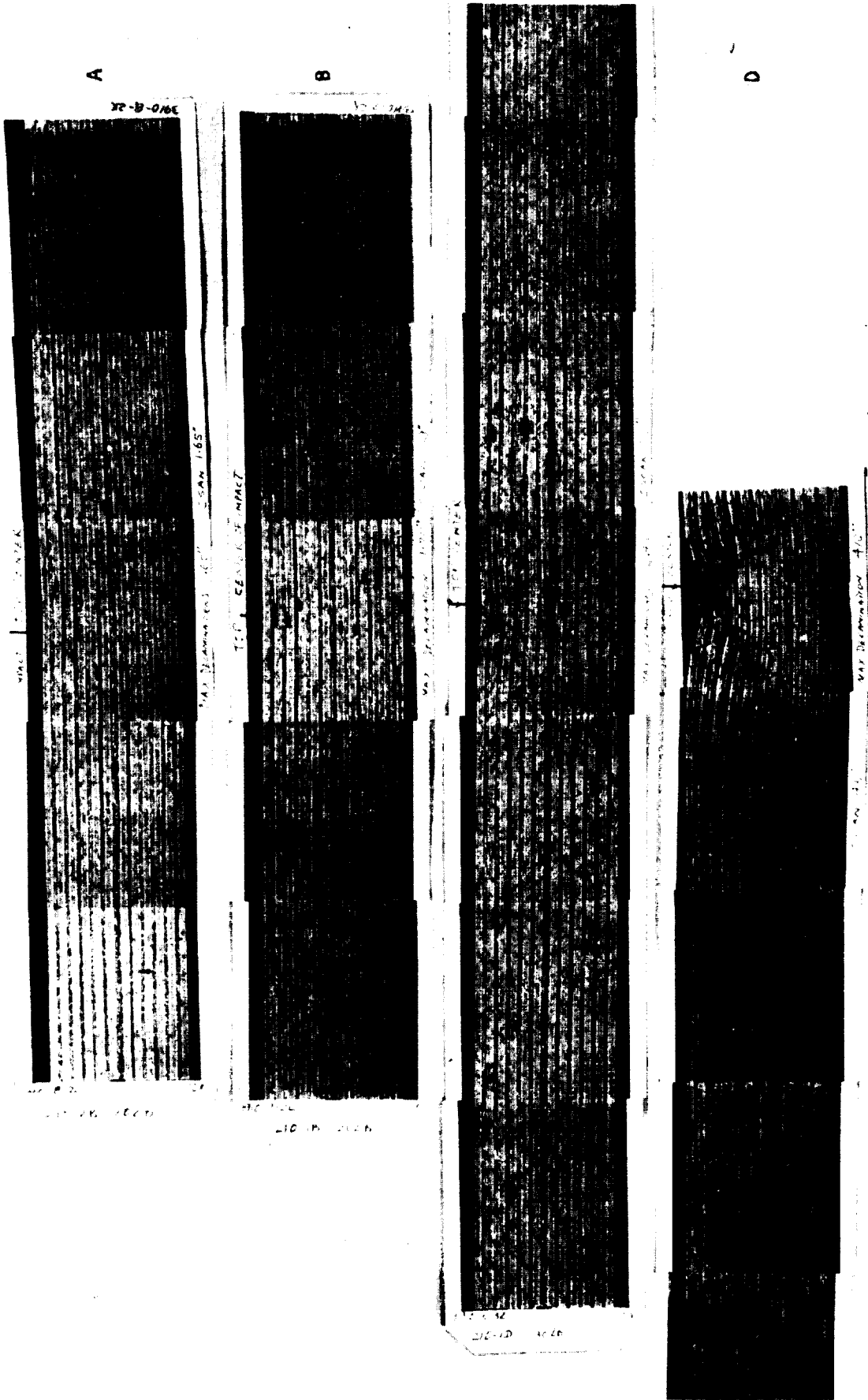
Photo No.
148405

(b)

Figure 2-16: Typical 30 ft-lb impact of Celion/5245: a) front surface,
b) back surface.

Photo No. 149887

Figure 2-17: Photomicrographs of a cross-section through the center of impacted damage regions of Celion HX1504: a) 10 ft-lb impact, b) 20 ft-lb impact, c) 30 ft-lb impact, d) 60 ft-lb impact. Impact locations are indicated by center vertical arrows. Outer vertical arrows indicate outermost extent of damage, which is from delaminations. Horizontal arrows indicate outer extent of matrix cracking. 3.2X magnification.



ORIGINAL PHOTOGRAPH
OF POOR QUALITY

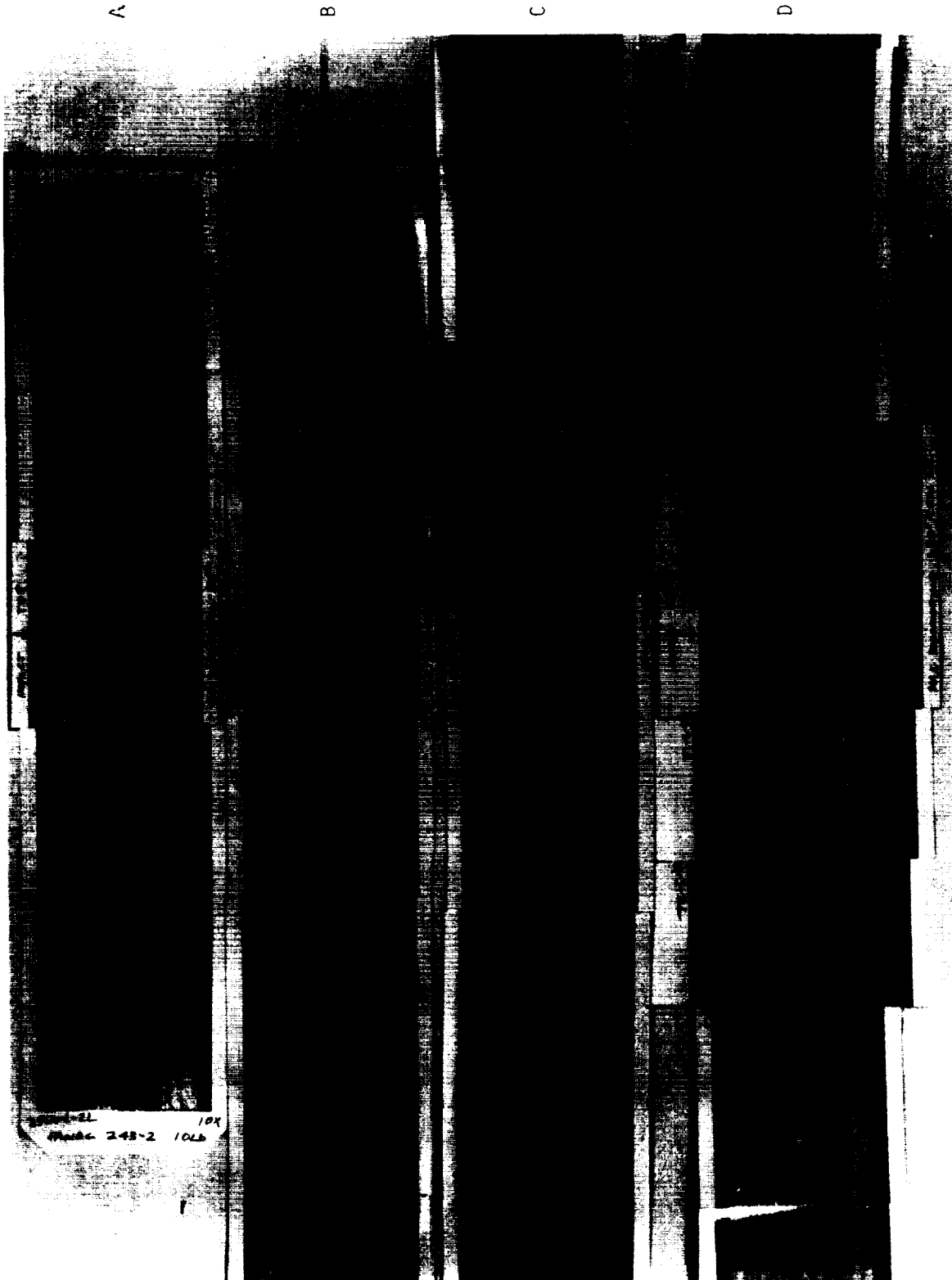
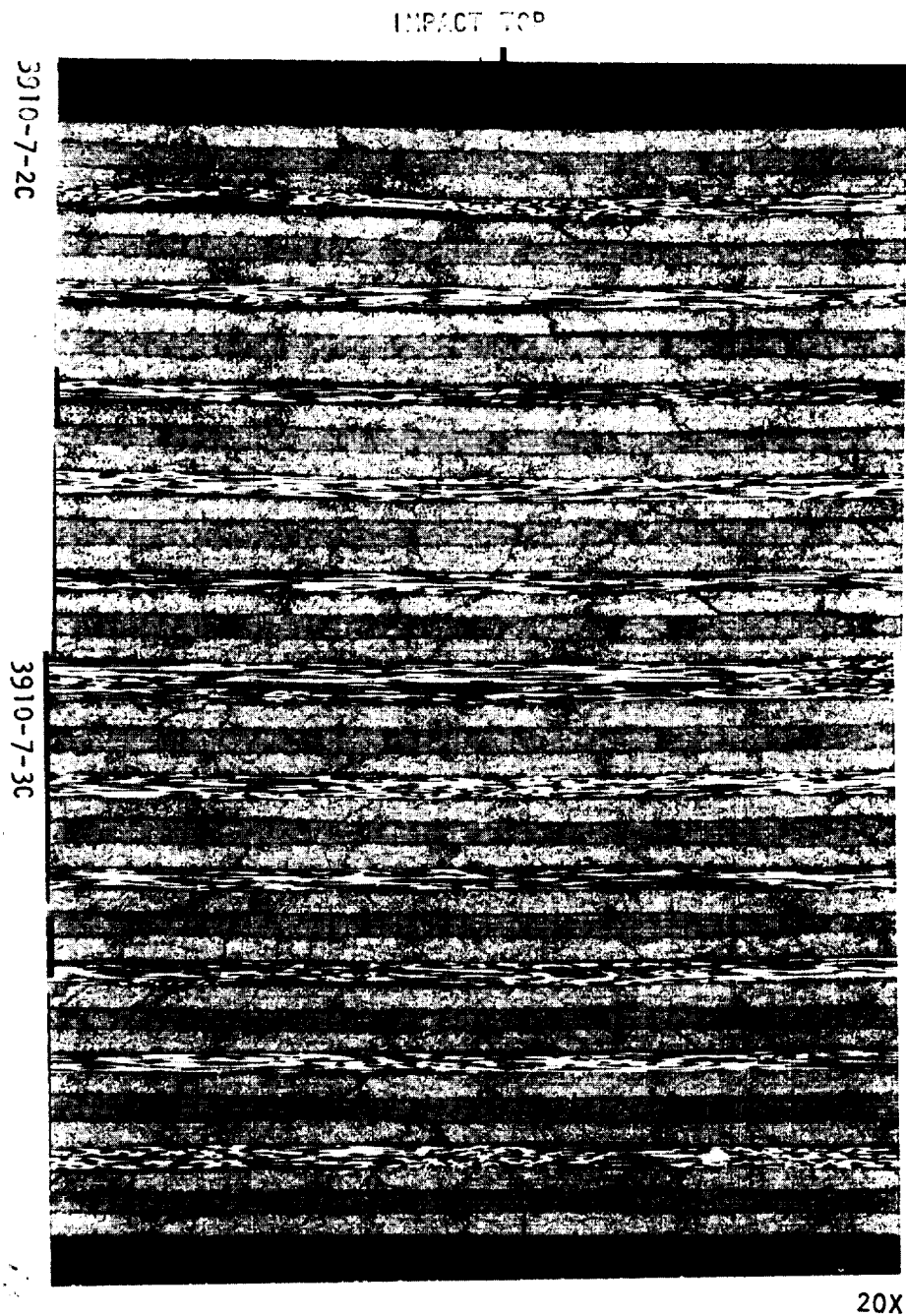


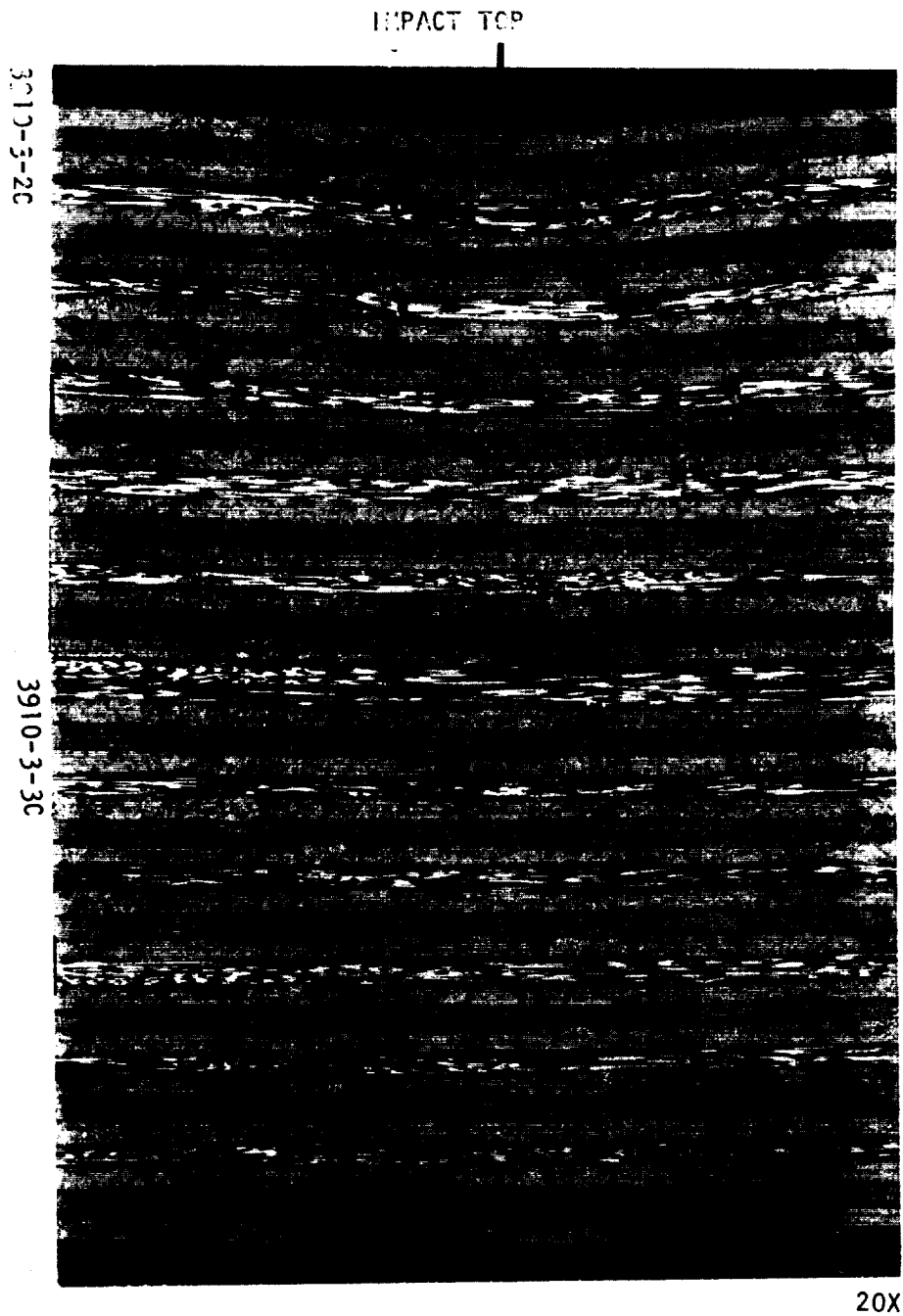
Photo No. 149884
Figure 2-16: Photomicrographs of a cross-section through the center of impacted damage regions of Celion/HX5245: a) 10 ft-lb impact, b) 20 ft-lb impact, c) 30 ft-lb impact, d) 60 ft-lb impact. Impact locations are indicated by center vertical arrows. Outer vertical arrows indicate outermost extent of damage, which is from delaminations. Horizontal arrows indicate outer extent of matrix cracking. 3.1X magnification.

ORIGINAL FILED
OF POOR QUALITY



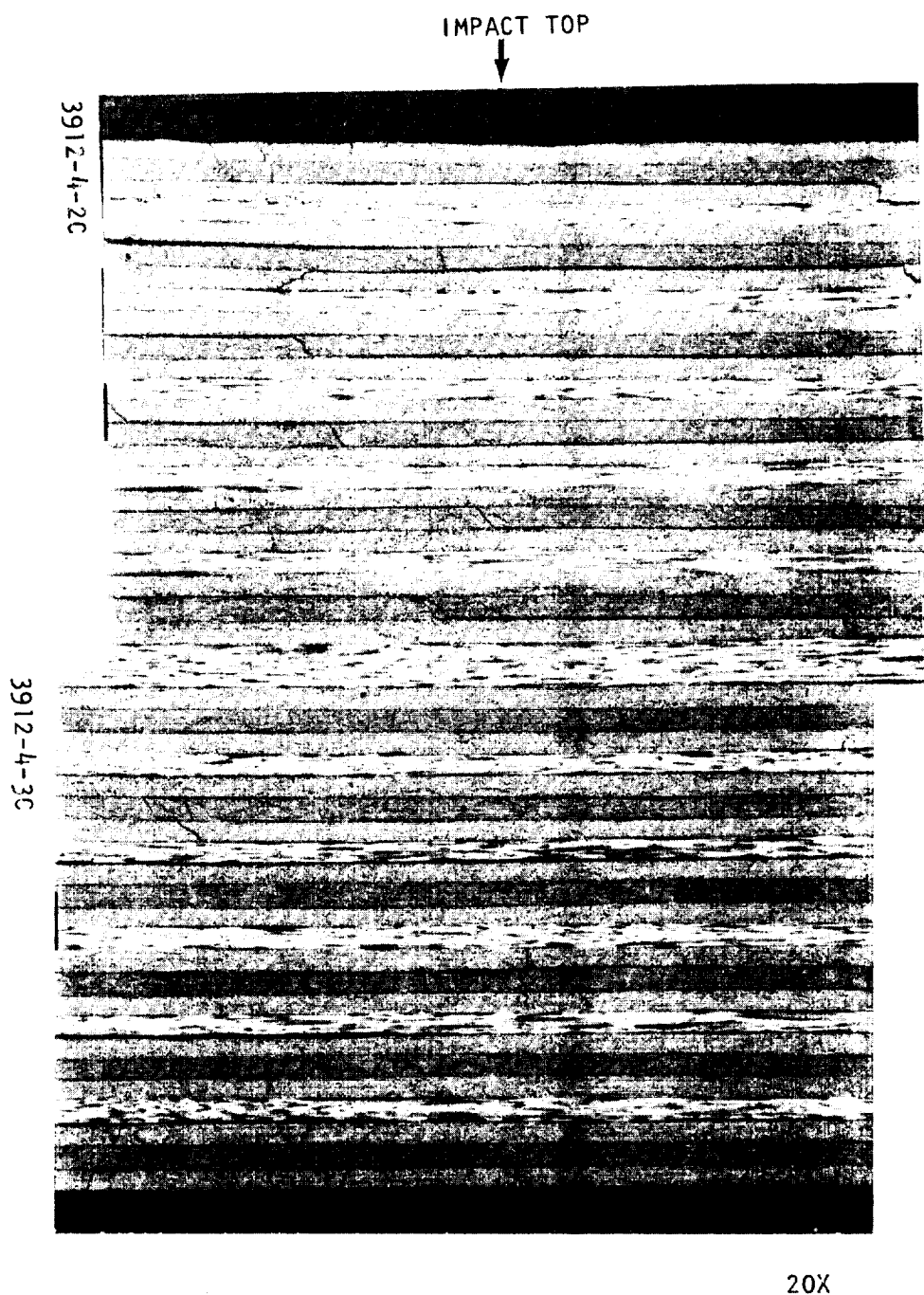
Panel 210-iB
20 ft-lbs

Figure 2-19: Center of impact area of high strain Celion/HX1504 at 20 ft-lbs. The arrow indicates the impact location. Note matrix cracking and delamination.



Panel 210-1D
30 ft-lbs

Figure 2-20: Center of impact area of high strain Celion/HX1504 at 30 ft-lbs. The arrow indicates the impact location. Note matrix cracking and delamination.



Panel 243-1B
20 ft-lbs

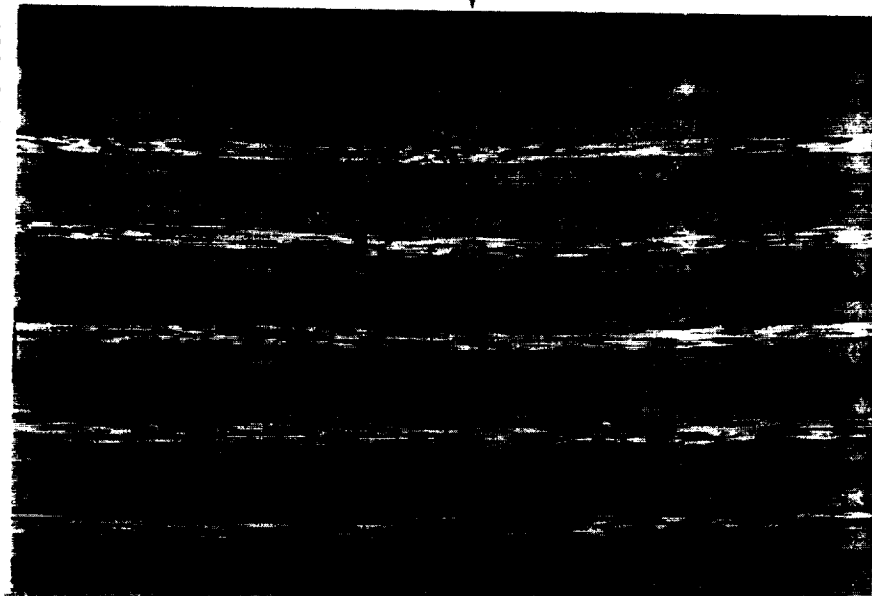
Figure 2-21: Center of impact area of high strain Celion/5245 at 20 ft-lbs. The arrow indicates the impact location. Note matrix cracking and delamination.

ORIGINAL PAGE IS
OF POOR QUALITY

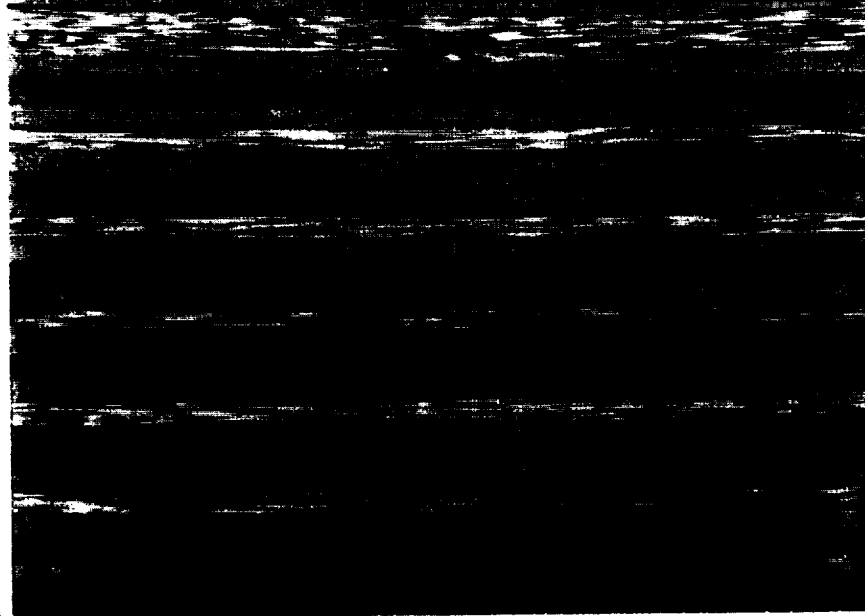
IMPACT TOP



3912-2-2C



3912-2-3C



20X

Panel 243-1D
30 ft-lbs

Figure 2-22: Center of impact area of high strain Celion/5245 at 30 ft-lbs impact. The arrow indicates the impact location. Note matrix cracking and delaminations.

TABLE 2.5: COMPARISON OF C-SCAN AND MICROSCOPE DELAMINATION MEASUREMENTS

Material	Impact Energy, ft-lbs	Specimen ID	C-Scan Damage Length, ^a in.	Microscope Delamination Length, ^a in.
Celion/HX1504	10	210-2B	1.65	1.60
	20	210-1B	1.90	1.70
	30	210-1D	2.60	2.45
	60	210-1C	4.60	4.10
Celion/5245	10	243-2B	1.45	1.45
	20	243-1B	2.00	1.90
	30	243-1D	2.40	2.43
	60	243-1C	3.30	3.30

a) The C-scan and microscope delamination measurements were made at approximately the same location.

delamination measured under a microscope for a particular impact energy corresponded very well, generally within 0.1 - 0.2 in., with the damage length measured from ultrasonic C-scans.

2.3 QUASI-ISOTROPIC COMPRESSION TESTS

Compression tests were conducted on 48-ply quasi-isotropic Celion/HX1504 and Celion/5245 laminates. The compression tests consisted of the following: three inch wide, unnotched specimens tested at 75⁰F dry and 180⁰F wet, (Figure 2-23); five inch wide specimens with a 1.0 inch hole or with a 20 or 30 ft-lb impact tested at 75⁰F dry (Figure 2-24). Notched and unnotched compression tests were performed per NASA Standard Test "ST-4: Specification for Inplane Open-Hole Compression Test". The wet conditioned specimens were immersed in water at 160⁰F for 45 days. The amount of weight gain within the coupon was monitored by weighing 1.0 x 1.0 in. weight gain travelers at two week intervals. The moisture absorption behavior of both materials was very similar (Figure 2-25). Both materials absorbed an average of 0.62% moisture after 45 days.

The specimens were tested in the simple supported composite compression fixture shown in Figure 2-26. The fixture has spherical seats on both loading ends to facilitate the alignment of the specimen. The specimens were tested in a 200 kip MTS machine at a stroke rate of 0.05 in./min. Preliminary runs to 5% of the anticipated failure load were conducted to ensure that the back-to-back strains were within 6% agreement, and adjustments were made to the specimen/fixture alignment when needed. The impacted compression tests were performed per NASA Standard Test "ST-1: Specification for Compression After Impact Test". The impact procedure was similar to that used for the trial impact tests (see Section 2.2).

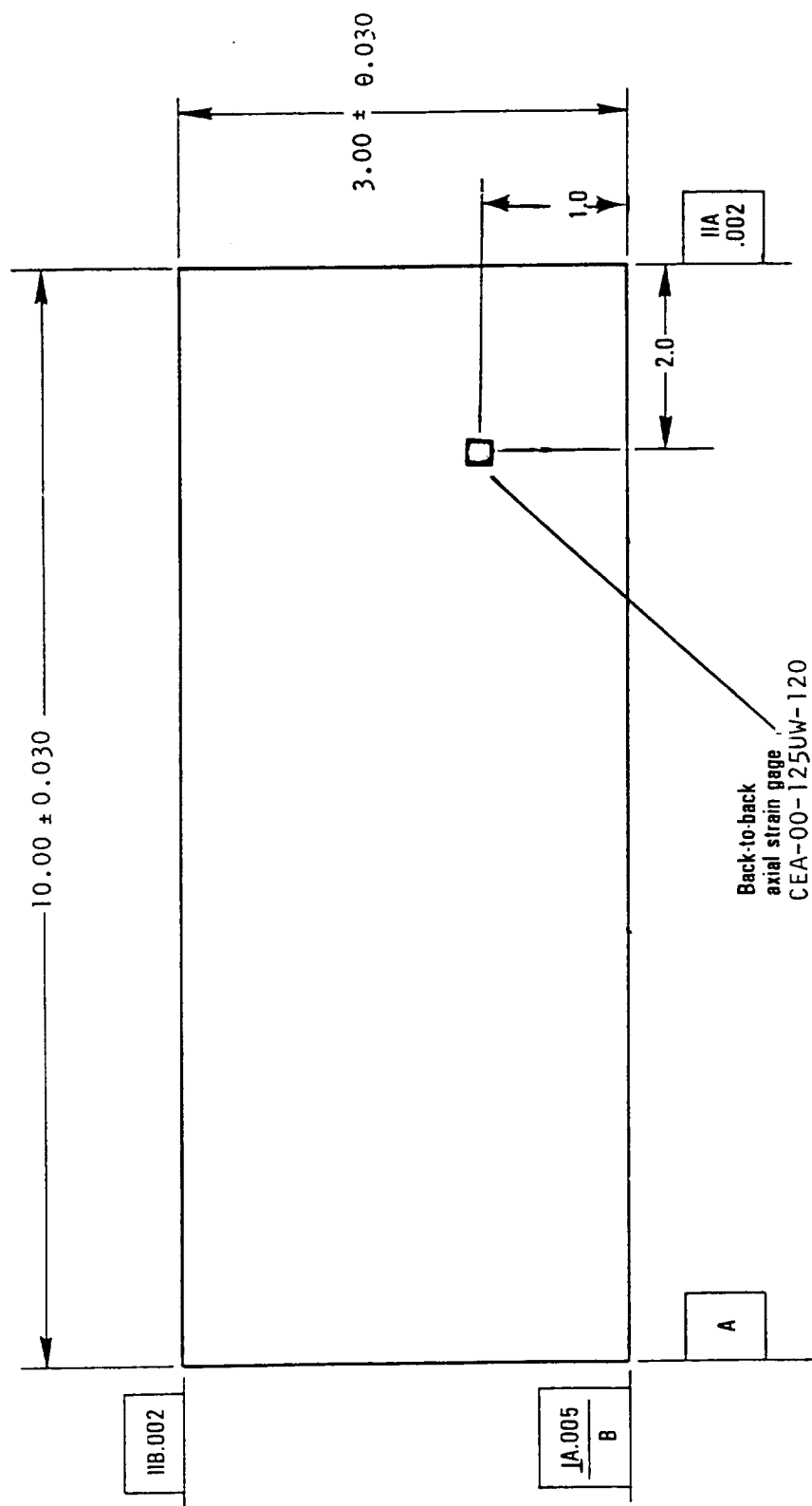


Figure 2-23: Compression coupon.

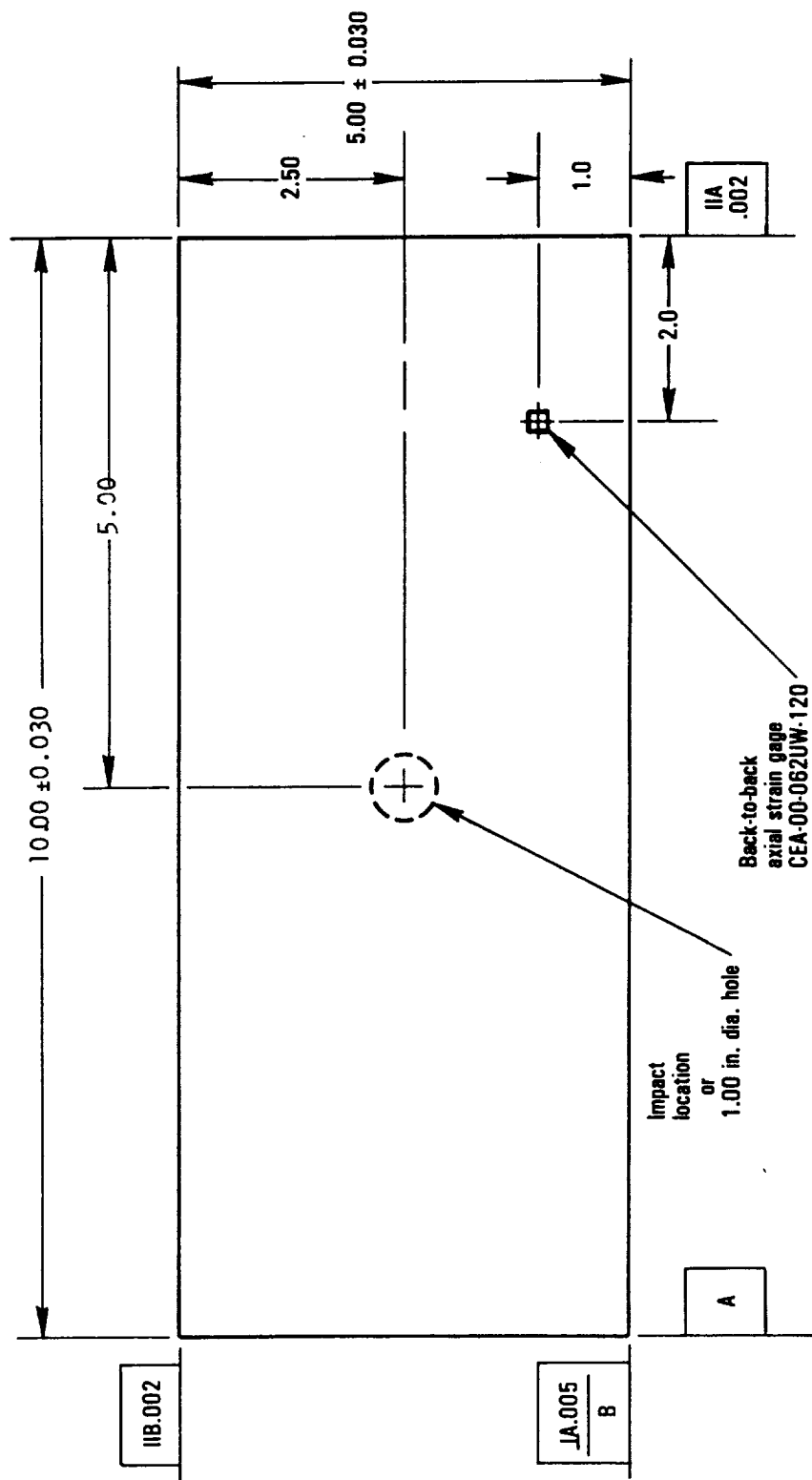
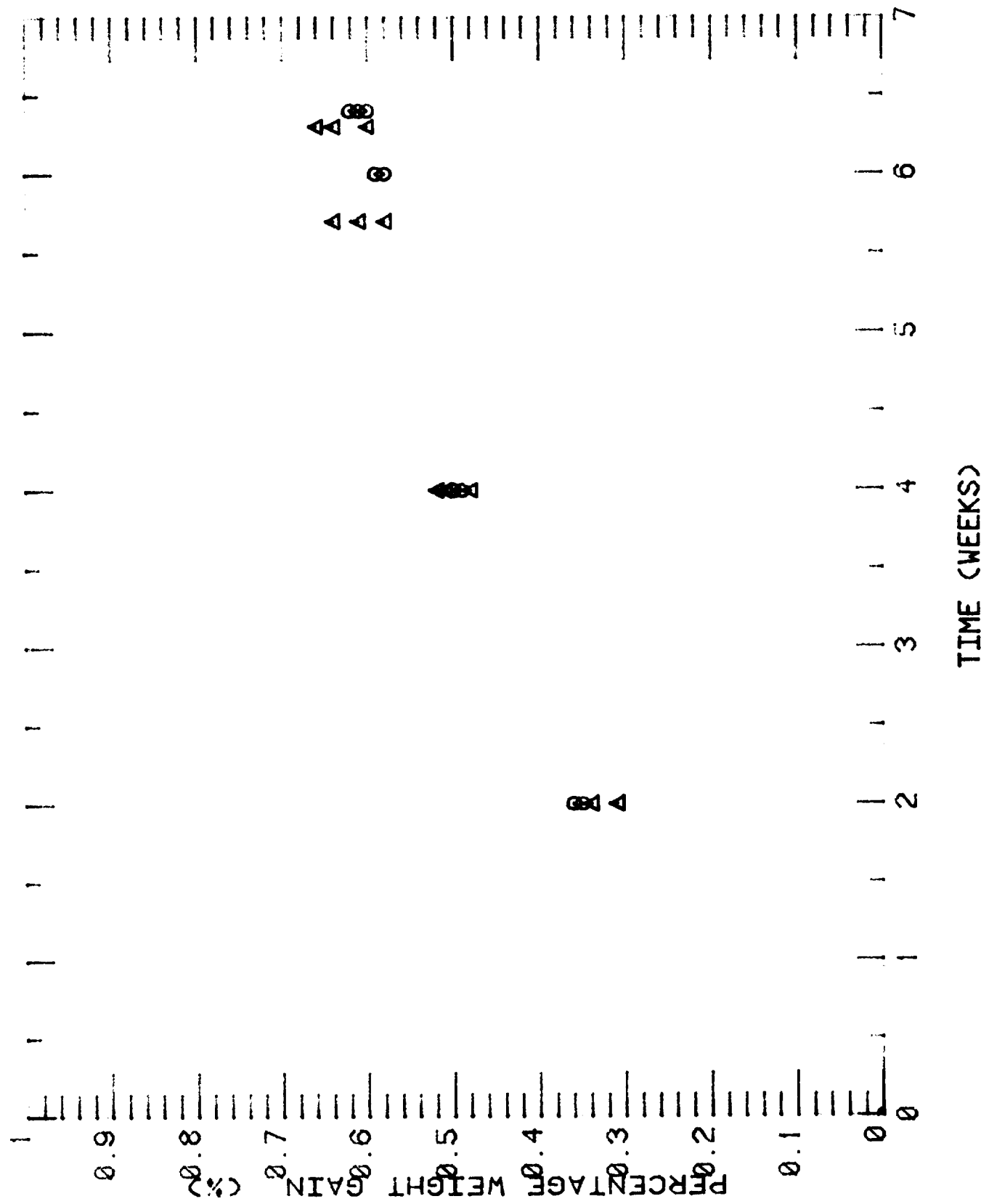


Figure 2-24: Compression Coupon

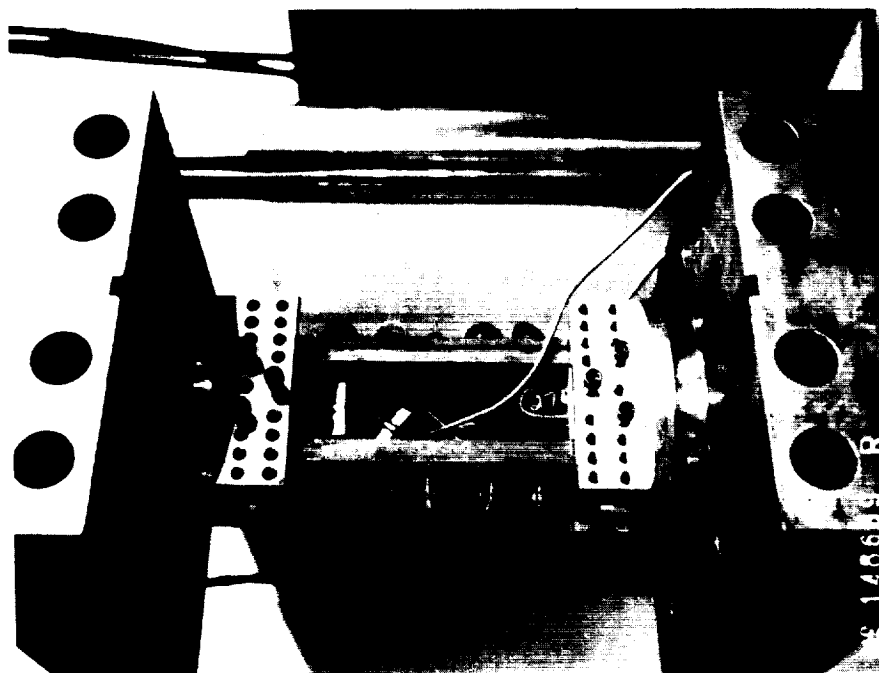
MOISTURE WEIGHT GAIN OF CELION/HX1504 AND CELION/5245



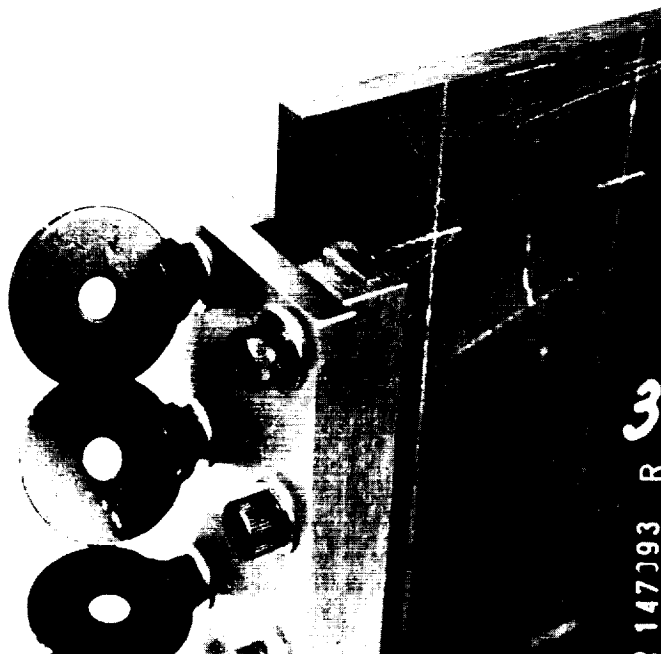
ORIGINAL PAGE IS
OF POOR QUALITY

TIME (WEEKS)

Figure 2-25 Percentage weight gain of Celion/HX1504 and Celion/5245 during immersion in 160°F water for 45 days. ○ Celion/5245, △ Celion/HX1504.



(a) Photo No. 148689



(b) Photo No. 147093

Figure 2-26: Compression test fixture: a) entire test fixture in test machine; b) side supports.

Tables 2.6 and 2.7 summarize the visible damage and damage area measurements resulting from the 20 and 30 ft-lb impacts. Close-up photos showing typical damage from these impacts are shown in Figures 2-15 and 2-16. The compression test results are summarized in Tables 2.8 and 2.9. Note that the reported failure strain value is the average of the back-to-back strain gage failure strains and that the failure stress is the gross stress for the notched coupons.

The unnotched 75⁰F dry failure strength and strain values for the Celion/HX1504 and Celion/5245 were 88 and 94 ksi, and 15600 and 16500 μ in/in, respectively. The most severe test condition was the 30 ft-lb impact, which reduced the failure strength values to 26 and 25 ksi, and the failure strain values to 4000 and 3700 μ in/in, respectively. The notched and unnotched, 75⁰F dry and 180⁰F wet Celion/5245 compression test values averaged 5 to 12% greater than the Celion/HX1504 values. However, while the Celion/HX1504 20 and 30 ft-lb damage areas were 13 to 18.5% greater than the corresponding Celion/5245 values, the Celion/HX1504 failure strengths were 3 to 4% greater than the Celion/5245 values. The relative effects of the various testing conditions on the failure strengths were fairly consistent from material to material. The unnotched room temperature strength decreased by around 38% with the notched room temperature tests, 16% with the notched 180⁰F wet conditioned test, 66% with the 20 ft-lb impacts, and 72% with the 30 ft-lb impacts. The percentage reductions for strain for the same conditions were a few percentage points higher than those mentioned for stress.

Typical failure modes for the unnotched compression tests conducted at room temperature are shown in Figure 2-27. The Celion/HX1504 180⁰F wet unnotched specimens had similar failure modes. The 1.00 inch hole diameter and 20 and 30 ft-lb impact specimens all had similar failure modes (Figures 2-28 and 2-29). The specimens failed across the width at the hole or impact sites and showed localized damage regions on the edges.

TABLE 2.6
IMPACT TEST RESULTS FOR HIGH STRAIN CELION/HX1504

Laminate Orientation: (45/0/-45/90) _{6s} Laminate Resin Content: 32.6% Laminate Thickness: 0.268						
Energy, ft-lbs	Location, ID	Ultrasonic Damage Measurements			Visual Indications	
		Width, in.	Length, in.	Area, in. ²	Front	Back
20	211-1A	2.12	2.18	3.55	Slight Dent	None
20	211-1B	2.14	2.20	3.45	Slight Dent	Slight Bulge
20	211-2A	2.18	2.10	3.55	Slight Dent	Slight Crack
30	211-2B	2.48	2.38	4.55	Small Dent	Slight Crack
30	211-3A	2.56	2.56	5.10	Small Dent	0.75" Delam.
30	211-3B	2.66	2.77	5.45	Small Dent	Slight Bulge

TABLE 2.7
IMPACT TEST RESULTS FOR HIGH STRAIN CELION/5245

Laminate Orientation: (45/0/-45/90) _{6s}						
Laminate Resin Content: 31.3%						
Laminate Thickness: 0.258						
Energy, ft-lbs	Location, ID	Ultrasonic Damage Measurements			Visual Indications	
		Width, in	Length, in.	Area, in. ²	Front	Back
20	248-1A	2.00	2.05	2.95	Small dent	Small lump
20	248-1B	2.00	2.02	2.95	Small dent	Small lump
20	248-2A	1.95	2.05	3.00	Small dent	None
30	248-2B	2.55	2.60	4.90	Small dent, broken fiber	0.25" Delam.
30	248-3A	2.45	2.40	4.35	Small dent	Small lump
30	248-3B	2.30	2.36	4.10	Small dent	Small lump

TABLE 2.8
HIGH STRAIN CELION/HX1504 COMPRESSION TEST DATA

Laminate Orientation: (45/0/-45/90)_{6s}
 Laminate Resin Content: Panel No. 210 Resin Content = 33.7%
 Panel No. 211 Resin Content = 32.6%

Coupon I.D.	Test Type and Cond.	Thickness (in.)	Width (in.)	Hole or Impact Area (in. ²)	Hole or Impact Width (in.)	Failure Load (Kips)	Failure Stress (Ksi)	Failure Strain (μ in/in)	Modulus (msi)
210-6	Unnotched at 75°F Dry	0.266	3.003	—	—	68.60	85.80	-15000	6.63
210-7		0.271	3.004	—	—	72.94	89.60	-15850	6.26
210-8		0.266	3.003	—	—	70.06	87.70	-15800	6.76
Avg						70.53	87.63	-15550	6.55
210-3	Notched at 75°F Dry	0.271	5.000	0.7853	1.00	47.56	36.0	-5609	6.46
210-4		0.271	5.002	0.7853	1.00	44.61	32.9	-5227	6.69
210-5		0.269	5.001	0.7853	1.00	44.34	33.0	-5190	6.32
Avg					1.00	45.50	33.97	-5342	6.49
210-9	Unnotched at 180°F Wet	0.273	3.003	—	—	52.34	63.84	-13816	6.83
210-10		0.273	3.002	—	—	59.57	72.68	-13337	6.71
210-11		0.267	3.000	—	—	63.20	78.80	-13604	6.89
Avg						58.37	71.77	-13586	6.81
211-1A	20 Ft-lb Impact at 75°F Dry	0.266	5.000	3.55	2.12	42.88	32.24	-4806	7.33
211-1B		0.268	4.999	3.45	2.14	40.69	30.37	-4658	6.53
211-2A		0.269	5.000	3.55	2.18	44.21	32.87	-5218	5.84
Avg				3.52	2.15	42.59	31.83	-4894	6.57
211-2B	30 Ft-lb Impact at 75°F Dry	0.270	5.000	4.55	2.48	36.10	26.74	-4181	6.18
211-3A		0.268	5.000	5.10	2.58	34.66	25.87	-3871	6.72
211-3B		0.269	5.000	5.45	2.66	34.71	25.81	-3964	6.54
Avg				5.03	2.57	35.16	26.14	-4005	6.48

TABLE 2.9
HIGH STRAIN CELION/5245 COMPRESSION TEST DATA

Laminate Orientation: (45/0/-45/90)6S Laminate Resin Content: Panel No. 243 Resin Content = 33.0%, Panel No. 248 Resin Content = 31.3%									
COUPON ID	TEST TYPE AND CONDITION	THICK (in.)	WIDTH (in.)	HOLE OR IMPACT AREA (in ²)	HOLE OR IMPACT WIDTH (in.)	FAILURE LOAD (kip)	FAILURE STRESS (ksi)	FAILURE STRAIN (μin/in)	MODULUS (Msi)
243-6 ^①	Unnotched 75°F Dry	0.268	2.995	—	—	-77.78	-96.82	-16930	6.60
243-7 ^①		0.266	2.995	—	—	-75.05	-94.31	-16840	6.69
243-8		0.267	2.995	—	—	-73.68	-92.03	-15737	6.72
Average		0.267	2.995			-75.50	-94.39	-16502	6.67
243-3	Open Hole at 75° Dry	0.263	5.000	0.78 ^②	1.00 ^②	-45.89	-34.85	-5292	6.64
243-4		0.265	4.999	0.78 ^②	1.00 ^②	-51.86	-39.13	-5800	6.58
243-5		0.266	5.000	0.78 ^②	1.00 ^②	-44.17	-33.16	-5154	6.55
Average		0.265	5.000	0.78	1.00	-47.31	-35.71	-5415	6.59
243-9	Unnotched at 180°F Wet	0.265	2.996	—	—	-67.40	-84.77	-14260 ^③	7.24
243-10		0.267	2.995	—	—	-66.75	-84.60	-13900	7.00
243-11		0.265	2.995	—	—	-57.33	-72.39	-11700	7.08
Average		0.266	2.995			-63.83	-80.59	-13270	7.11
248-1A	20 Ft-lb Impact at 75°F Dry	0.258	5.019	2.95	2.00	-39.36	-30.4	-4400	6.85
248-1B		0.258	5.021	2.95	2.00	-40.06	-30.9	-4400	6.94
248-2A		0.259	5.021	3.00	1.95	-39.70	-30.6	-4400	6.91
Average				2.97	1.98	-39.71	-30.6	-4400	6.90
248-2B	30 Ft-lb Impact at 75°F Dry	0.259	5.022	4.90	2.55	-32.81	-25.2	-3700	6.84
248-3A		0.258	5.022	4.35	2.45	-32.40	-25.0	-3600	6.83
248-3B		0.258	5.021	4.10	2.30	-33.09	-25.6	-3700	6.78
Average				4.45	2.43	-32.77	-25.3	-3700	6.82

① Specimen failed in the grip.

② Hole diameter was not recorded. A 1.00 in. diameter hole was assumed.

③ This value was measured by one of the strain gages, the other strain gage failed before the specimen failed.

ORIGINAL PAGE IS
OF POOR QUALITY

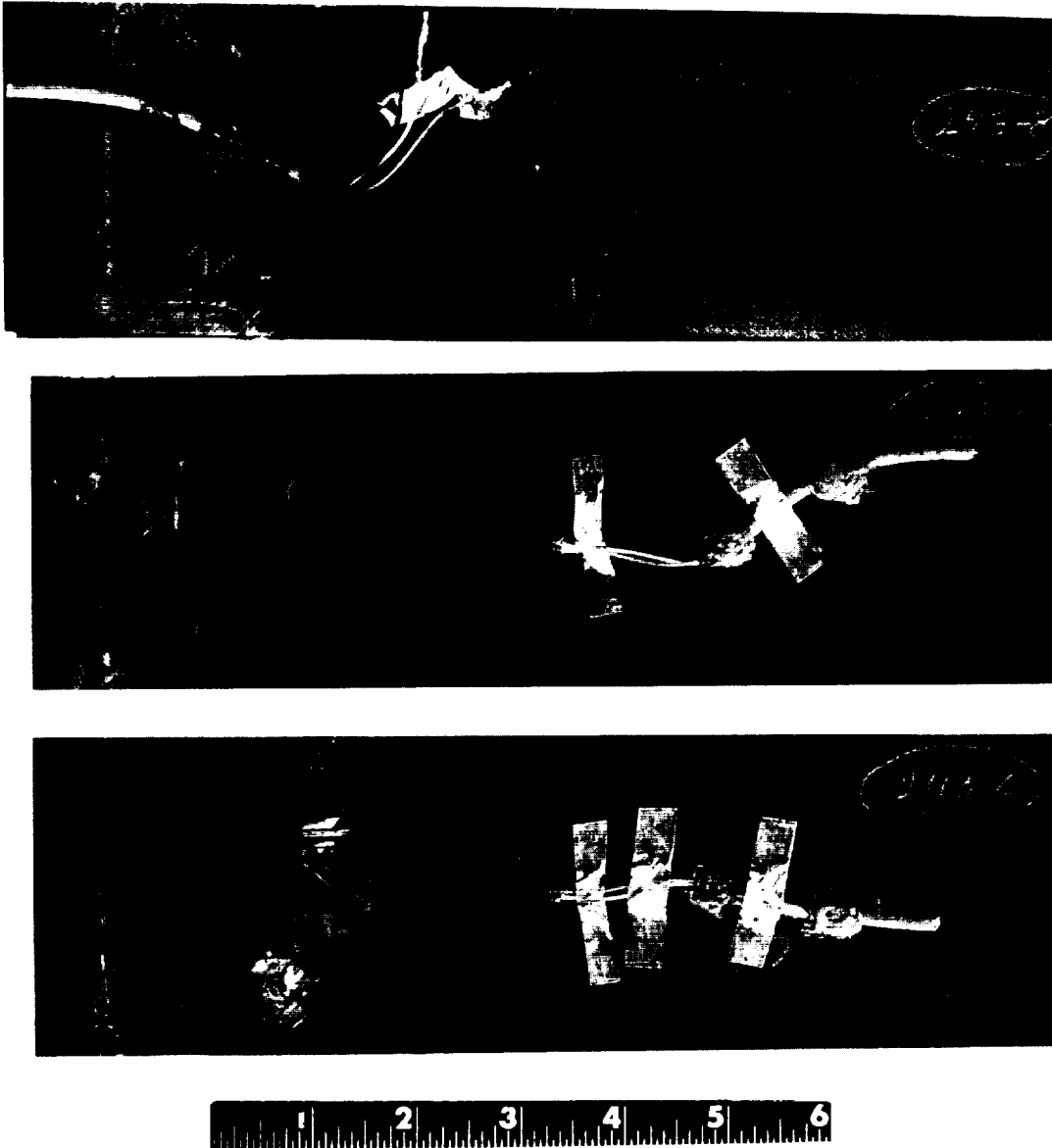


Photo No. 149895R

Figure 2-27a: Typical failures of unnotched compression specimens tested at room temperature: front view.

ORIGINAL PAGE IS
OF POOR QUALITY



Photo No. 149896

Figure 2-27b: Typical failures of unnotched compression specimens tested at room temperature: edge view.

UNCLASSIFIED
OF POOR QUALITY

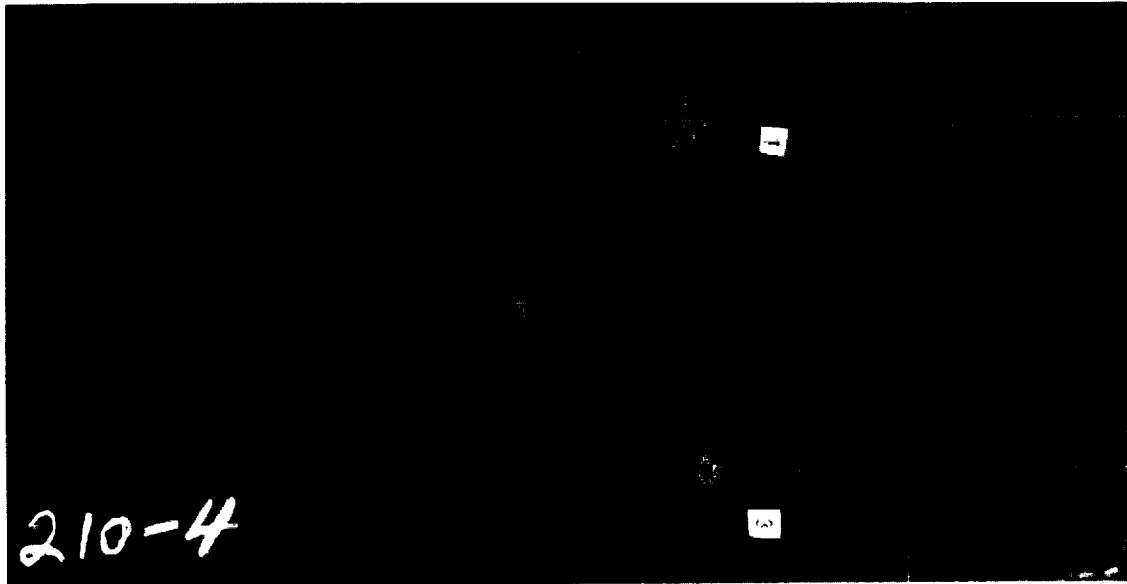


Photo No. 148004

(A)

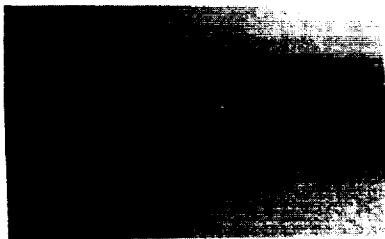


Photo No. 148009
210-3

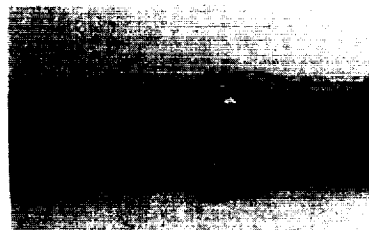


Photo No. 148005
210-4



Photo No. 148007
210-5

(B)

Figure 2-28: Typical failures of 1.00 in. diameter hole compression specimens.
a) front view, b) edge views.

Check for
OF POOR QUALITY

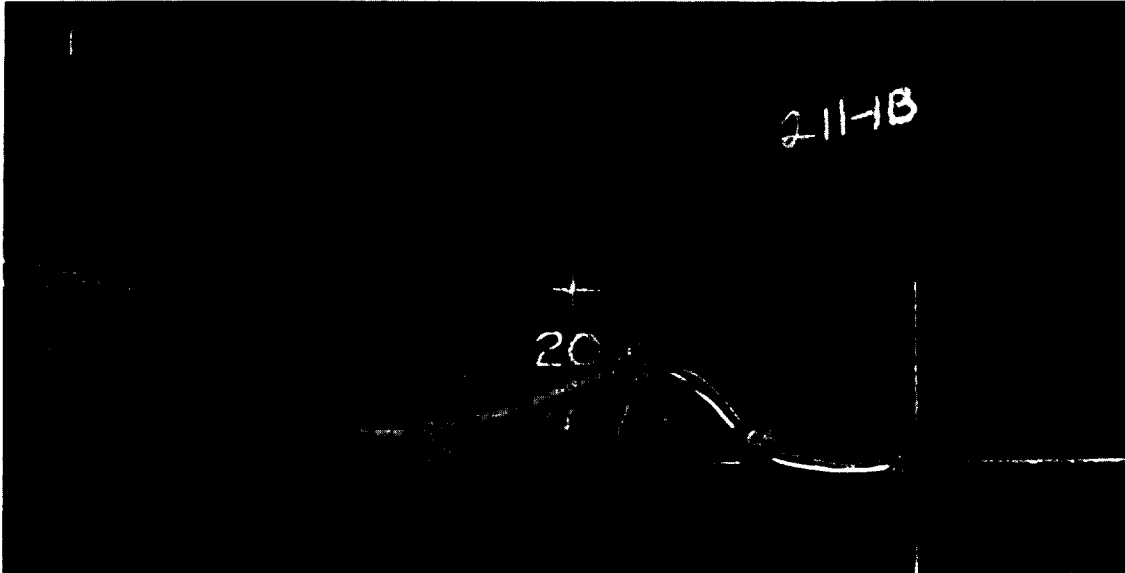


Photo No. 148148

(A)



Photo No. 148143
211-1A



Photo No. 148149
211-1B



Photo No. 148145
211-2A

(B)

Figure 2-29: Typical failures of compression specimens impacted at 20 ft-lbs:
a) front view, b) edge views through impact region. 30 ft-lb
impact failures were similar to those above.

2.4 QUASI-ISOTROPIC TENSION TESTS

Tension tests were conducted on 48-ply quasi-isotropic (45/0/-45/90)_{6s} laminates of Celion/HX1504 and Celion/5245. The test conditions were unnotched and notched room temperature dry, and notched or unnotched -65°F dry. The tension tests were conducted according to the procedures of NASA Standard Test "ST-3: Specification for Open-Hole Tension Test".

All the tension specimens had the configuration shown in Figure 2-30, except the Celion/HX1504 unnotched -65°F and 75°F dry tests, which had the configuration shown in Figure 2-31. These later test specimens were reconfigured because they were initially incorrectly machined. The notched specimens were tested in a 50 kip MTS machine and the unnotched specimens were tested in a 200 kip MTS machine. Both machines were equipped with 4.0 in. wide hydraulic grips (Figure 2-32). The specimens were tested at a 0.05 in./min. stroke rate. Lexan tabs were used instead of bonded tabs, and an 80-120 grit open mesh sanding cloth was put between the tabs and specimen to improve load transfer.

The test results are summarized in Tables 2-10 and 2-11. All of the Celion/HX1504 48-ply unnotched room temperature dry specimens failed or slipped in the grips. As a result, the 32-ply processability data is recorded in Table 2-10 for this condition. The unnotched and notched room temperature dry Celion/5245 values were greater than the Celion/HX1504 values by 15% for the failure strength, 9 to 13% for the failure strain, and 4% for the modulus. Unnotched 75°F dry Celion/5245 tension failures are shown in Figure 2-33. The 1.00 x 8.00 in. unnotched -65°F Celion/HX1504 failures were similar. Two of the three unnotched 75°F dry Celion/5245 specimens failed in the grips. Figure 2-34 shows notched specimen failures typical of Celion/HX1504 and Celion/5245.

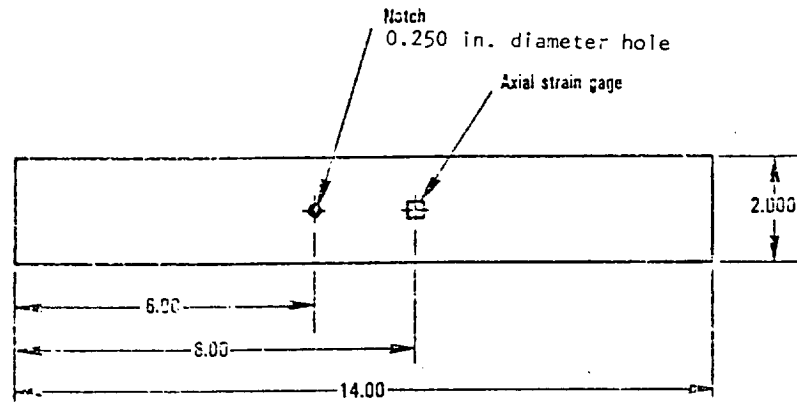


Figure 2-30: Inplane tension specimen geometry. Only notched specimens had hole.

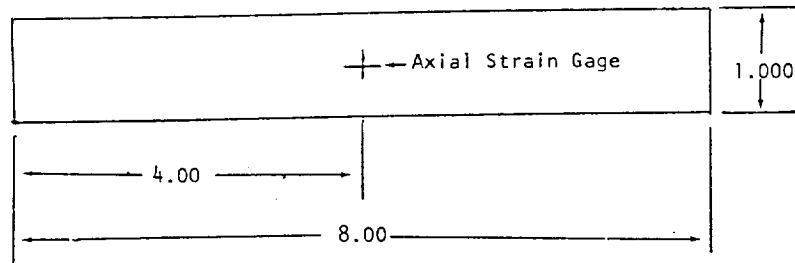


Figure 2-31: Inplane tension specimen geometry.

ORIGINAL PAGE IS
OF POOR QUALITY



Figure 2-32: Tension test set-up.

TABLE 2.10: HIGH STRAIN CELION/HX1504 QUASI-ISOTROPIC TENSION TEST DATA

Laminate Orientation: (45 0 -45 90)°S									
Laminate Resin Content: Panel #202 Resin Content = 32.0% Panel #211 Resin Content = 32.6%									
Coupon ID	Test Type and Condition	Thickness (in.)	Width (in.)	Impact Area (in. ²) or Hole Dia (in.)	Failure Load (kip)	Failure Stress (ksi)	Failure Strain (μ in/in)	Modulus (Msi)	
202 - 1	Unnotched at 75°F Dry	0.1829	(2)	-	(2)	98.3	14,300	6.90	
- 2		0.1867		-		104.1	14,700	7.10	
- 3		0.1790		-		80.0	10,600 (3)	7.50	
Average						94.13	13,200	7.17	
211 - 10	Open Hole at 75°F Dry	0.271	1.955	0.250	24.14 (4)	45.63	6,768	6.74	
- 11		-	-	-	- (5)	-	-	-	
- 12		0.268	2.003	0.250	31.95	59.50	8,398	7.19	
Average					28.045	52.57	7,583	6.965	
211 - 7	Unnotched at -65°F Dry	0.270	1.002	-	23.50	86.811	- (6)	- (6)	
- 8		0.271	1.002	-	23.84	87.71	13,490	5.60	
- 9		0.273	1.002	-	23.16	84.61	12,020	7.066	
Average					23.50	86.37	12,755	6.33	

① 32-ply laminate data. Reference Periodic Technical Progress Report No. 21, June 1983.

② Data not available.

③ Slipped in grip.

④ Specimen slipped in grip, damaged strain gage wiring. Repaired and loaded to failure. Specimen may have been damaged.

⑤ Computer malfunction - lost data.

⑥ Strain gage malfunction.

TABLE 2.11 HIGH STRAIN CELION/5245 QUASI-ISOTROPIC TENSION TEST DATA

Laminate Orientation: (45/0/- 45/90) _{6S}								
Laminate Resin Content: 31.3%								
Coupon ID	Test Type and Condition	Thickness (in.)	Width (in.)	Notch Dia.(in.)	Failure Load (kip)	Failure Stress (ksi)	Failure Strain (μ in./in.)	Modulus (Msi)
248-10 ^①	Unnotched at 75°F Dry	0.259	2.014	—	55.64	106.7	14600	7.33
248-11 ^①		0.257	1.998	—	56.01	109.0	14800	7.67
148-12		0.257	2.007	—	57.52	111.7	15300	7.42
Average					56.39	109.1	14900	7.47
248-4	Notched at 75°F Dry	0.258	2.006	0.250	31.71	61.26	8200	7.42
248-5		0.260	2.009	0.250	31.56	61.42	8600	6.92
248-6		0.255	2.004	0.250	30.89	60.47	8000	7.50
Average					31.39	61.05	8300	7.28
248-7	Notched at -65°F Dry	0.257	2.006	0.250	30.10	58.38	7600	7.47
248-8		0.256	2.004	0.251	30.23	58.93	7700	7.47
248-9		0.257	2.012	0.252	30.05	58.02	7600	7.53
Average					30.13	58.44	7600	7.49

① Specimen failed at grips.

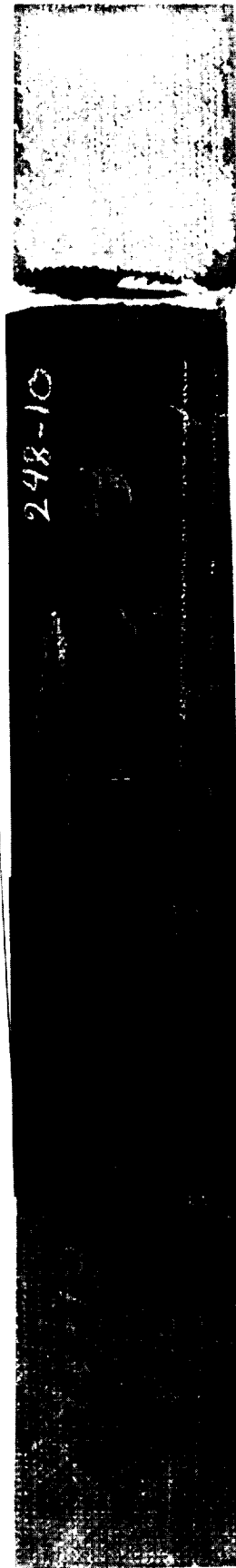


Photo No. 149894

Figure 2-33: Typical failures of unnotched tension tests.

ORIGINAL PAGE IS
OF POOR QUALITY

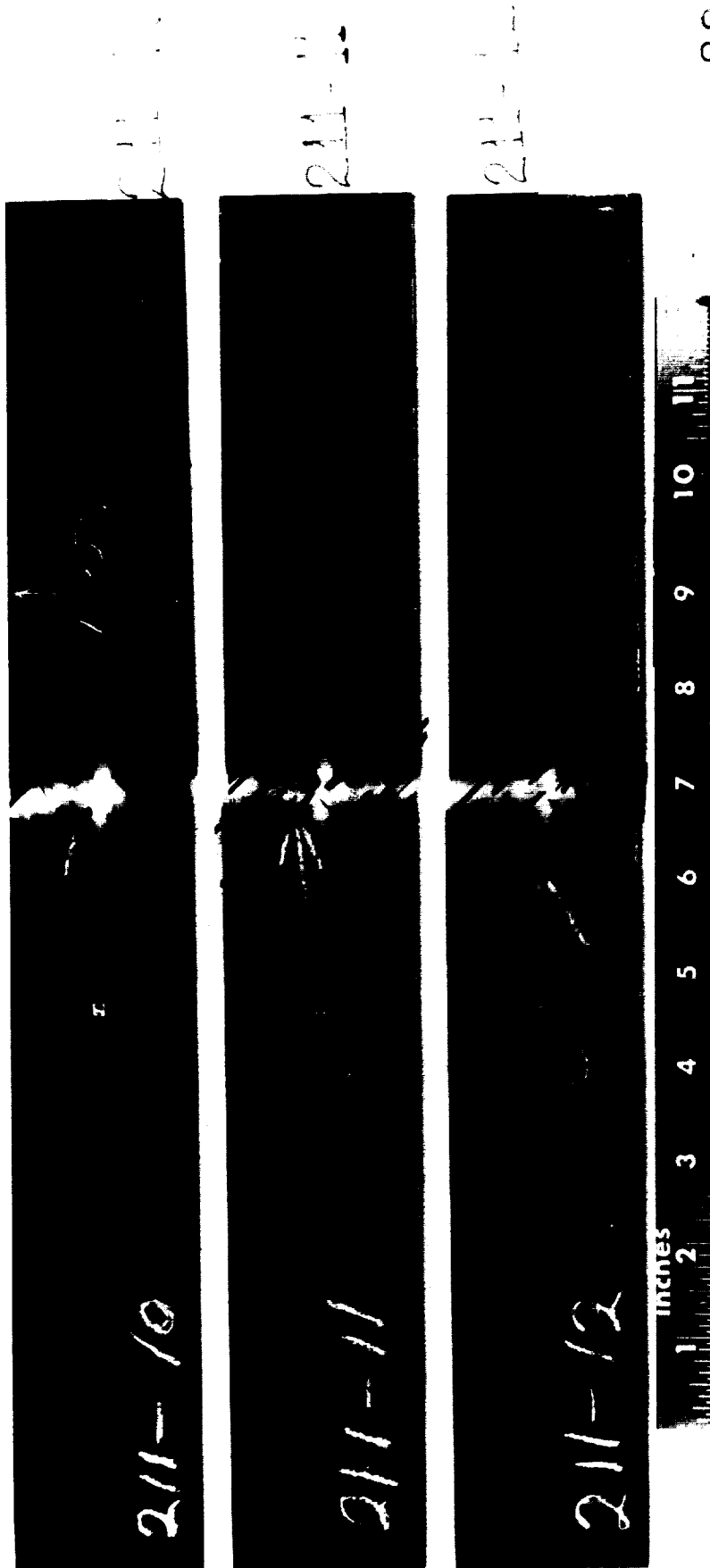


Photo No. 147906

Figure 2-34: Typical failure of notched tension tests.

2.5 0° TENSION TESTS

Tension tests were performed on 12-ply 0° laminates of Celion/HX1504 and Celion/5245. The specimens had the geometry shown in Figure 2-35 with one T type strain gage for recording axial and transverse strain to failure. Fiberglass tabs were bonded to the specimen grip ends. Tests were run in an MTS machine with hydraulic grips at a loading rate of 0.05 in./min. Typical failed specimens are shown in Figure 2-36. Test results are summarized in Tables 2-12 and 2-13. The Celion/HX1504 failure stress and strain values were on the average 9% greater than the Celion/5245 values.

2.6 90° TENSION

Unidirectional 0°, 12-ply high strain Celion/HX1504 and high strain Celion/5245 laminates were fabricated into 90° sandwich beam specimens shown in Figure 2-37. The graphite/epoxy laminates were bonded to an aluminum honeycomb core with an opposite face sheet of 12-ply fiberglass per Lockheed Drawing TL1031-5. Cross sectional dimensions of the beams are listed in Table 2-14. A single axial strain gage was mounted on the specimen center line of the graphite/epoxy side.

Specimens were loaded in a four point bending fixture with the graphite/epoxy laminate on the lower tension surface of the beam, Figure 2-38. The loading rate was 0.05 in./min. Valid specimen failures were considered to be those that occurred within the center 4 inches between the center supports. For those failures the laminate broke sharply in two, with no core crushing occurring (Figure 2-39). Some specimens did fail outside of that region towards the ends of the specimens and exhibited core crushing. These failures were considered invalid for the 90° tension test.

Test data are summarized in Tables 2-15 and 2-16. The average Celion/HX1504 values were greater than the Celion/5245 values by 36% for the failure stress, 27% for the failure strain, and 9% for the modulus.

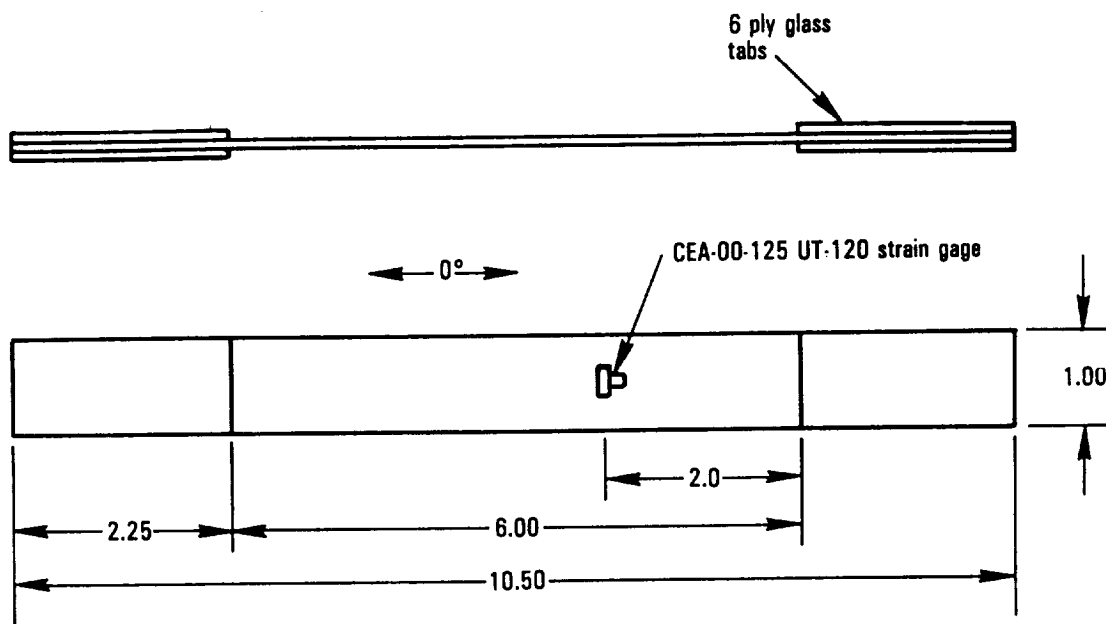
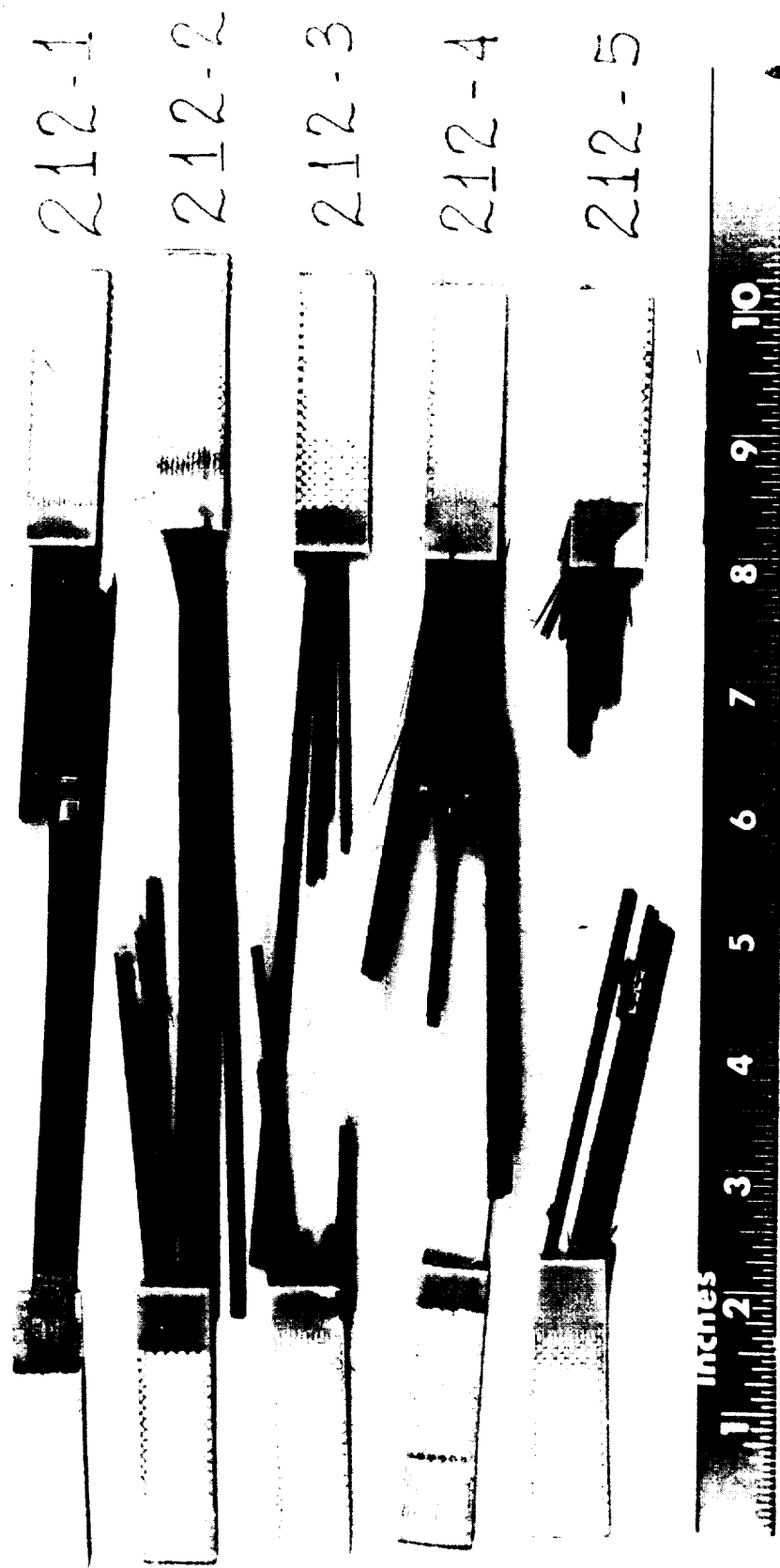


Figure 2-35: $+45^{\circ}$ and 0° Tensile Test Specimen Geometry
All dimensions are in inches.



GROUP 2: FAILURE
OF POOR QUALITY

Photo No. 147909

Figure 2-36: Typical failures of 0° tension tests.

TABLE 2.12: HIGH STRAIN CELION/HX1504 0° TENSION TEST DATA

Laminete Orientation: 0 ₁₂ Laminete Resin Content: 28.4% Test Condition: 75°F Dry							
Coupon ID	Thick. (in.)	Width (in.)	Failure Load (kips)	Failure Stress (ksi)	Failure Strain (μin/in)	Modulus (Msi)	Poisson's Ratio
212 - 2	0.068	0.502	10.41	305.0	14,820	18.33	0.256
212 - 3	0.066	0.502	10.56	319.0	15,200	19.33	0.288
212 - 4	0.066	0.502	11.02	334.9	15,690	19.17	0.281
212 - 5	0.064	0.502	<u>10.91</u>	<u>339.6</u>	<u>15,770</u>	<u>19.17</u>	<u>0.305</u>
Average ①			10.73	324.63	15,370	19.00	0.283

① No data recorded for specimen 212-1 because initial load scale was not set high enough.

TABLE 2.13: HIGH STRAIN CELION/5245 0° TENSION TEST DATA

Laminete Orientation: 0 ₁₂ Laminete Resin Content: 31.2% Test Condition: 75°F Dry							
Coupon ID	Thick (in.)	Width (in.)	Failure Load (kips)	Failure Stress (ksi)	Failure Strain (μin./in.)	Modulus (Msi)	Poisson's Ratio
245-2	0.072	0.506	10.56	291.0	13200	19.74	0.274
245-3	0.072	0.506	11.25	311.1	14700	19.61	0.284
245-4	0.070	0.506	10.57	292.4	14400	18.99	0.299
245-5	0.068	0.506	<u>10.00</u>	<u>288.6</u>	<u>14700</u>	<u>18.52</u>	<u>0.269</u>
Average ①			10.59	295.8	14200	19.22	0.282

① No data recorded for specimen 245-1 because high grip pressure caused failure.

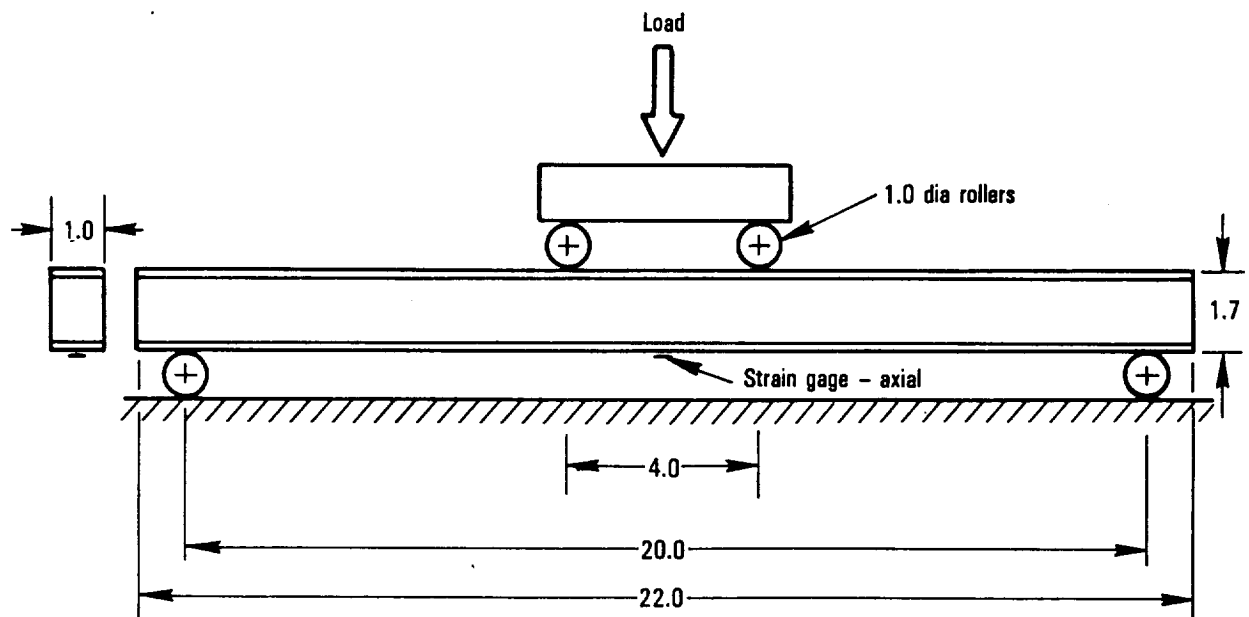


Figure 2-37: 90° Tension Test Setup Geometry. All Dimensions in Inches

TABLE 2.14 SANDWICH BEAM GEOMETRY

Specimen ID	$T_{G/E}$ (in.)	T_{FG} (in.)	T_o (in.)
213-1	0.114	0.112	1.732
213-2	0.109	0.114	1.720
213-3	0.110	0.115	1.723
213-4	0.108	0.115	1.728
213-5	0.107	0.114	1.717
233-1	0.115	0.120	1.740
233-2	0.116	0.126	1.740
233-3	0.110	0.128	1.739
233-4	0.115	0.128	1.738
233-5	0.113	0.128	1.738

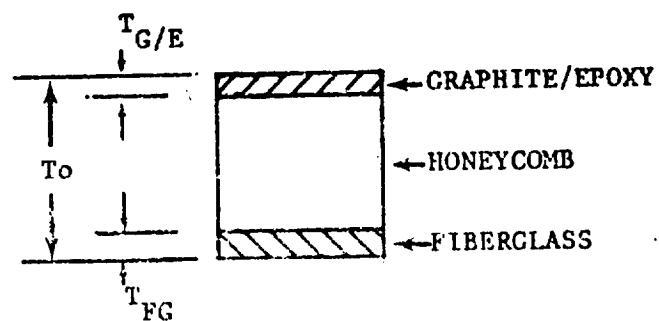
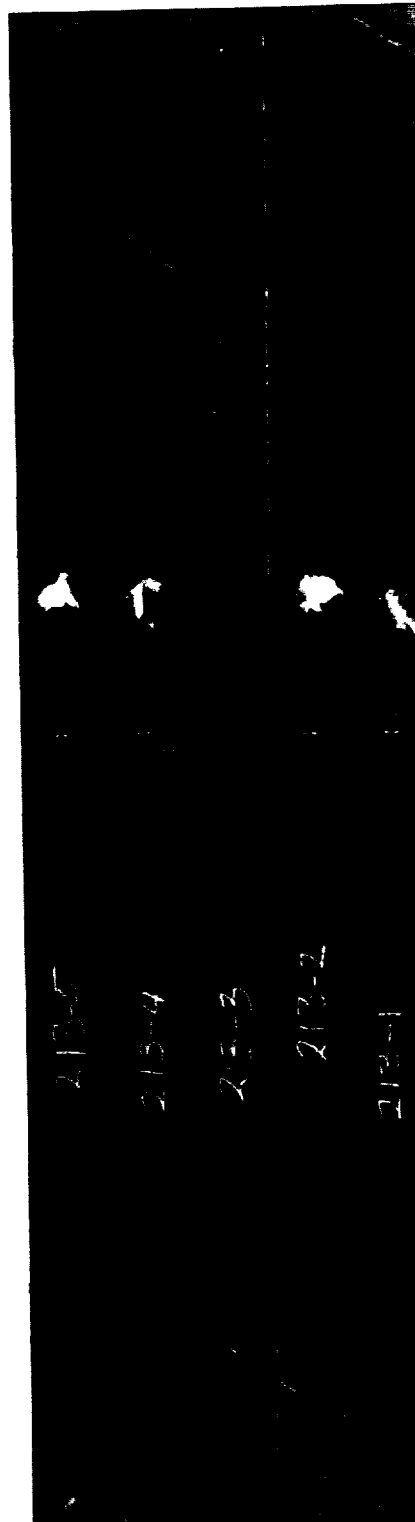


Photo No. 146179

Figure 2-38: 90° Tension Test Setup. Graphite/Epoxy Sheet is on the Bottom Surface of the Sandwich Beam.

4



4

Photo No. 148043R

ORIGINAL PAGE IS
OF POOR QUALITY

Figure 2-39: Typical failures of 90° sandwich beam tests.

TABLE 2.5 HIGH STRAIN CELION/HX1504 90° TENSION TEST DATA

Laminate Orientation: 90° ₁₂ Laminate Resin Content: 31.7% Test Condition: 75°F Dry						
Coupon ID	Thick. T G/E (in.)	Width G/E (in.)	Failure Load (lb)	Failure Stress (ksi)	Strain (μ in/in)	Modulus (Msi)
213 - 1	0.114	0.972	520	12.11	9366	1.29
- 2	0.109	1.000	535	13.11	9791	1.34
- 3	0.110	1.007	532	12.91	9789	1.32
- 4	0.108	1.010	519	12.77	9264	1.38
- 5	0.107	1.015	<u>477</u>	<u>11.92</u>	<u>8499</u>	<u>1.40</u>
Average			517	12.56	9342	1.35

TABLE 2.16 HIGH STRAIN CELION/5245 90° TENSION DATA

Laminate Orientation: 90° ₂₀ Laminate Resin Content: 29.6% Test Condition: 75°F Dry						
Coupon ID	Thick. T _{G/E} (in.)	Width G/E (in.)	Failure Load (lb)	Failure Stress (ksi)	Strain (μin./in.)	Modulus (Msi)
233-1	0.115	1.000	394	8.44	6600	1.28
233-2	0.116	0.999	471	10.04	8300	1.21
233-3 ①	0.110	0.999	152	3.42	2600	0.90
233-4 ②	0.115	0.995	498	10.77	8800	1.22
233-5 ③	0.113	0.995	314	6.91	5500	1.26
Average ④			432	9.24	7400	1.24

- ① Specimen failed in center test section. Value very anomalous with respect to other values for no apparent reason.
- ② Specimen failed at bottom support.
- ③ Specimen failed 2.5 in. inboard from bottom support.
- ④ Average values do not include values from specimens 233-3, 233-4 and 233-5.

2.7 + 45° TENSILE TESTS

Tensile tests were performed on 12-ply ($+45^{\circ}$)_{3S} laminates of Celion/HX1504 and Celion/5245. The test specimen geometry and T strain gage location for transverse and longitudinal strain monitoring are shown in Figure 2-35. Lexan was used as tab material and the specimen was tested in a 50 kip MTS machine with hydraulic grips at a 0.05 in./min. stroke rate. Characteristic failures are shown in Figure 2-40. The results are summarized in Tables 2-17 and 2-18. The tensile and shear failure stresses of Celion/HX1504 were 10% greater than those of Celion/5245. The other values did not differ significantly between the two materials.

Strain to failure data were not presented due to the high strain levels reached prior to failure. A trade-off in computer data taking rate versus the total data capacity led to terminating strain recording beyond 40,000 in/in in order to improve data resolution of the lower part of the stress-strain curve which contains the primary data of interest.

2.8 EDGE DELAMINATION TENSION TESTS

Tensile tests were conducted on Celion/HX1504 and Celion/5245 per NASA Standard Test "ST-2 Specification for Edge Delamination Tension Test". Two layups were tested: an 8-ply ($+35/0/90$)_S layup and an 11-ply ($+30_2/90/90$)_S layup. Ten specimens of each type were made, five of which were tested and five sent to NASA untested. After testing the five in our laboratory, these were also sent to NASA for post test analysis. For each five specimens, only two were tested to failure, except for the Celion/HX1504 $+30^{\circ}$ specimens, none of which were tested to failure.

TABLE 2.17: HIGH STRAIN CELION/HX1504 $\pm 45^\circ$ TENSION TEST DATA

Laminate Orientation: $(\pm 45^\circ)_3S$ Laminate Resin Content: 30.5% Test Condition: 75°F Dry								
Coupon ID	Thick. (in.)	Width (in.)	Failure Load (lb)	Tensile Failure Stress (ksi)	Tensile Modulus (Msi)	Shear Failure Stress (ksi)	Shear Modulus (Msi)	Poisson's Ratio
214 - 1	.070	1.000	2832	40.45	3.33	20.23	0.84	0.89
214 - 2	.073	0.999	3006	41.46	2.77	20.73	0.78	0.95
214 - 3	.073	0.999	2831	38.72	2.66	19.36	0.75	0.71
214 - 4	.073	1.000	2973	41.01	2.80	20.51	0.83	0.77
214 - 5	.073	1.000	2903	40.04	2.67	20.02	0.83	0.70
Average	.0724	0.9996	2909	40.34	2.85	20.17	0.81	0.76

TABLE 2.18: HIGH STRAIN CELION/5245 $\pm 45^\circ$ TENSION TEST DATA

Laminate Orientation: $(\pm 45^\circ)_3S$ Laminate Resin Content: 33.0 Test Condition: 75°F Dry								
Coupon ID	Thick. (in.)	Width (in.)	Failure Load (lb)	Tensile Failure Stress (ksi)	Tensile Modulus (Msi)	Shear Failure Stress (ksi)	Shear Modulus (Msi)	Poisson's Ratio ①
239-1	0.068	0.999	2421	35.64	2.66	17.82	0.73	0.85
239-2	0.068	0.999	2461	36.23	2.63	18.12	0.76	0.76
239-3	0.067	0.999	2434	36.36	2.67	18.18	0.74	0.82
239-4	0.067	0.999	2519	37.63	2.66	18.82	0.78	0.75
239-5	0.067	0.999	2482	37.08	2.65	18.54	0.73	0.81
Average	0.067	0.999	2463	36.59	2.65	18.30	0.75	0.80
① Calculated at 10.00 ksi								

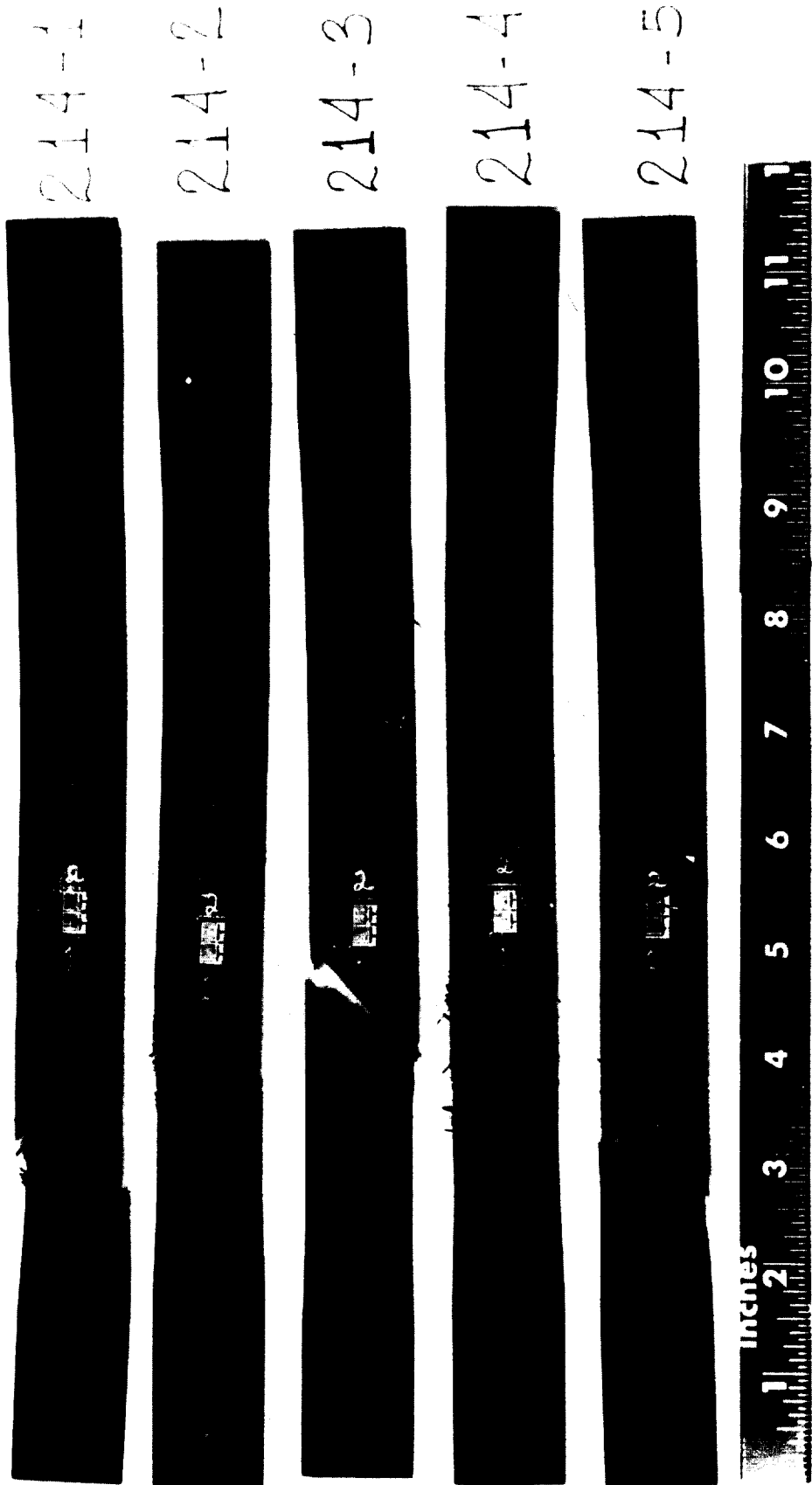


Photo No. 147907R

Figure 2-40: Typical $+45^\circ$ tension test failures.

The specimen configuration is shown in Figure 2-40. Small aluminum tabs were bonded onto the specimen four inches apart and an extensometer was attached to the specimen (Figure 2-41). An extension on the extensometer enabled the 4 inch gage length. Figure 2-42 shows a close up view of the extensometer knife edge biting into the small aluminum tabs and the clamp securing the extensometer.

An X-Y recorder at the test site plotted the load versus extension data. The test was performed in a 50 kip MTS test machine at a stroke rate of 0.00008 in./sec (0.002 mm/sec). The objective was to find the onset of edge delamination. In most cases, the test was then terminated. The onset of delamination was detected by an audible cracking noise. Just past that point, the load was held constant and the specimen edges were examined to verify the initiation of delamination. The X-Y curve was checked for any deviation of the curve from a straight line. Delamination initiation was marked on the load/extension plot. In addition, load/strain data were taken by the computer.

The results are summarized in Tables 2-19, 2-20, 2-21, and 2-22. Note that the load/deflection or load/strain curves were linear until the initiation of delamination for the 8 and 11 ply layups of both materials. Therefore, no secant moduli were reported. The interlaminar fracture toughness of the 8-ply Celion/5245 laminate was 29% greater than that for Celion/HX1504. The interlaminar fracture toughness of the 11-ply Celion/5245 laminate was 75% greater than that for Celion/HX1504. Figures 2-43 and 2-44 show the edges of 8 and 11 ply Celion/5245 specimens.

2.9 DOUBLE CANTILEVER BEAM (DCB) TESTS

Double cantilever beam tests were conducted to determine the fracture toughness of Celion/5245. The tests were performed according to NASA Standard Test "ST-5: Specification for Hinged Double Cantilever Beam Test",

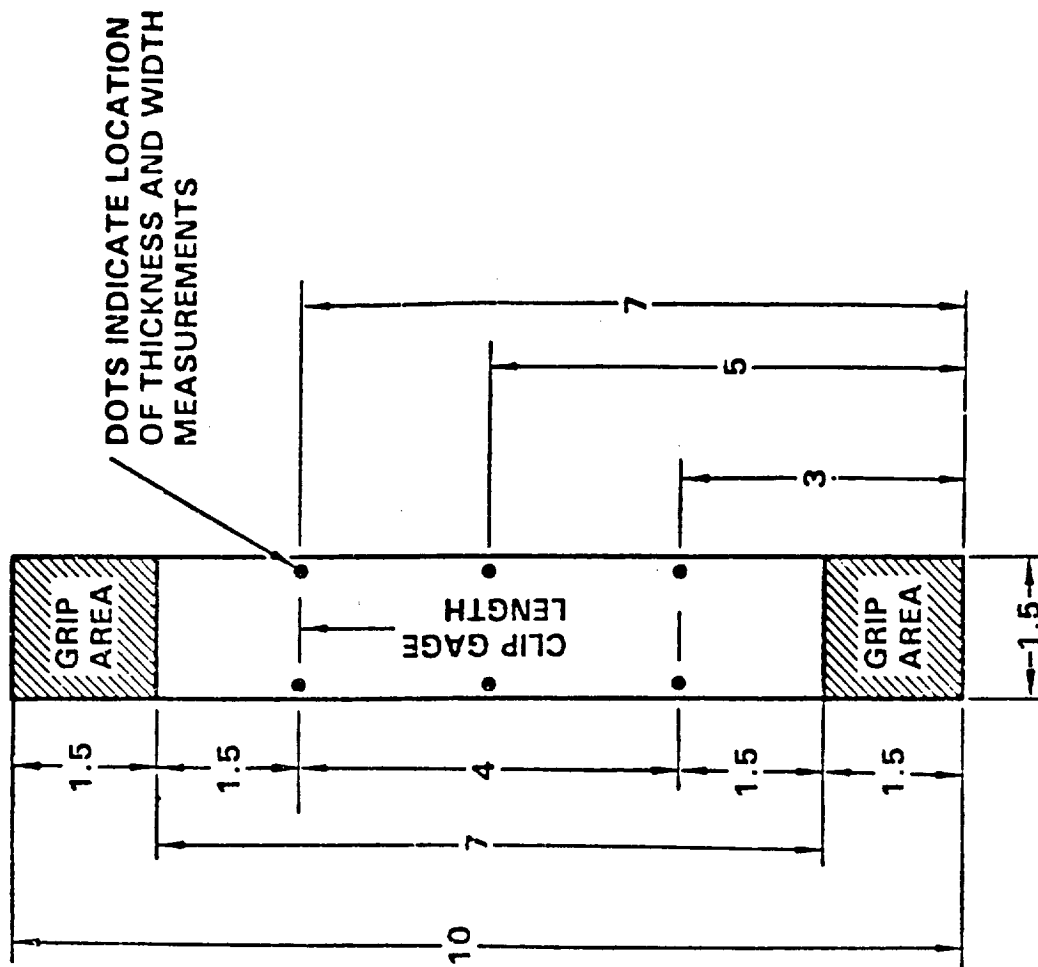
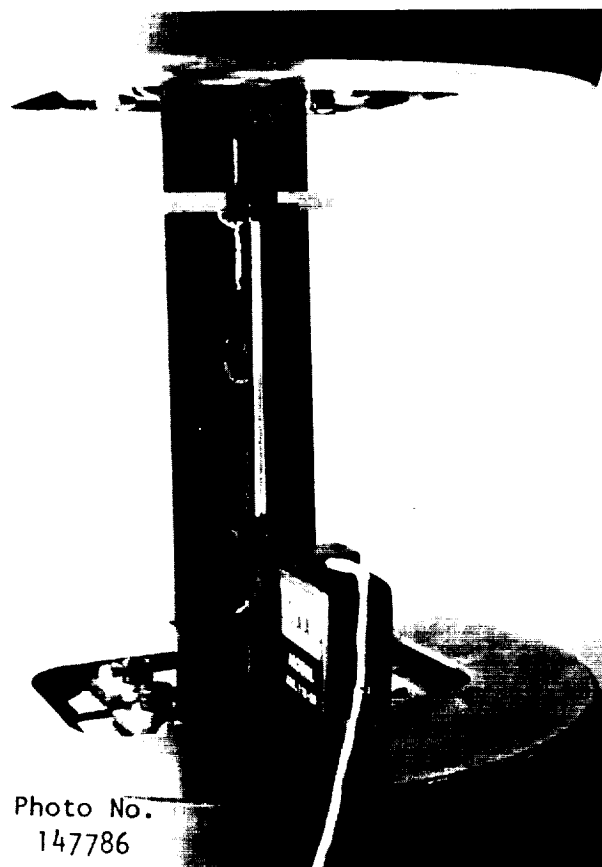


Figure 2-41: Edge Delamination Tension Test Specimen (Dimension Are In Inches).



ORIGINAL PAGE IS
OF POOR QUALITY

Photo No.
147786

Figure 2-42a: Edge delamination test specimen in test machine with extensometer attached.



148586

Figure 2-42b: Close-up of extensometer attachment to edge delamination specimen. Note extensometer knife edge bites into aluminum tab which is epoxied to specimen.

TABLE 2.19: 8 PLY HIGH STRAIN CELION/HX1504 EDGE DELAMINATION TEST DATA

Laminate Orientation: $(\pm 30_2 / 90 / 90)_S$ Laminate Resin Content: 30.6% Test Condition: 75°F, Dry						
Coupon ID	Thick. (in.)	Width (in.)	Delam. Onset Strain ($\mu\text{in/in}$)	Failure Strain ($\mu\text{in/in}$)	Tensile Modulus (Msi)	Interlaminar Fracture Toughness, G_c (lb/in)
215 - 1	0.061	1.505	4438	Specimens	7.38	1.425
215 - 2	0.063	1.505	4850	not Tested to	7.40	1.716
215 - 3	0.063	1.505	4662	Failure	7.32	1.532
215 - 4	0.062	1.506	4725		7.28	1.546
215 - 5	0.062	1.506	<u>4588</u>		<u>7.56</u>	<u>1.641</u>
Average			4653		7.39	1.572

TABLE 2.20: 11 PLY HIGH STRAIN CELION/HX1505 EDGE DELAMINATION TEST DATA

Laminate Orientation: $(\pm 35 / 0 / 90)_S$ Laminate Resin Content: 31.7% Test Condition: 75°F, Dry						
Coupon ID	Thick. (in.)	Width (in.)	Delam. Onset Strain ($\mu\text{in/in}$)	Failure Strain ($\mu\text{in/in}$)	Tensile Modulus (Msi)	Interlaminar Fracture Toughness, G_c (lb/in)
216 - 1	0.046	1.505	6075	①	8.70	1.071
216 - 2	0.046	1.505	5600	①	8.85	1.020
216 - 3	0.046	1.504	5775	①	8.81	1.054
216 - 5	0.046	1.505	6450	13,388	8.18	0.701
216 - 11	0.046	1.506	<u>5900</u>	<u>14,207</u>	<u>8.65</u>	<u>0.969</u>
Average			5960	13,798	8.64	0.963

① Specimen not tested to failure.

TABLE 2.21
8-PLY HIGH STRAIN CELION/5245
EDGE DELAMINATION TEST

Laminate Orientation: $(\pm 35/0/90)_S$ Laminate Resin Content: 28.3% Test Condition: 75°F, Dry						
Coupon ID	Thick (in.)	Width (in.)	Delam. Onset Strain ($\mu\text{in./in.}$)	Failure Strain ($\mu\text{in./in.}$)	Tensile Modulus (Msi)	Interlaminar Fracture Toughness G_c (lb/in.)
247-1	0.0436	1.503	6200	①	9.42	1.25
247-4	0.0431	1.507	6000	①	9.34	1.23
247-5	0.0434	1.507	6400	①	9.37	1.24
247-2	0.0432	1.500	6200	13800	9.17	1.24
247-3	0.0431	1.505	6200	13700	9.19	1.23
Average	0.0433	1.504	6200	13800	9.30	1.24

① Specimen not tested to failure.

TABLE 2.22
11-PLY HIGH STRAIN CELION/5245
EDGE DELAMINATION TEST

Laminate Orientation: $(\pm 30_2/90/90)_S$ Laminate Resin Content: 29.1% Test Condition: 75°F, Dry						
Coupon ID	Thick (in.)	Width (in.)	Delam. Onset Strain ($\mu\text{in./in.}$)	Failure Strain ($\mu\text{in./in.}$)	Tensile Modulus (Msi)	Interlaminar Fracture Toughness G_c (lb/in.)
246-3	0.060	1.508	6200	①	7.45	2.84
246-4	0.060	1.507	5900	①	7.60	2.57
246-5	0.060	1.506	6400	①	7.33	3.02
246-1	0.060	1.508	6000	17800	7.63	2.66
246-2	0.060	1.508	6000	20700	7.63	2.66
Average	0.060	1.507	6100	19200	7.53	2.75

① Specimen not tested to failure.

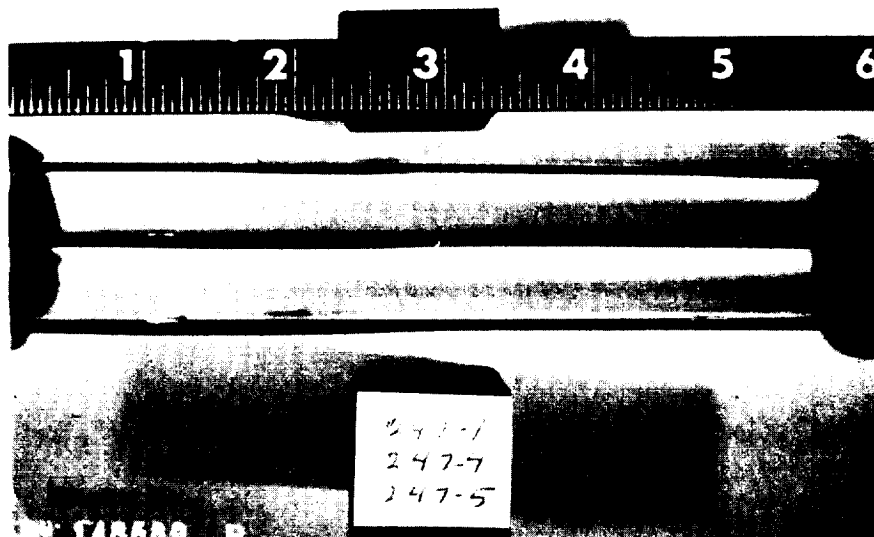


Figure 2-43: Edge of 8-ply, $\pm 35^{\circ}$ Celion/5245 edge delamination specimens.

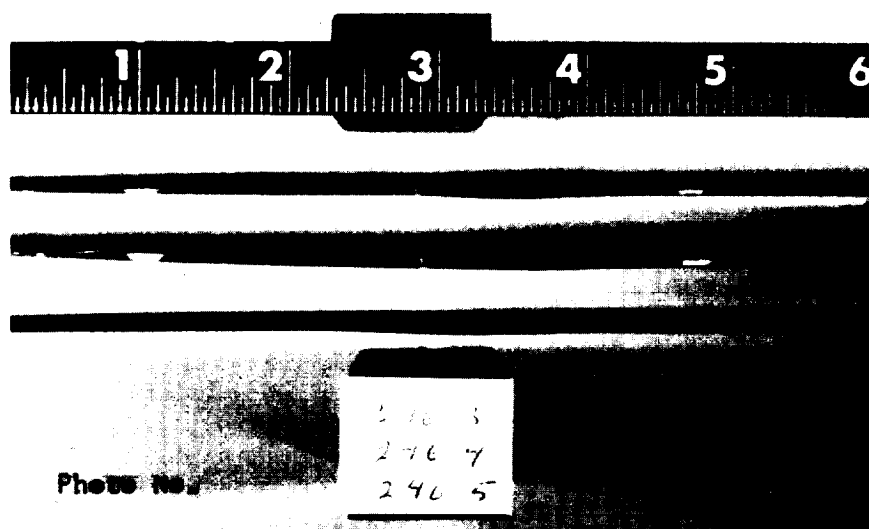


Figure 2-44: Edges of 11-ply, $\pm 30^{\circ}$ Celion/5245 edge delamination specimens.

presented in the revised edition of the NASA Reference Publication 1092, Standard Tests for Toughened Resin Composites, 1983.

The 24-ply, all 0^0 ply specimens were configured as shown in Figures 2-45 and 2-46. A 1.0 mil thick Teflon sheet insert was placed between the center plies to act as a crack starter in the beam. The piano hinges attached to the specimens were pin loaded with clevises. The specimens were tested in an MTS machine with the load applied at a rate of 0.05 in./min (Figure 2-47). Load/deflection (stroke) curves were recorded on an X-Y plotter for the deflection at the load line. Crack lengths were measured from the load line on both sides of the specimen with a dial gage and microscope while the specimen was held under load.

The specimen was loaded until the initial crack length was 2 in. Then the stroke (deflection) was held constant while the location on the load/deflection plot was marked and the crack lengths were measured. This procedure was repeated at 1 in. intervals until the total crack length was 6 in.

The strain energy release rate, G_{IC} , was calculated by two methods. The modified direct beam equation method is detailed in NASA ST-5. The final expression for the modified direct beam equation is

$$G_{IC} = \frac{P \delta}{2ab} \frac{(3a - 4a_0)}{a - a_0},$$

where

G_{IC} = Critical strain energy release rate

P = Load

δ = Deflection

a = Crack length

b = Width of beam

a_0 = Constant used for curve fit, defined in detail in NASA ST-5

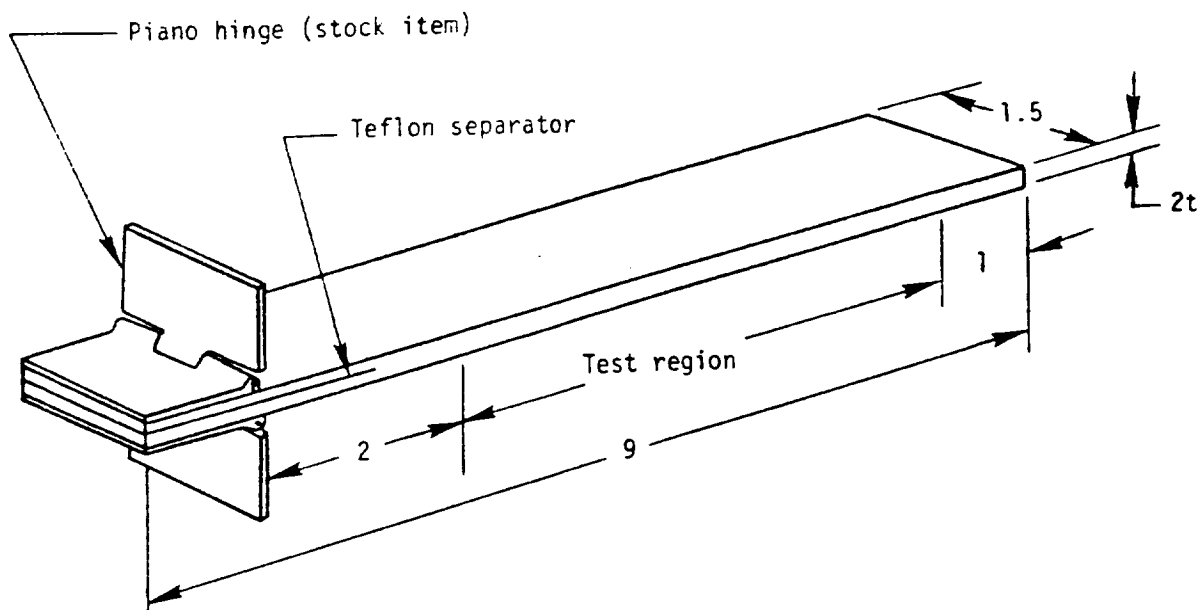


Figure 2-45: Hinged double cantilever beam (HDCB) specimen.
Dimensions are in inches.

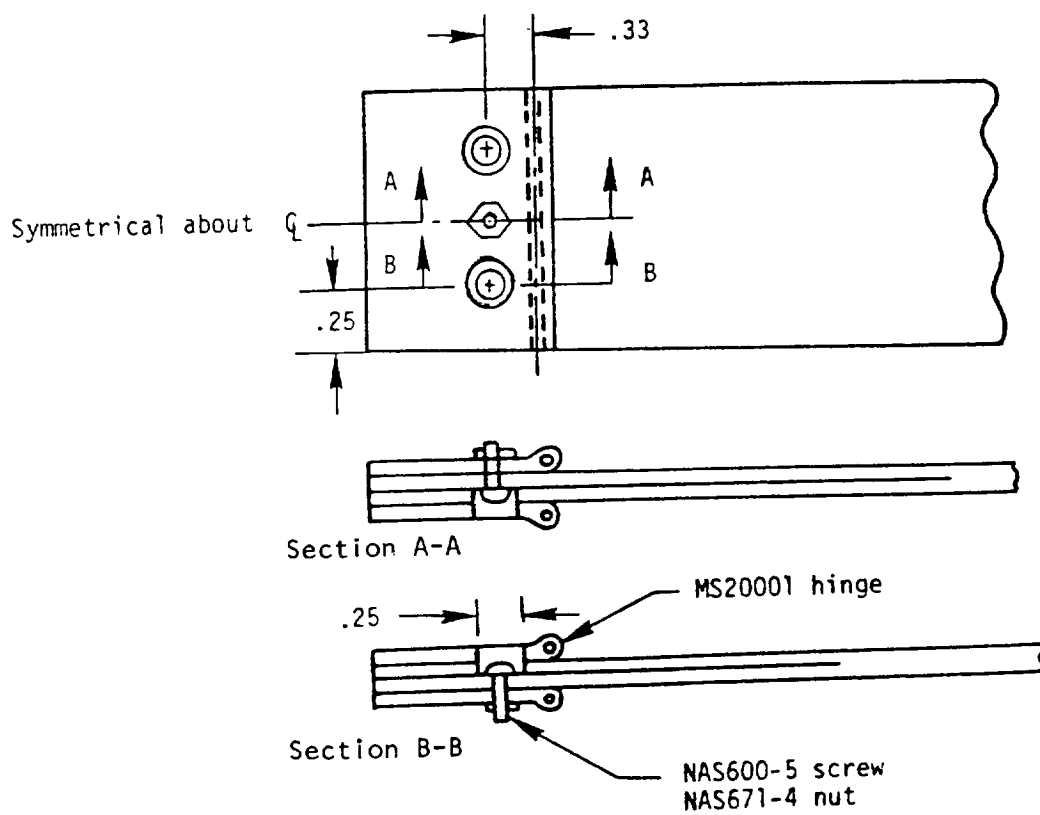


Figure 2-46: Hinge attachment details.

ORIGINAL PAGE IS
OF POOR QUALITY

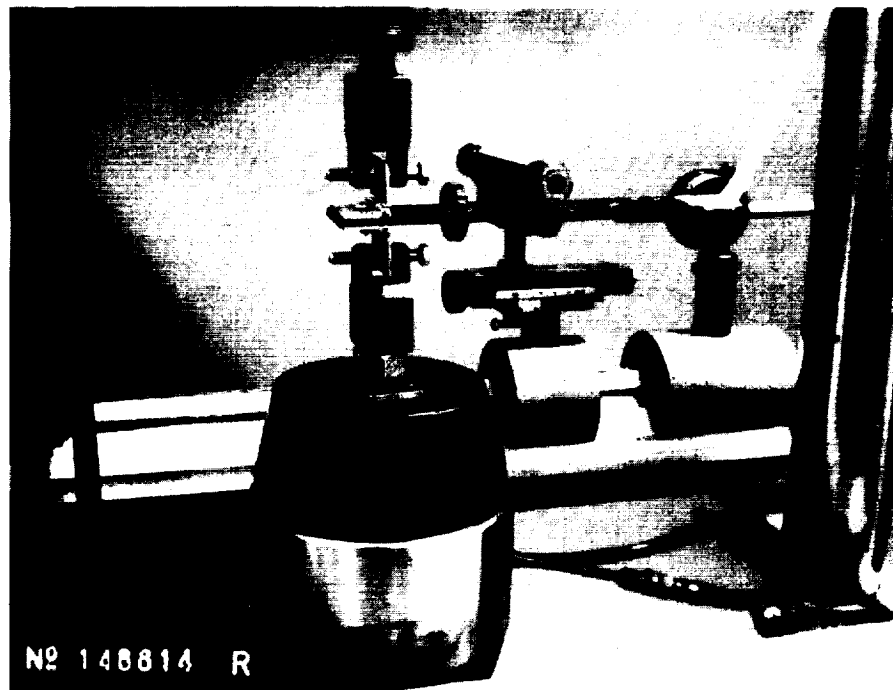


Figure 2-47: Double cantilever beam test set-up.

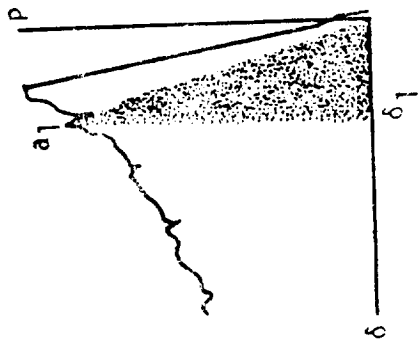
A computer program was written to calculate the G_{IC} values on a Tektronix 4052 minicomputer. The program was entitled "Double Cantilever Beam: Modified Direct Beam Equation Method. NASA ST-5".

The strain energy release rate was also calculated by the energy-area integration method which was described in NASA ST-5 and is illustrated in Figure 2-48. The total energy required to propagate the crack from a_1 to a_2 was the sum of (a) the energy stored in the beam prior to the crack propagation at a_1 , and (b) the energy required to propagate the crack from a_1 to a_2 by further flexing the beam, minus (c) the energy remaining in the flexed beam after the crack propagation is halted at a_2 . This total energy was then divided by the area created by the crack extension from a_1 to a_2 to determine the strain energy release rate.

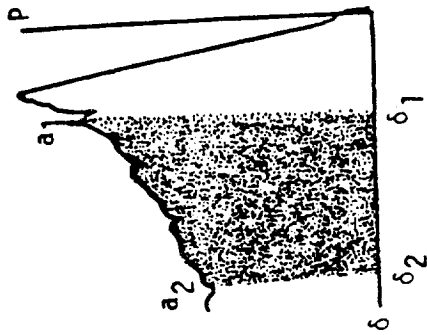
Table 2-23 contains the test data and the G_{IC} values calculated by the modified direct beam equation method. Table 2-24 summarizes the G_{IC} values obtained by both methods. The values of the strain energy release rate determined for each specimen using the two methods vary slightly, but the overall average values for the four test specimens are the same. This indicates very good agreement between the two methods.

2.10 SUMMARY

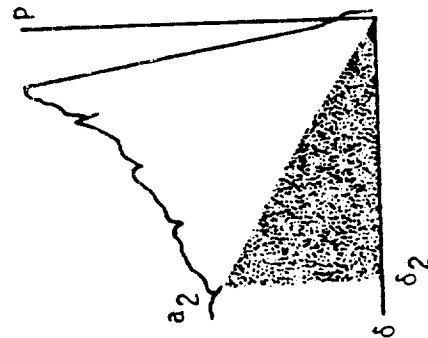
In this section, the data obtained during Phase II of the material characterization task is compared with comparable data obtained during Phase I of the Task (Reference 1). A summary of the quasi-isotropic compression data is shown in Table 2-25. For the unnotched and notched quasi-isotropic compression tests, the Celion/5245 had the highest and the Celion/HX1504 the next highest failure stress and strain values. Of the unnotched 180°F wet tests, Celion/5245 and Celion/HX1504 have similar failure strains, in the 13300 - 13600 μ in/in range, but the Celion/5245 failure stress is 12% greater than



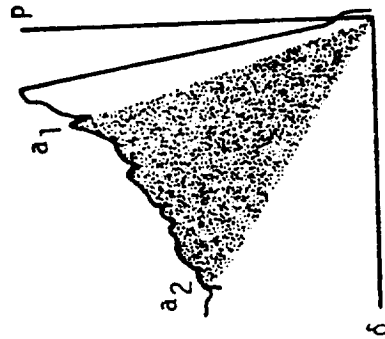
(a) Energy to flex beam to crack initiation.



(b) Additional energy to propagate crack and flex beam further.



(c) Energy remaining in flexed beam after crack propagation.



(d) Total energy to propagate crack ((a) + (b) - (c)).

Figure 2-48: Energy-area integration method for calculating G_{Ic} .

ORIGINAL PHOTOGRAPH
OF POOR QUALITY

TABLE 2-23
HIGH STRAIN CELION/5245 DOUBLE CANTILEVER BEAM TEST DATA
MODIFIED DIRECT BEAM EQUATION METHOD

Laminate orientation: (0) ₂₄ Resin content: 26.87% Test condition: 75 ⁰ F dry																		
Coupon ID	Total Thick, in	Width, in.	A ₁ , in.	δ ₁ , in.	P ₁ , lb	A ₂ , in.	δ ₂ , in.	P ₂ , in.	A ₃ , in.	δ ₃ , in.	P ₃ , in.	A ₄ , in.	δ ₄ , in.	P ₄ , in.	A ₅ , in.	δ ₅ , in.	P ₅ , in.	G _{1c} ^① $\frac{\text{in.-lb}}{\text{in}^2}$
249-1	0.1356	1.505	2.19	0.21	15	3.13	0.40	12	4.10	0.70	9	5.06	1.04	8	6.04	1.46	6	1.42
249-2	0.1246	1.504	2.10	0.18	13	3.07	0.38	10	4.10	0.69	8	5.07	1.03	6	6.06	1.48	5	1.18
249-3	0.1225	1.505	2.10	0.18	13	3.07	0.39	10	4.08	0.68	7	5.07	1.08	6	6.05	1.72	5	1.25
249-5	0.1280	1.504	2.05	0.18	14	3.08	0.40	10	4.04	0.66	8	5.05	1.01	7	6.11	1.49	5	1.21
Average																		$\frac{1.26}{}$

① Each reported G_{IC} value is the average of five values determined per specimen.

TABLE 2-24: HIGH STRAIN CELION/5245 DOUBLE CANTILEVER BEAM TEST DATA SUMMARY

Laminate Orientation: 0 ₂₄ Resin Content: 26.87% Test Condition: 75°F, dry			Coupon ID	Modified Direct Beam Equation Method G _{IC} (in.-lb/in ²)	Energy-Area Integration Method G _{IC} (in.-lb/in ²)
			249-1	1.42	1.54
			249-2	1.18	1.14
			249-3	1.25	1.16
			249-5	1.21	1.21
			Average	1.27	1.26

TABLE. 2 25
COMPRESSION TEST DATA COMPARISON,
(45/0/135/90)_{6s} QUASI-ISOTROPIC LAMINATE

Test Type and Condition		Material			
		High Strain Celion/5245 ^①	High Strain Celion/HX1504 ^①	Celion/982 ^②	AS4/2220-1 ^②
Unnotched at 75°F Dry	Resin Content	33.0%	33.7%	36.3% ^③	34.3% ^③
	Failure Strain (μin/in)	-16502	-15550	-12690	-13808
	Failure Stress (ksi)	-94.39	-87.63	-75.28	-81.90
	Modulus (msi)	6.67	6.55	6.79	6.88
1.00 inch Open Hole at 75°F Dry	Resin Content	33.0%	33.7%	36.3% ^④	34.3% ^④
	Failure Strain (μin/in)	-5415	-5342	-4960	-4713
	Failure Stress (ksi)	-35.71	-33.97	-30.43	-31.09
	Modulus (msi)	6.59	6.49	6.33	6.64
Unnotched at 180°F Wet	Resin Content	33.0%	33.7%	⑤	⑤
	Failure Strain (μin./in.)	13300	13600	⑤	⑤
	Failure Stress (ksi)	80.59	71.77	⑤	⑤
	Modulus (msi)	7.11	6.81	⑤	⑤
1.00 inch Open Hole at 180°F Wet	Resin Content	⑤	⑤	36.3% ^③	34.3% ^④
	Failure Strain (μin./in.)	⑤	⑤	3500	3700
	Failure Stress (ksi)	⑤	⑤	22.60	24.89
	Modulus (msi)	⑤	⑤	6.82	7.09
20 ft-lb Impact at 75°F Dry	Resin Content	31.3%	33.7%	36.3% ^④	34.3% ^④
	Failure Strain (μin/in)	-4400	-4894	-5257	-4050
	Failure Stress (ksi)	-30.6	-31.83	-31.68	-26.43
	Modulus (msi)	6.90	6.57	6.08	6.78
	Impact Damage Area (in ²)	2.97	3.52	2.46	1.94
	Impact Damage Width (in)	1.98	2.15	1.73	1.46
30 ft-lb Impact at 75°F Dry	Resin Content	31.3%	32.6%	⑤	⑤
	Failure Strain (μin/in)	-3700	-4005	⑤	⑤
	Failure Stress (ksi)	-25.3	-26.14	⑤	⑤
	Modulus (msi)	6.82	6.48	⑤	⑤
	Impact Damage Area (in ²)	4.45	5.03	⑤	⑤
	Impact Damage Width (in)	2.43	2.57	⑤	⑤

- ① Simple support compression test fixture, NASA Standard Test "ST-1: Specification for Compression after Impact Test".
- ② Reference 1.
- ③ V-groove compression test fixture, Reference 1.
- ④ 5 x 12 inch compression test fixture, Reference 1.
- ⑤ These tests not run.

that of Celion/HX1504. For the 1.00 in. open hole 180⁰F wet tests, the Celion/982 and AS4/2220-1 have similar failure values. With a 20 ft-lb impact, the Celion/982 had the highest failure strain value at -5300 μ in/in. The Celion/HX1504 and Celion/5245 had the next highest strain at -4900 and -4400 μ in/in respectively. The Celion/982 was not tested with a 30 ft-lb impact. For both the 20 and 30 ft-lb impacts, the Celion/HX1504 failure strains were 8 to 12% greater than the Celion/5245 strains.

The quasi-isotropic tension data is summarized in Table 2-26. For the unnotched and notched room temperature tests, the Celion/5245 had the highest failure strains of 14900 and 8300 μ in/in and the second highest failure stresses of 109 ksi and 61 ksi, respectively. AS4/2220-1 had the second highest failure strains of 14000 and 7700 μ in/in and the highest failure stresses of 136 ksi and 73 ksi, respectively. The Celion/HX1504 notched room temperature strain was essentially that of AS4/2220-1.

For the unnotched -65⁰F dry tests, the Celion/HX1504 failure strain was slightly greater than that of AS4/2220-1, and the AS4/2220-1 failure stress was significantly greater than that of Celion/HX1504.

For all the 0⁰, +45⁰, and 90⁰ tension tests, the Celion/HX1504 had consistently the highest failure stress and strain values of all the materials (Table 2-27). The Celion/HX1504 0⁰ failure stress and strain values were 33 and 28% greater than the AS4/3502 values; the +45⁰ failure stress was 40% greater, and the 90⁰ failure stress and strain values were 19 and 42% greater. Generally speaking, the Celion/HX1504, Celion/5245 and AS4/2220 stress and strain values were greater than the AS4/3502 values. The 0⁰ tension stress and strain values and the 90⁰ strain values were similar for both the Celion/5245 and AS4/2220.

Interlaminar fracture toughness, G_c , values were calculated from the 8 and 11 ply edge delamination data per formulae presented in NASA Standard Test "ST-2: Specification for Edge Delamination Tension Test." The average of

TABLE 2.26: QUASI-ISOTROPIC TENSION TEST DATA COMPARISON

TEST TYPE	PROPERTY	MATERIAL			AS4/3502 (1)
		HIGH STRAIN CELION/ 5245	HIGH STRAIN CELION/ HX1504	AS4/2220-1	
Unnotched at 75°F Dry	Resin Content	31.3%	32.0% (2)	35.0%	35.1%
	Failure Strain ($\mu\text{in./in.}$)	14900	13200	14000	11200
	Failure Stress (ksi)	109.1	94.13	136.35	112.80
	Modulus (msi)	7.47	7.17	10.01	10.14
0.2500 Open Hole at 75°F Dry	Resin Content	31.3%	32.6%	34.5%	35.1%
	Failure Strain ($\mu\text{in./in.}$)	8300	7600	7700	6000
	Failure Stress (ksi)	61.05	52.57	72.87	61.35
	Modulus (msi)	7.28	6.96	9.48	10.11
0.500 Open Hole at 75°F Dry	Resin Content	(3)	(3)	35.0%	35.1%
	Failure Strain ($\mu\text{in./in.}$)	(3)	(3)	6200	4800
	Failure Stress (ksi)	(3)	(3)	59.97	50.02
	Modulus (mpsi)	(3)	(3)	9.71	10.42
Unnotched at -65°F Dry	Resin Content	(3)	(3)	35.7%	32.2%
	Failure Strain ($\mu\text{in./in.}$)	(3)	32.6%	12500	9100
	Failure Stress (ksi)	(3)	12800	134.73	100.62
	Modulus (msi)	(3)	86.37 6.33	10.29	10.38
0.250 Open Hole at -65°F Dry	Resin Content	31.3	(3)	(3)	(3)
	Failure Strain ($\mu\text{in./in.}$)	7600	(3)	(3)	(3)
	Failure Stress (ksi)	58.4	(3)	(3)	(3)
	Modulus (msi)	7.49	(3)	(3)	(3)

Note: All laminates are 48 ply Quasi-Isotropic layups except Celion/HX1504 unnotched 75°F Dry.

(1) Reference 1.

(2) Data from 32 ply laminate

(3) These tests not run on this material

TABLE 2.27: TENSION TEST DATA COMPARISON ^①

Orientation	Property	Material			
		High Strain Celion/5245	High Strain Celion/HX1504	AS4/2220 ^②	AS4/3502 ^②
0°	Resin Content	31.2%	31.2%	30.8%	28.4%
	Failure Strain (μ in/in)	14200	14917	14176	11612
	Failure Stress (ksi)	295.8	314.42	299.42	236.04
	Modulus (Msi)	19.22	18.98	20.24	21.42
±45°	Resin Content	33.0	30.5%	29.8%	31.5%
	Tensile Failure Stress (ksi)	36.59	40.34	31.40	24.81
	Tensile Modulus (Msi)	2.65	2.85	2.41	2.65
	Shear Modulus (Msi)	0.75	0.81	0.70	0.77
90°	Resin Content	29.6%	31.7%	30.8%	28.4%
	Failure Strain (μ in/in)	7300	9342	7260	6577
	Failure Stress (ksi)	9.04	12.56	10.54	10.58
	Modulus (Msi)	1.24	1.35	1.49	1.64

① Reference periodic technical progress report #10, July 1982.

② Average values.

TABLE 2.28: 8 and 11 PLY EDGE DELAMINATION TEST DATA COMPARISON

Material	Reported G_c (lb/in) ^①	
	8-Ply ^②	11-Ply ^③
AS4/2220-1	0.520	1.370
AS4/3502	0.692	0.590
High Strain Celion HX/1504	0.963	1.572
High Strain Celion/5245	1.26	2.75

① Reference Periodic Technical Progress Report No. 24, September, 1983.

② 8-Ply Laminate Orientation: $(+35/0/90)_s$

③ 11-Ply Laminate Orientation: $(+30_2/90/90)_s$

SECTION 3

POST IMPACT FUEL LEAK

3.1 INTRODUCTION

This section summarizes tests performed to evaluate the ability of selected coatings, films, and materials to prevent fuel leakage through 32-ply AS4/2220-1 laminates impacted at three different energy levels. Trial impacts were conducted to determine visible damage threshold, delamination area as measured by ultrasonic C-scan, and to select leak test energy levels. Leak tests of up to 50 hours duration at 10 psi fuel pressure were conducted on sections which had been impacted at selected impact levels. After test several impact locations were sectioned for investigation of impact damage.

3.2 TEST LAMINATES

Two 32-ply quasi-isotropic laminates were fabricated from AS4/2220-1 material. Table 3.1 lists these two panels as 280 and 281 and the various surface treatments used with each. Panel 280 had a polyurethane film located at the midplane in one region of the laminate from which panels 280-1A and 280-1B were cut. Panel 281 had a ply of 120 glass fabric cocured to one surface in one region of the laminate from which panels 281-1A and 281-1B were cut. The remaining panels were treated as listed in Table 3.1.

After curing, the laminates were ultrasonically inspected and tag end portions were removed for resin content and grind down measurements. Coatings were then applied as-required. Weights of the various treatments are given in Table 3.2. After coating the two laminates were machined into 12 subpanels 7 x 21 inches. Panels identified by "A" were used for trial impact tests and those by "B" were impacted and used for leak testing.

TABLE 3-1
PANEL COATING

Panel I.D.	Coating Requirements
280-1A, -1B	Embedded film ^a -- no coating
280-2A, -2B	Control panel -- no coating
280-3A, 3B	Coated with PRC ^b (R)
281-1A, 1B	Fiberglass ^c on one surface coated with 5 mil chemglaze ^d
281-2A, 2B	5 mil Chemglaze ^d
281-3A, 3B	10 mil Chemglaze ^d

a = 13 mil film: Polyurethane

b = 21 mil coating: A Permapol (R) based, sprayable, fuel resistant, polyurethane material having 15% swell. Intended as an elastomeric coating for aircraft integral fuel tanks and full cell cavities. The PRC type used was RW-1722-83, made by Product Research Corporation.

c = 5 mil layer: Fiberglass

d = 5 or 10 mil coating: A polyurethane based paint having high elongation.

TABLE 3.2
WEIGHTS OF POST-IMPACT FUEL LEAK COATINGS

Configuration	Weight (lb/in ² x 10 ⁻⁴)	Impact Energy to Puncture Coating (ft-lb)
Polyurethane Film Within Laminate	5.56	50
Untreated Laminate	—	—
PRC Elastomeric Coating	9.06	30
Fiberglass Fabric (0.005 in.) + Chemglaze (0.005 in.)	3.51	50
Chemglaze (0.005 in.)	3.41	50
Chemglaze (0.010 in.)	6.68	50

3.3 TRIAL IMPACT TESTS

Trial impacts were conducted on six panels as listed in Table 3.3 with a 0.5 inch diameter hemispheric head impactor and a 12 pound weight. The panels were restrained during impact in a 5 x 5 inch open area frame shown in NASA Reference Publication 1092. Impact locations are shown in Figure 3-1. The visual extent of damage is described in Table 3.4. After impacting the panels were ultrasonically inspected and the damage area measured (Table 3.5).

3.4 LEAK TESTING

After reviewing the ultrasonic inspection results 10, 20, and 30 foot-pounds were selected as impact energies for leak testing. The "B" panels were then impacted in the same manner as the trial impacts. Locations of the impacts on each panel are shown in Figure 3-2. Photographs of each side of the impacted panels are contained in Appendix B.

Prior to leak testing a panel, flat black paint was sprayed below the impact site to provide contrast between the leaking fuel and the exterior painted surface (light grey) that could be easily noticeable on the video tape recorder-camera used for each 50 hour test. Eight hour video tapes with a camera stop watch running in the upper left hand corner were used with white light to indicate the onset of leakage. For spray painting, paper or scotch tape lightly pressed over the impact site was used to mask the site from the effect of the paint. The panels were also previously inspected using a black light to detect the dye in the simulated fuel.

After the black paint was dry, a fuel box assembly was attached to each impact area as shown in Figures 3-3 and 3-4. The seal between the coating on the panel and the fuel box was achieved by means of 1/8" thick rubber gasket (shore 60) which overlapped the perimeter of the fuel box by $\pm 1/8"$.

TABLE 3.3
TRIAL PANEL IMPACT ENERGY

Panel I. D.	Impact Energy (Ft. - lbs.)				
	A	B	C	D	
280 -1A	20	40	5 [Ⓐ]	10	10 [Ⓐ] 30
280 -2A	10	20	5		15
280 -3A	30	40	20		10
281 -1A	10	50	40		20
281 -2A	20	40	50		10
281 -3A	30	40	60		30

Ⓐ = These impacts were 1 1/8" to the left of and 1 7/8" to the right of the C impact.

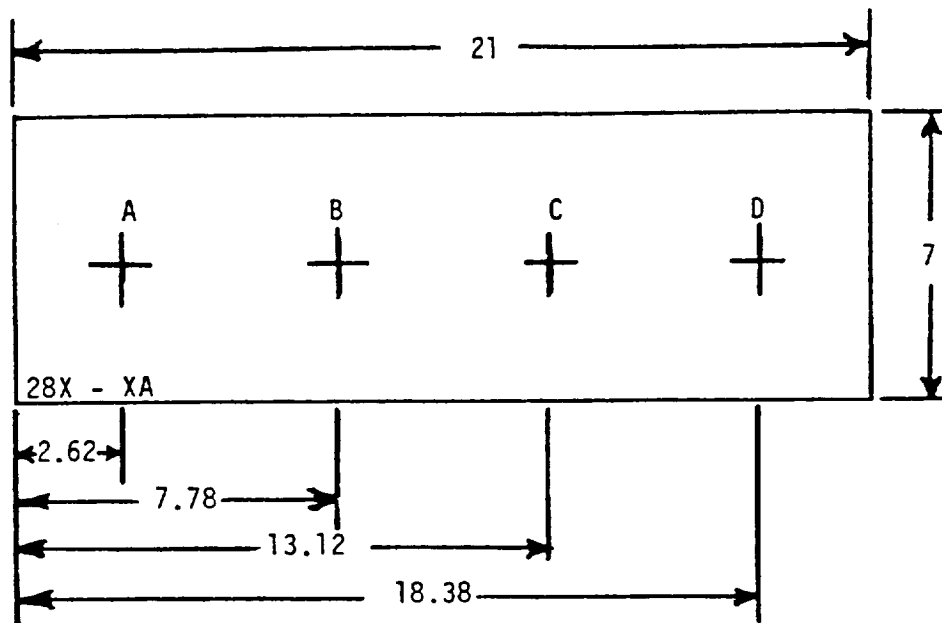


FIGURE 3-1: TRIAL IMPACT PANEL LAYOUT

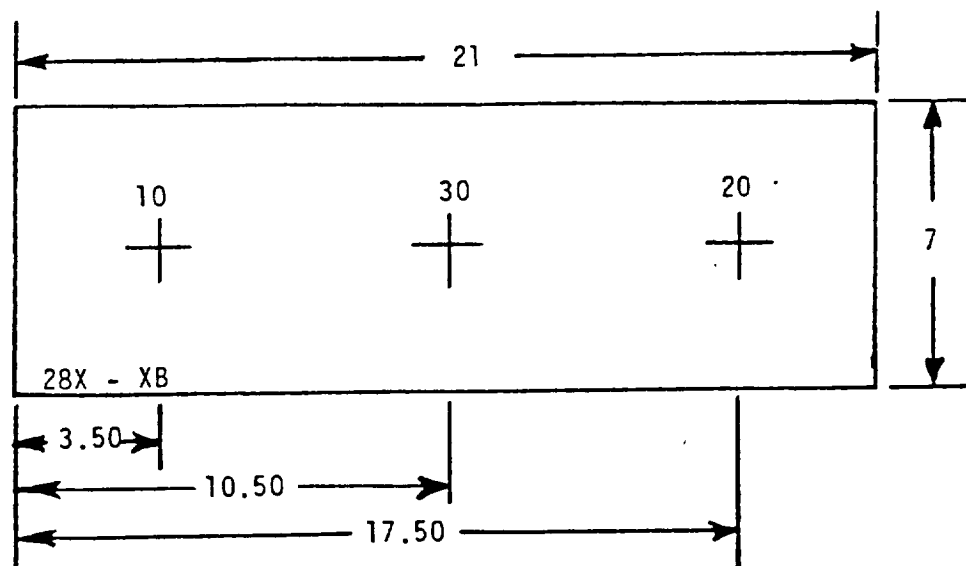


FIGURE 3-2: TEST PANEL LAYOUT

TABLE 3.4
VISUAL OBSERVATIONS OF TRIAL IMPACT TEST DAMAGE

Panel ID	Impact Energy ft-lbs	Front	Back
280-1A	20	Large dent	3" delamination
	40	Partial Penetration	6½" delamination
	5	None	None
	10	None	None
	10	Slight dent	None
	30	Many broken fibers	6" delamination
280-2A	10	Slight dent	None
	20	Dent, few broken fibers	4" delamination
	5	Slight dent	None
	15	Slight dent	2" delamination
280-3A	30	Many broken fibers	4½" bulge, 1" delamination in coating.
	40	Penetration	2 3/4" bulge, 1½" delam. in coating.
	20	Dent, few broken fibers	1½" bulge, coating not broken.
	10	Slight dent	None
281-1A	10	Slight dent	0.2" bulge
	50	Penetration	2" bulge, 1½" coating rupture
	40	Penetration	2" bulge no rupture
	20	Dent, some broken fibers	1" bulge no rupture
281-2A	20	Dent, some broken fibers	3" bulge no rupture
	40	Penetration	6" bulge 0.8" rupture
	50	Penetration	7" bulge 2" rupture
	10	Slight dent	0.3" ripple, no rupture
281-3A	20	Dent, some broken fibers	2" bulge, no rupture
	40	Penetration	6" bulge, no rupture
	60	Penetration	6" bulge, 0.5" rupture
	30	Many broken fibers	4½" bulge, no rupture

The three boxes were then filled in parallel with fuel simulant Shell Pella-A, with a fluorescent dye additive, entering from the bottom, while air was let out the top. Each hydraulic fitting on the fuel box was capped as fuel overflowed, and when all three boxes were full, fittings were added to complete the parallel hookup, then more fuel was added to fill the fittings. The test setup is shown in Figures 3-3 and 3-4. The filling reservoir to the fuel boxes was capped off, and a pressure of 10 psig applied.

After a particular impact site started to leak, the pressure was temporarily released and the associated fuel box disconnected from the system. At the end of test, each box was drained, and the volume of the drained fuel was checked to show that fuel was at least above the impact site for the duration of the test -- the volume of full fuel box being 900 cc.

Results of the panel leak tests are shown in Table 3-6. The ten ft-lb impact sites did not leak in any of the six panels in fifty hours, and the impact itself was not severe enough to crack the light grey paint. The twenty and thirty ft-lb impacts caused leaking except in panels coated with Chemglaze.

The Chemglaze coating in the 30 and 20 ft-lb leak tests produced interesting results in that even if oil did not flow out, fluorescence of the dye in the impact site could be seen with an ultraviolet light. To be sure the dye came from the fuel side of the panel, a Q-tip was put in front of the ultraviolet light and showing no fluorescence, rolled gently in the impact site, and put in front of the ultraviolet light again. Dye was transferred to the Q-tip from the impact site as dye was removed from the impact site. But the fluorescence came back after a time suggesting either a very fine puncture of the Chemglaze or the Chemglaze acted as a molecular sieve holding back the fuel simulant Shell Pella-A but passing the dye.



Figure 3-3: Overall view of test set-up

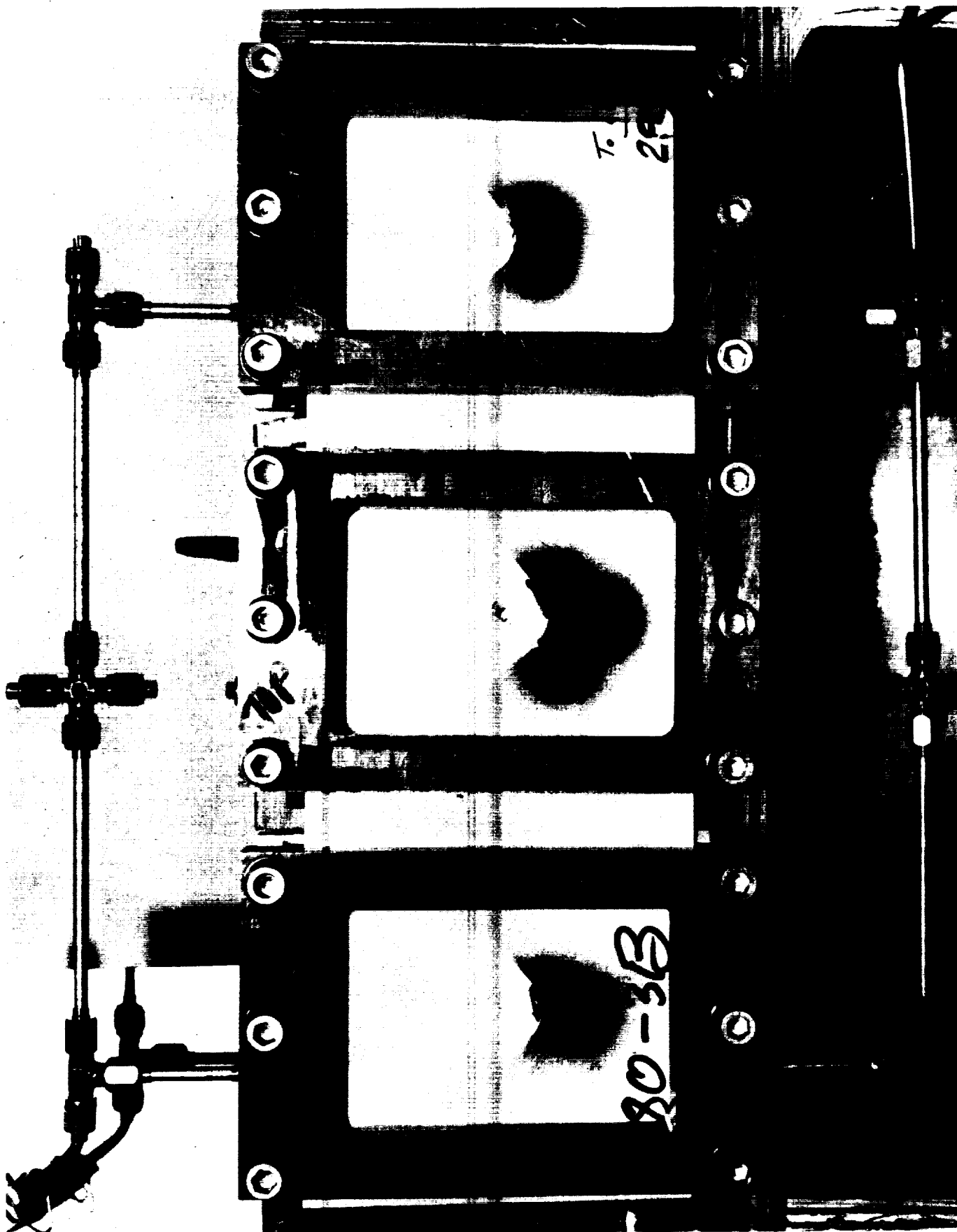


Figure 3-4: A close up of the test showing where fuel has leaked and flowed over the black paint.
The center impact was 30 ft-lbs.

TABLE 3.5
TRIAL IMPACT ULTRASONIC INSPECTION DAMAGE AREAS

Panel #	Impact Energy (ft. lbs.)	Area (in. ²)
280-1B	10	0.70
	20	0.71+
	30	1.13+
280-2B	10	0.90
	20	1.22
	30	1.32+
280-3B	10	1.06
	20	1.35
	30	1.58+
281-1B	10	1.48
	20	1.64
	30	1.80
281-2B	10	1.05
	20	1.38+
	30	1.69+
281-3B	10	0.97
	20	1.61+
	30	1.76+

+ Indicates a splitting of the back surface ply/plies giving a larger C-scan indication. The split area is not included.

TABLE 3.6
SUMMARY OF TIME OF LEAK

Coating Description	Panel I.D.	10 ft. lbs.	20 ft. lbs.	30 ft. lbs.
embedded film-no coating	280 -1B	50 hr. no leak @ 10 PSIG	50 hrs. no leak @ 10 PSIG	16 min @ 0 PSIG
control panel -no coating	280 -2B	50 hr. no leak @ 10 PSIG	14 min. @ 0 PSIG	1 sec. @ 0 PSIG
PRC coating 21 mil	280 -3B	50 hr. no leak @ 10 PSIG	50 hr. no leak @ 10 PSIG	4 min. @ 0 PSIG
fiberglass on one surface coated with 5 mil chemglaze	280 -1B	50 hr. no leak @ 10 PSIG	①	leak @ 7 PSIG while Pressurizing
5 mil Chemglaze	281 -2B	50 hr. no leak @ 10 PSIG	②	③
10 mil Chemglaze	281 -3B	50 hr. no leak @ 10 PSIG	①	④

- ① = Crack in paint fluoresces but no flow of oil noticed at 50 hours.
 ② = Crack in paint fluoresces but no flow of oil noticed at 18 hours.
 ③ = Fluorescence but no flow noticed at 1 hour 35 minutes.
 ④ = Fluorescence but no flow noticed at 50 hours.

SECTION 4

DESIGN DEVELOPMENT TESTS

4.1 INTRODUCTION

The objective of this phase of the program was to verify the structural integrity of the technology demonstration article structural details. Test specimens were cut from two AS4/2220-1 panels fabricated by Lockheed Manufacturing Research as a part of the technology demonstration article process development work. One such panel is shown in Figure 4-1 in the as-received condition. Both panels were painted on the exterior surface with a greyish-white paint and on the interior with a 5-mil coating of Chemglaze except on the stiffener blades which were uncoated. The following types of tests were conducted.

- o Stiffener pull-off
- o Stiffener side load
- o Undamaged compression, single stiffener
- o Impacted compression, single stiffener
- o Impacted compression, two-stiffener panel
- o Trial impact, two stiffener panel
- o Stiffener failsafe

All of these test panels were tested in the as-received condition under normal laboratory environmental conditions of $75 \pm 10^{\circ}\text{F}$ and $50 \pm 10\%$ relative humidity. In areas where strain gages were applied, the Chemglaze and paint were locally removed by mechanical methods. Table 4.1 lists details of each test and Figure 4-2 shows test configurations and loading directions. Figures 4-3 and 4-4 show the location of each specimen in the two process development panels.

ORIGINAL FACTORY
OF POOR QUALITY

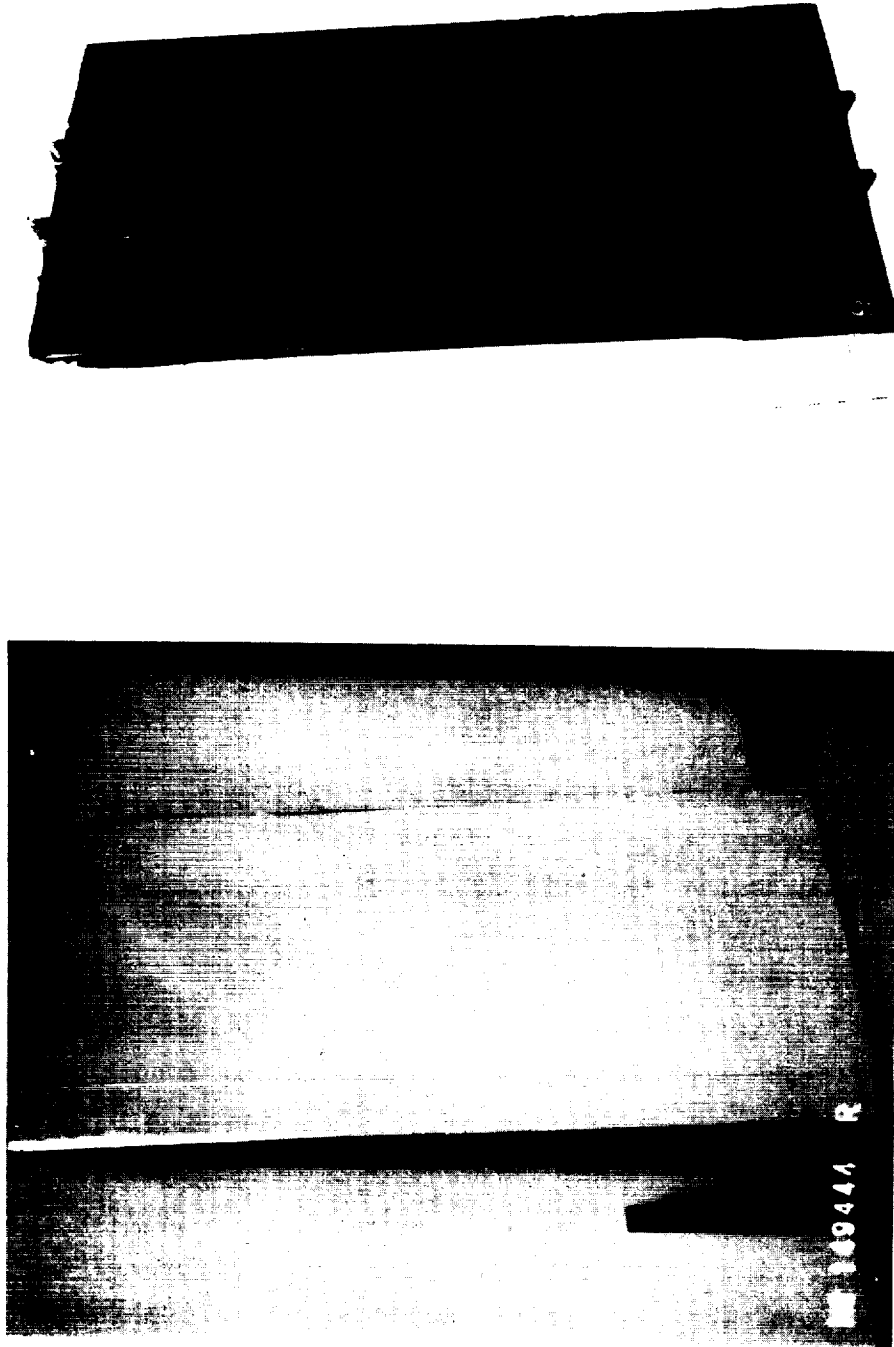


Figure 4-1: Skin and stiffener side views of process development panel. Scale is in inches.

TABLE 4.1
DESIGN DEVELOPMENT TESTS

Specimen I.D.	Specimen Description	Specimen Dimensions		Type of Test	Number of Tests
		Length (in.)	Width (in.)		
A	Undamaged Stiffener	18.0	5.75	Compression	1
B	Impacted Stiffener	18.0	5.75	Compression	1
C	Stiffener Pull-Off	3.0	5.75	Tension	4
D	Stiffener Side Load	3.0	5.75	Tension	4
E	Stiffener Fail-Safe	18.0	5.75	Tension	2
F	Trial Impact Panel	24.75	18.0	--	1
G	Impacted Stiffened Panel	25.0	18.0	Compression	1

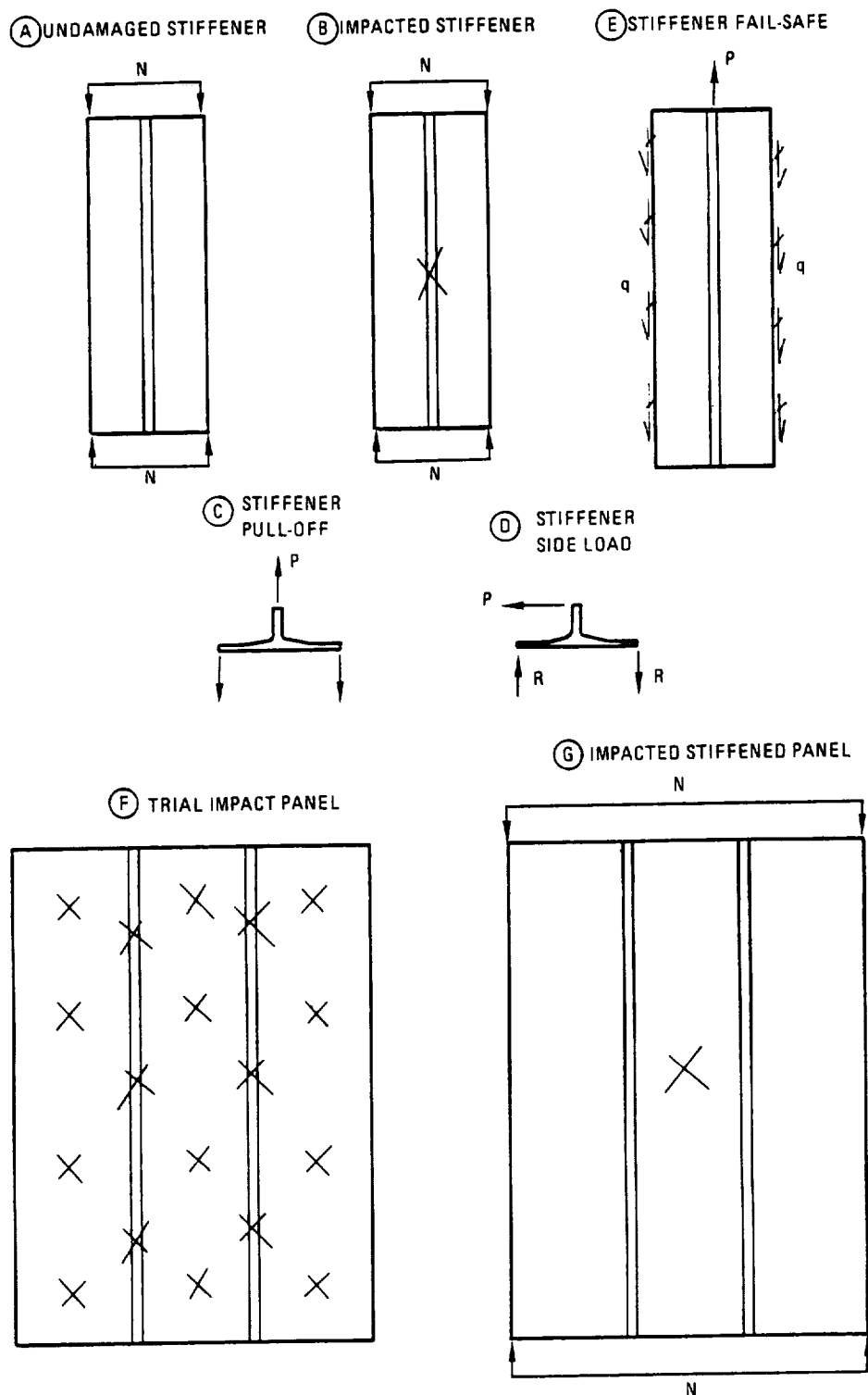


Figure 4-2: Process development test specimen configurations and loading directions.

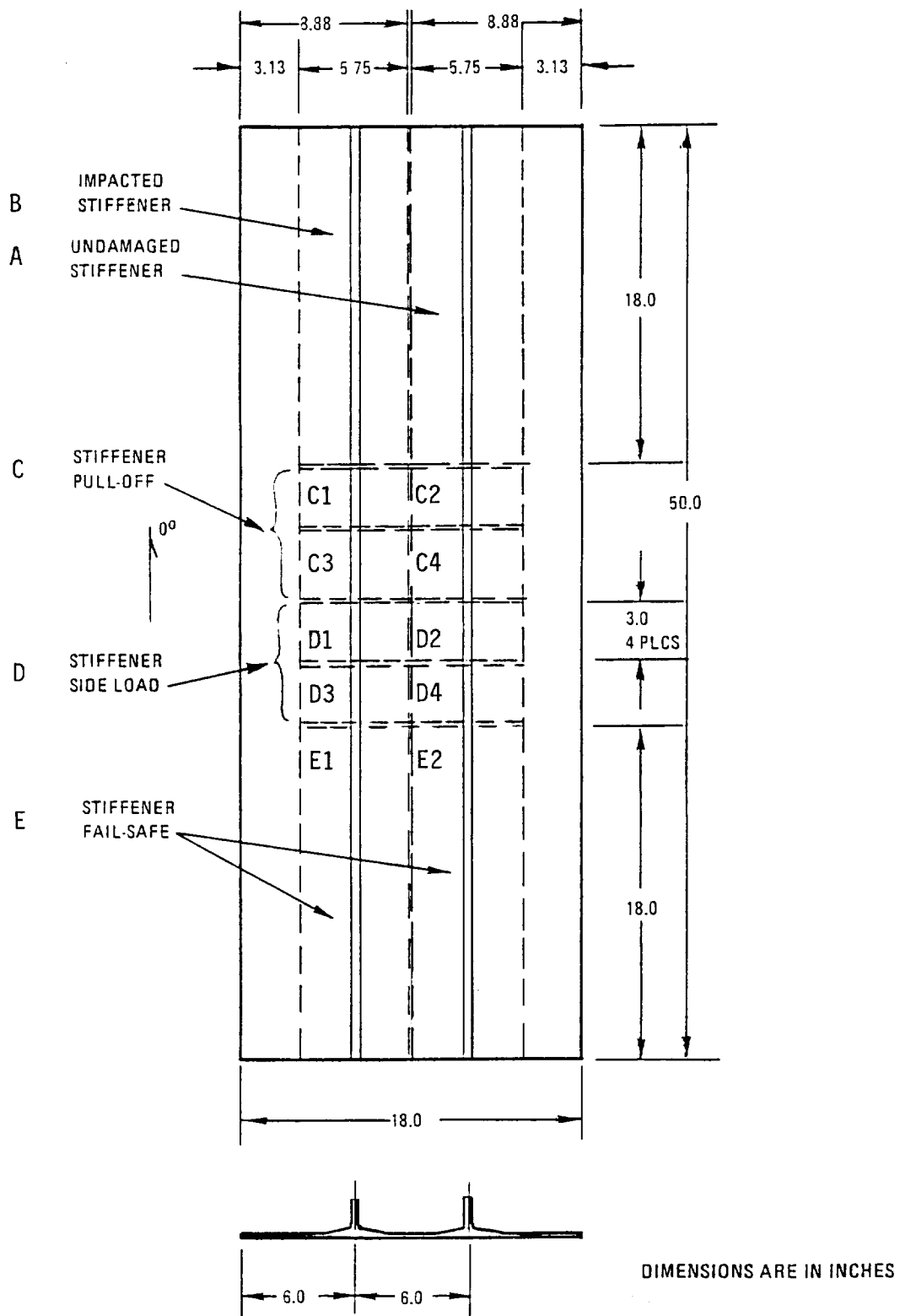


Figure 4-3: Stiffened panel process development test specimens.
Panel #2.

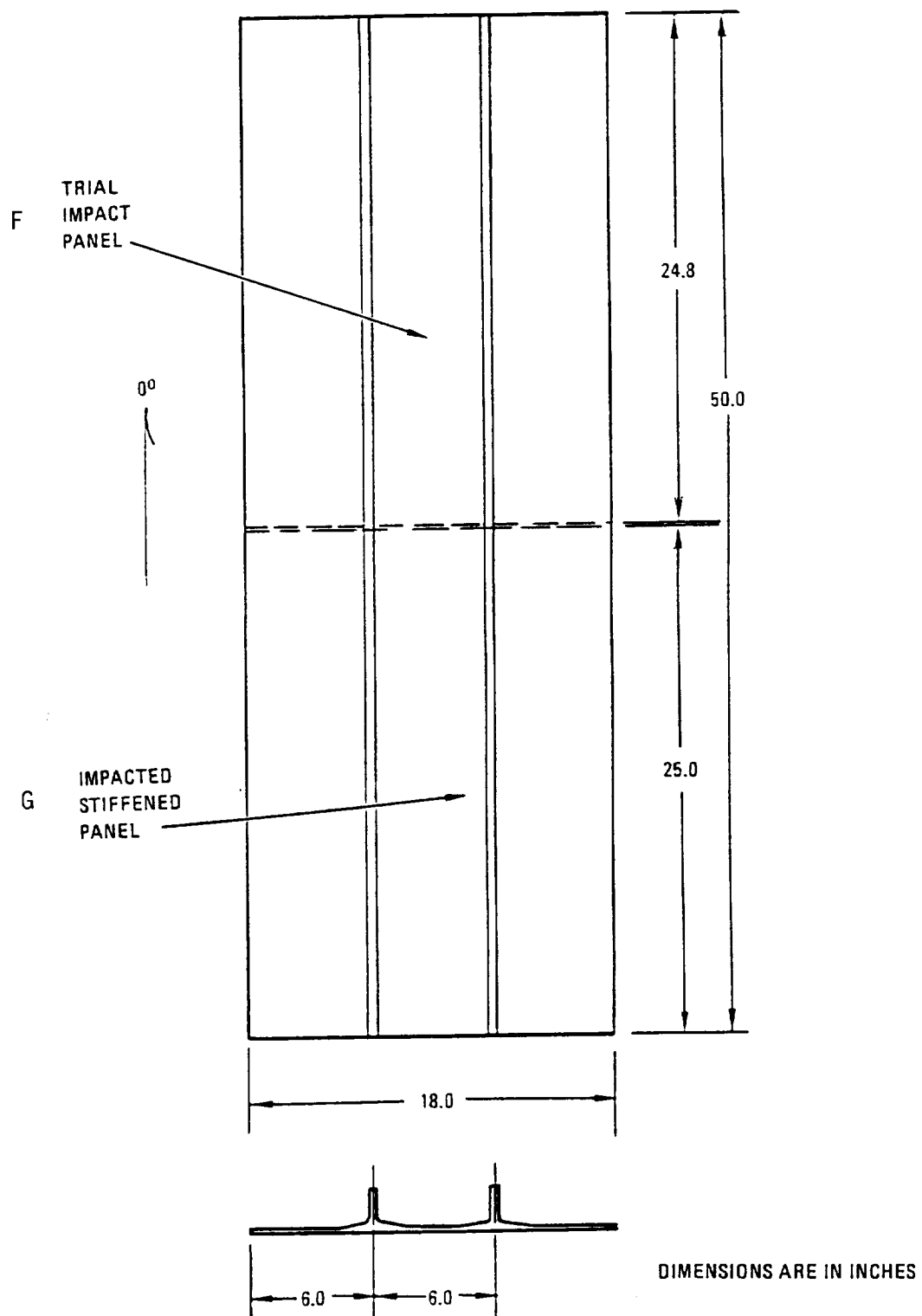


Figure 4-4: Stiffened panel process development test specimens.
Panel #1.

4.2 TRIAL IMPACT TESTS (F)

The trial impact tests were conducted on a two stiffener panel, 25-inches long by 18-inches wide. Twelve impacts were made on the skin surface of the panel and eight impacts on the stiffeners. The panel was first impacted with a 12-pound impactor having a 0.5 inch diameter hemispherical steel tup. The trial impact panel was supported by a wooden panel support frame that was contoured to mate with the bottom or inside of the panel to uniformly distribute impact load over the entire panel. Impact locations and energies are shown in Figure 4-5. Impacts on the skin areas of the panel produced barely visible front side damage at between 20 ft-lb and 30 ft-lb energy levels. Visible damage to the back side of the skin occurred at 40 ft-lb energy and greater. Because the panel had a 5 mil Chemglaze coating on the back surface, damage that did not cause broken fibers to lift the coating was not readily visible. Stiffener impacts were made normal to the stiffener on the same panel at 10 ft-lb, 20 ft-lb, 40 ft-lb, and 50 ft-lb energy levels. Impacts on the stiffener produced barely visible damage to the fiberglass outer layer at 10 ft-lb to 20 ft-lb energy levels and visible damage at 50 ft-lb. Ultrasonic inspection of the stiffener impacts indicated that no internal damage was done to the stiffener by any of the impacts. Therefore, additional impacts were made on the panel at 40 ft-lb, 60 ft-lb, 80 ft-lb and 100 ft-lb energy levels. Visual inspection of the top of the impacted stiffener revealed delamination of the stiffener by impacts of 60 ft-lb energy and greater. The delamination caused by the 100 ft-lb impact propagated through the other impacts on the same stiffener and delaminated 80 percent, as measured by ultrasonic C-scan, of the stiffener. As a result of the trial impact test, a skin impact energy level of 30 ft-lb was chosen for the impacted stiffened panel compression test specimen, and a stiffener impact of 40 ft-lb was chosen for the damaged stiffener specimen. Difficulties were encountered in measuring delamination areas by C-scan in the region of stiffener runout. A copy of a C-scan of the skin is shown in Figure 4-6.

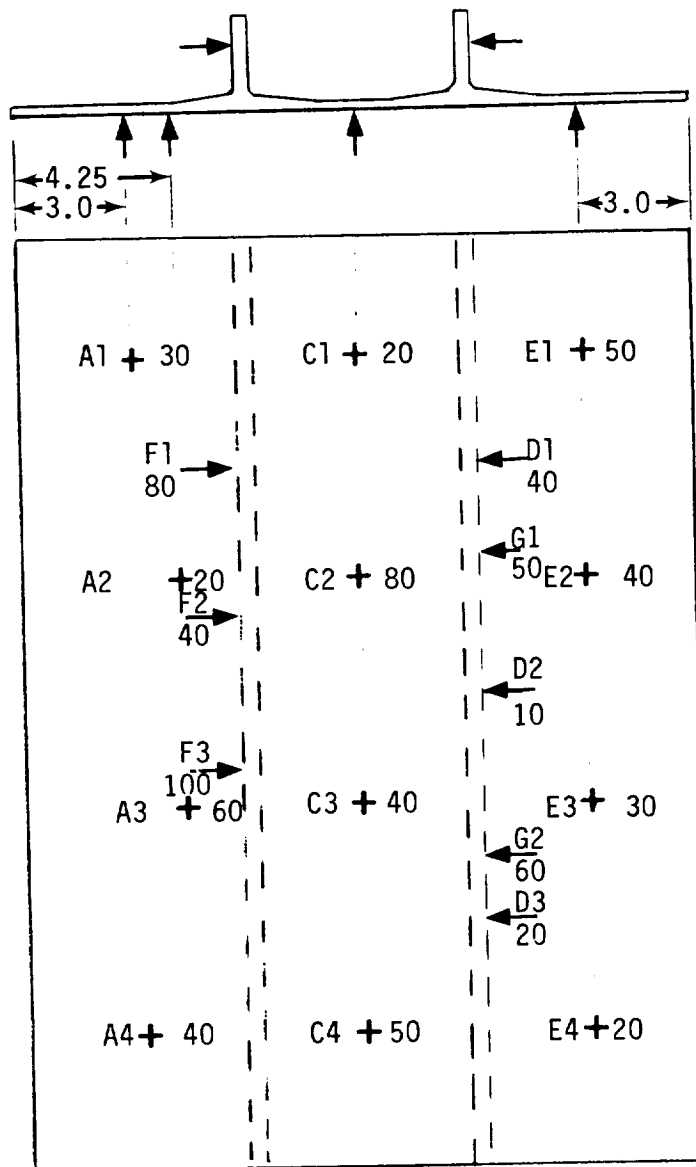


Figure 4-5: Trial impact panel impact locations and energies in ft.-lbs.

ORIGINAL FILED IN
OF POOR QUALITY

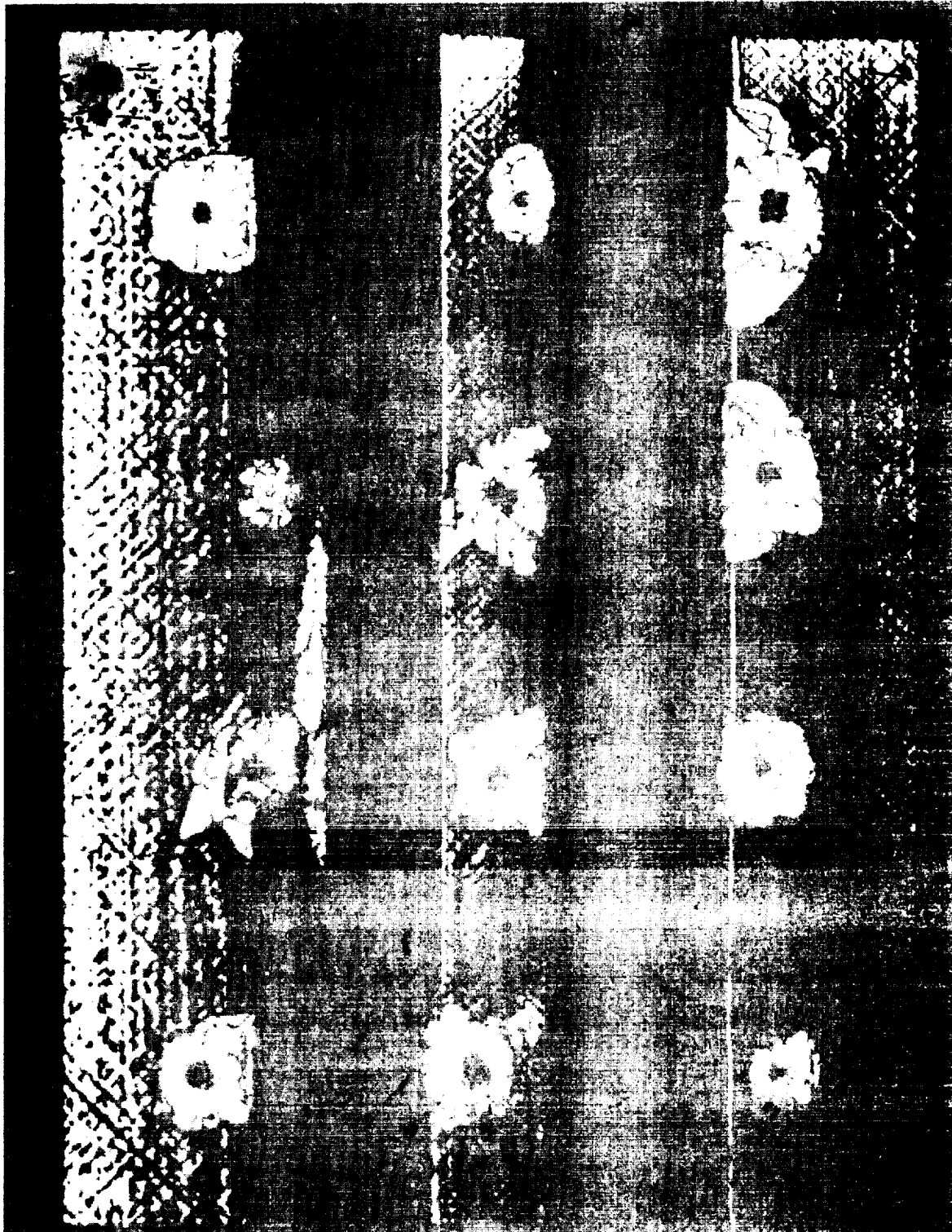


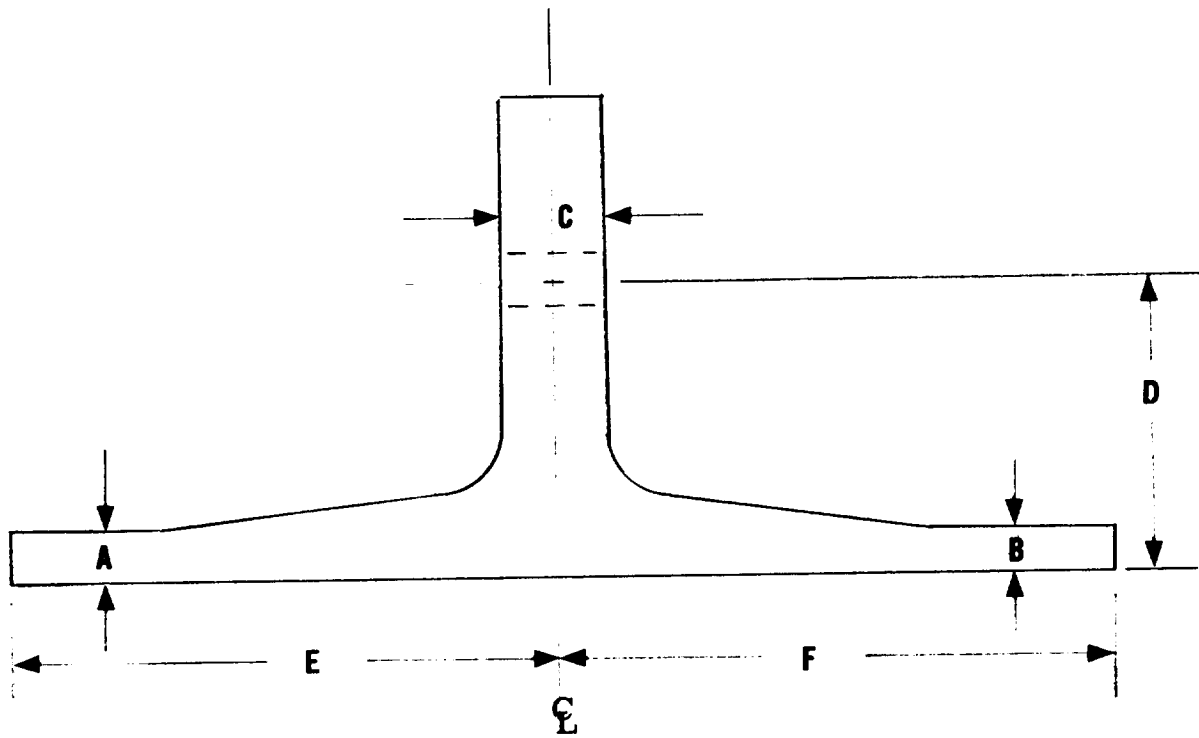
Figure 4-6: C-scan of trial impact panel.

4.3 STIFFENER PULL-OFF TESTS (C)

Four stiffener pull-off specimens were machined from Panel #2 (Figure 4-3) and are identified as C1→C4. Dimensions of each specimen are given in Table 4.2. Test configuration is shown in Figure 4-7 with the skin side clamped down to a steel plate by two bars clamping outboard of the stiffener runout region. This test setup is more clearly seen in Figure 4-8. Steel plates were attached to the stiffener and pin loaded in the transverse plane. Load was continuously applied at a displacement rate of 0.10 in./minute to failure in a stroke controlled mode. The average failure load of the pull-off specimens was 1687 lbs as listed in Table 4.3. Load and deflection were recorded and the results are presented in Figures 4-9 through 4-12.

Failure was initiated by interlaminar cracking in the upstanding portion of the precured stiffener insert above the corner radius between the upstanding portion of the stiffener and the flanges of the stiffener insert. Secondary cracks occurred in the corner radius of the precured stiffener insert after maximum load was reached. Final failure of the specimens occurred as delaminations in the precured stiffener insert near the bondline between the precured stiffener insert and the skin. Generally the maximum load was reached before any visible cracking occurred and each subsequent mode had progressively lower strength. These correspond to the major vertical load drops in Figures 4-9 through 4-12. For example in Figure 4-9 at a deflection of 0.200 in., after a drop in load from 800 lbs to 500 lbs, the bondline delamination became visible. Further loading only resulted in delamination growth, the load increase was due to end restraint of the clamping blocks. Figure 4-8 shows specimen C3 under load at maximum deflection. Figures 4-13 through 4-16 show the tested specimens with no load applied. These figures demonstrate the areas of cracking relative to the bond lines.

TABLE 4.2
STIFFENER PULL-OFF AND STIFFENER SIDE LOAD
SPECIMEN DIMENSIONS



Spec. ID	A	B	C	D	E	F
C1	.234	.209	.510	1.60	2.73	2.97
C2	.218	.211	.508	1.60	2.83	2.92
C3	.234	.211	.514	1.60	2.70	3.05
C4	.214	.212	.512	1.60	2.83	2.92
D1	.235	.211	.511	1.37	2.80	2.95
D2	.214	.212	.518	1.37	2.87	2.82
D3	.234	.211	.510	1.37	2.65	3.05
D4	.212	.211	.509	1.37	2.85	2.90

ORIGINAL PAGE IS
OF POOR QUALITY

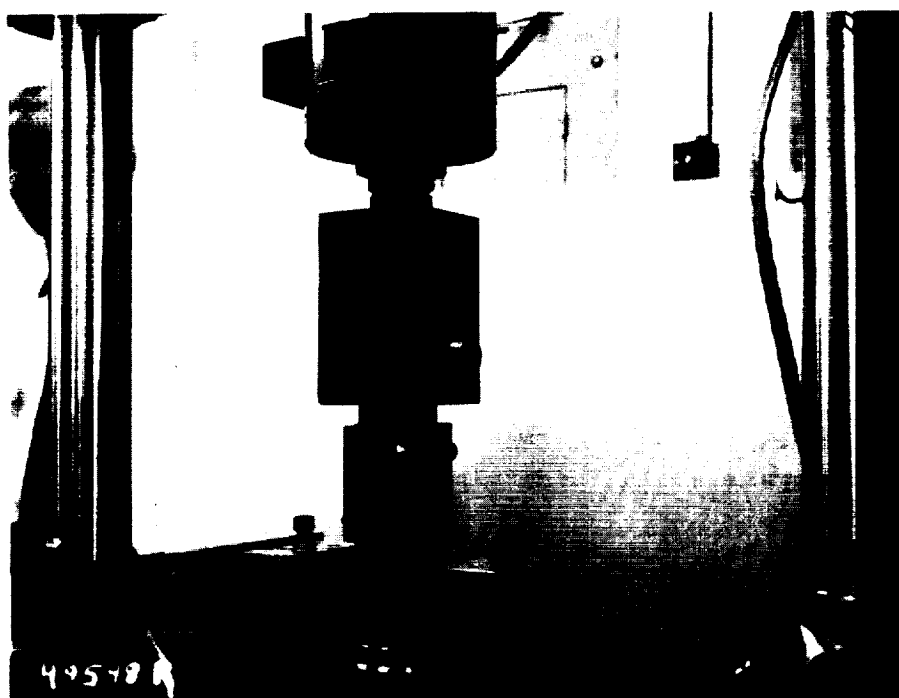
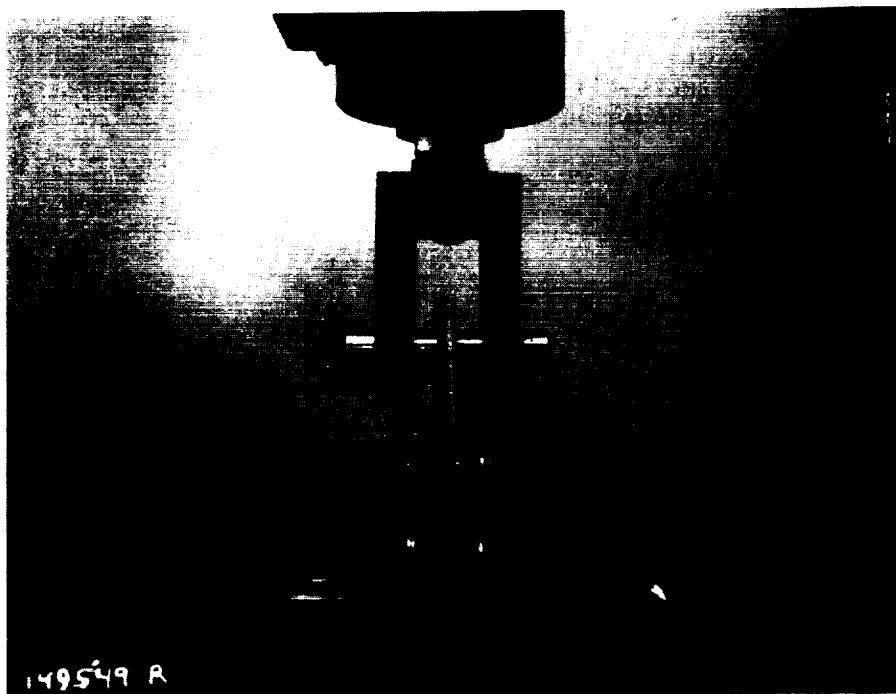


Figure 4-7: Stiffener pull-off test setup.

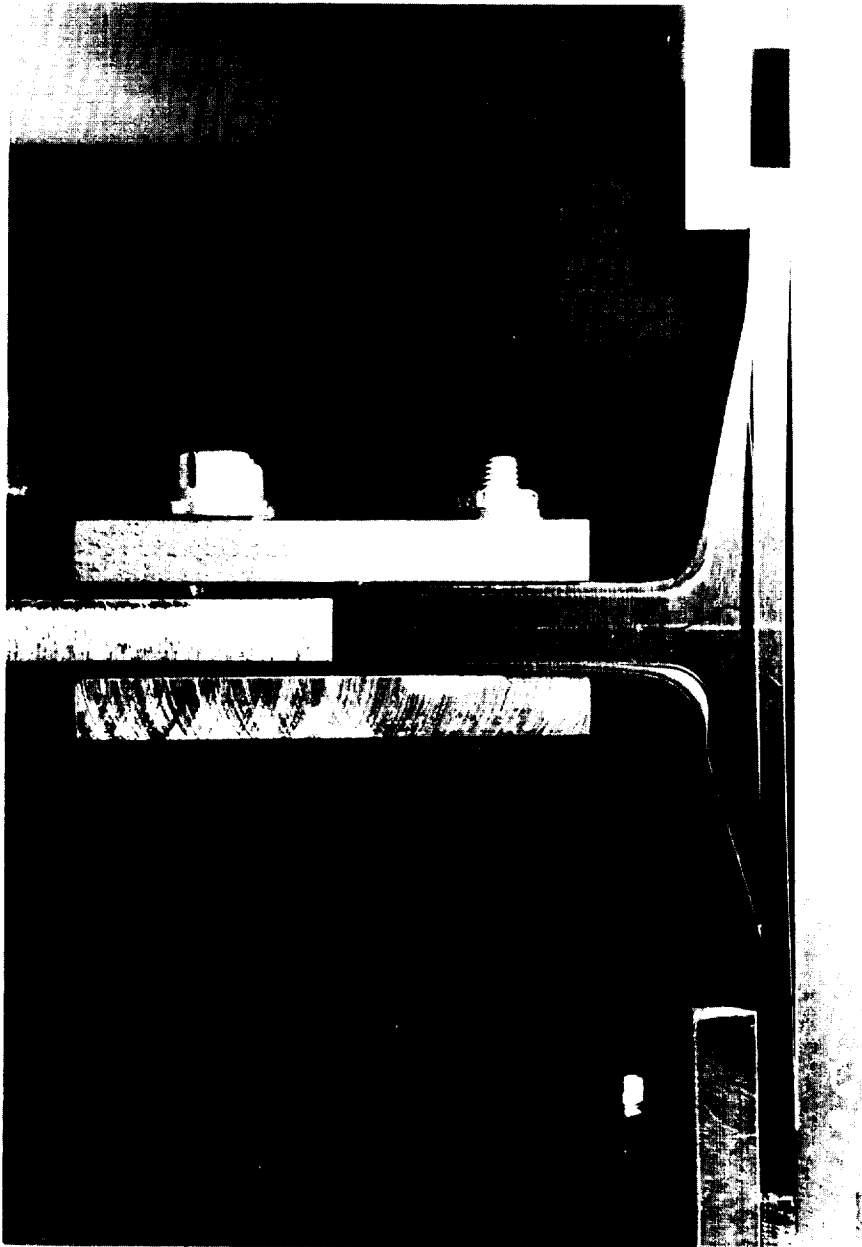


Figure 4-8: Typical failure of stiffener pull-off specimen (C3). First cracks were in the blade, second around the radius, and lastly horizontal delamination.

TABLE 4.3
STIFFENER PULL-OFF AND SIDE LOAD TEST RESULTS

SPECIMEN ID	TEST CONDITION	FAILURE LOAD (LB)
C1	PULL-OFF 75°F, DRY	1711
C2		1862
C3		1638
C4		<u>1536</u>
AVERAGE		1687
D1	SIDE LOAD 75°F, DRY	1191
D2		1309
D3		1220
D4		<u>1309</u>
AVERAGE		1257

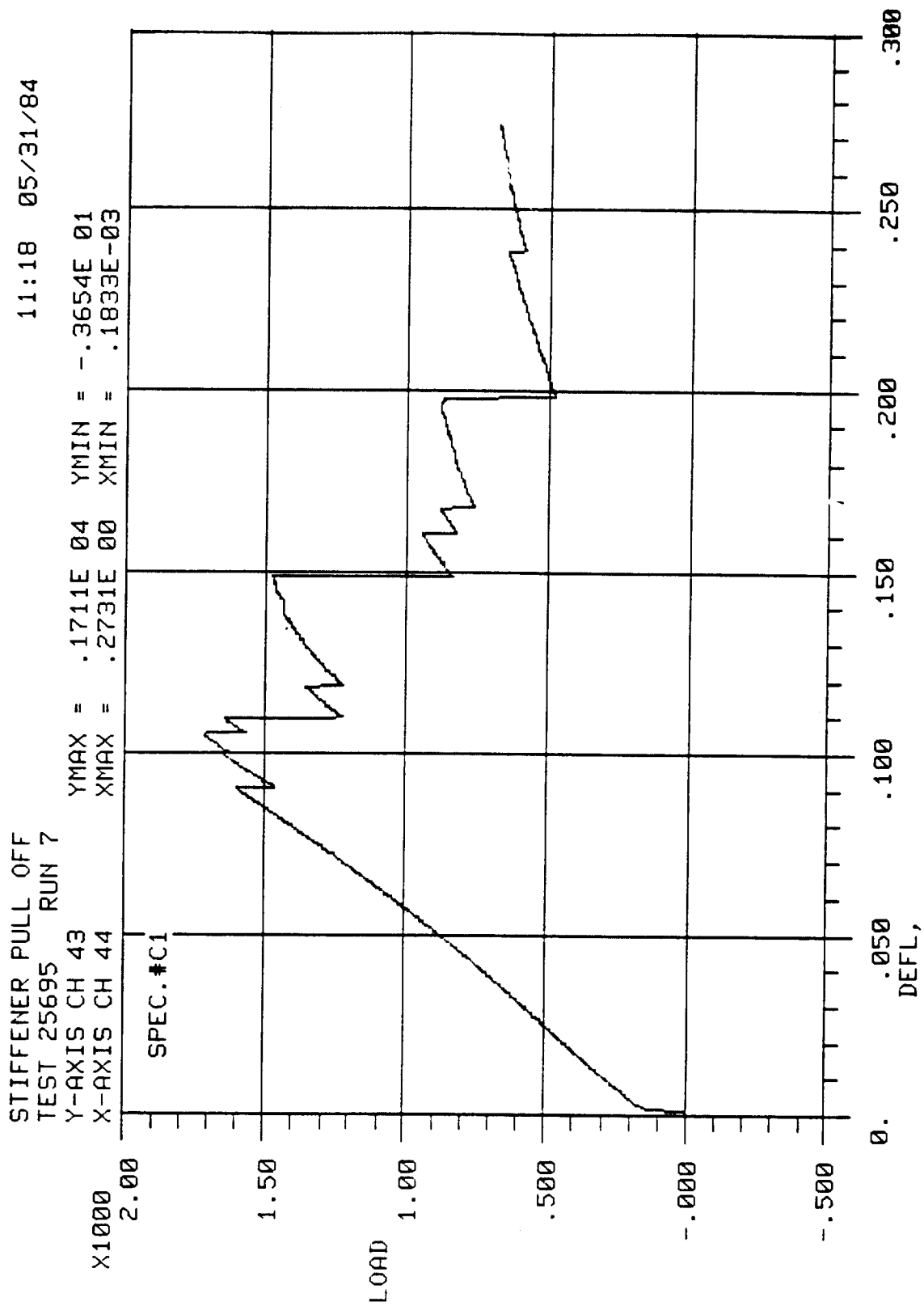


Figure 4-9: Load-deflection curve for stiffener pull-off specimen C1.

13:35 05/31/84

STIFFENER PULL OFF

TEST 25695 RUN 12

Y-AXIS CH 43

X-AXIS CH 44

YMAX = .1862E 04 YMIN = -.7922E 01

XMAX = .1573E 00 XMIN = -.2905E-04

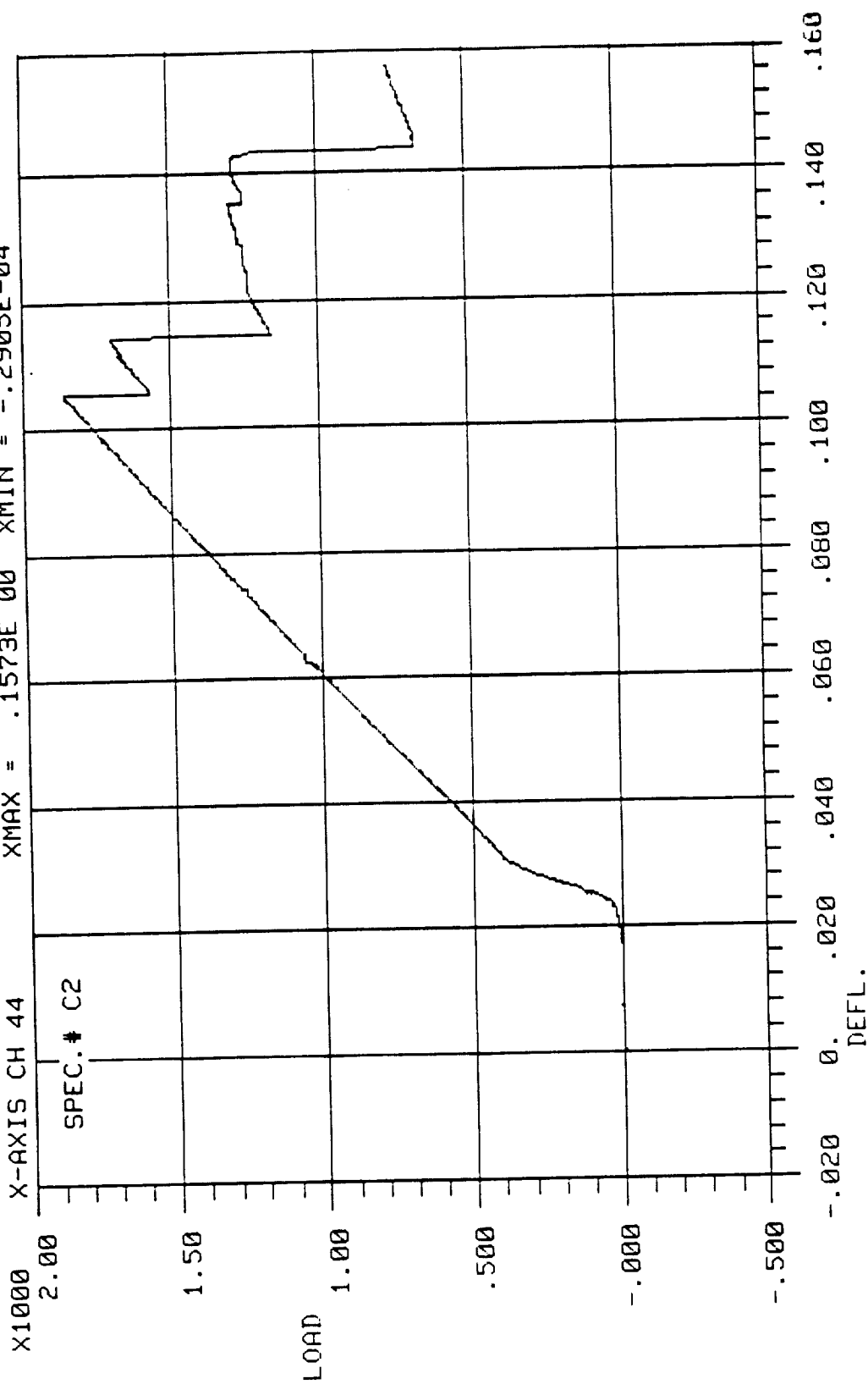


Figure 4-10: Load-deflection curve for stiffener pull-off specimen C2.

13:55 05/31/84

STIFFENER PULL OFF
TEST 25695 RUN 13
Y-AXIS CH 43
X-AXIS CH 44

YMAX = .1638E 04 YMIN = -.1831E 01
XMAX = .1415E 00 XMIN = -.2124E-03

X1000

SPEC. # C3

LOAD

DEFL.

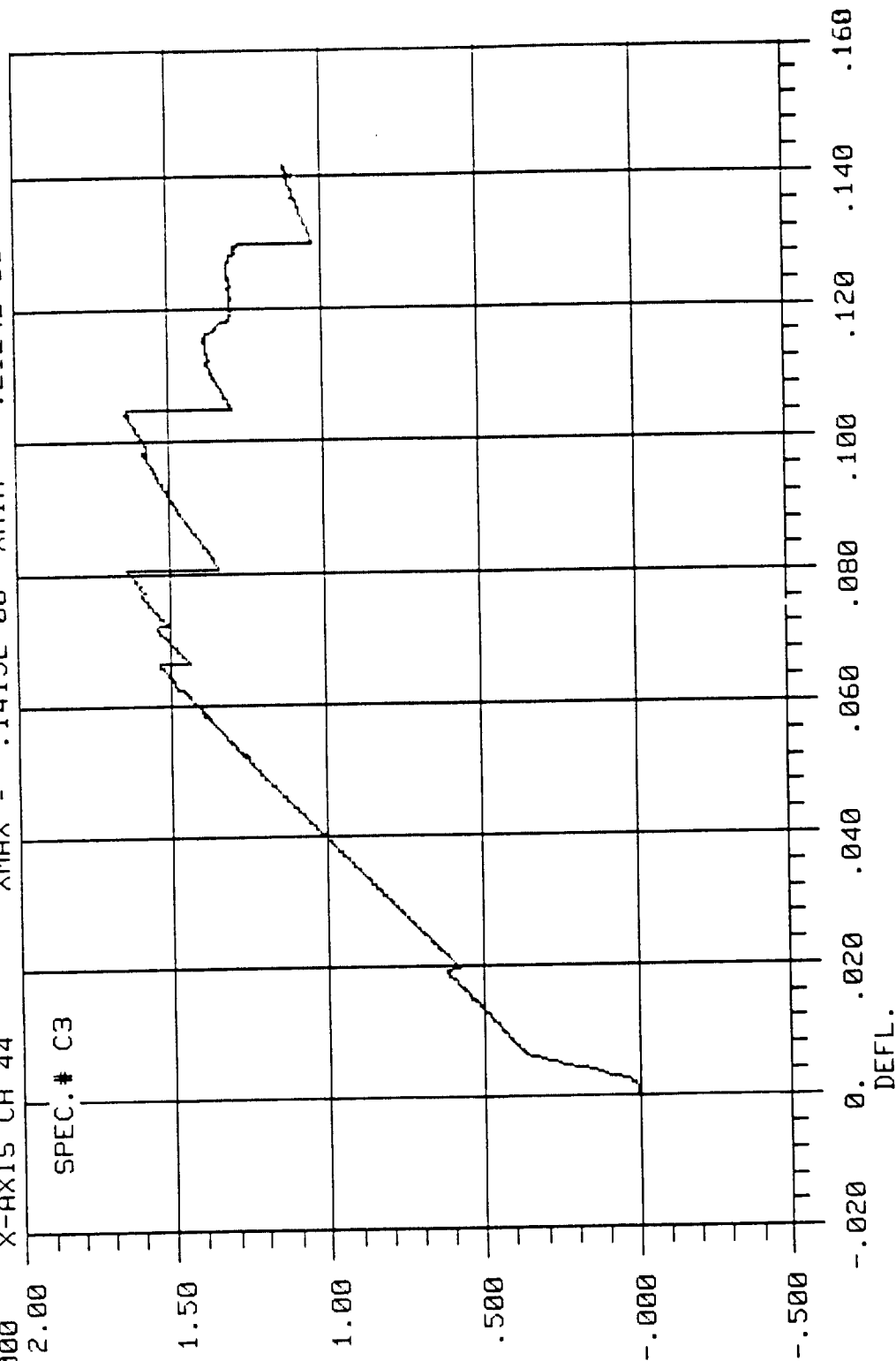


Figure 4-11: Load-deflection curve for stiffener pull-off specimen C3.

14:18 05/31/84

STIFFENER PULL OFF
TEST 25695 RUN 14
Y-AXIS CH 43
X-AXIS CH 44

YMAX = .1536E 04 YMIN = -.2437E 01
XMAX = .1528E 00 XMIN = -.2441E-03

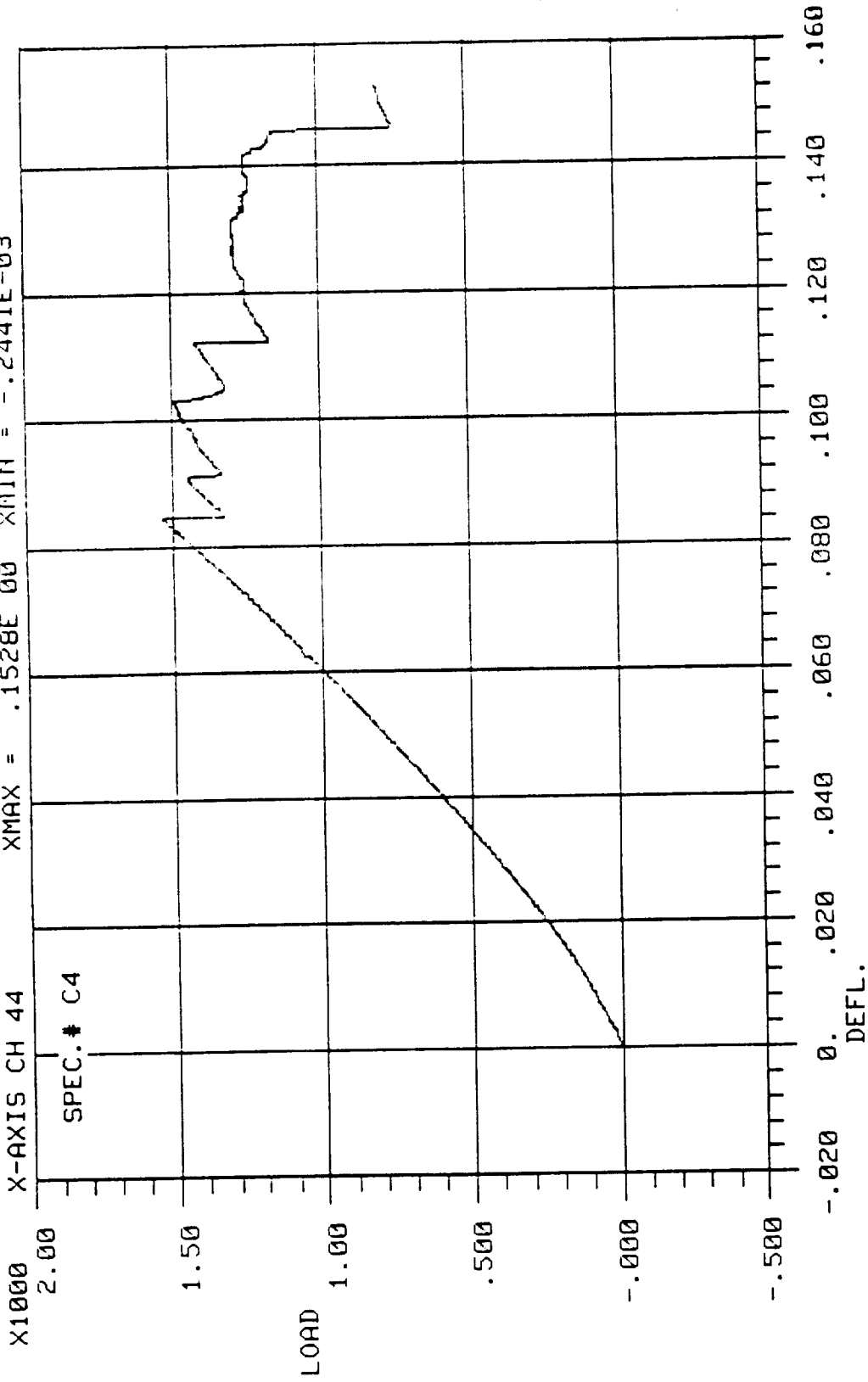


Figure 4-12: Load-deflection curve for stiffener pull-off specimen C4.

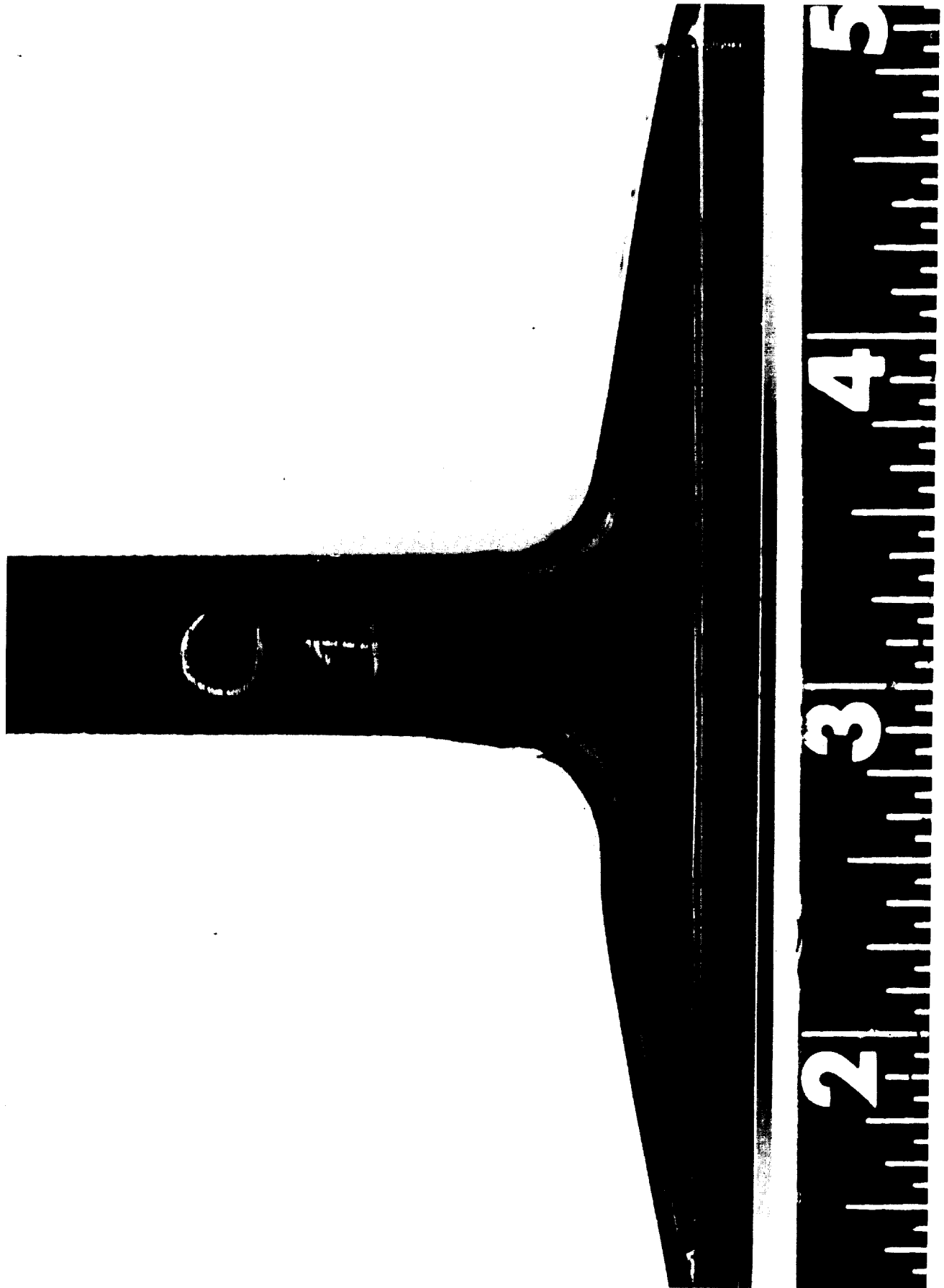


Photo No. 149616R

Figure 4-13: Stiffener pull-off specimen C1 failure.

ORIGINAL PAGE IS
OF POOR QUALITY

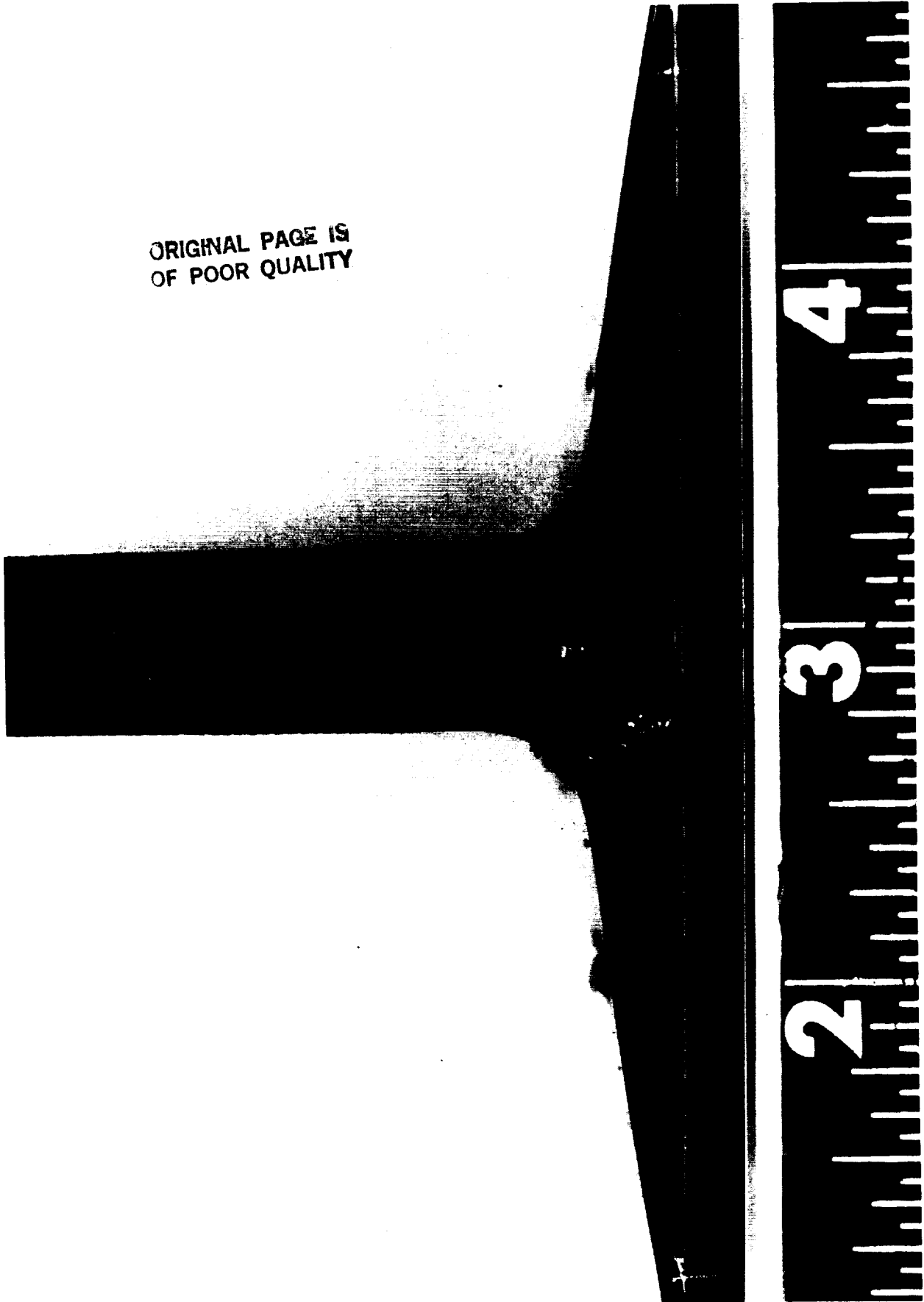


Photo No. 149617R

Figure 4-14: Stiffener pull-off specimen C2 failure.

ORIGINAL PAGE IS
OF POOR QUALITY

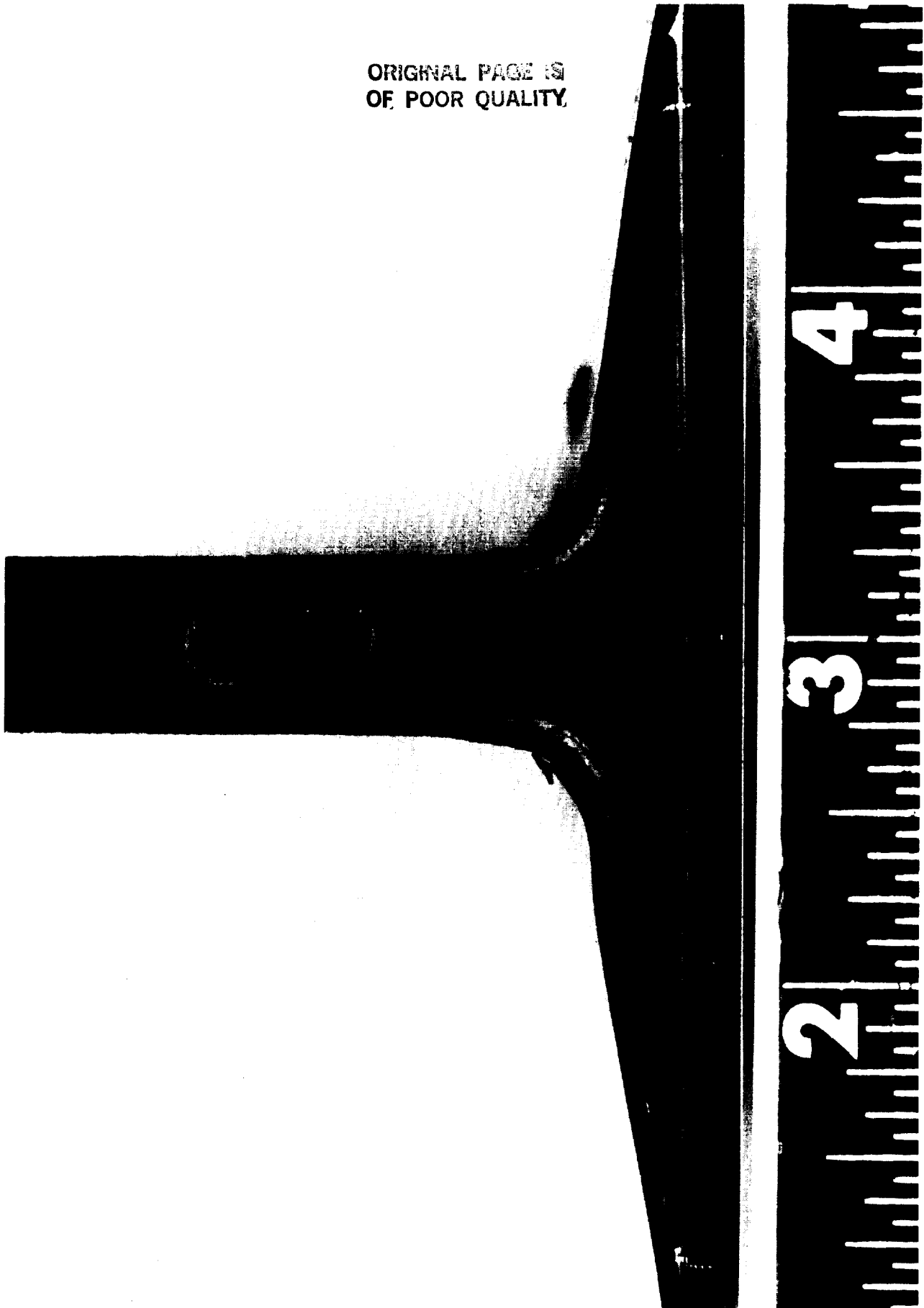


Photo No. 149618R

Figure 4-15: Stiffener pull-off specimen C3 failure.

ORIGINAL PAGE IS
OF POOR QUALITY

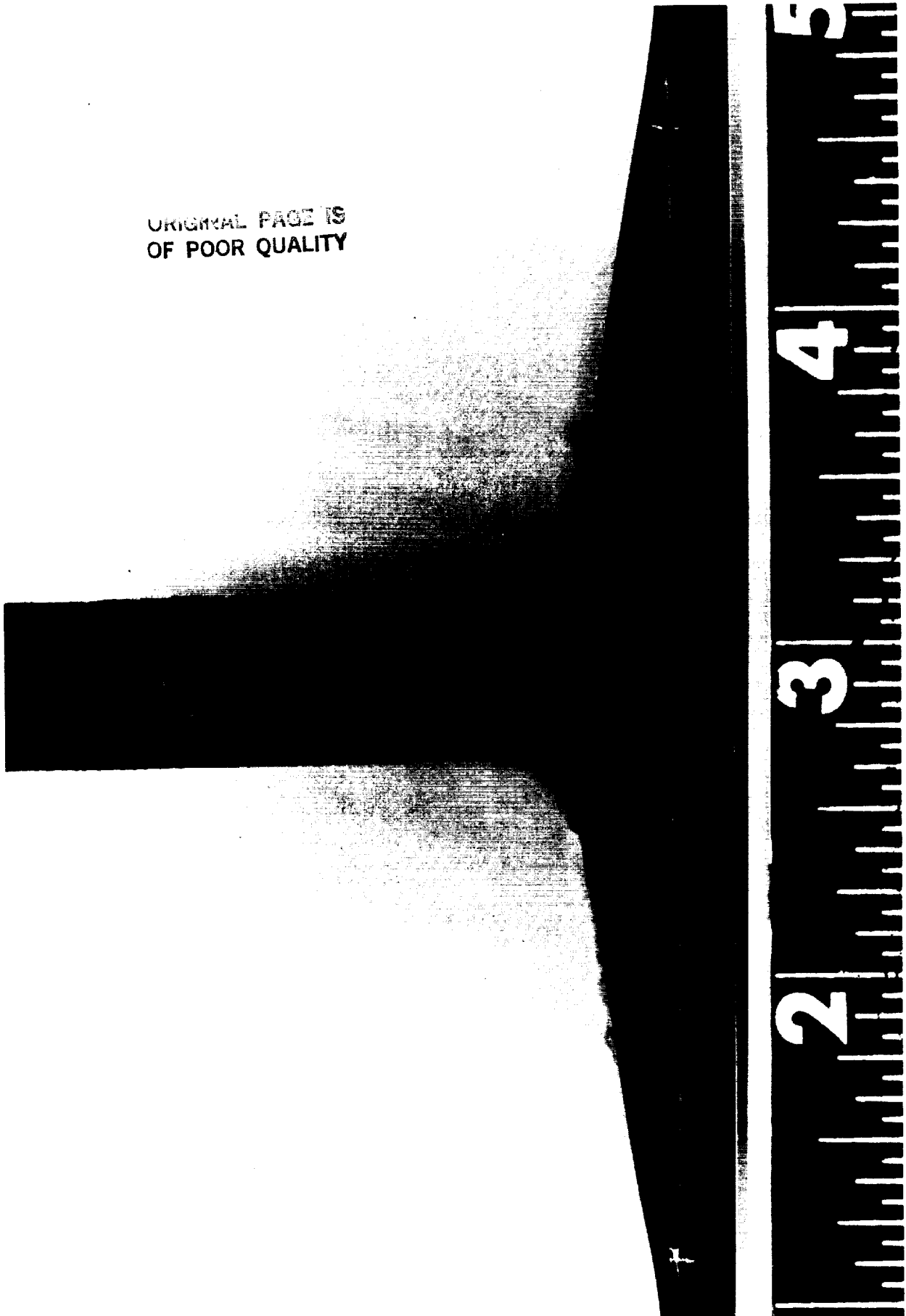


Figure 4-16: Stiffener pull-off specimen C4 failure.

4.4 STIFFENER SIDE LOAD TESTS (D)

Four stiffener side load specimens were machined from Panel #2 (Figure 4-3) and are identified as D1→ D4. Dimensions of each are given in Table 4.2. The test setup is shown in Figure 4-17. Load was applied through a pinned hinge to allow for alignment changes as the stiffener bends. The test fixture was off-center so that the load was applied perpendicular to the blade

tip. The upper end of the skin bears against the clamping bolt preventing it from moving upward during loading. Load was continuously applied at a displacement rate of 0.10 inch/minute to failure in a stroke controlled mode (except for D2).

The average failure load of the side load specimens was 1257 lbs as listed in Table 4.3. Load-Deflection plots for each specimen are given in Figures 4-18 through 4-21. Post test failure photographs are shown in Figures 4-22 through 4-25.

During the test of specimen D2 photographs were made after each major load drop which was accompanied with loud cracking noises and readily visible fracture. Loading was halted for a few seconds while each photograph was made. The sequence of damage is shown in Figure 4-26 and can be correlated to the load drops identified in Figure 4-19 as numbers 1 through 6. As shown the first crack initiated in the precured stiffener insert from near the bondline up the stiffener center. Delaminations then progressed along the skin two to three plies above the bond line with a small extension of the vertical mid-stiffener crack. Additional cracks then formed in the stiffener radius between the upstanding portion of the stiffener and the stiffener flange. At this point the load carrying capability had dropped by over 50% and the test was terminated. The other three specimens failed in a similar manner.

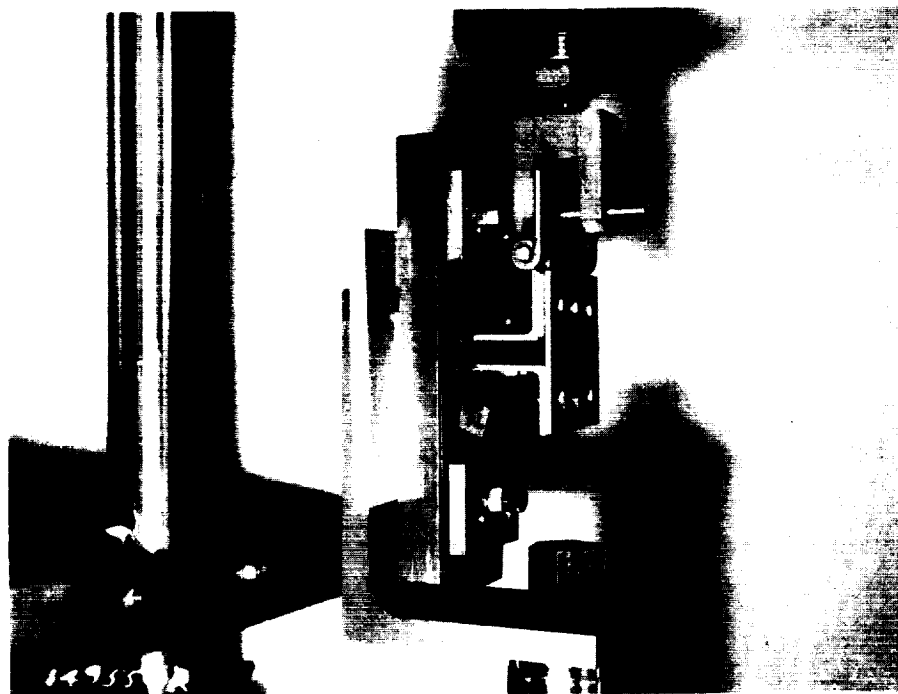
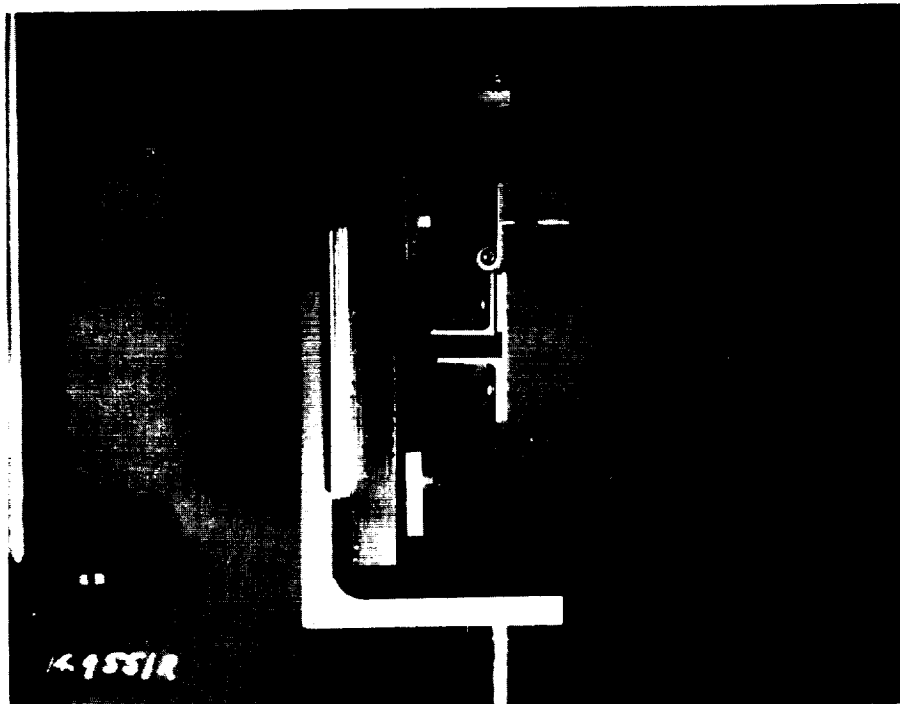


Figure 4-17: Stiffener side load test set-up.

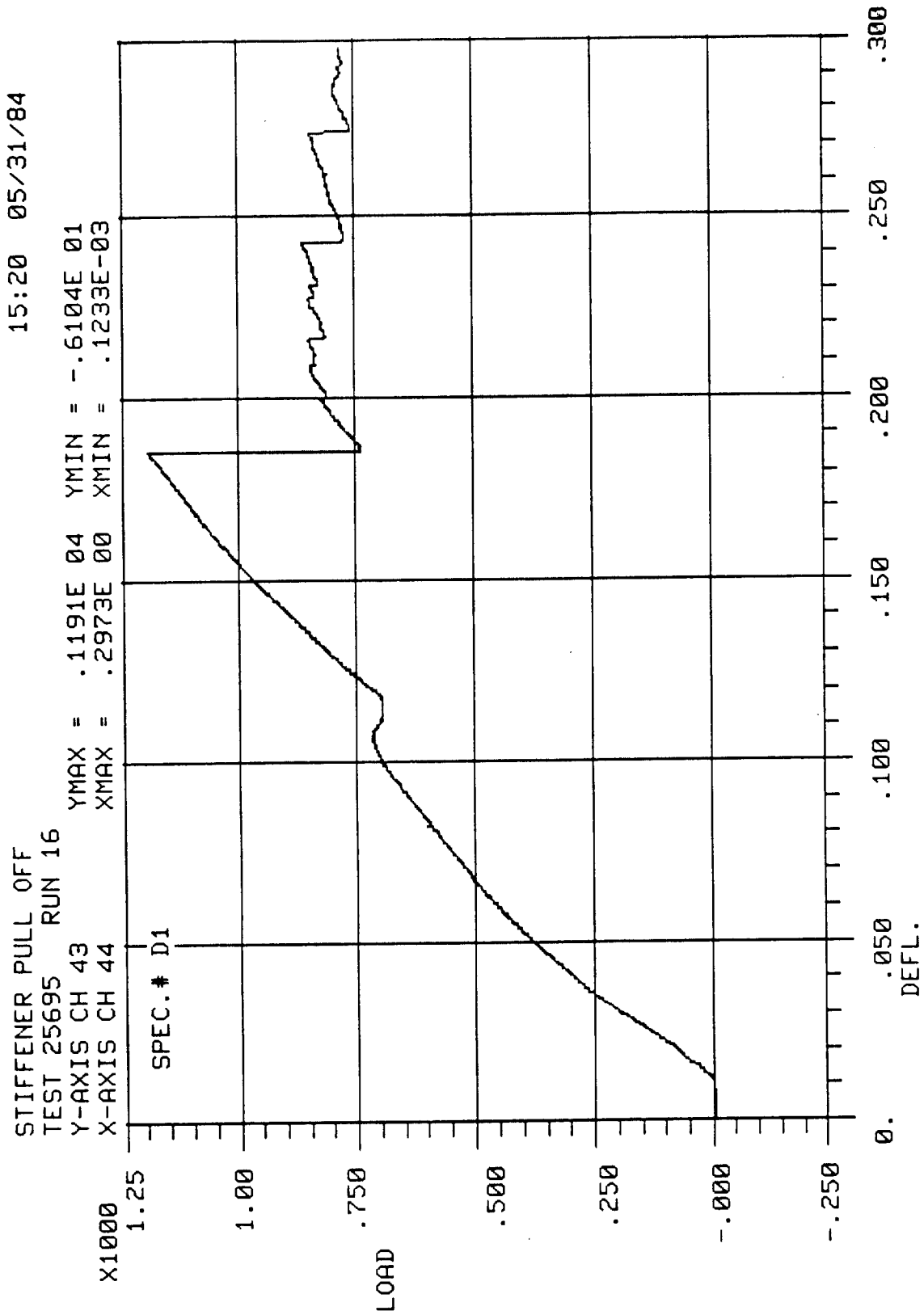


Figure 4-18: Load-deflection curve for stiffener side load specimen D1.

08:49 06/01/84

STIFFENER SIDE LOAD

TEST 25701 RUN 2

Y-AXIS CH 43

X-AXIS CH 44

YMAX = .1309E 04 YMIN = .3052E 01

XMAX = .3358E 00 XMIN = .3052E-03

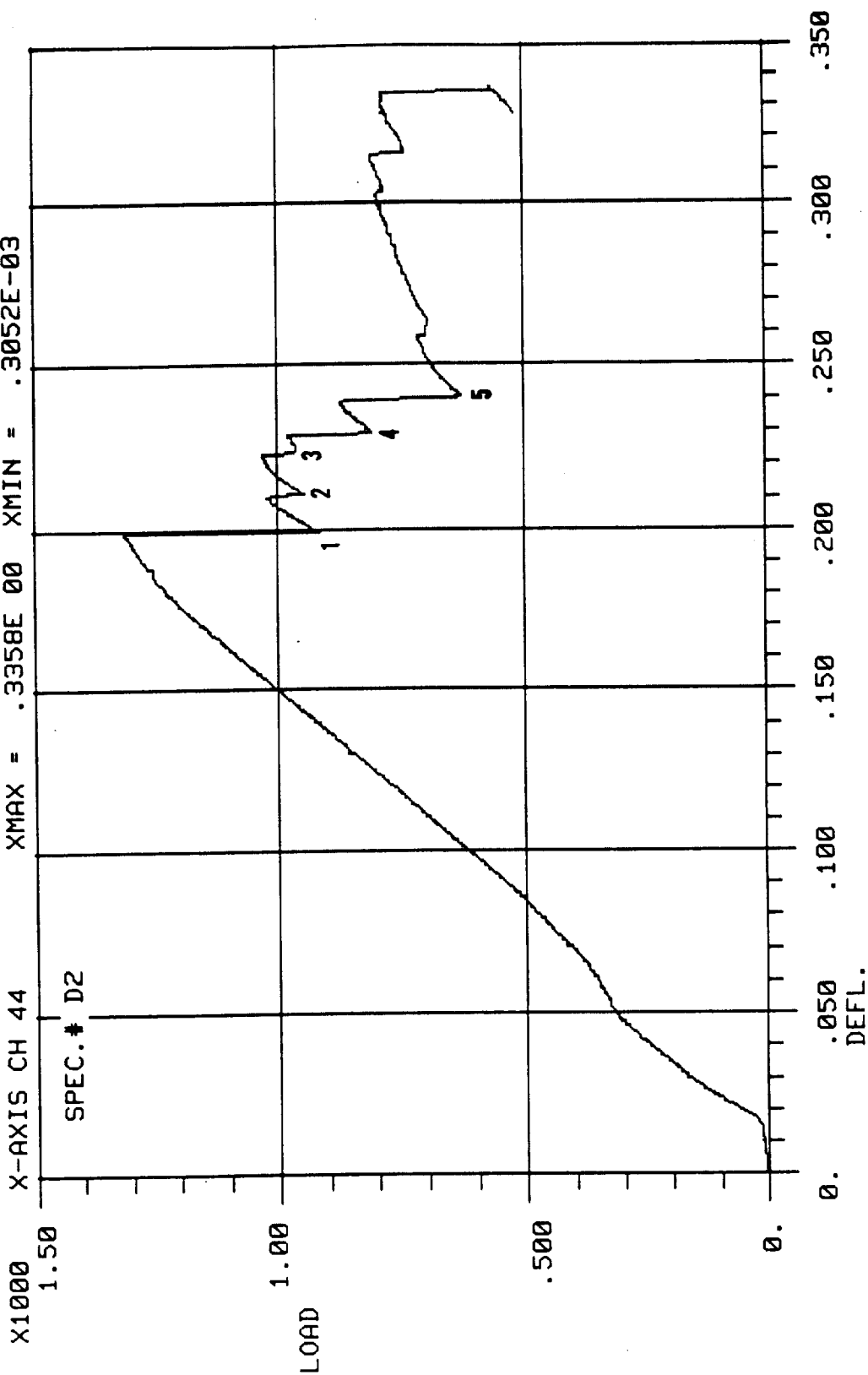


Figure 4-19: Load-deflection curve for stiffener side load specimen D2. Numbers refer to failure sequence in Figure 4-26.

11:12 06/01/84

STIFFENER SIDE LOAD

TEST 25701 RUN 4

Y-AXIS CH 43

X-AXIS CH 44

YMAX = .1220E 04 YMIN = .1837E 01

XMAX = .2240E 00 XMIN = .9190E-04

SPEC. # D3

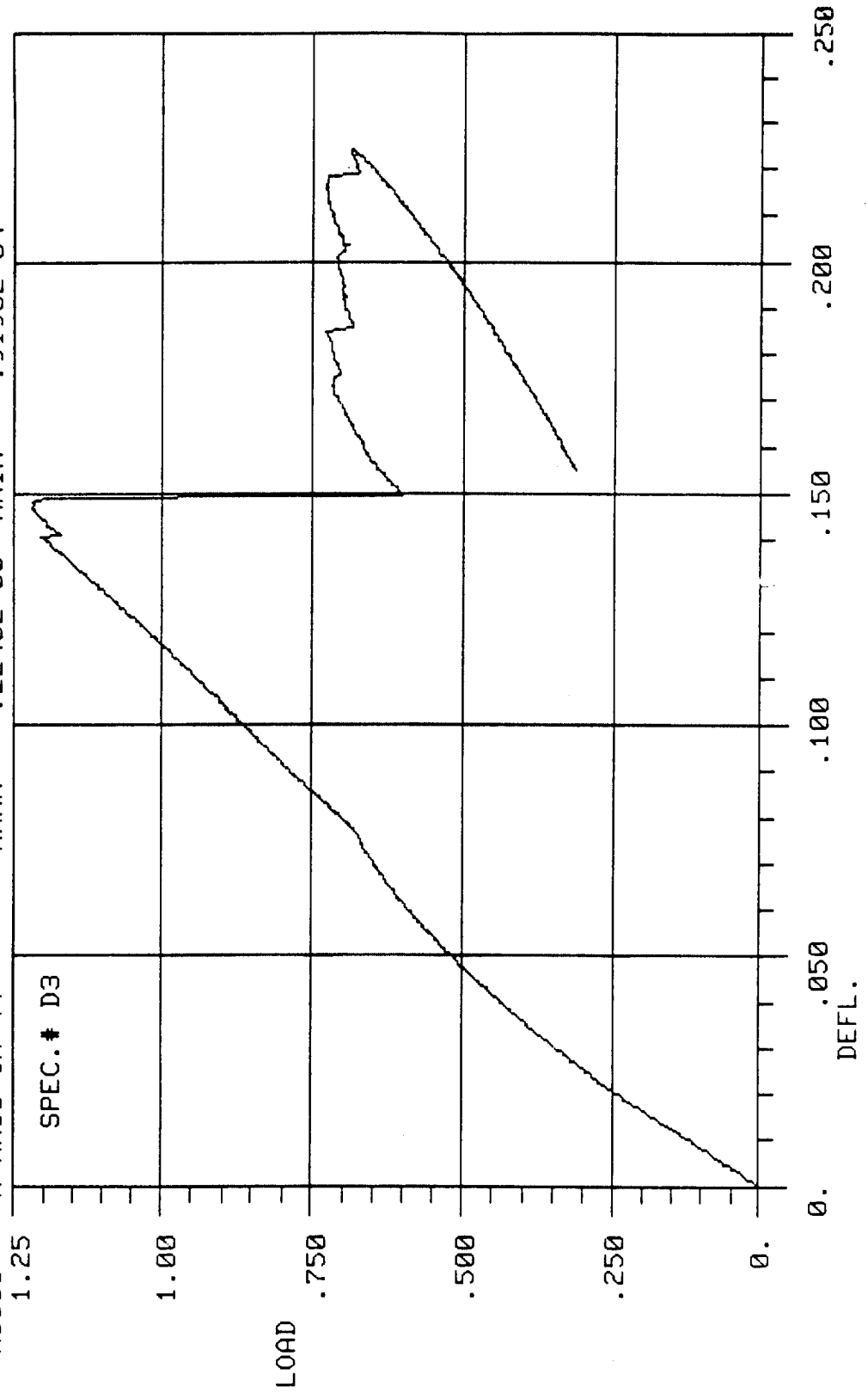


Figure 4-20: Load-deflection curve for stiffener side load specimen D3.

10:06 06/01/84

STIFFENER SIDE LOAD

TEST 25701 RUN 3

Y-AXIS CH 43

X-AXIS CH 44

YMAX = .1309E 04 YMIN = -.1827E 01

XMAX = .2680E 00 XMIN = .2140E-03

X1000

SPEC. # D4

LOAD

DEFL.

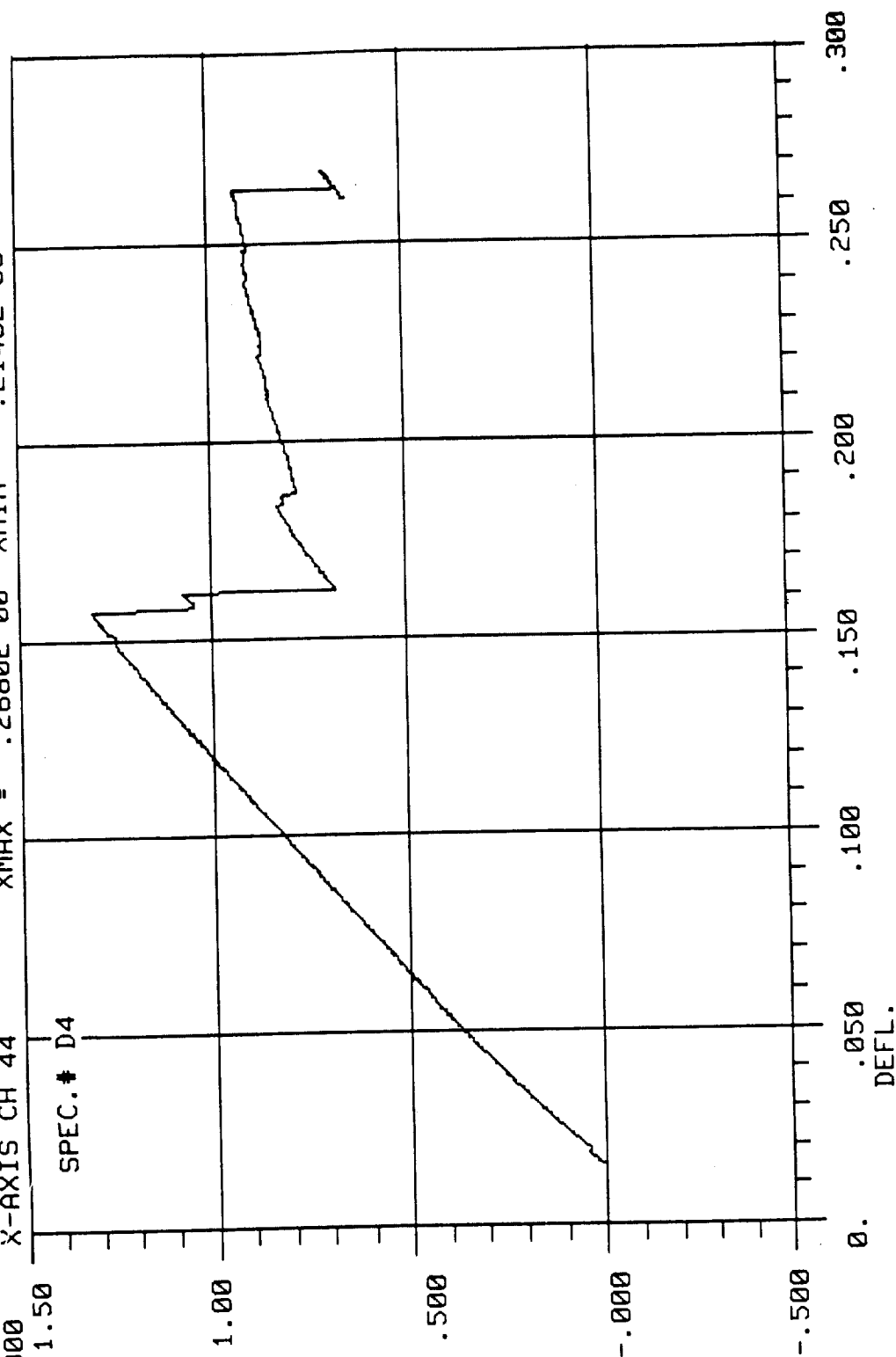


Figure 4-21: Load-deflection curve for stiffener side load specimen D4.

ORIGINAL PAGE IS
OF POOR QUALITY

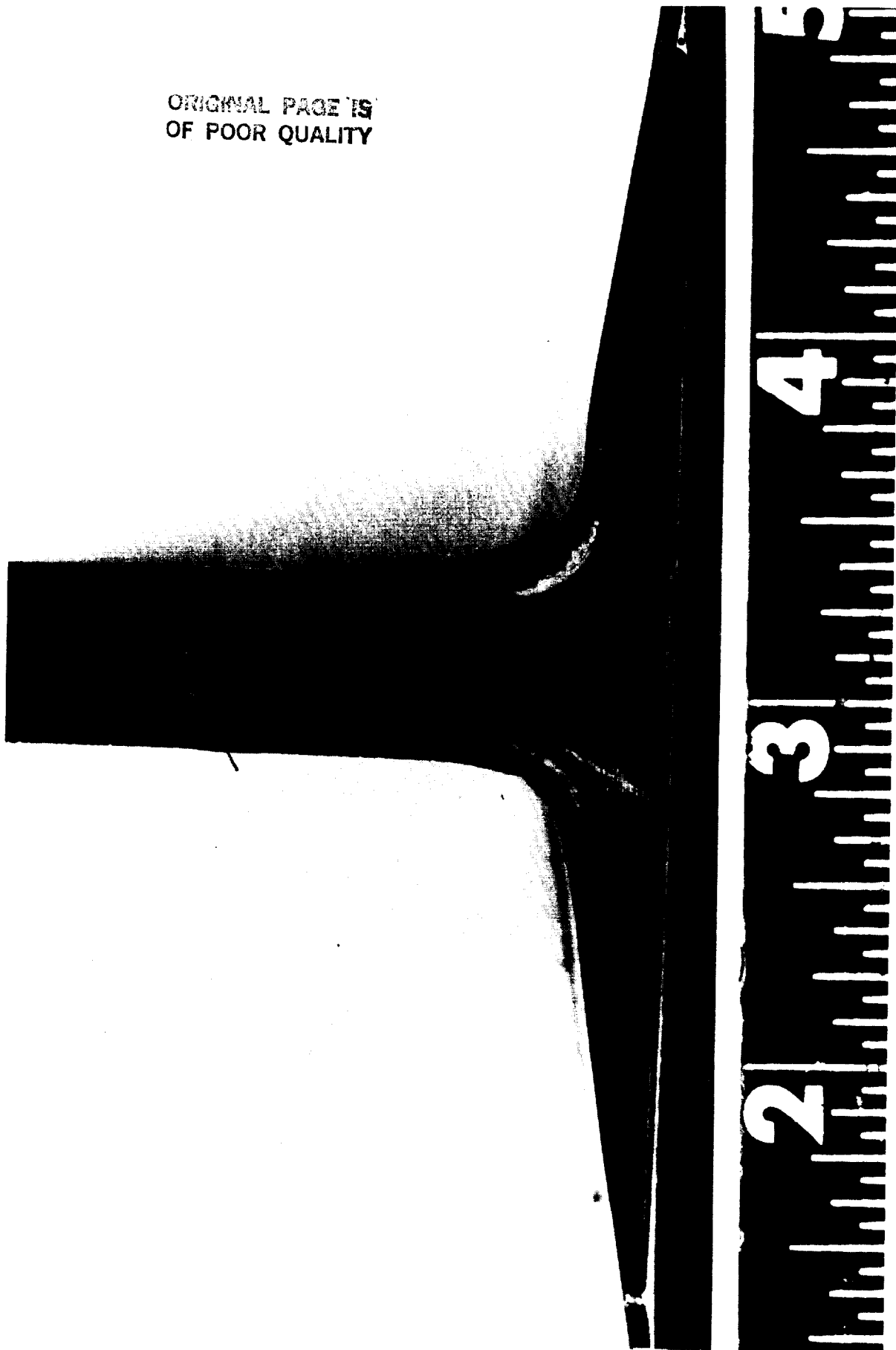


Photo No. 149620R

Figure 4-22: Stiffener side load specimen D1 failure.

ORIGINAL PAGE IS
OF POOR QUALITY

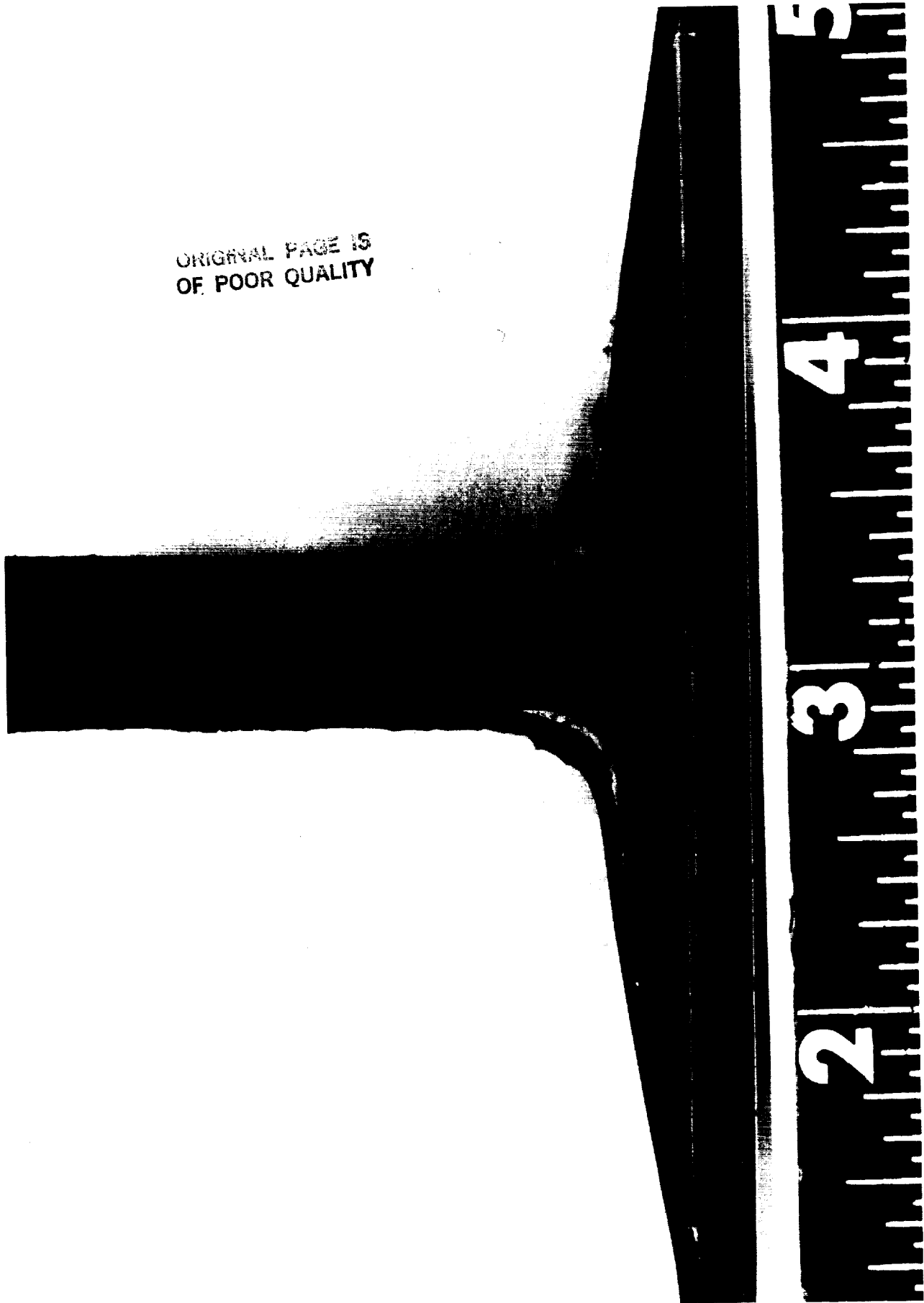


Photo No. 149621R

Figure 4-23: Stiffener side load specimen D2 failure.

ORIGINAL PAGE IS
OF POOR QUALITY

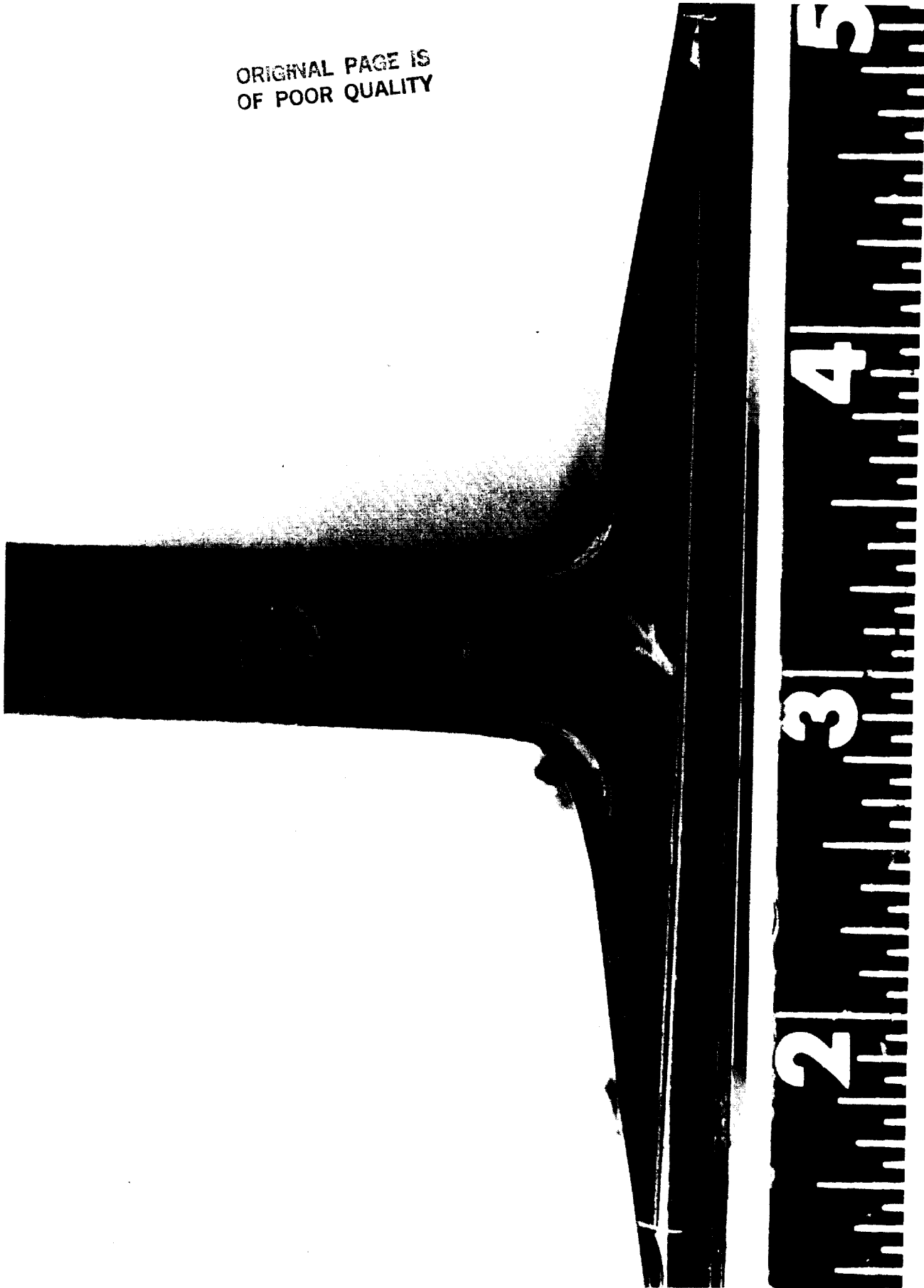


Photo No. 149622R

Figure 4-24: Stiffener side load specimen D3 failure.

ORIGINAL PAGE IS
OF POOR QUALITY

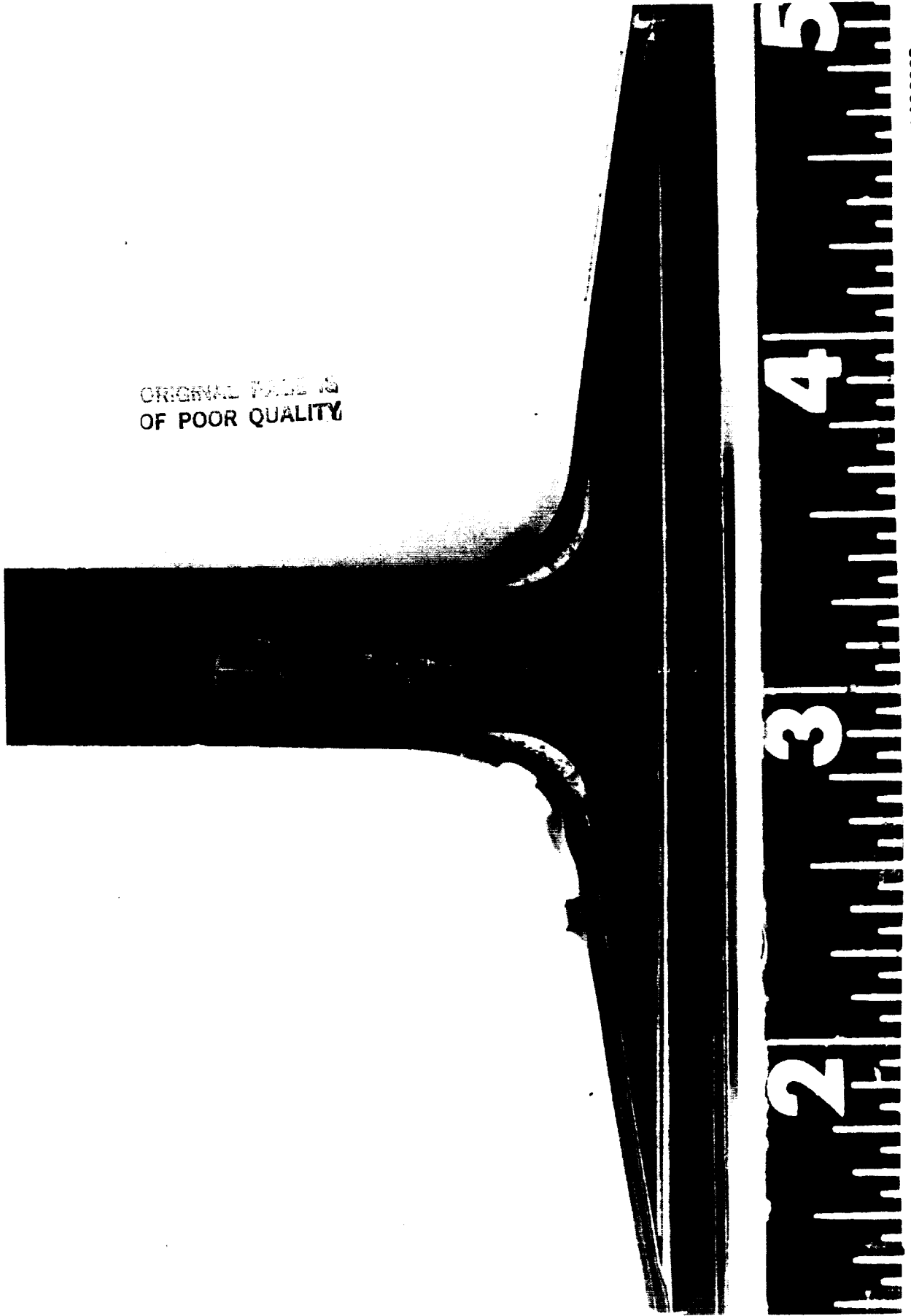
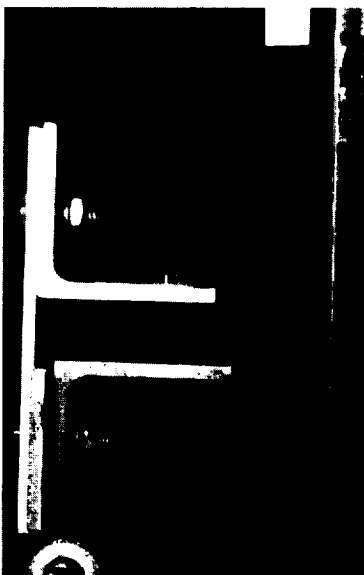
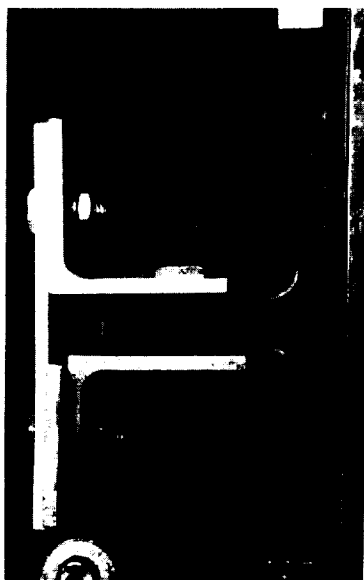


Photo No. 149623R

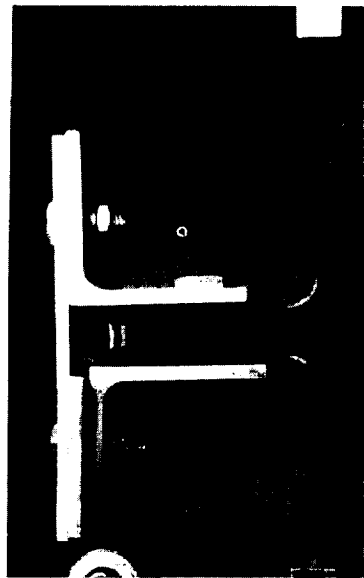
Figure 4-25: Stiffener side load specimen D4 failure.



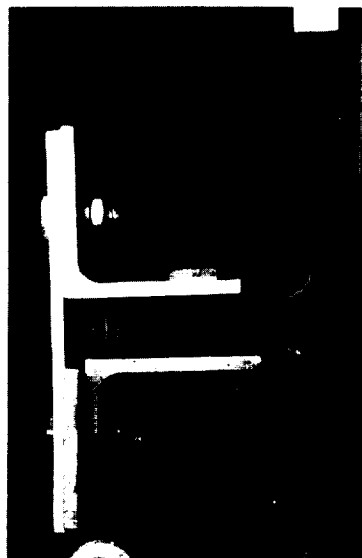
0 No Load



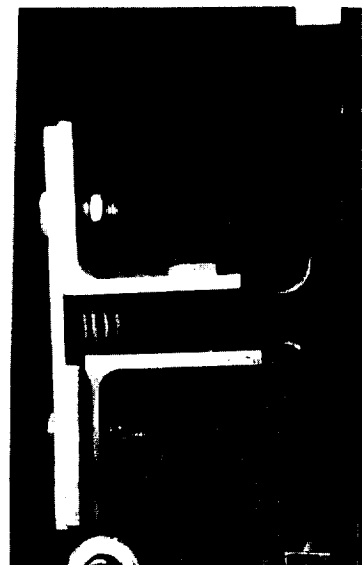
1 First crack



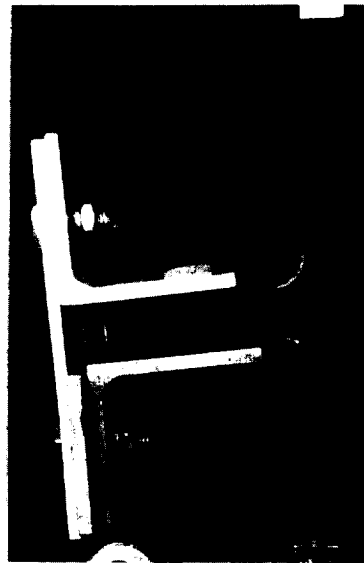
2



3



4



5

Figure 4-26: Sequence of damage progression in stiffener side load test. Photos were taken after each load pop after the load had dropped off.

Copyright 2000 by Lockheed Martin Corp.
All rights reserved.

4.5 FAIL SAFE TESTS (E)

Two specimens were tested in a setup designed to load the joint between the stiffener and the surrounding panel in the same manner that it would be loaded if a stiffener in a wing were broken under load. Figure 4-27 shows the test arrangement, the test hardware was configured so that load was applied along the specimen centroid. The skin piece was attached to a steel plate with 16 NAS 1103-11 bolts on either side of the blade stiffener, the stiffener was attached to the steel side rails on both sides of the blade stiffener by 17 NAS 1104-29 bolts. Both ends of the test assembly were pin loaded to allow for rotation during test.

Ten strain gages (CEA-00-125-UW-120) were attached as shown in Figure 4-28. A cutout was made in the skin side steel plate and in one side rail on the stiffener over the gages. During bolt torquing, a side rail damaged gages 4A and 5A because of insufficient clearance, so the cutouts were enlarged for the second test.

Tests were conducted in a 200 kip MTS hydraulic machine. On specimen E-1, tensile loading was applied at 0.05 in./min. to failure. Specimen E-2 was accidentally loaded at 5 in./min. and was not a valid test. Both specimens failed interlaminarly in the base of the stiffener two to three plies above the skin/stiffener bond line. The design requirement for the failsafe specimen was 54,500 pounds, based on the stiffener pitch of 6.00 inches, the design axial load intensity of 12,972 lb/in, and 70 percent of the axial load being carried in the stiffener. The one valid specimen failed at 57,870 pounds. Failure occurred catastrophically into two pieces. Figures 4-29 and 4-30 and 4-31 show the failure overall and closeup. Figure 4-31 shows how the fastener heads pulled through the stiffener runout. Figure 4-32 is an end-on view showing the failure plane two to three plies above the skin/stiffener bond line.

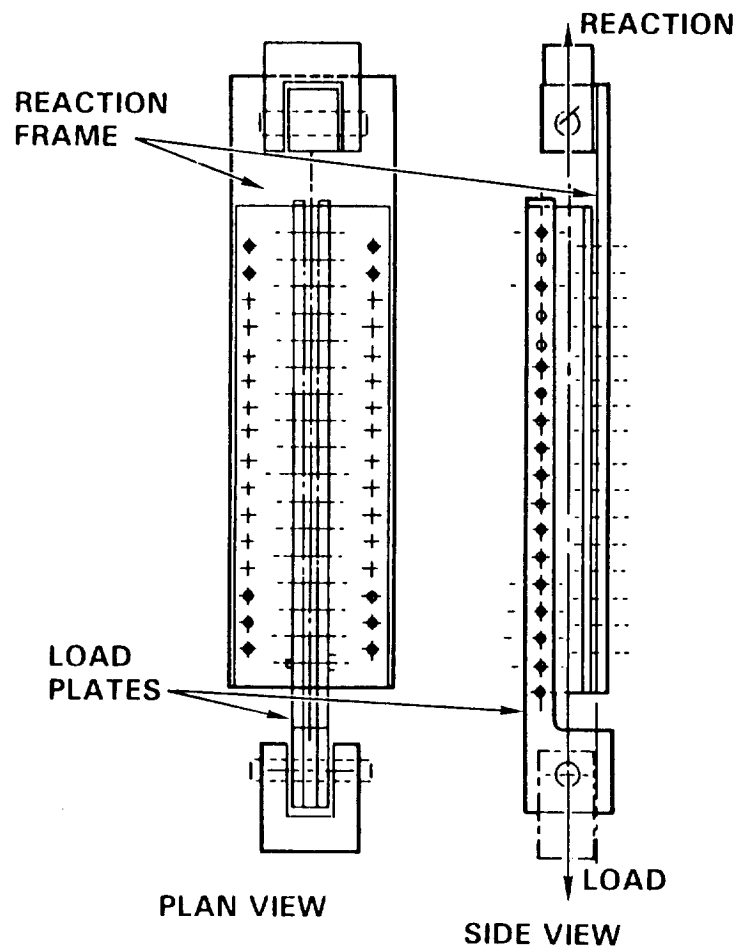
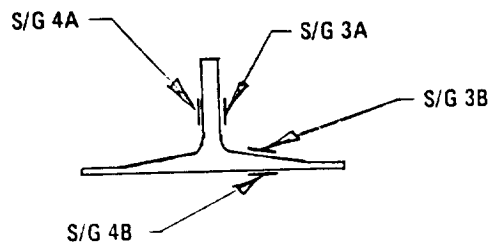
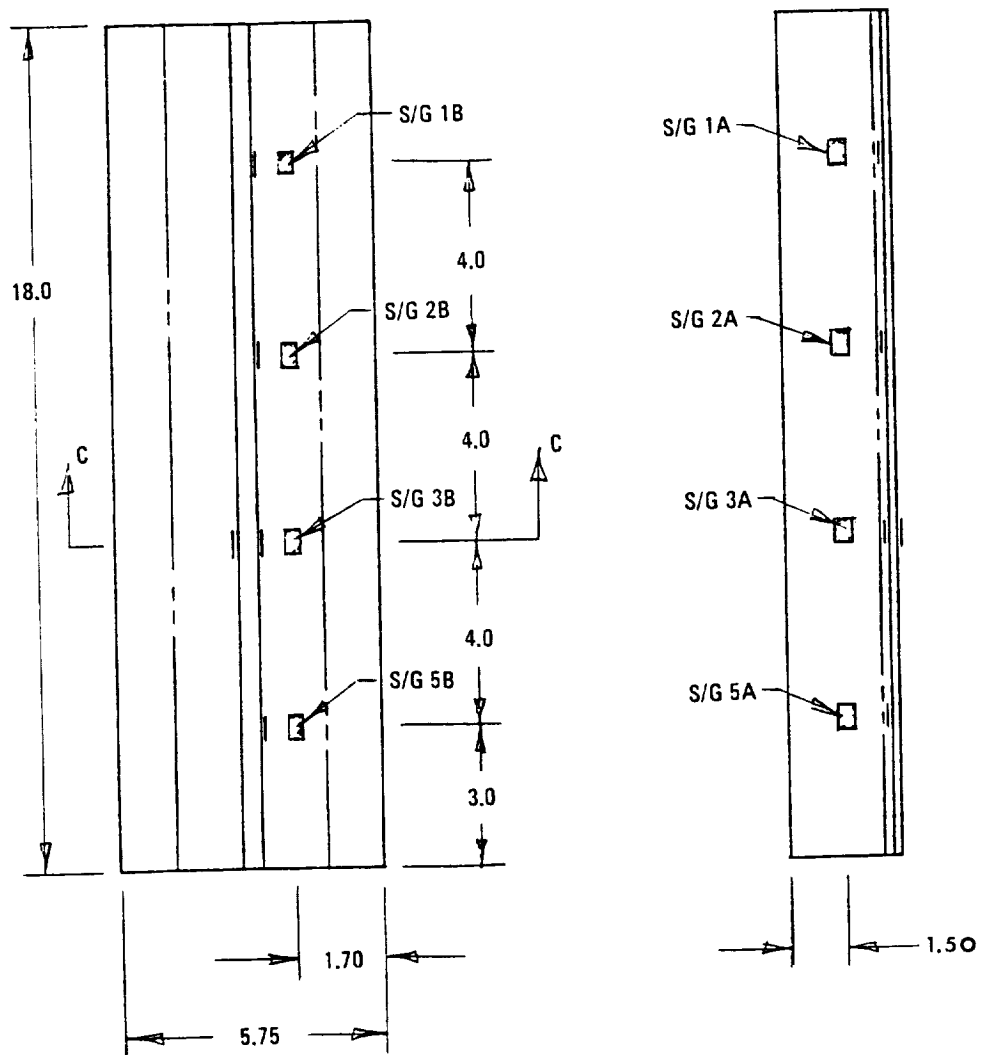


Figure 4-27: Stiffener failsafe test set-up.



SEC C-C

Figure 4-28: Fail safe specimen strain gage locations.

ORIGINAL PAGE IS
OF POOR QUALITY

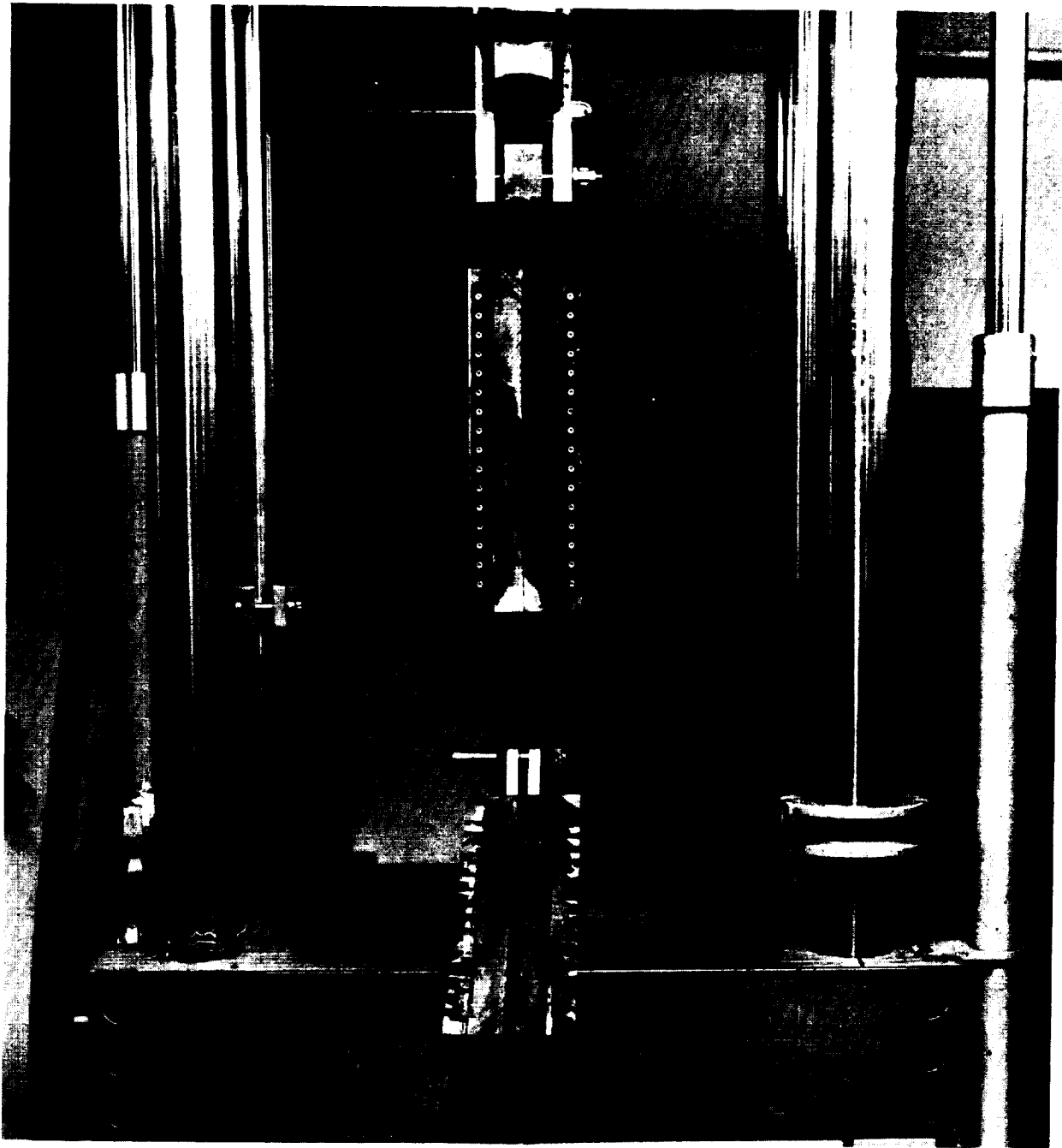


Photo No. 149753

Figure 4-29: Failure of fail-safe specimen.

ORIGINAL PHOTO OF
OF POOR QUALITY

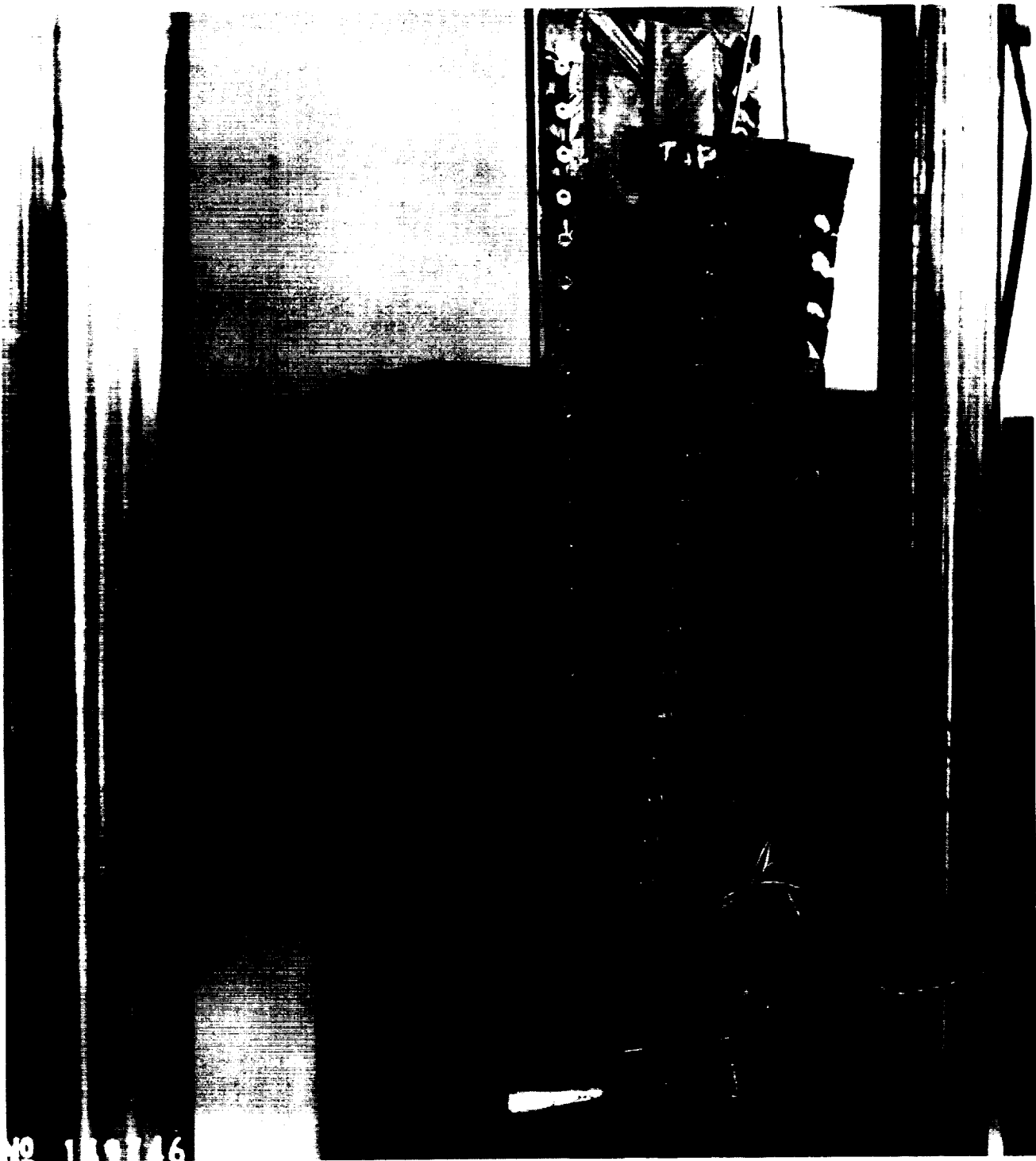
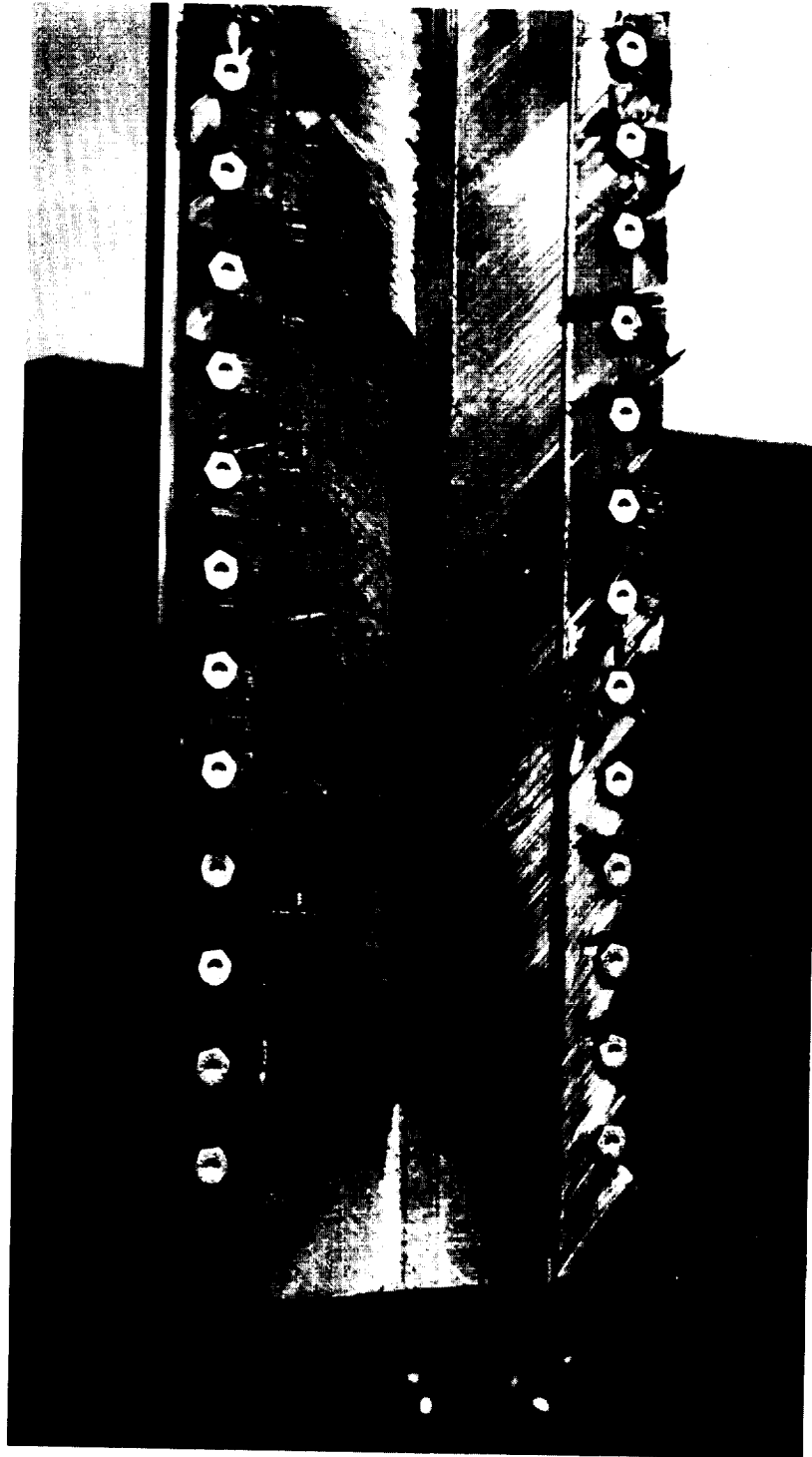


Figure 4-30: Failure showing fastener head tearout.

ORIGINAL PAGE IS
OF POOR QUALITY



149744R

Figure 4-31: Closeup of skin side of failed fail-safe specimens.

ORIGINAL PAGE IS
OF POOR QUALITY

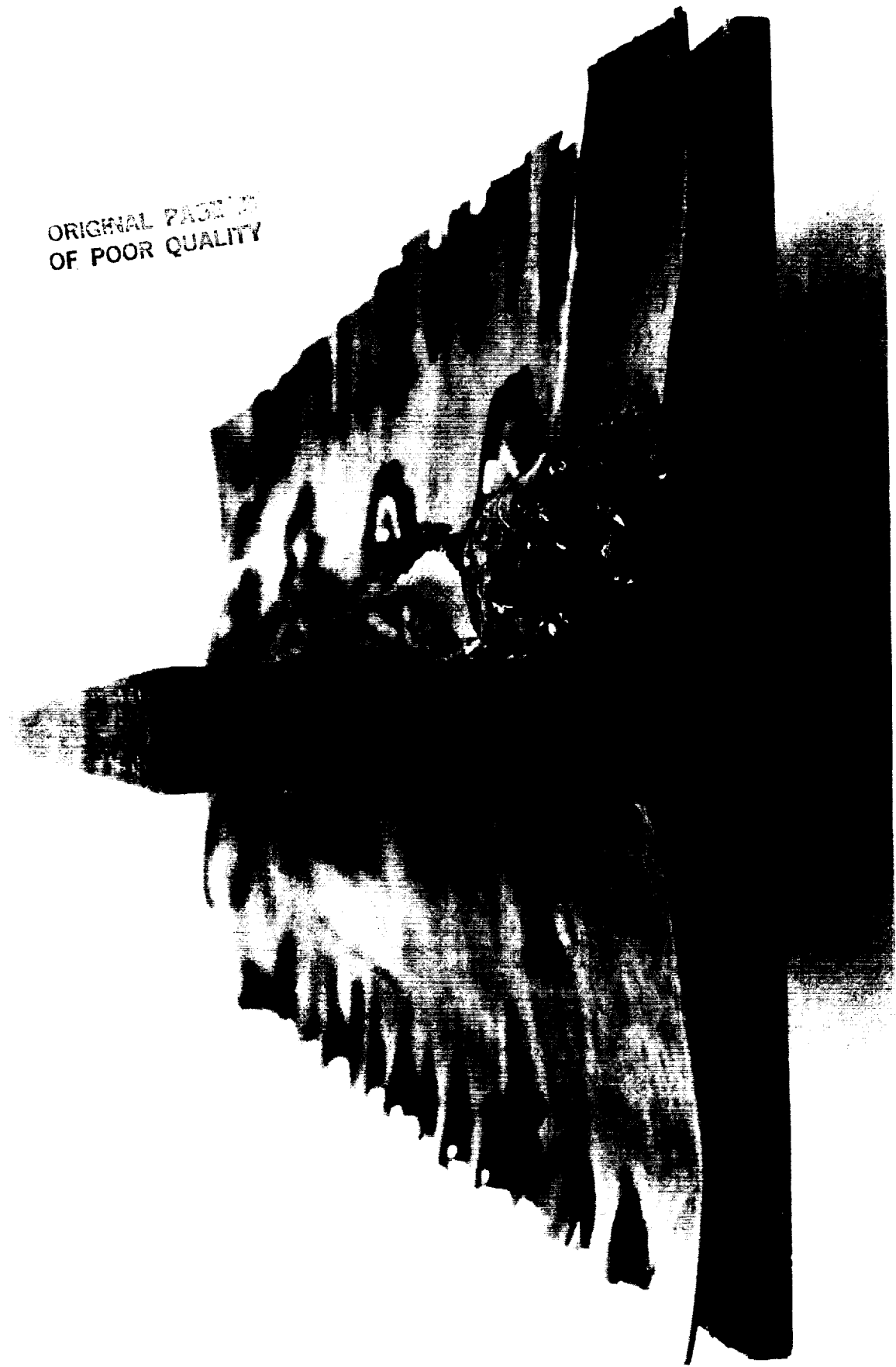


Photo No. 149957R

Figure 4-32: Fail safe specimen failure showing delamination above the secondary bond line.

Load-deflection and load-strain curves are given in Figures 4-33 through 4-36. Strain response is not linear with load particularly for the "A" gages. This was partly due to their close proximity to the fastener holes and being under the edge of the clamped loading bar. Audible damage occurred at about 32 kip which resulted in some load redistribution as noted on Figure 4-35. The initial offset in gage 1A in Figure 4-36 was due to the loading bar being too close to the gage, rendering the data invalid.

4.6 UNDAMAGED STIFFENER COMPRESSION TESTS (A)

A compression test was conducted on one 18 inch long by 5.75 inch wide single blade stiffened panel with no prior damage. Dimensions of the panel are given in Table 4.4. The specimen was instrumented with six strain gages in back-to-back pairs as shown in Figure 4-37. Panel ends were machined flat and parallel prior to potting in welded steel boxes with the inside and outside of the bottom plates also machined flat and parallel. The panel centroid was positioned in the center of the potting box. The potting material was Kerstone, a ceramic with approximately a one-half percent volumetric expansion during curing. Kerstone was selected due to its low cost, non-corrosive effects on steel, lack of contraction on cure, and ease of removal from the boxes after test without using a parting agent. Due to the mass of the potting boxes two steel angles were attached to two diagonal corners of the potting boxes after potting to prevent any bending loads being applied to the panel during handling. These angles were removed just prior to testing.

Compression testing was done in a 400 kip static test machine. A thin coat of Devcon A was applied to the bottom of the lower potting box prior to installation. After installation a 1/4 inch thick layer of Devcon was applied to the top of the upper potting box. The test machine head was then lowered until the Devcon was squeezed out on all sides, giving a thickness

11:44 07/05/84

FAIL SAFE SPECIMEN E-1

TEST 26042 RUN 2

Y-AXIS CH 43

X-AXIS CH 44

YMAX = .5787E 05 YMIN = -.1526E 03

XMAX = .3506E 00 XMIN = .2930E-02

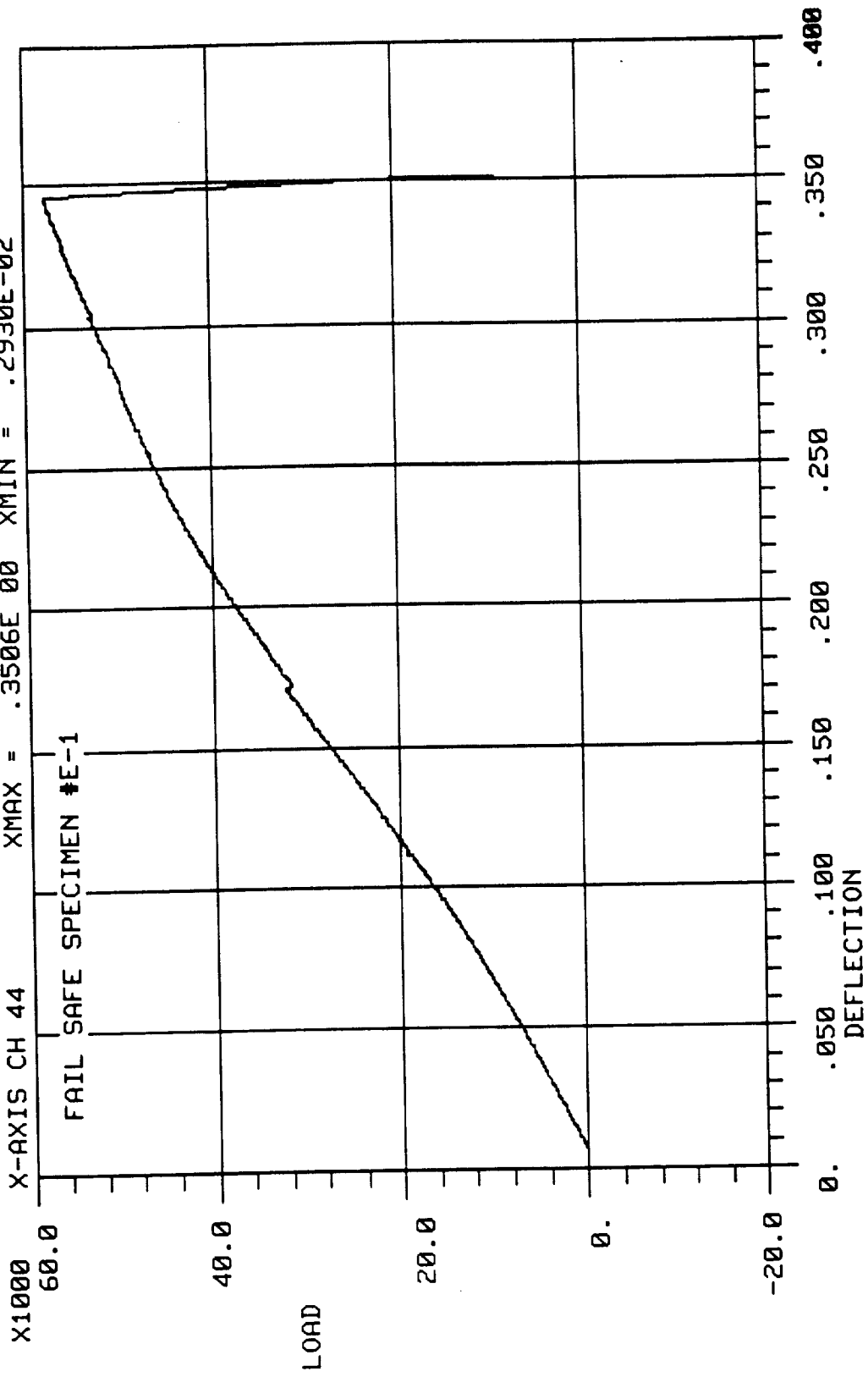


Figure 4-33: Load-deflection curve for fail-safe specimen E1.

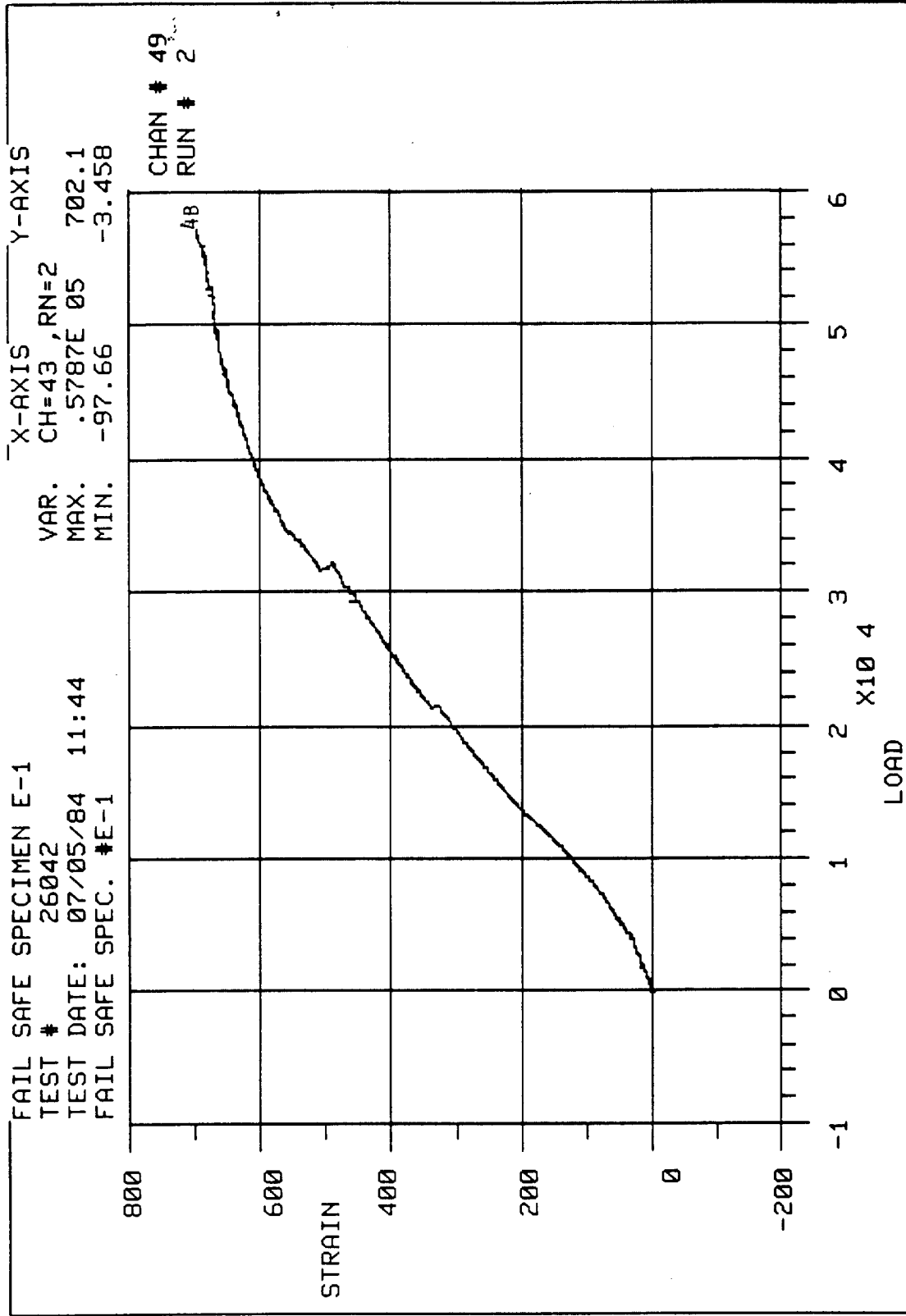


Figure 4-34 Load-strain curve for fail-safe specimen E1, strain gage in location 4B.

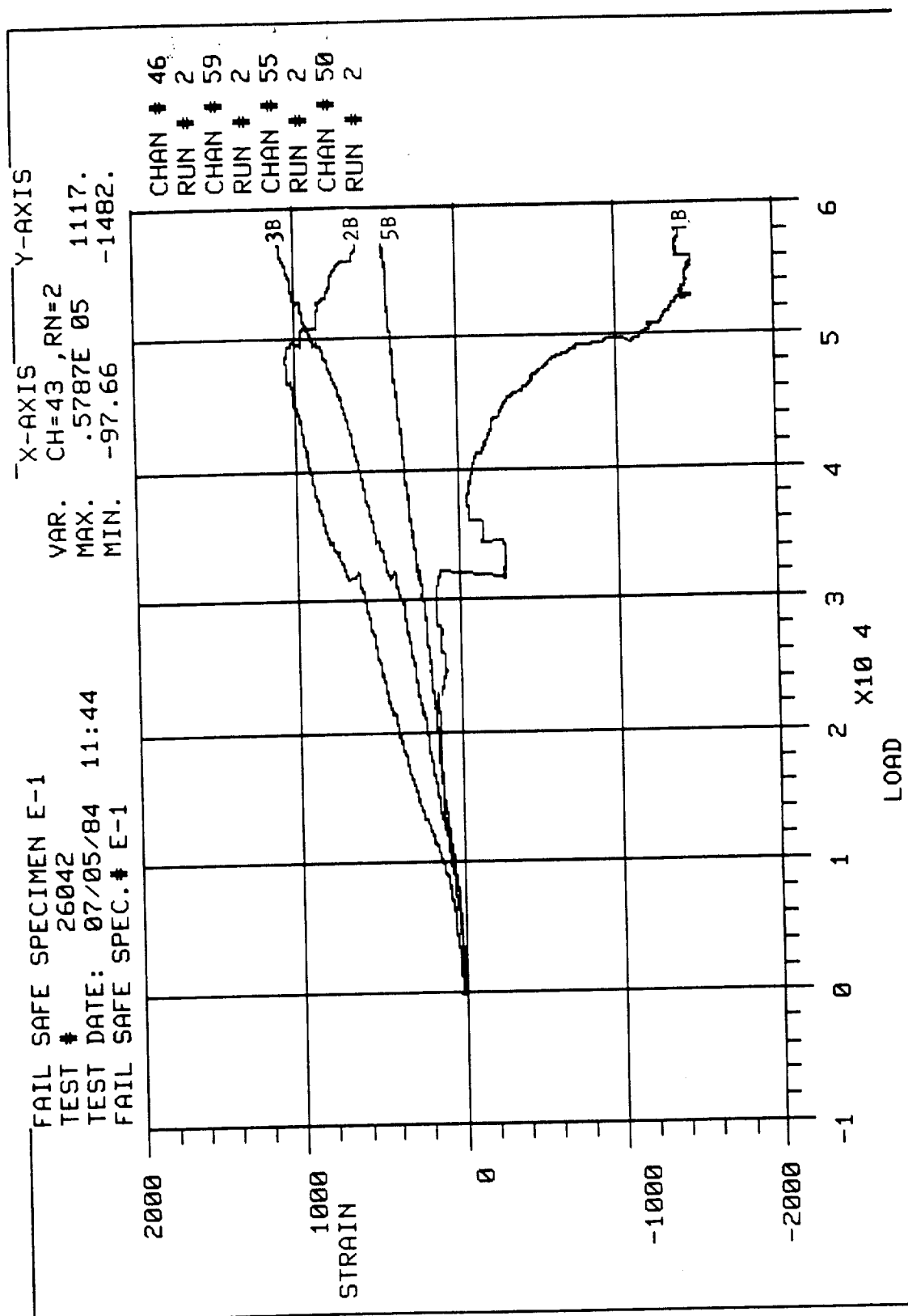


Figure 4-35: Load-deflection curve for fail-safe specimen E1, strain gages in locations 1B, 2B, 3B and 5B.

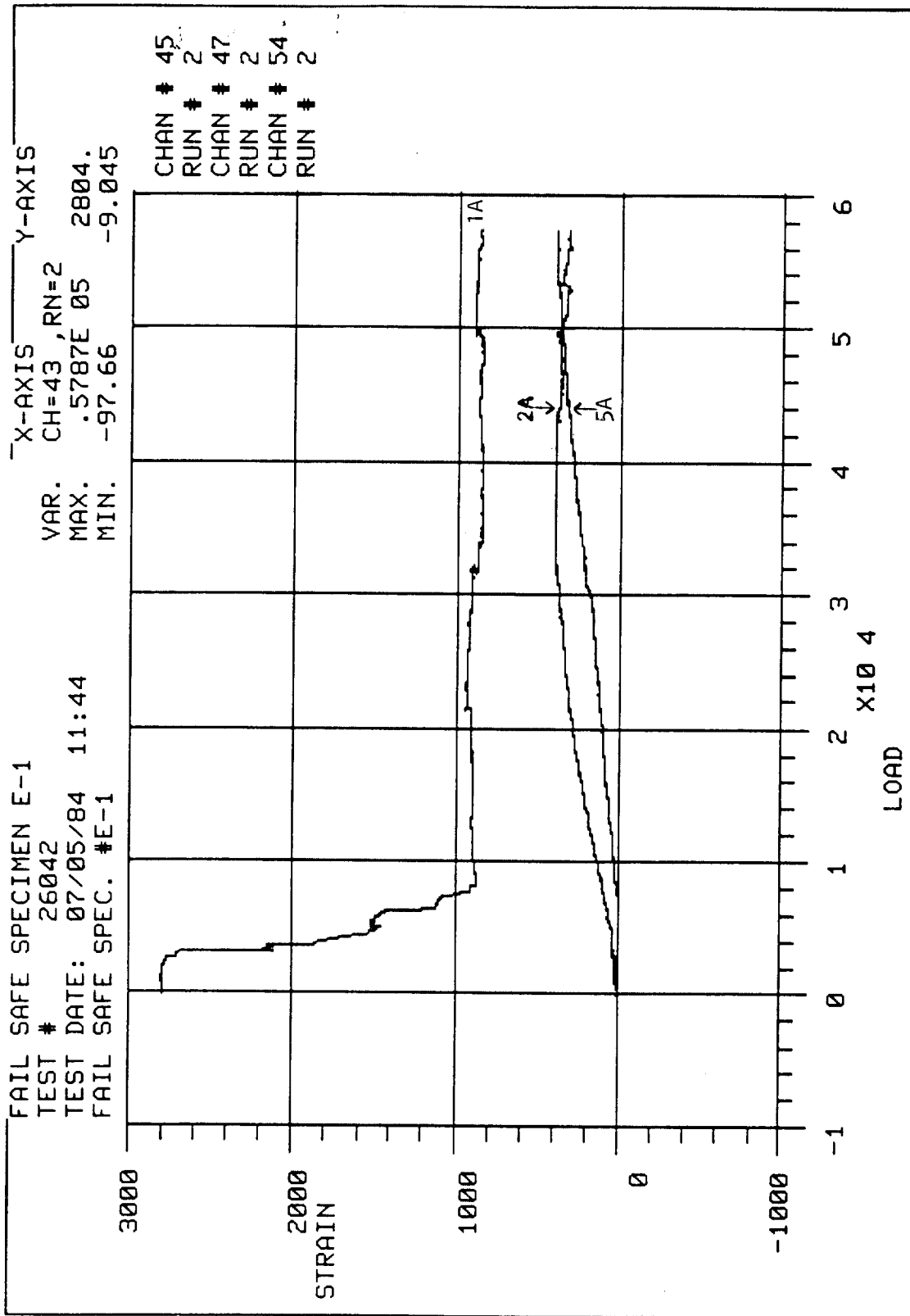


Figure 4-36: Load-deflection curve for fail-safe specimen E1, strain gages in locations 1A, 2A, and 5A.

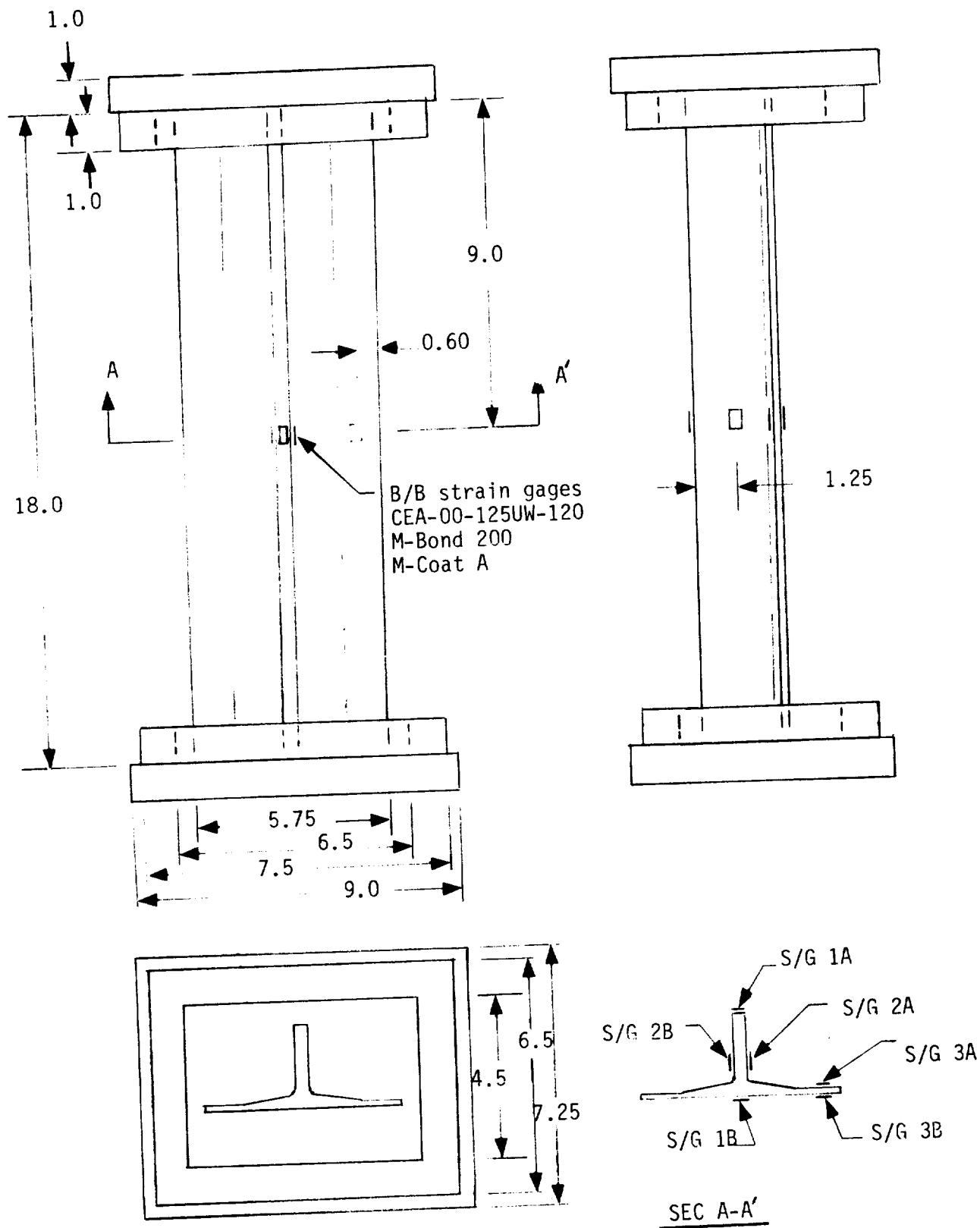


Figure 4-37: Undamaged stiffener panel test configuration and strain gage layout.

of approximately 1/8 inch. The machine head was locked into place and allowed to sit overnight to obtain a full cure of the Devcon. Figure 4-38 shows the panel just prior to testing. Testing then proceeded at a head deflection loading rate of 0.05 inches/minute to failure. The predicted failure load of the undamaged stiffener specimen was -275,000 pounds based on the stiffener critical buckling strain of 10,500 μ in/in. The specimen failed at -189,500 pounds and a maximum strain level of -8,783 μ in/in.

The panel failed in a combined compression bending mode in both the skin and stiffener near the top end. Which area failed first was not determined because of the catastrophic nature of the failure. Figures 4-39 through 4-41 show close-ups of the failure area from different angles.

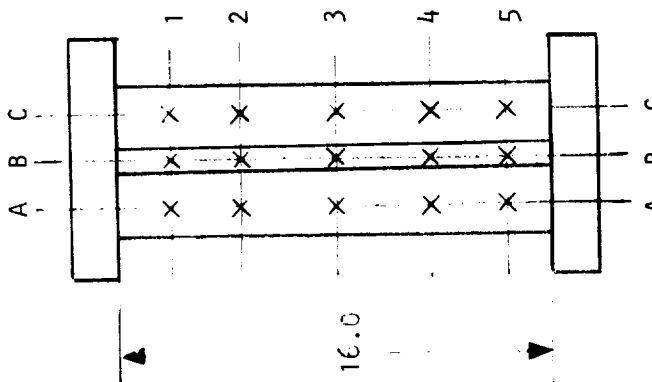
Load-deflection and load-strain plots were made and are presented in Figures 4-42 through 4-45. Strain gage identification/locations are shown in Figure 4-37. Higher strains (Figure 4-43) were recorded in the skin directly under the stiffener than on the stiffener top (gages 1A and 1B in Figure 4-37). The other back-to-back strain gage pairs showed no divergence to failure (Figures 4-44 and 4-45).

After removal from the potting boxes the panel ends were inspected for bearing or brooming failure - none was found. The potting box configuration and kerstone were judged as satisfactory from a panel support standpoint.

4.7 IMPACTED STIFFENER COMPRESSION TEST (B)

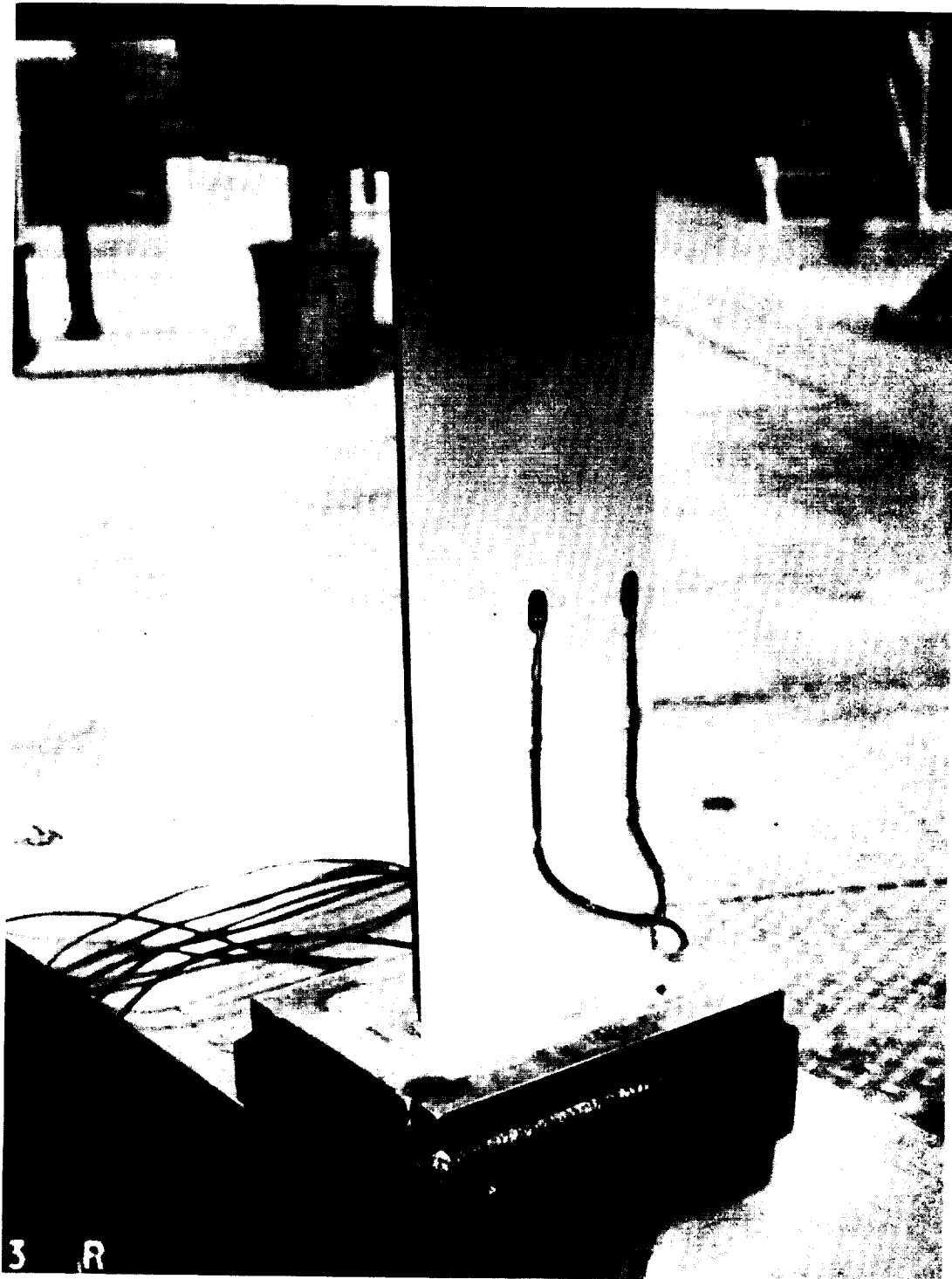
One panel 18 inches long and 5.75 inches wide with a single stiffener was impacted and tested to failure in compression. The panel was instrumented with six strain gages in back-to-back pairs identical to the unimpacted panel in Figure 4-37. One impact was made with a 0.5 inch hemispheric tip on a 12 pound impactor on the side of the stiffener 1.25 inches from the edge of the upstanding flange and nine inches from one end. The impact caused clearly visible damage to the side of the stiffener and produced 0.68

TABLE 4.4
UNDAMAGED STIFFENER PANEL DIMENSIONS



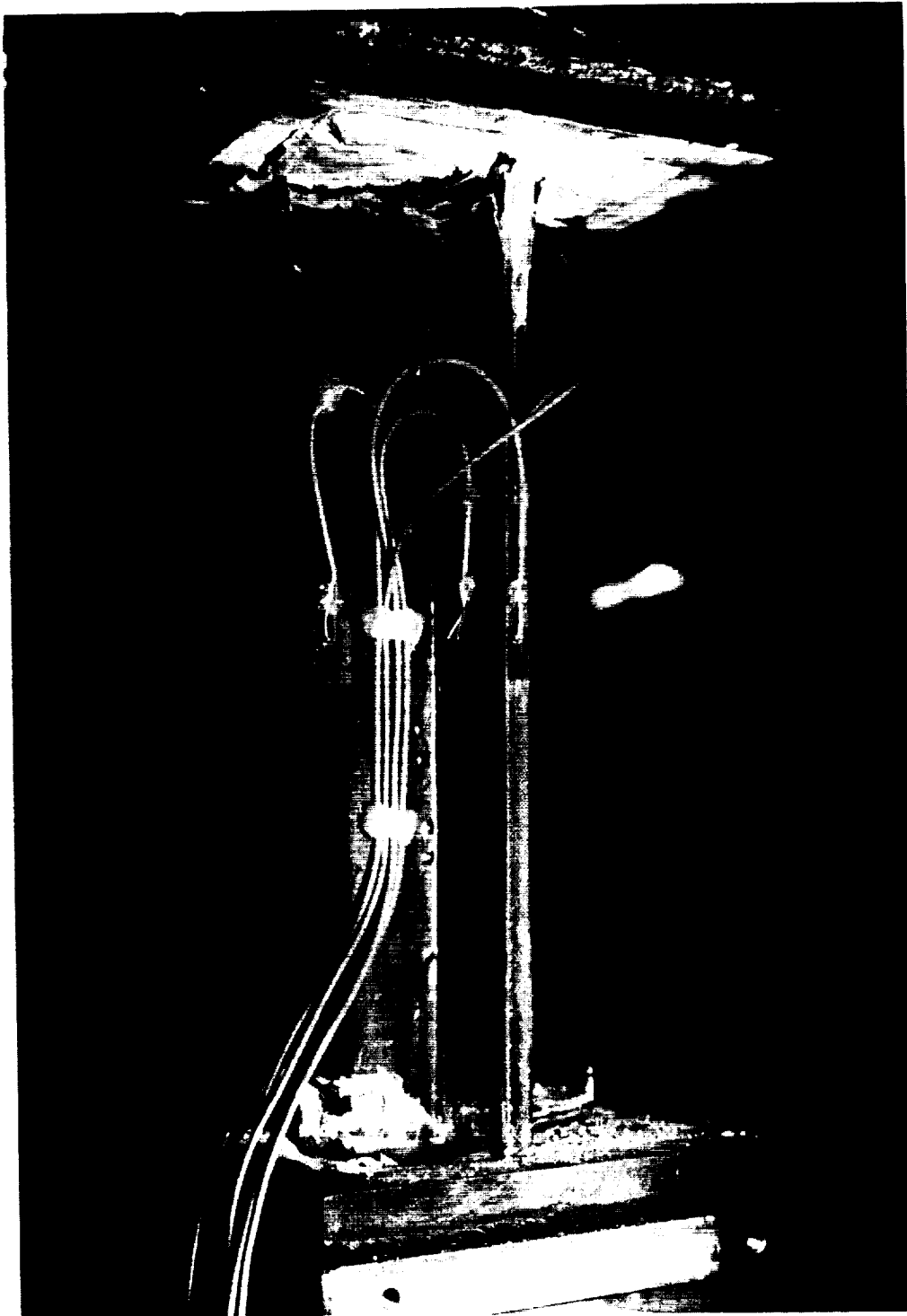
THICKNESS		
PANEL A	STIFFENER B	PANEL C
.2135	.5021	.2222
.2113	.5047	.2039
.2128	.5053	.2035
.2156	.5121	.2043
.2150	.5112	.2075

1
2
3
4
5



149763R

Figure 4-38: Stiffened compression panel A ready for test. Devcon squeeze-out is visible on top potting box.



149757R

Figure 4-39: Overall view of failed stiffened Panel A.

149761k
OF POOR QUALITY

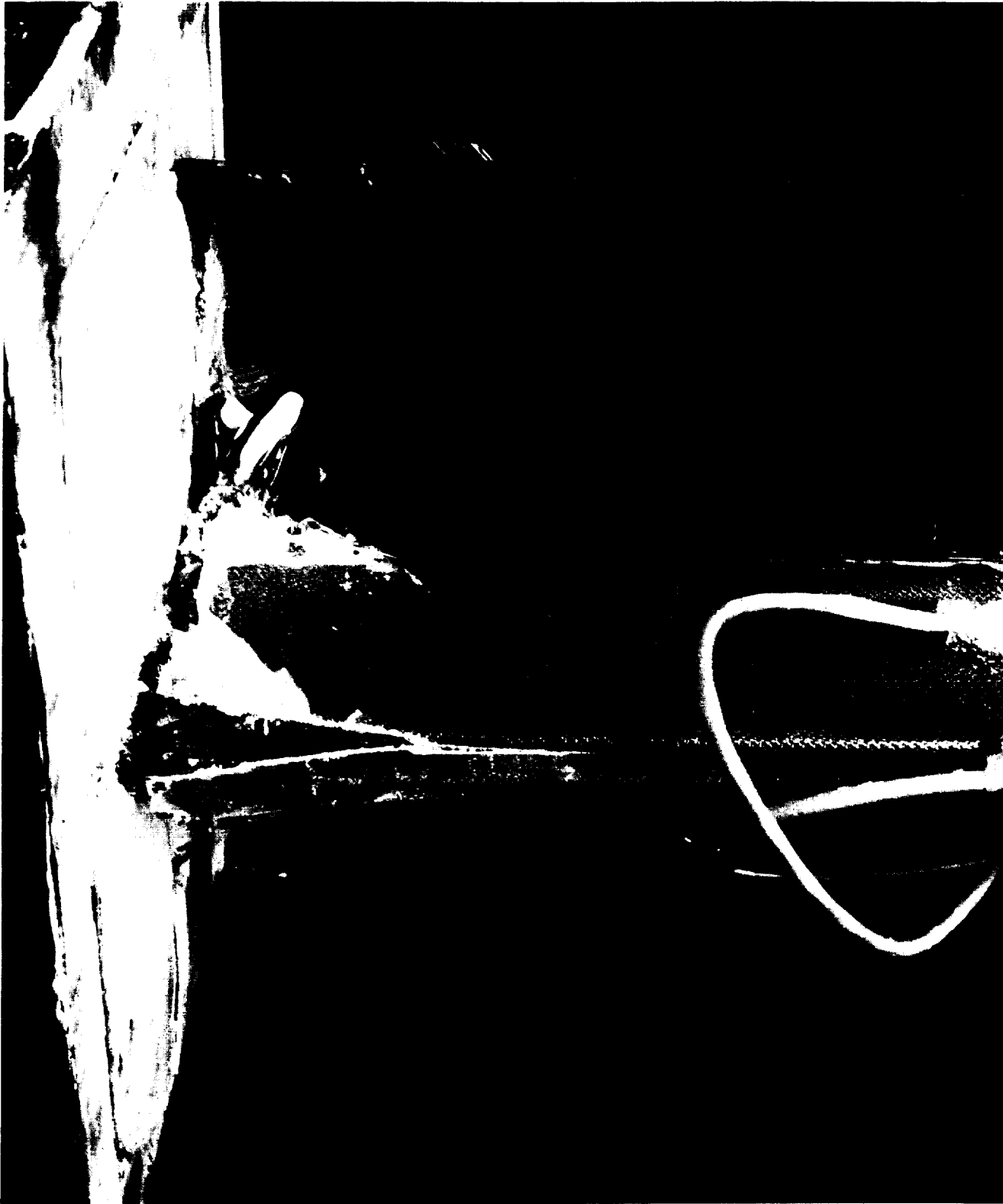


Photo No. 149761k

Figure 4-40: Failure of stiffener of Panel A.



Photo No. 149756R

Figure 4-41: Skin failure of stiffened Panel A.

TEST 26025 RUN 3

Y-AXIS CH 14

X-AXIS CH 13

YMAX = .9674E-01

XMAX = .1825E 00

YMIN = -.1895E 03

XMIN = -.1220E-02

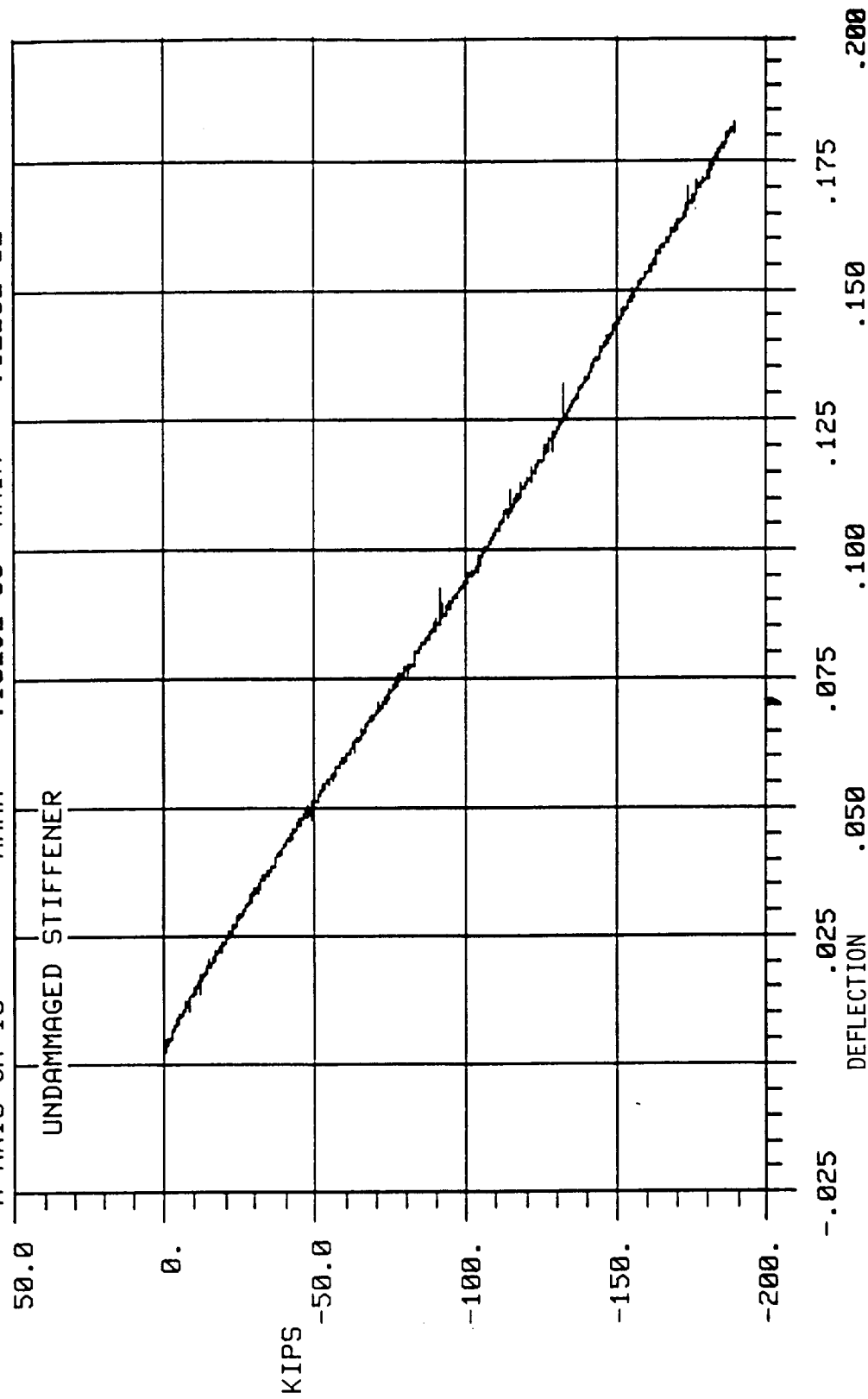


Figure 4-42: Load-deflection plot for undamaged stiffened compression Panel A.

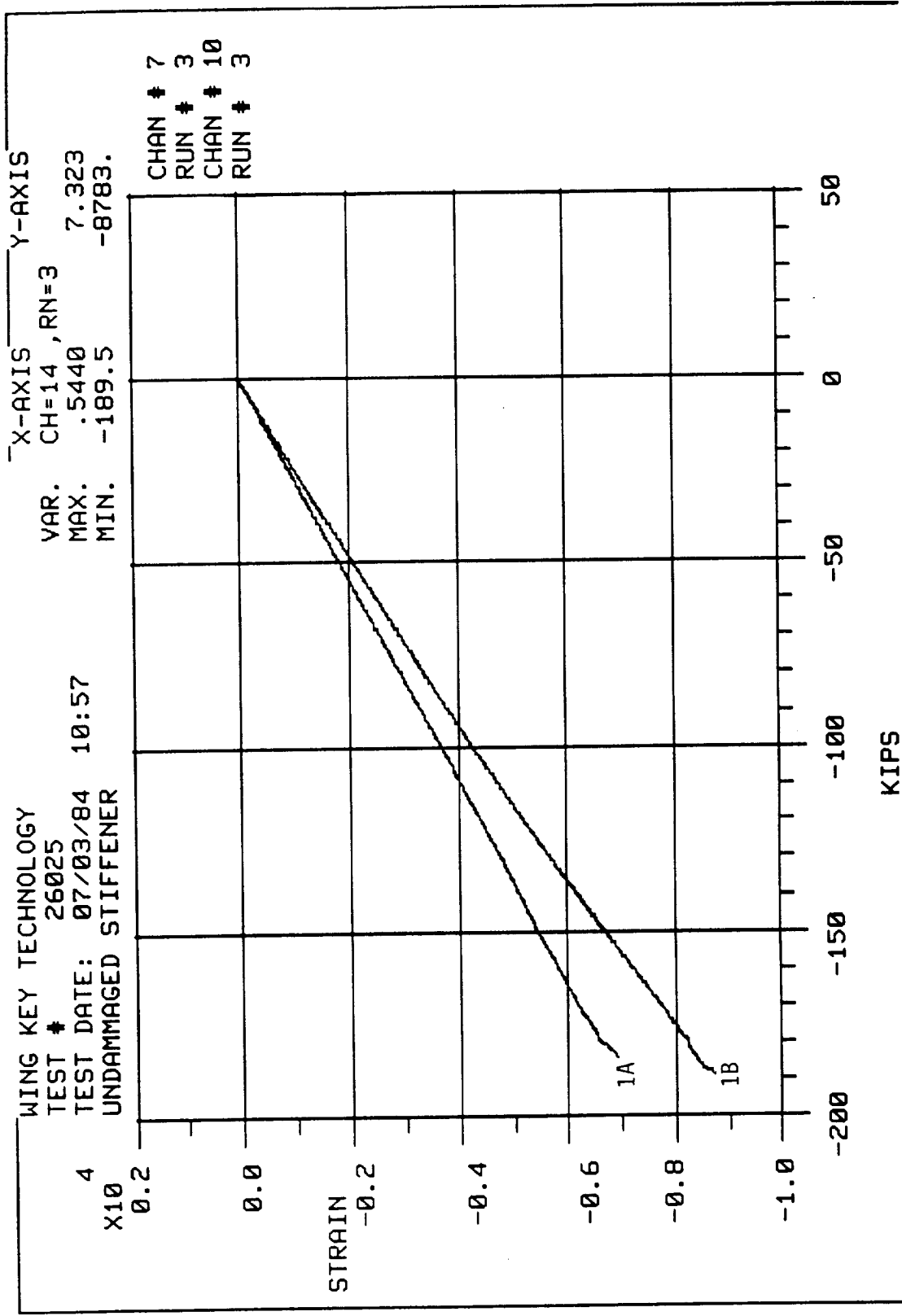


Figure 4-43: Load-strain plot of strain gages 1A and 1B on Panel A.

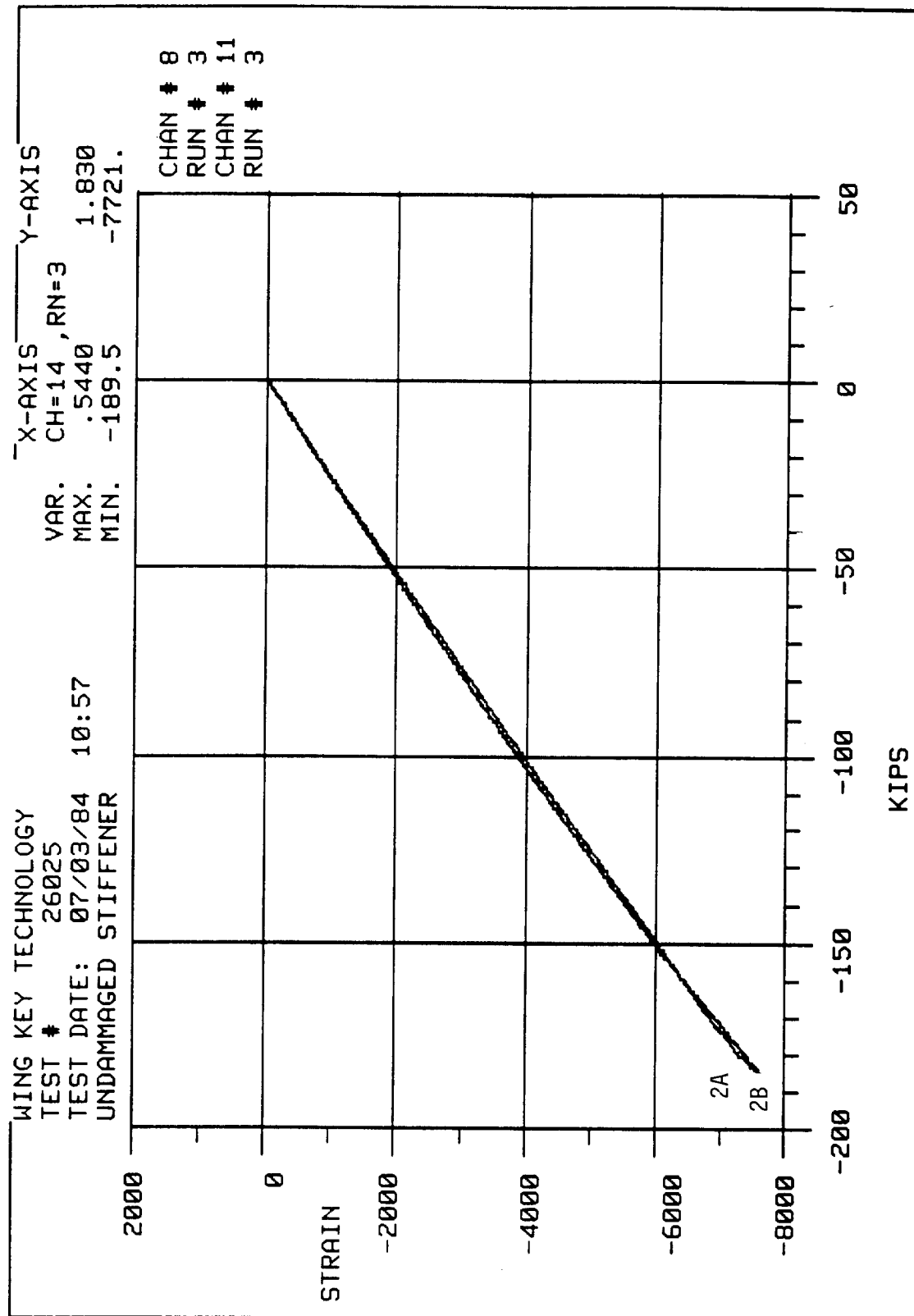


Figure 4-44: Load-strain plot of strain gages 2A and 2B on Panel A.

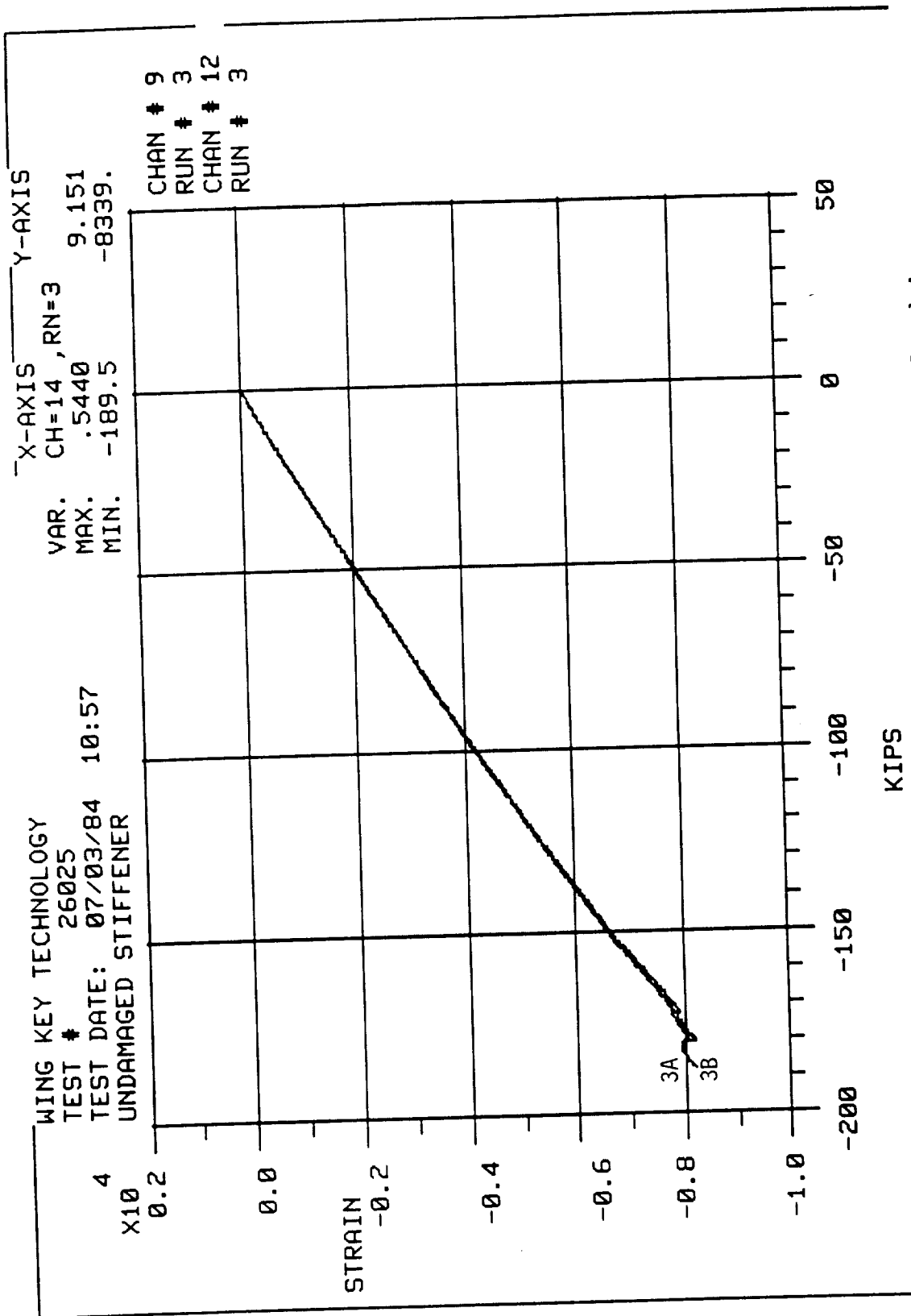


Figure 4-45: Load-strain plot of strain gages 3A and 3B on Panel A.

in² of internal damage as measured by C-scan. A delamination of 0.6-in. diameter was visible in the fiberglass cloth outer layer with total crushing and removal in a center area 0.2-inch in diameter. Some broken graphite fibers were visible under this area. No back surface damage was observed.

A different type potting box was used with the unimpacted panel. This one consisted of a one inch thick steel welded box three inches high with no bottom and it was filled with Kerstone as in the previous test. After potting the ends were machined flat and parallel. The reason for potting prior to machining was that the available machining cutters at the time produced some delamination in the stiffener if it were unsupported by potting material. This problem was resolved with different tooling thus peprmitting the configuration used in the unimpacted stiffener test which is the recommended design. Figure 4-46 shows the panel and potting box ready for test. No Devcon was applied to either end of the potted panel. Table 4.5 lists the panel dimensions prior to test.

Testing was done continuously to failure in the 400 kip machine at a head deflection loading rate of 0.05 inches/minute. The predicted failure load of the impact damaged stiffener was -126,000 pounds. This was based on the average failure strain of AS4/2220-1 laminates, impacted with 20 ft-lb, tested in phase 1 of this program. The impact damaged panel failed at -178,500 pounds and a maximum strain level of $-8505 \mu \text{ in./in.}$ The failure was not catastrophic although there was a loud noise and a load drop. The only visible damage was a buckle two or three plies deep in the stiffener at one end as shown in Figures 4-47 and 4-48. After removal from the potting box this buckle was found to run to the outboard end of the panel through the potting box. The end of the panel had some localized crushing; whether this debond and crushing was responsible for the failure observed or a result of a secondary compression wave pulse caused by elastic energy stored in the test machine frame was not determined.

ORIGINAL PAGE IS
OF POOR QUALITY

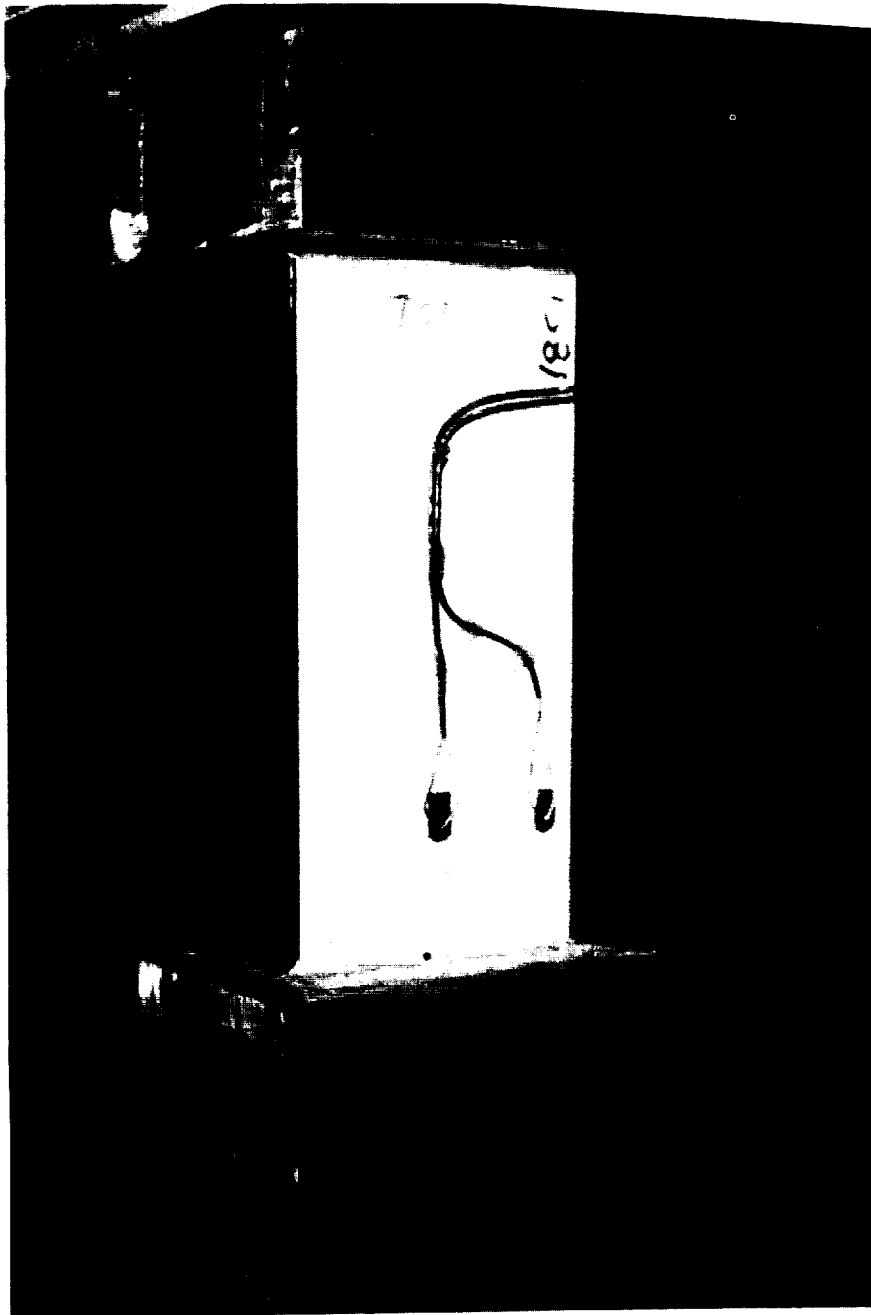
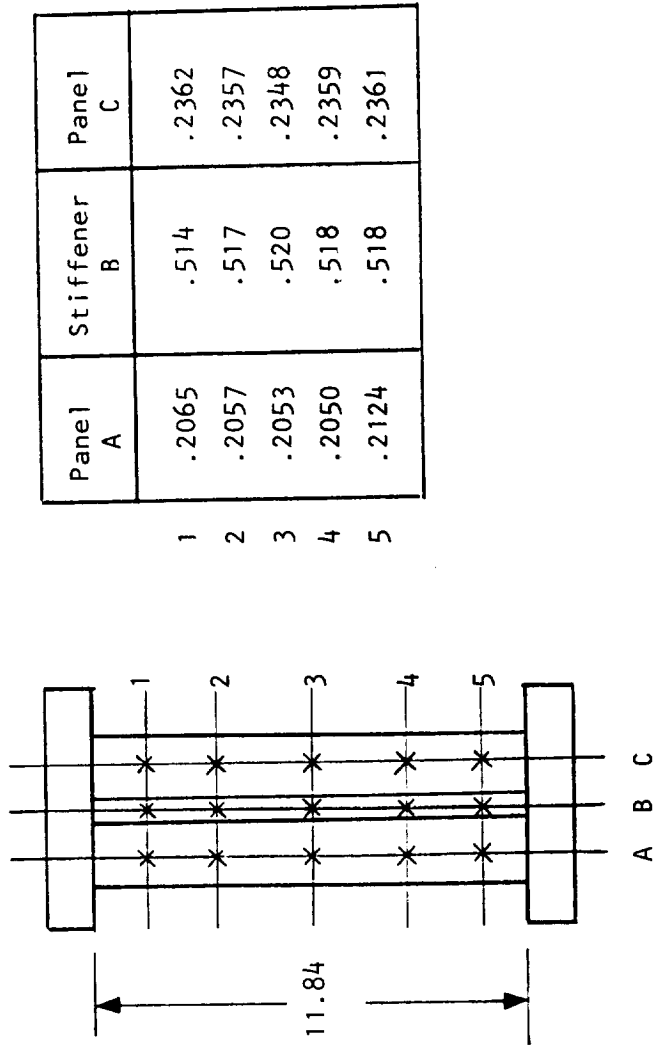


Photo No. 149755

Figure 4-46: Impacted stiffener compression test B setup.

TABLE 4.5
IMPACTED STIFFENER PANEL DIMENSIONS



	Panel A	Stiffener B	Panel C
1	.2065	.514	.2362
2	.2057	.517	.2357
3	.2053	.520	.2348
4	.2050	.518	.2359
5	.2124	.518	.2361

ORIGINAL PAGE
OF POOR QUALITY

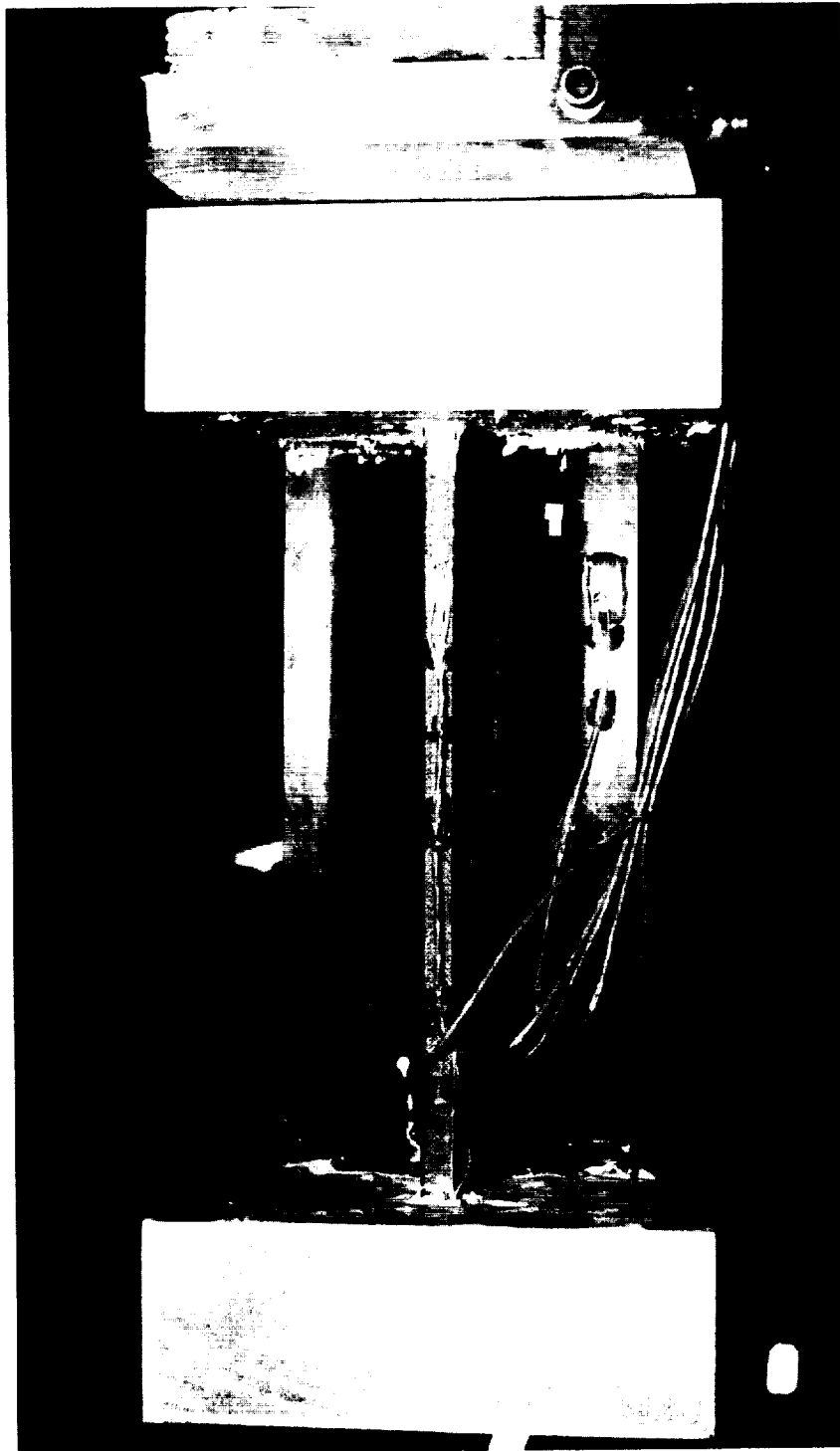


Photo No. 149758R

Figure 4-47: Overall view of failure of impacted stiffened Panel B.

ORIGINAL PAGE IS
OF POOR QUALITY



Photo No. 149760

Figure 4-48: Closeup of stiffener buckle in test of impacted stiffened
Panel B.

A load-head deflection plot is presented in Figure 4-49. Stress-strain curves for the three sets of back-to-back gages are given in Figures 4-50, 4-51 and 4-52. As in the undamaged stiffener test, the strain gage under the stiffener (1B vs 1A in Figure 4-50) measured the highest strain (-8505_{μ} in./in.) of all six gages. It diverged sharply from the gage on top of the stiffener (-5222_{μ} in./in. maximum). Gage locations are the same as shown in Figure 4-37. The two gages back-to-back on the stiffener side (2A and 2B) gave the same readings as shown in Figure 4-51. The gages on the skin (3A and 3B) diverged somewhat with the outer gage (3B) being the highest at -8408_{μ} in./in. versus the inner (3A) at -7658_{μ} in./in. as shown in Figure 4-52.

Because the damage was so localized, it was subsequently decided to machine off the damaged end and retest using the potting boxes from the undamaged stiffener test. After re-machining the total panel length was 13.625 inches of which one inch on each end was embedded in the potting material giving a clear test length of 11.625 in. versus the 11.84 in. of the first test. Strain gages were reinstalled on the same points. All other test conditions remained the same.

During loading a loud noise was heard at 141,000 pounds with a load drop-off to 140,000 pounds. There was no visible damage so loading was resumed. Failure occurred catastrophically at 159,700 pounds. Figures 4-53 through 4-56 show details of the failure. Both the skin and stiffener buckled, the origin being approximately 3 1/2 inches below the impact point. It does not appear that the impact had any significant influence either on this retest failure or the first failure.

Load-deflection and stress-strain plots are given in Figures 4-57 through 4-60. Response is similar to the first test except for major damage being apparent at 141,000 pounds where the loud noise was heard. Less divergence was noted in gages 3A and 3B (Figure 4-60) and slightly more in gages 2A and 2B (Figure 4-59).

14:19 07/03/84

WING KEY TECHNOLOGY
TEST 26031 RUN 2

Y-AXIS CH 14 YMAX = .1276E 00 YMIN = -.1785E 03
X-AXIS CH 13 XMAX = .1324E 00 XMIN = -.2712E-03

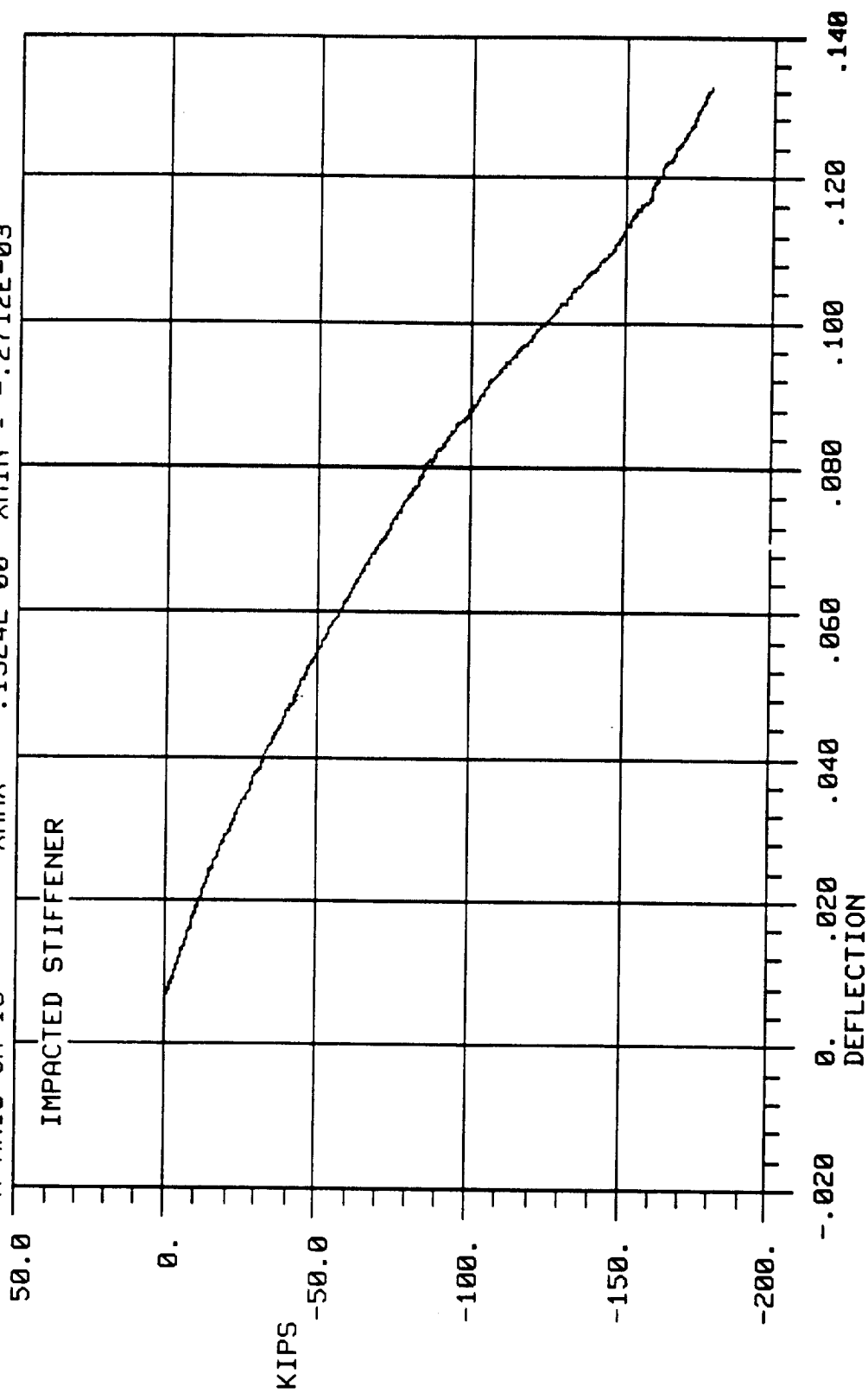


Figure 4-49: Load-deflection plot for impacted stiffened compression Panel B.

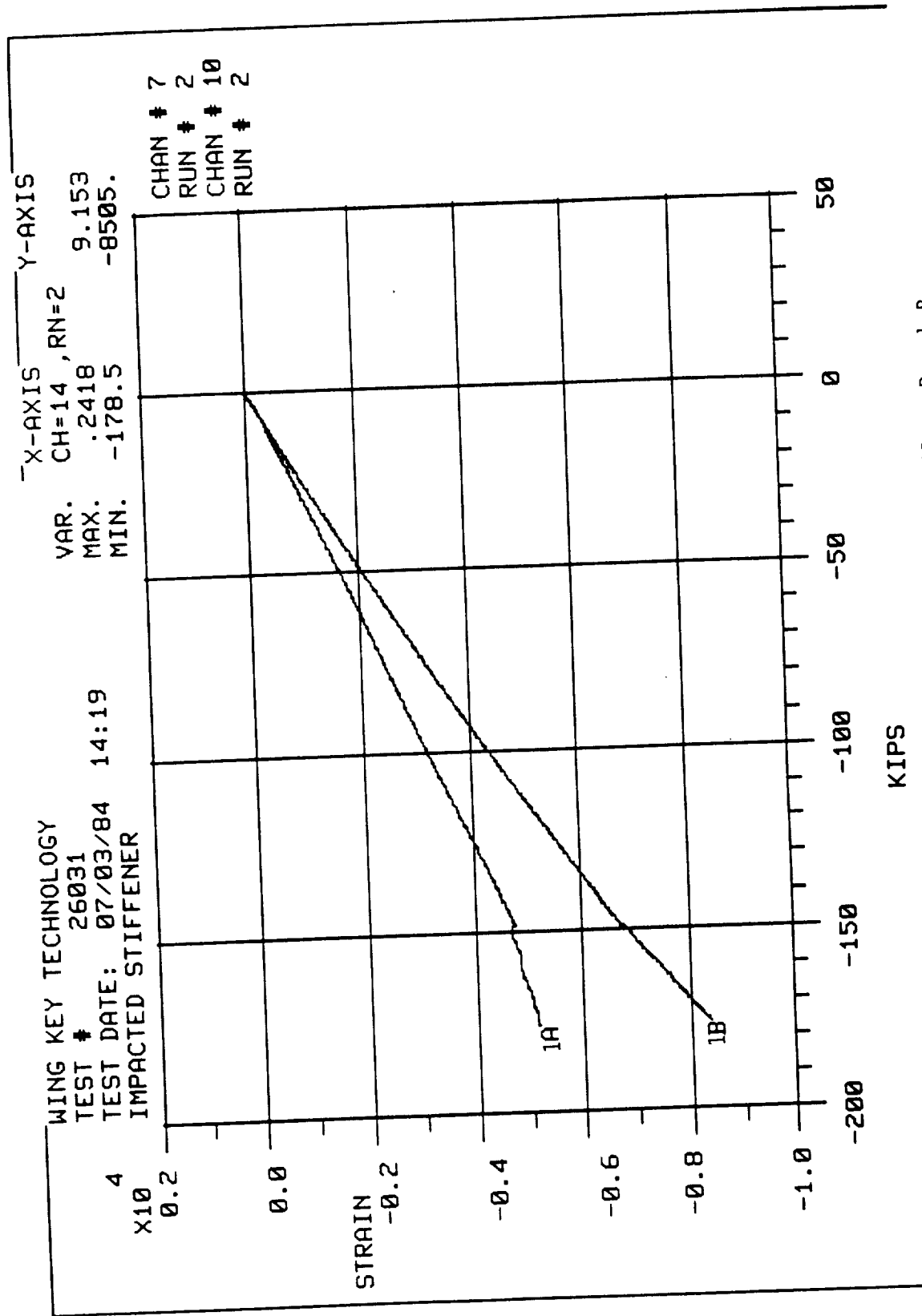


Figure 4-50: Load-strain plot of strain gages 1A and 1B on Panel B.

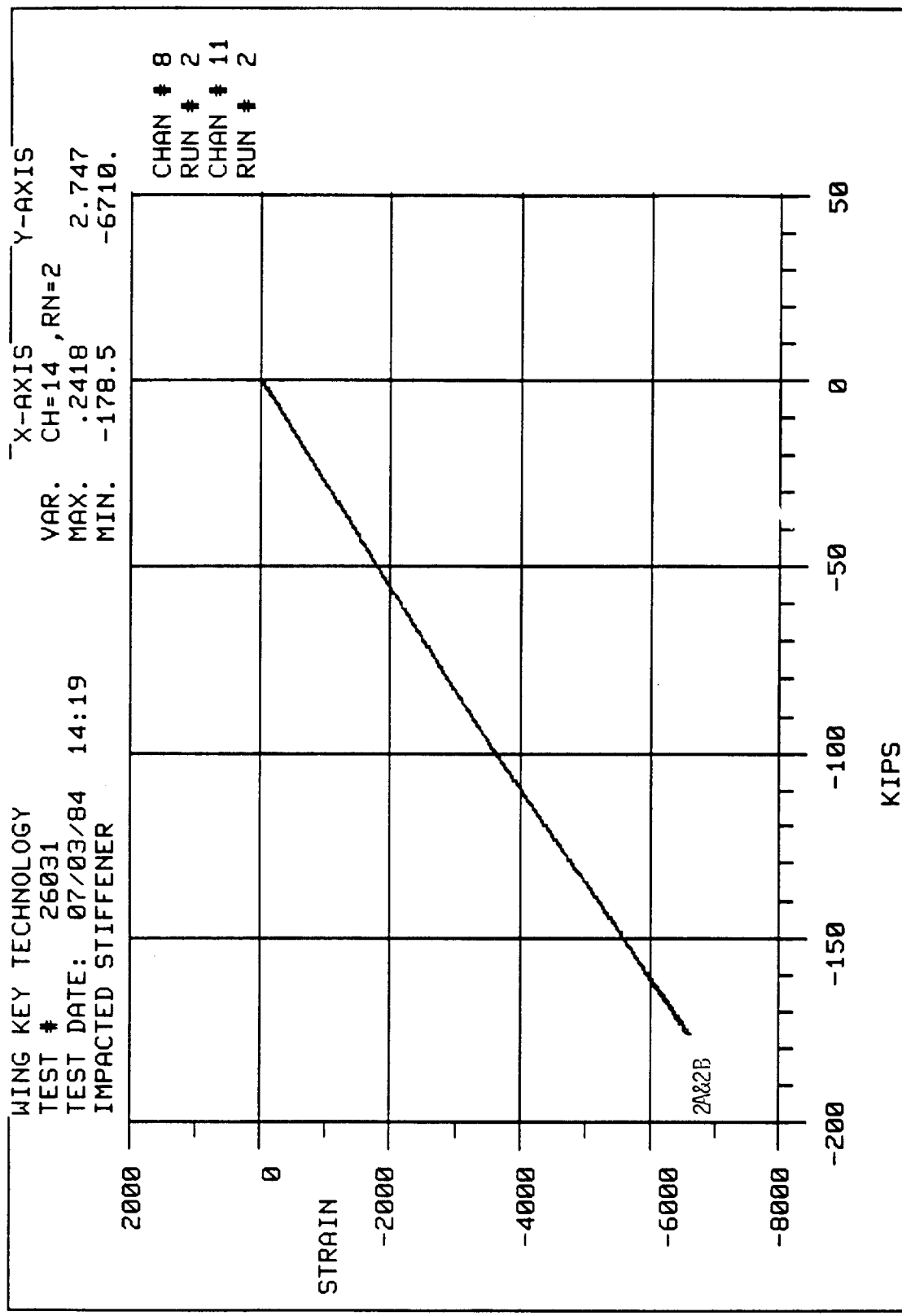


Figure 4-51: Load-strain plot of strain gages 2A and 2B on Panel B.

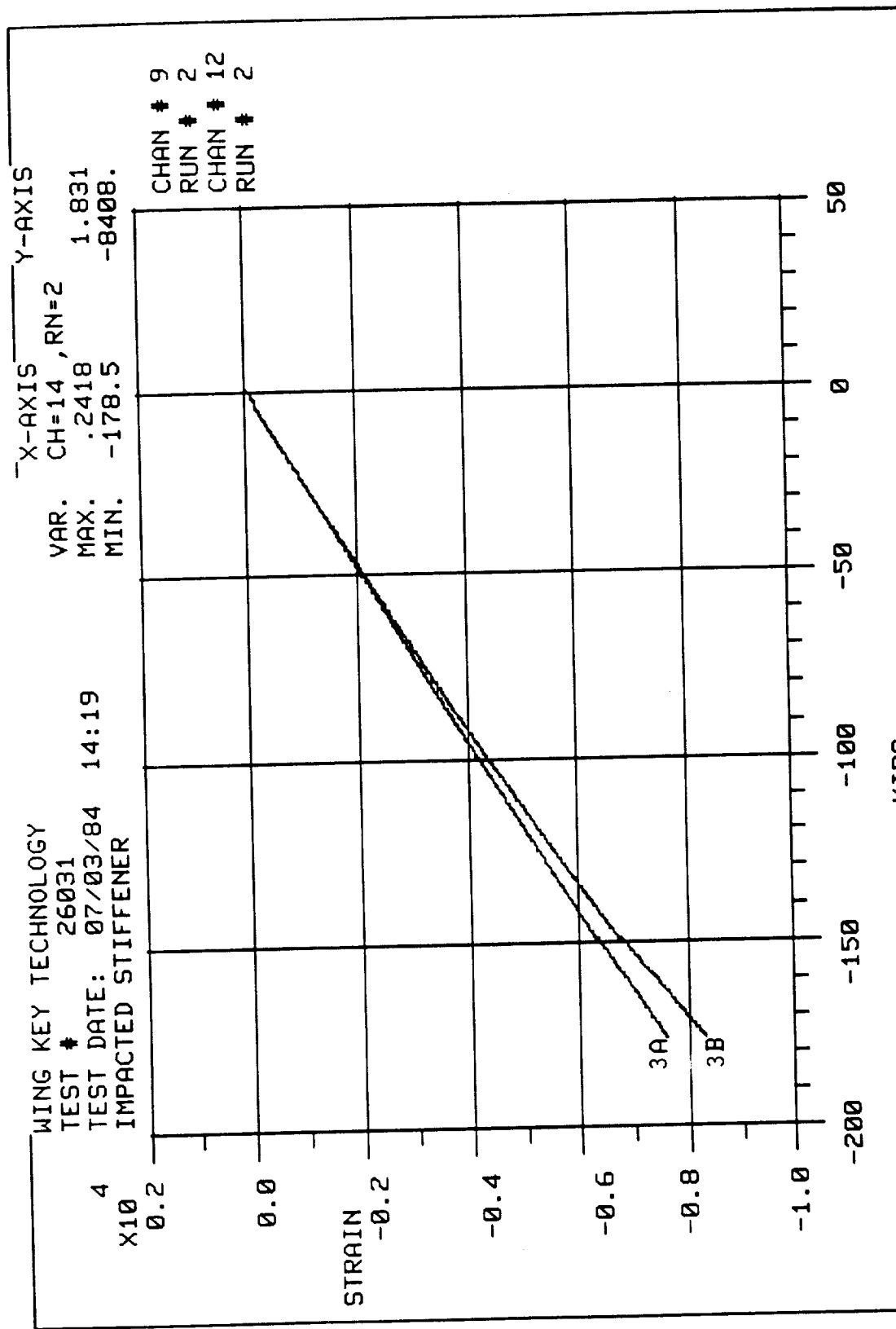


Figure 4-52: Load-strain plot of strain gages 3A and 3B on Panel B.

ORIGINAL PAGE IS
OF POOR QUALITY



Photo No. 149918R

Figure 4-53: View of skin and stiffener failure modes of retest of impacted stiffener specimen.

ORIGINAL PAGE IS
OF POOR QUALITY



Photo No. 149916R

Figure 4-54: Stiffener failure detail view of impacted stiffener retest.

ORIGINAL PAGE IS
OF POOR QUALITY

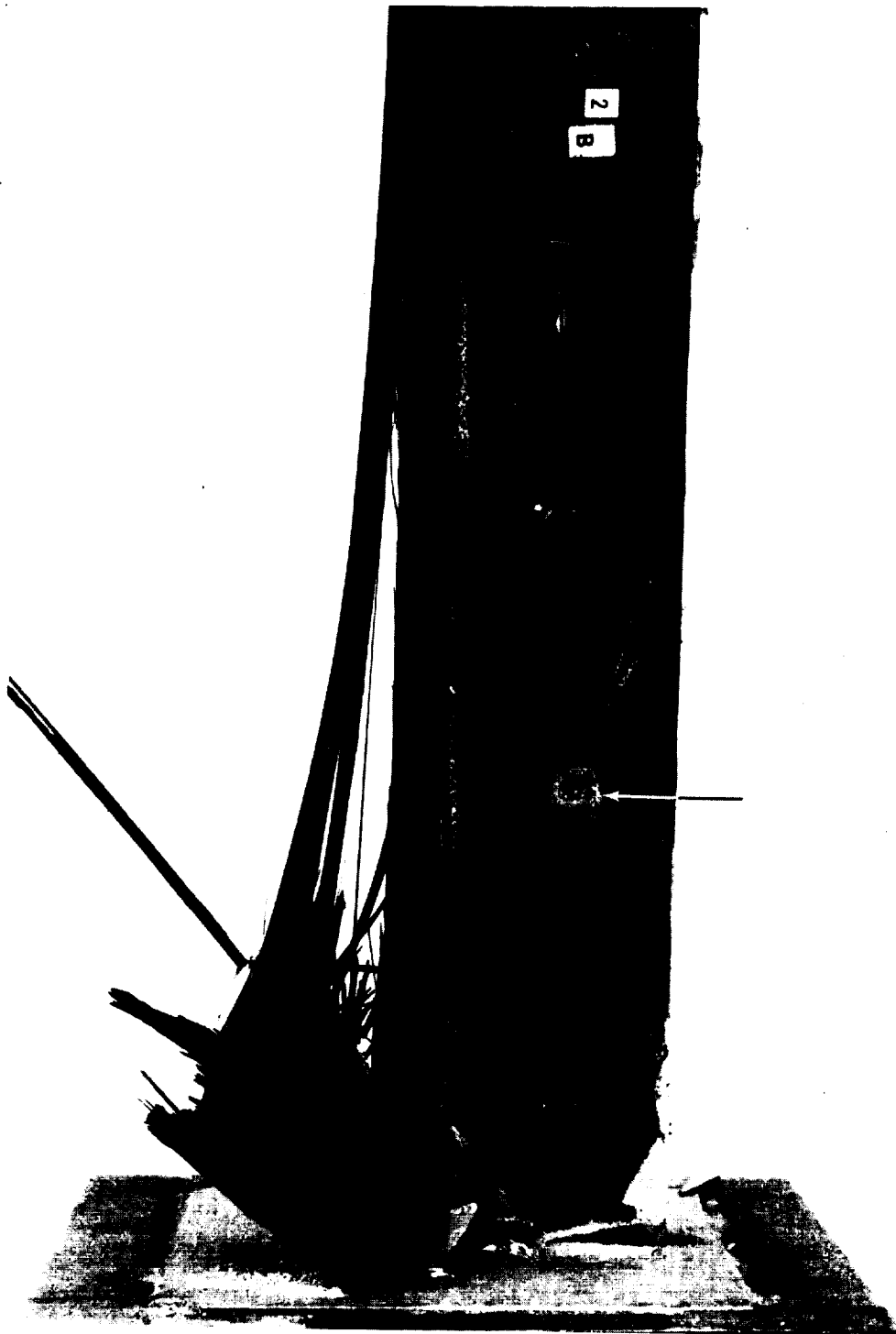


Photo No. 149917R

Figure 4-55: Side view of retest of impacted stiffener showing location of impact relative to failure.

ORIGINAL PAGE IS
OF POOR QUALITY

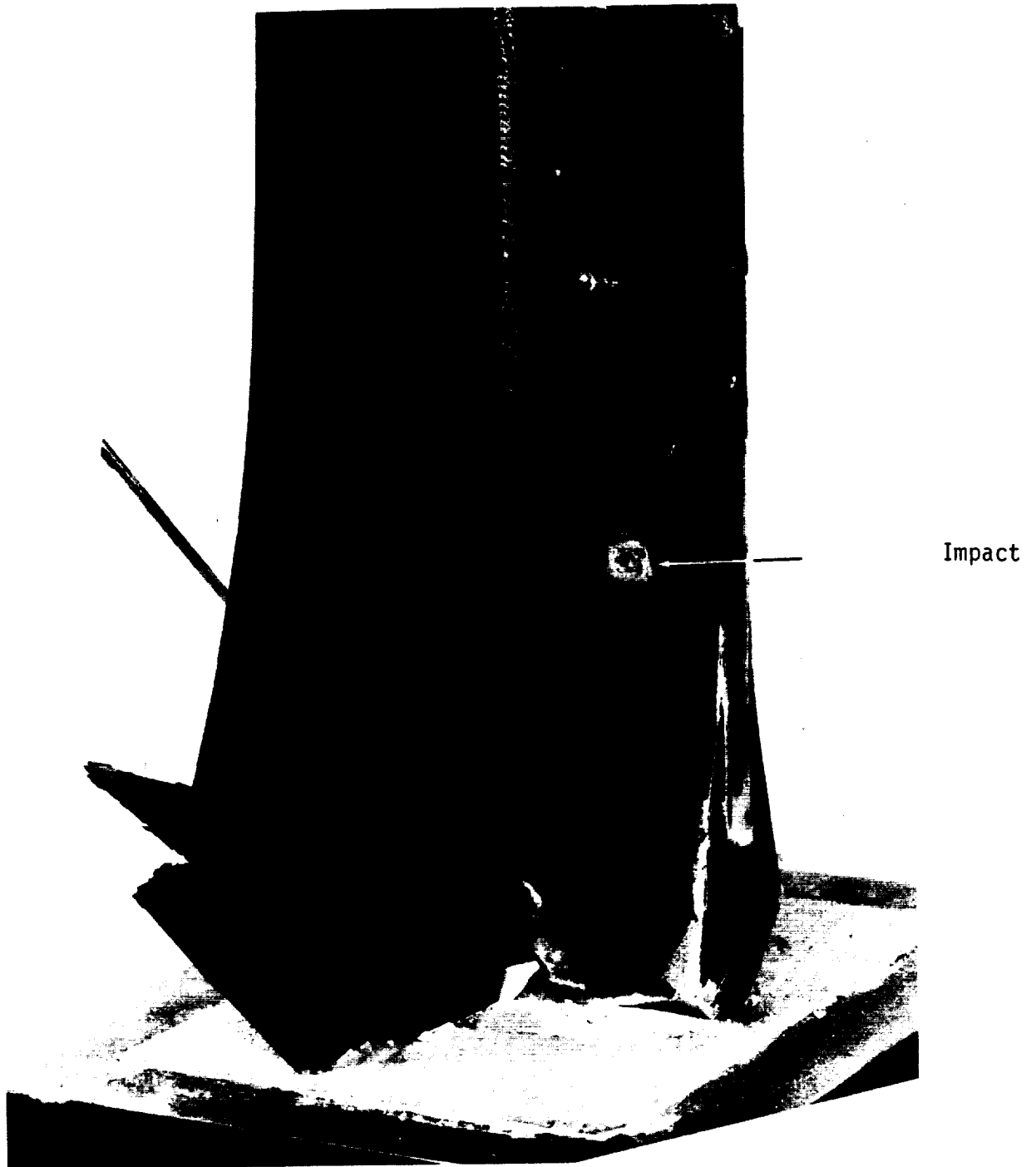


Photo No. 149919R

Figure 4-56: View of skin and stiffener of failure of retest of impacted stiffener. Location of impact is shown.

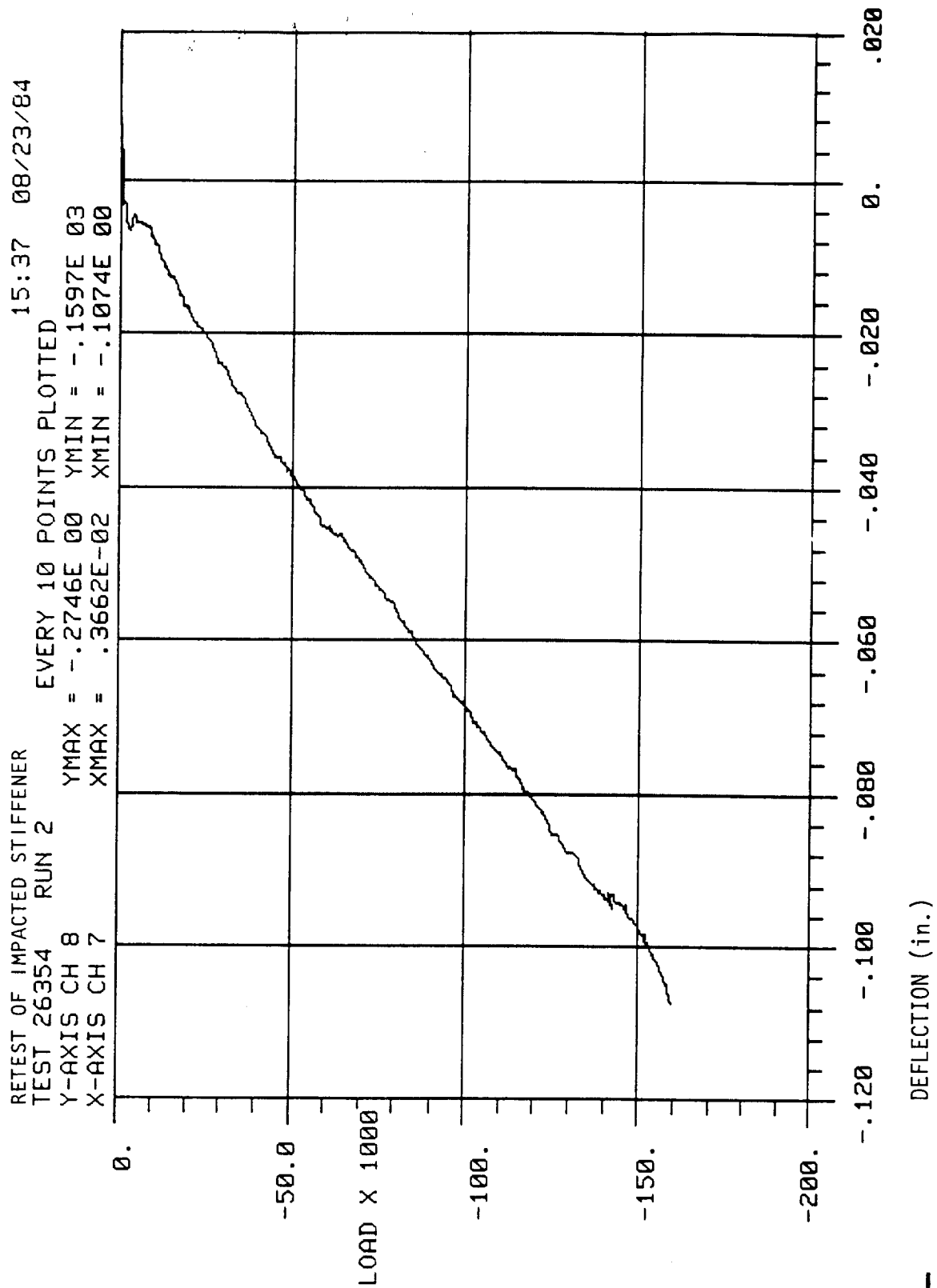


Figure 4-57: Load-deflection plot of retest of impacted stiffened Panel B.

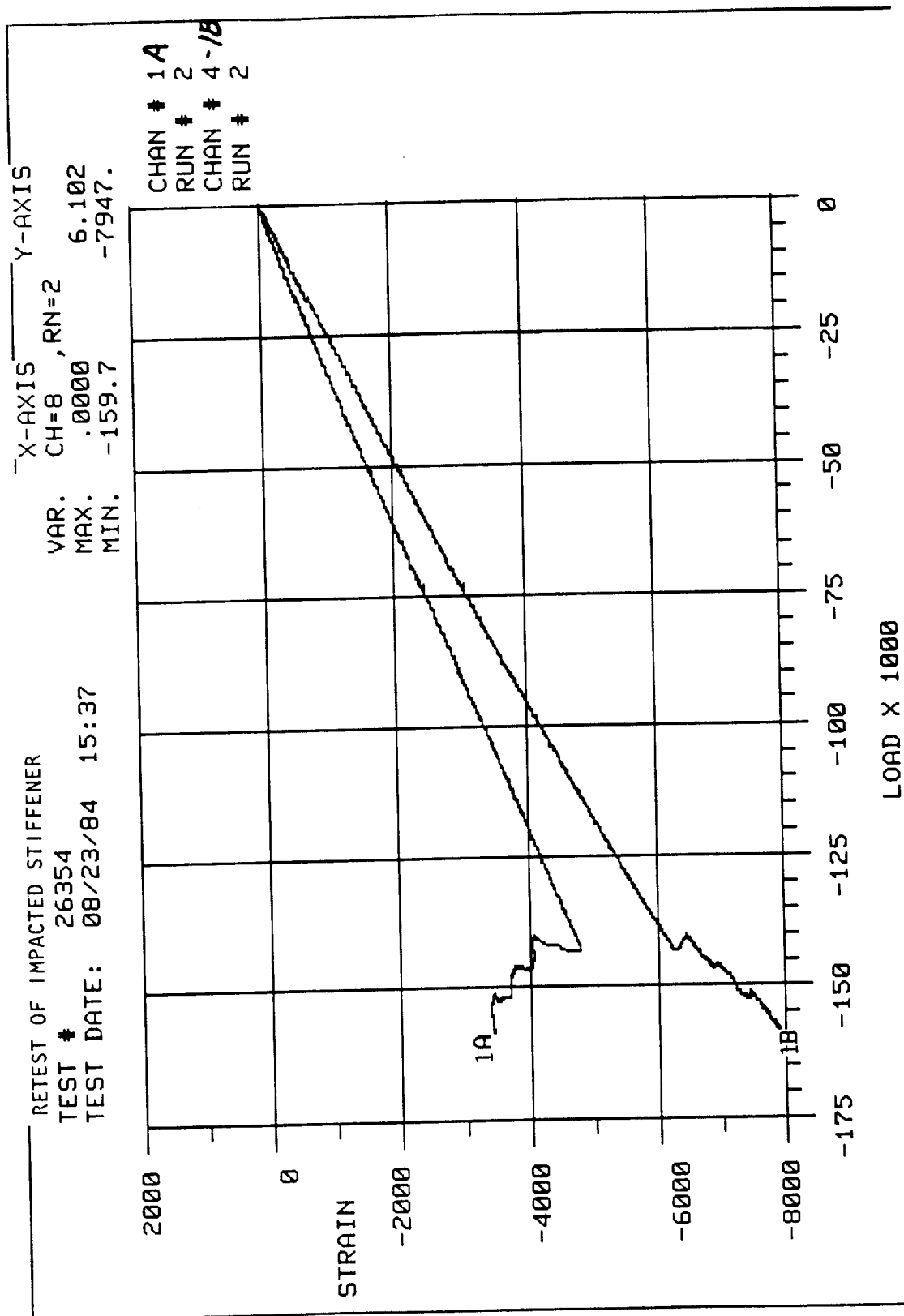


Figure 4-58: Load-strain plot of strain gages 1A and 1B on retest of Panel B.

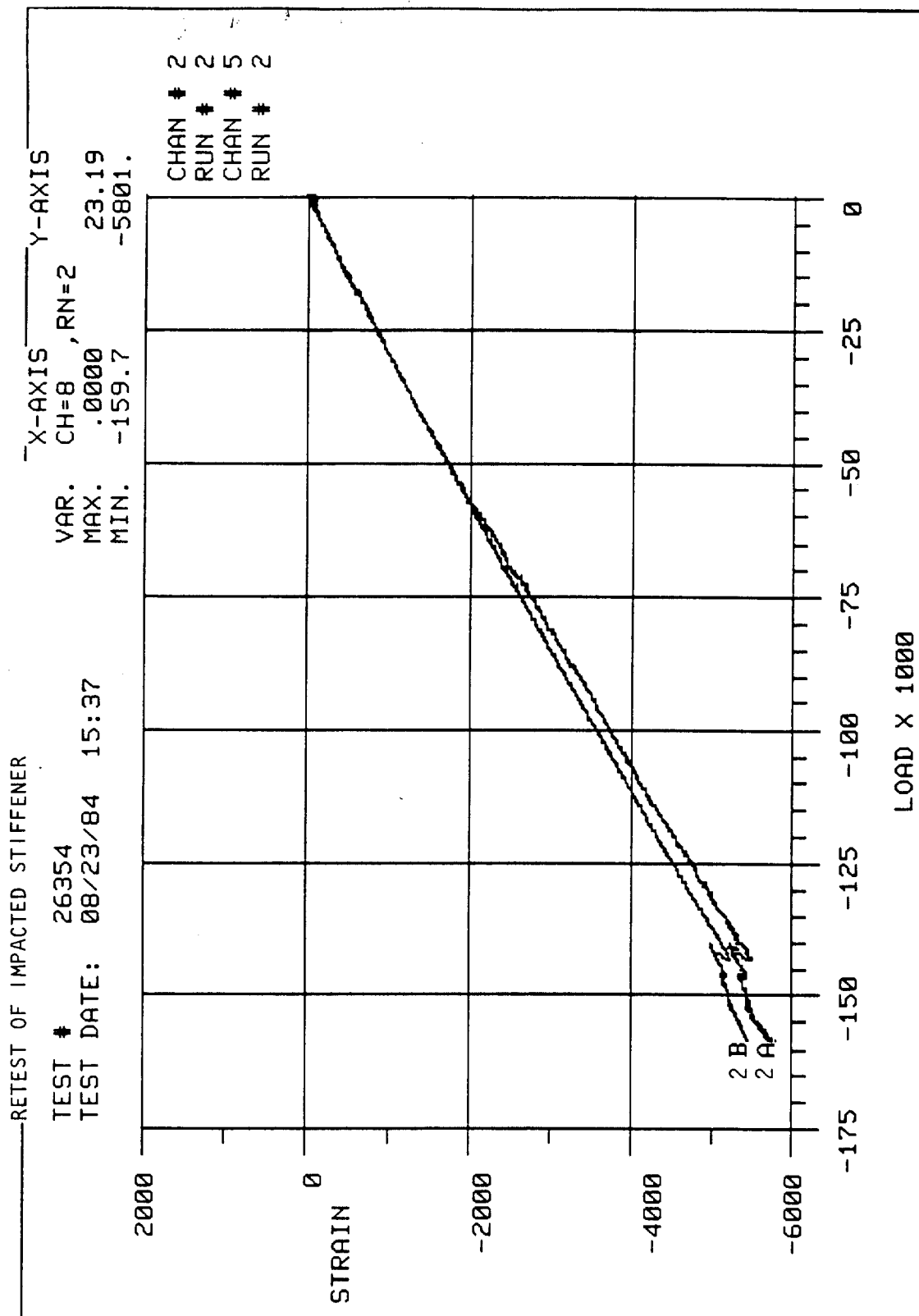


Figure 4-59: Load-strain plot of strain gages 2A and 2B on retest of Panel B.

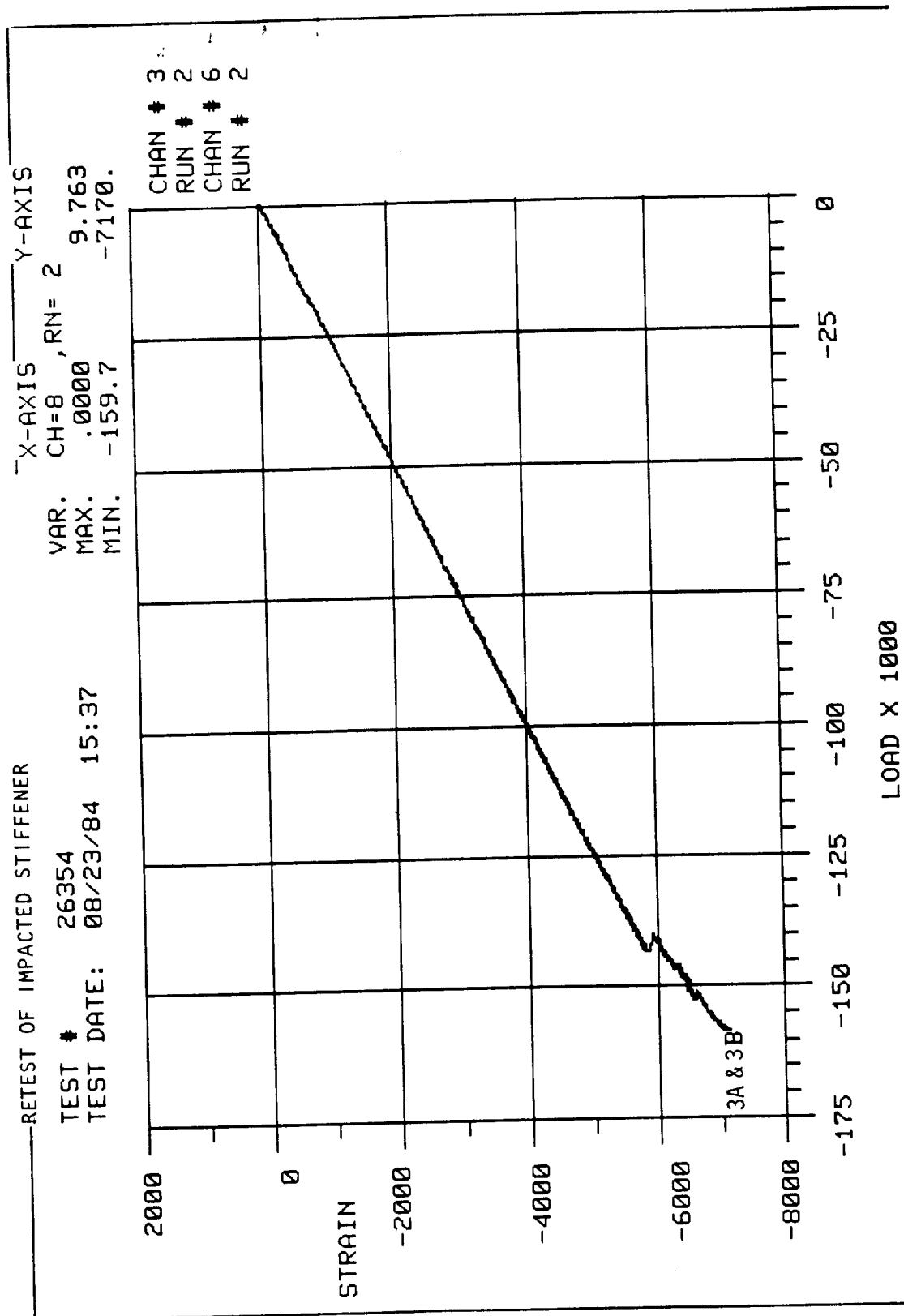


Figure 4-60: Load-strain plot of strain gages 3A and 3B on retest of Panel B.

Examination of the potted end nearest the failure after removal of the potting material indicated that no crushing of the end occurred (Figure 4-61), although the delamination ran to the specimen end. Since this retest failed at a lower load than the original test (159,000 vs 178,500 lbs) it appears that all of the original damage may not have been removed by the remachining.

4.8 IMPACTED STIFFENED PANEL COMPRESSION TEST (G)

One 25 inches long by 18 inches wide two-stiffener panel was tested in compression. The panel was first impacted in the center, between the stiffeners, at 30 ft-lb with a 12-pound impactor having a 0.5 inch diameter hemispherical steel tup. As with the trial impact panel the wooden panel support frame was contoured to mate with the bottom or inside of the panel to uniformly distribute impact load over the entire panel. The stiffener caps also carried bearing load at each end. The impact caused 4.3 square inches of internal damage as measured by ultrasonic C-scan.

After inspection the panel ends were machined flat and parallel then strain gaged with 12 gages as shown in Figure 4-62. Strain gages were CEA-00-125UW-120 types bonded with M-Bond 200. After gaging the panel was placed in steel boxes and potted with Kerstone. The centroid of the panel was placed in the geometric center of the potting boxes. Steel angles were attached to the potting boxes at two diagonal corners for handling protection. Panel edge supports consisting of 1/4 x 2 x 2 inch steel angles were then added to prevent buckling. Test configuration and gage locations are shown in Figure 4-62. Panel dimensions are given in Table 4.6. Devcon was placed on the bottom and top of the potting boxes as in the single stiffener tests.

The test was run in the same 400 kip machine as the single stiffener tests. Failure occurred at 232,900 pounds and at a maximum strain $-5343 \mu \text{ in/in}$.

ORIGINAL PAGE IS
OF POOR QUALITY.



Photo No. 149964R

Figure 4-61: Potted end of impacted stiffened compression retest. One inch was contained in the potting compound.

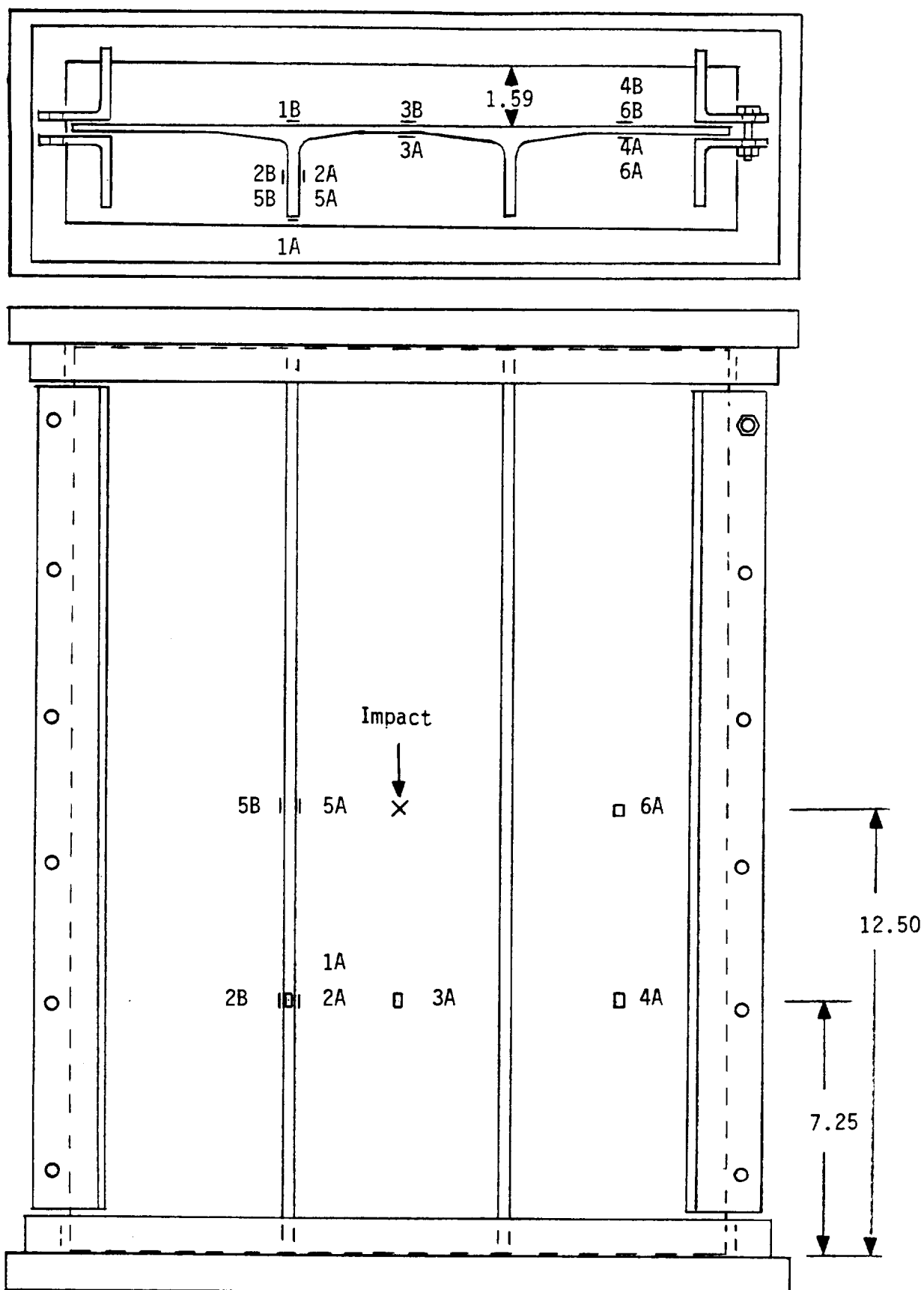
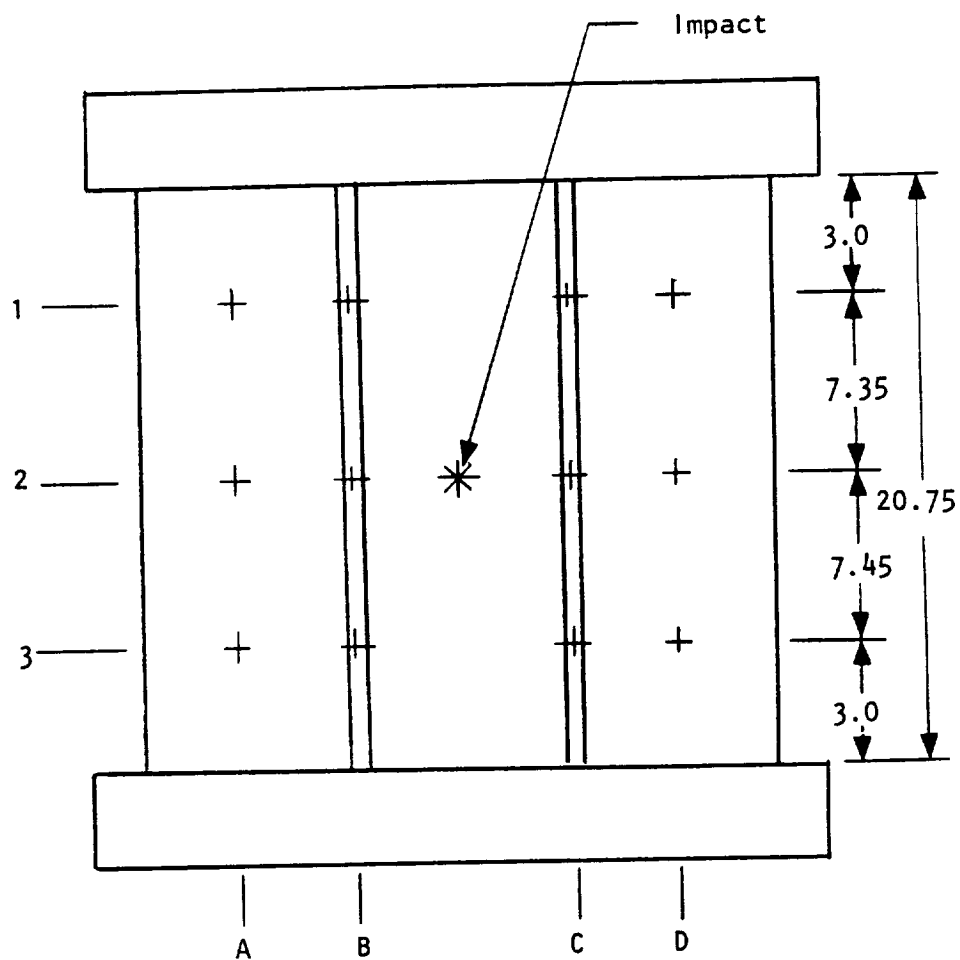


Figure 4-62: Impacted compression test setup. Numbers are strain gage identifications.



	A	B	C	D
	PANEL	STIFFENER	STIFFENER	PANEL
1	.2223	.5010	.4952	.2125
2	.2225	.5019	.4951	.2167
3	.2134	.4986	.4955	.2177

Table 4.6: Impacted Stiffened Panel G Thickness Dimensions (in.).

The predicted failure load was 239,000 pounds. Figures 4-63 and 4-64 show both front and back views of the failed panel. Figures 4-65 and 4-66 are close-ups of the failure area. The key observation from these figures is that the failure does not appear to go through the impact area. The nearest visible damage is on the back side three inches from the impact.

Due to the 5 mil Chemglaze coating on the back surface much of the damage was masked. To evaluate the interior damage the panel was sawed transversely at five locations shown in Figure 4-64. An end-on view of these resulting sections is shown in Figure 4-67. This reveals extensive damage throughout the panel. Splits in the stiffeners run the full length of each. Delaminations in the skin are more restricted and occur only near the failure zone. One section is through the center of the impact, which is indicated by the arrow in Figure 4-67. Close observation of the area reveals only minor delamination resulting from the impact and verifying that the impact probably did not contribute to the failure. Examination of the other sections reveals damage typical of other tests in this series -- that is delamination between the skin and stiffener, splitting of the stiffeners, and corner cracking around the filler.

Load deflection and stress-strain curves are presented in Figures 4-68 through 4-71. Again the strain in the skin is higher than on the stiffener top (Figure 69). Stiffener strains are generally lower than skin strains. Gages 3A and 3B were located in a failure zone but had the lowest strain values (Figure 70) and remained linear to failure. Gage 1B was located on the skin under the stiffener and was centered in the damage region, however the stress-strain curve (Figure 4-69) shows no deviation prior to failure. Gages 4A and 4B show a divergence (Figure 4-70), indicating that the failure may have originated in the area below these gages near the potting box.

ORIGINAL PAGE IS
OF POOR QUALITY

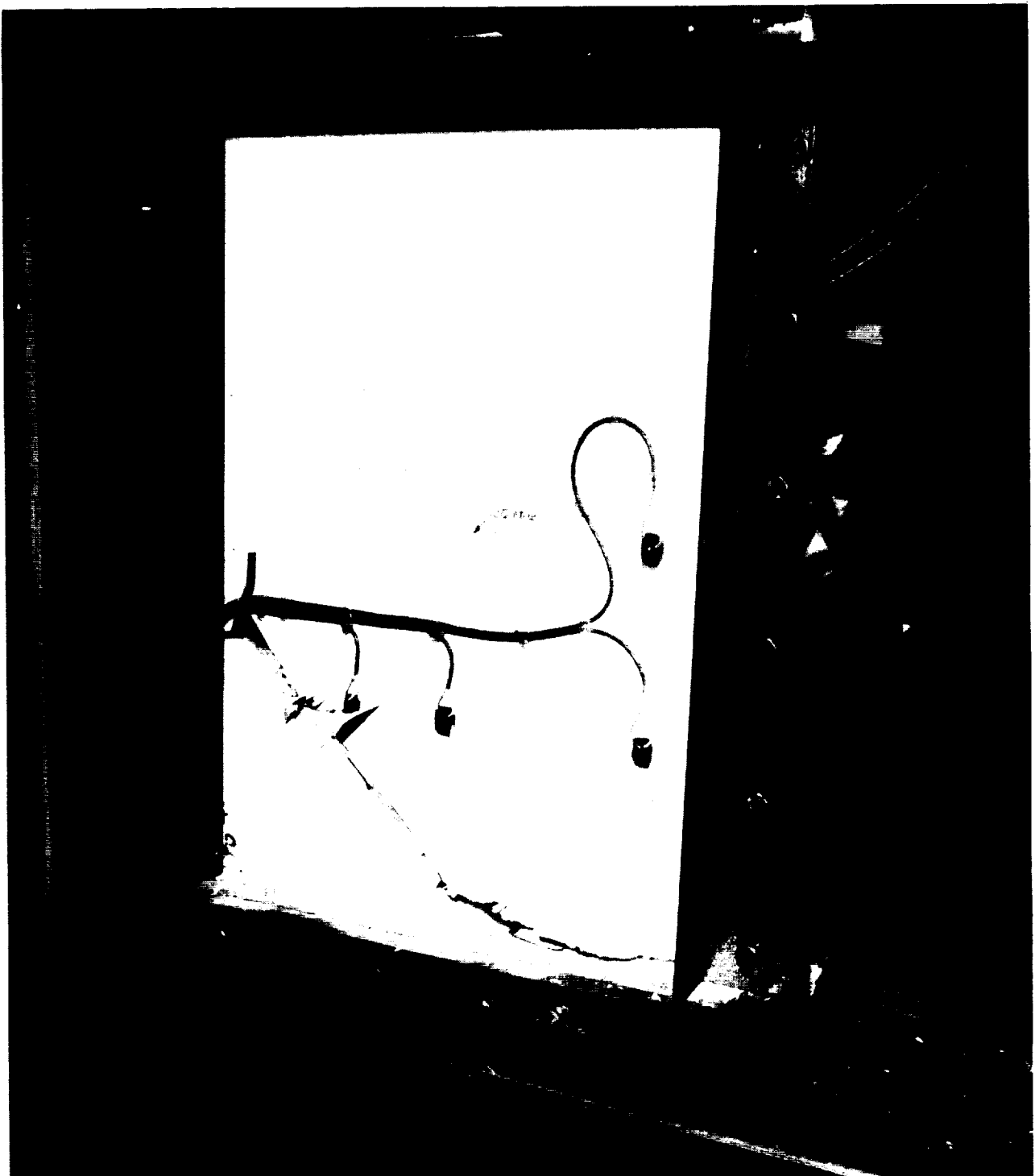


Figure 4-63: Front side of failed impacted stiffened panel. Photo No. 149751R

ORIGINAL PAGE IS
OF POOR QUALITY

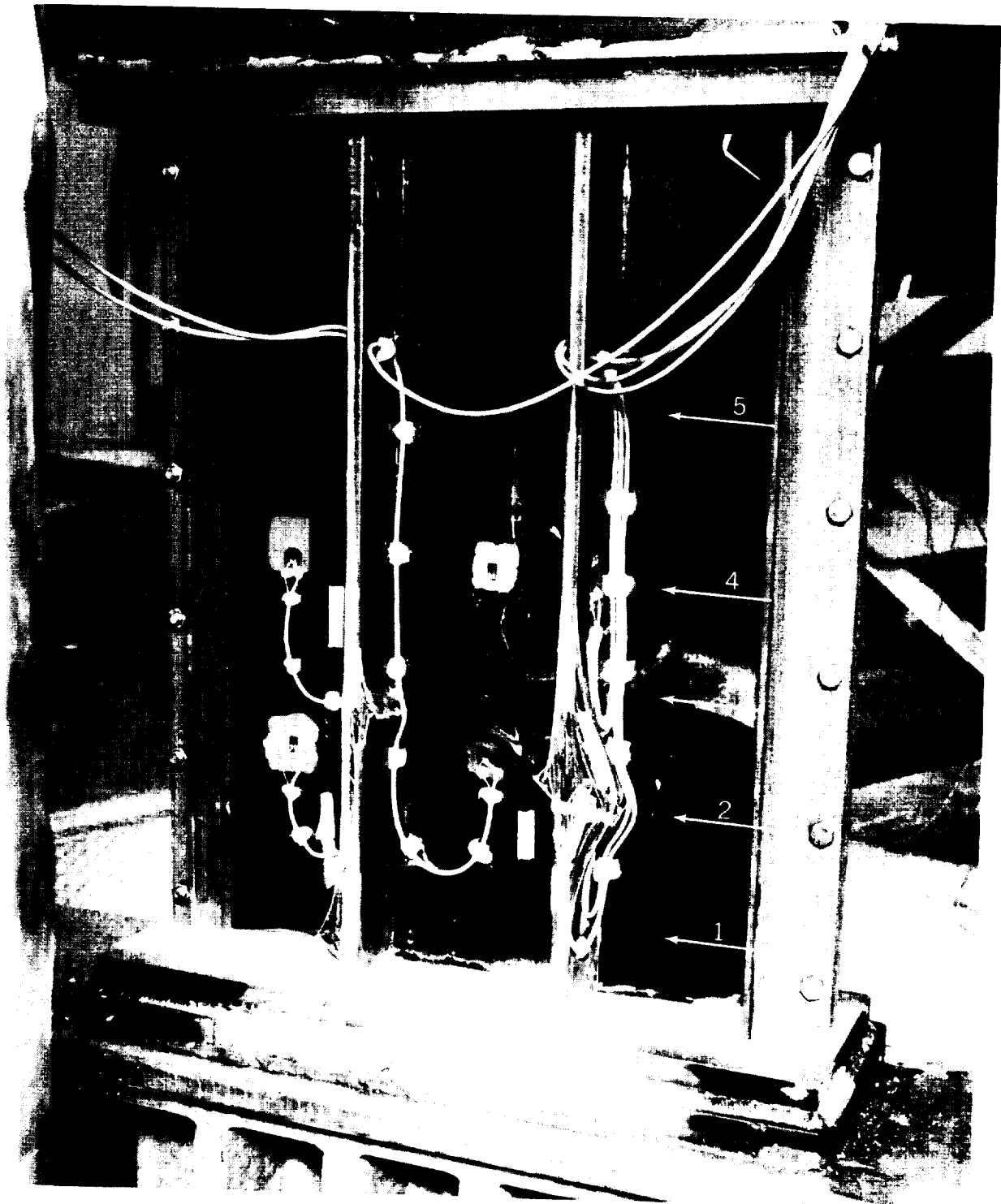


Photo NO. 149748R

Figure 4-64: Back side of failed impacted stiffened panel. White arrows indicate section plane.

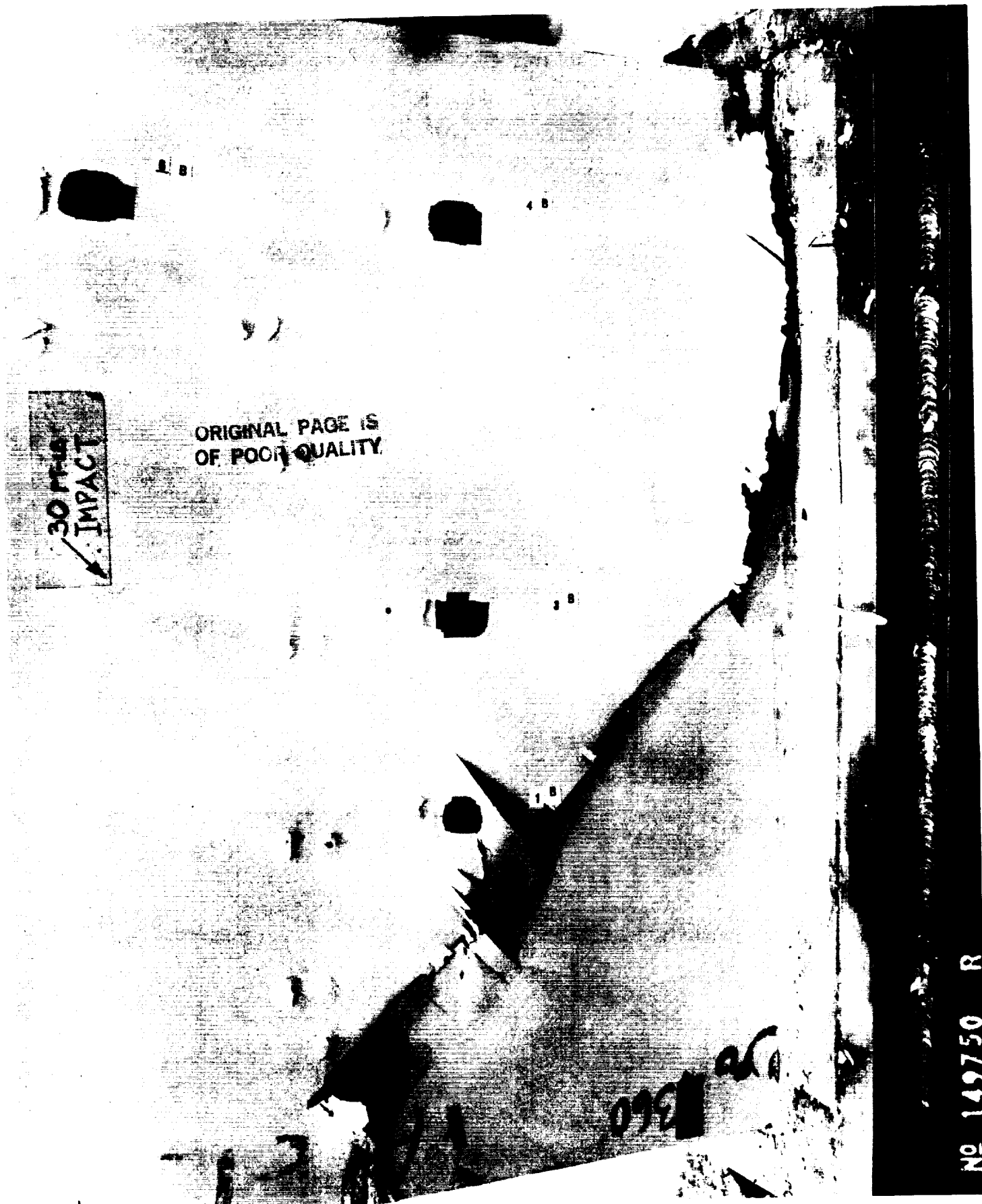


Figure 4-65: Closeup of skin side failure zone.



Figure 4-66: Closeup of failure zone.

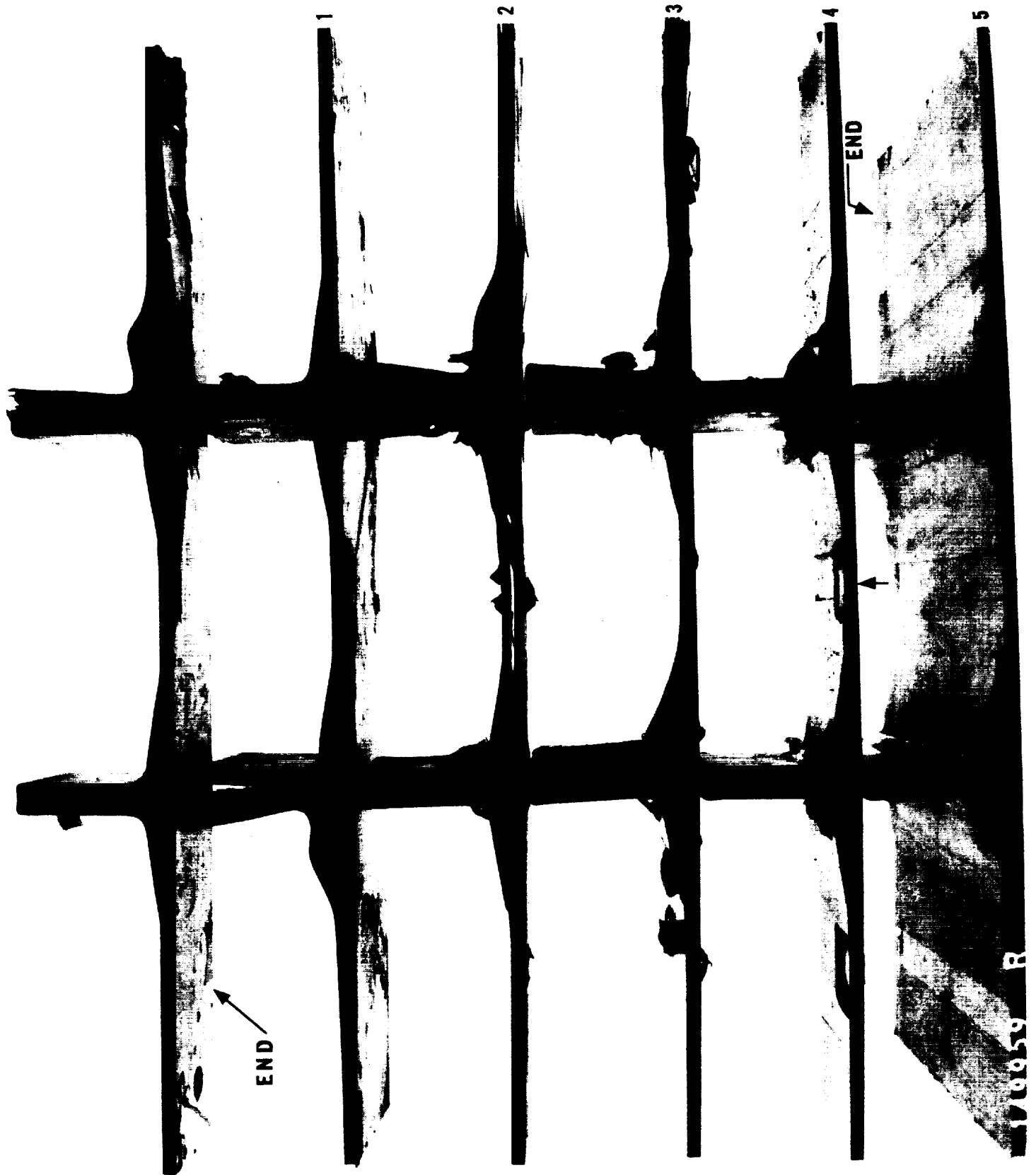


Figure 4-67: Sections of failed impacted panel. Arrow indicates impact site. Locations are shown in Figure 64.

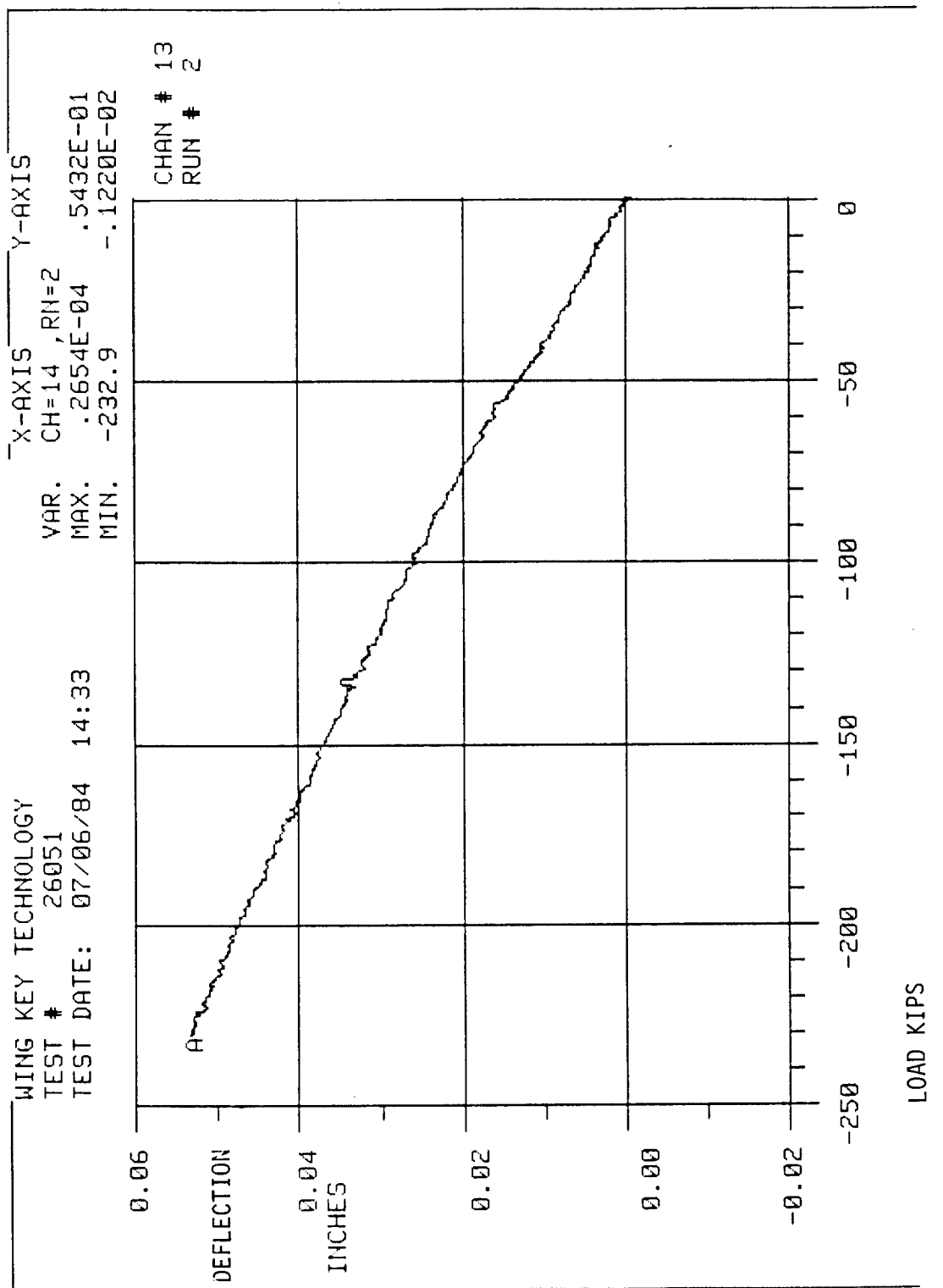


Figure 4-68: Load-Deflection curve for impacted compression panel G.

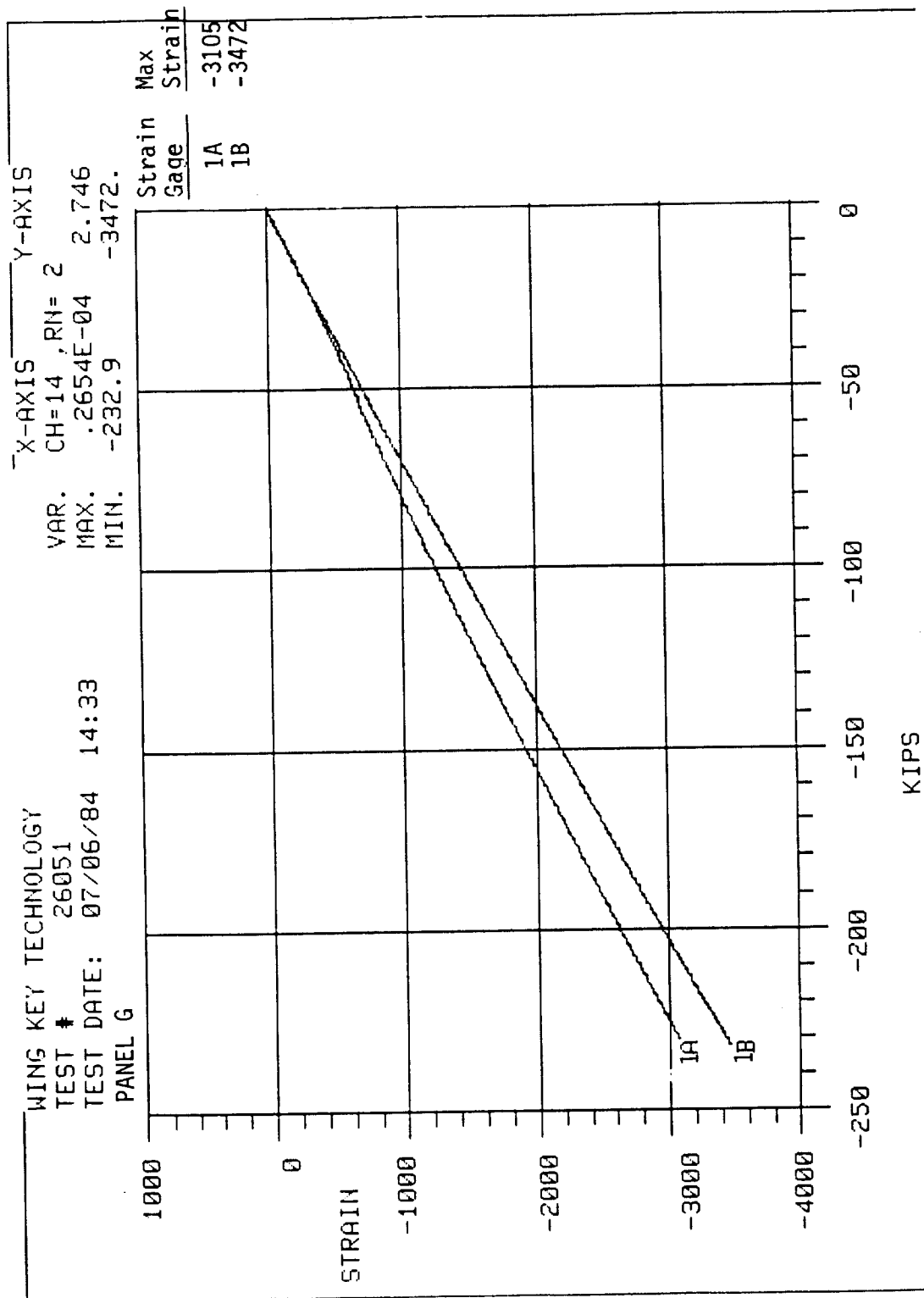


Figure 4-69: Load-strain plot of strain gages 1A and 1B on Panel G.

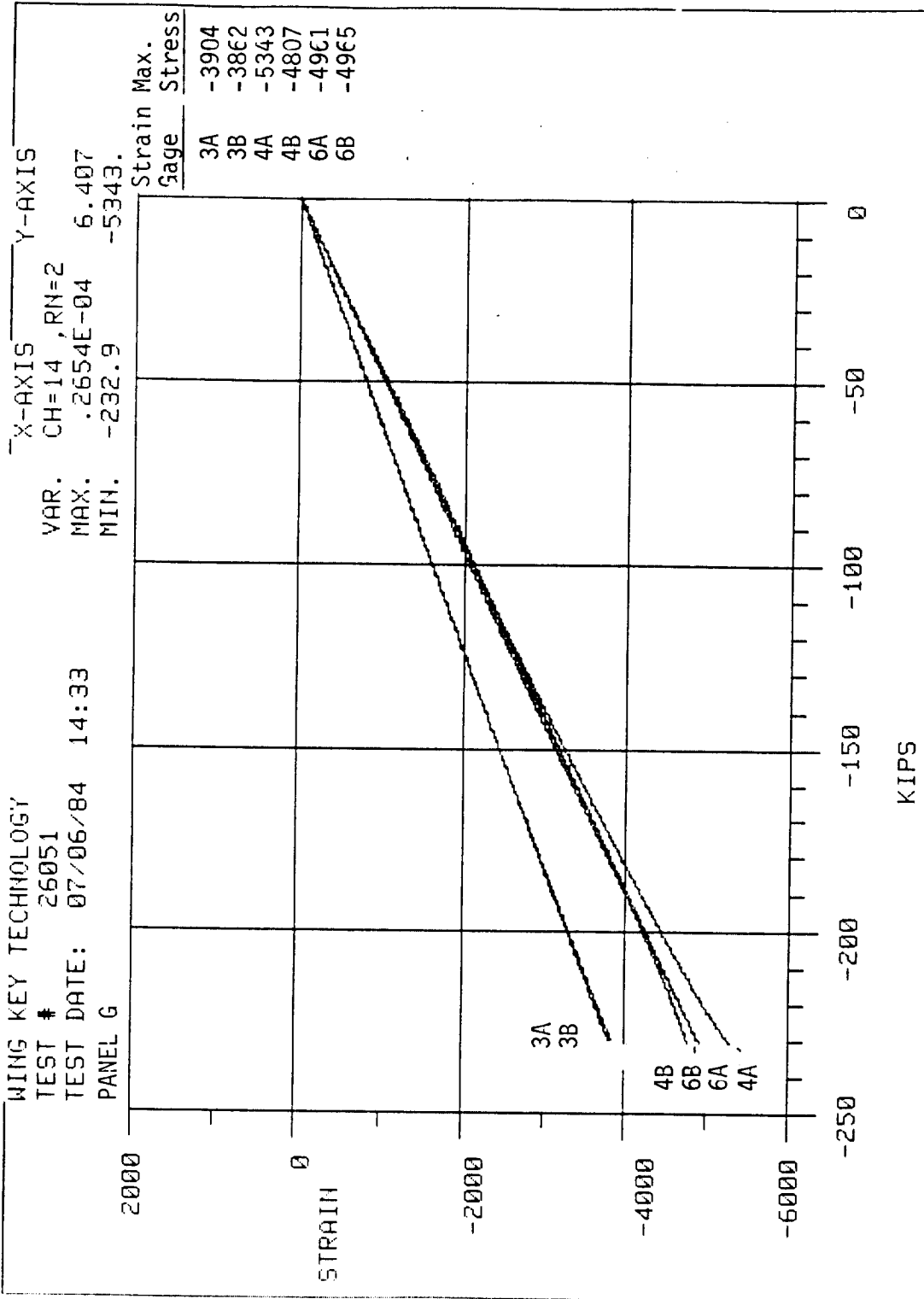


Figure 4-70: Load-strain plot of strain gages 3A, 3B, 4A, 4B, 6A and 6B on Panel G.

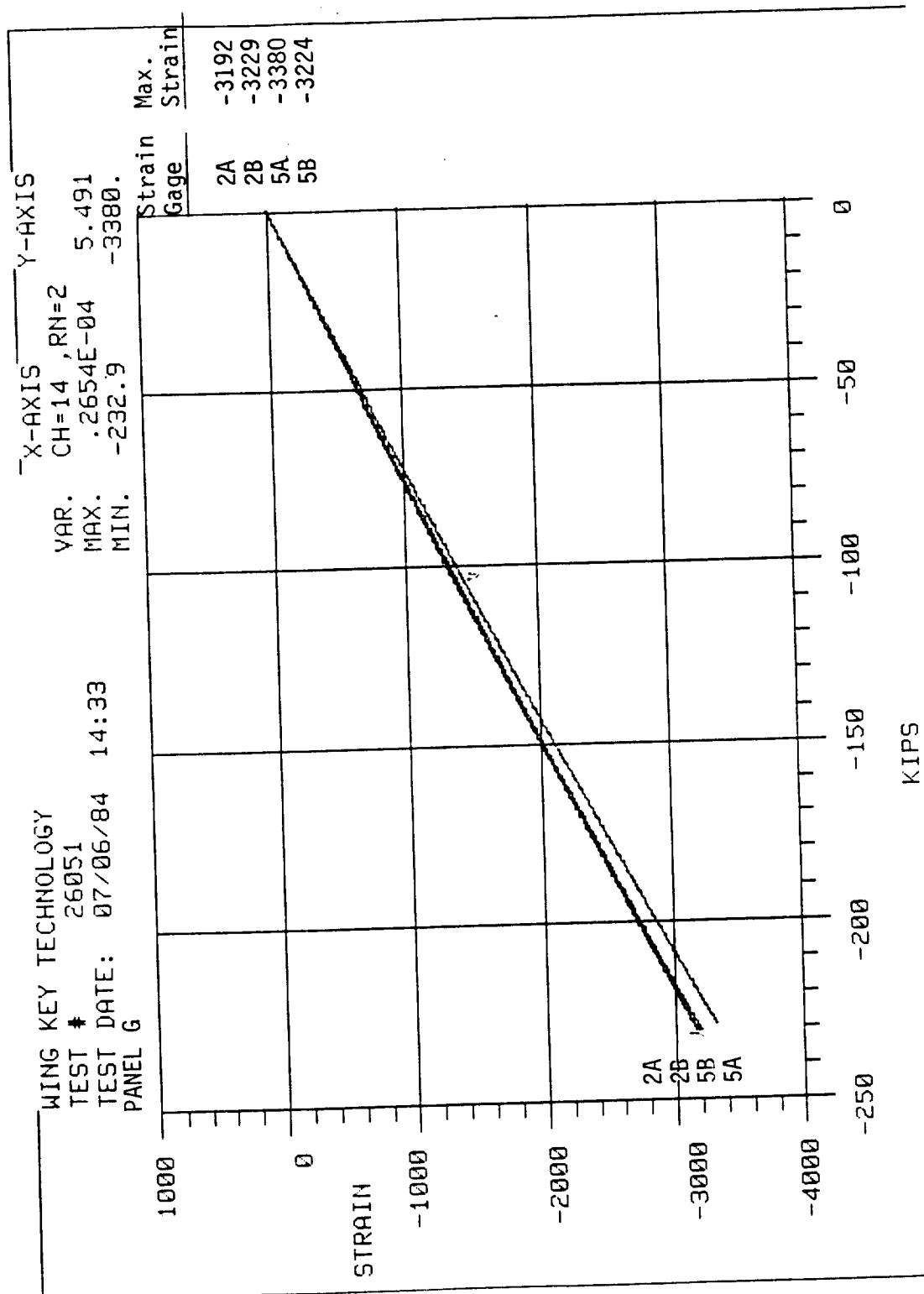


Figure 4-71: Load-strain plot of strain gages 2A, 2B, 5A and 5B on Panel G.

4.9 CONCLUSIONS

An examination of each failed specimen reveals that if one were to consider only the area under the stiffeners out to one to two inches on either side they all appear to have failed in essentially the same manner. That is the delamination resulting from a compression test is the same as the delamination of a stiffener side load or stiffener pull-off test. This seems to indicate that the critical failure mode in all of these tests was interlaminar tension between the stiffener flange and the skin. In almost all cases the failure was 2 to 3 plies above the secondary bond line. This would explain why the impacted specimens did not fail through the impacts -- the impacts were less critical than the natural stiffener/skin interface.

SECTION 5

LIGHTNING STRIKE DAMAGE AND UNDAMAGED COMPRESSION TESTS

5.1 INTRODUCTION

The objective of this task was to determine the amount of strength degradation caused by a Zone II lightning strike in a composite wing surface substructure. Two panels from the Lightning Strike Test Series IV which had been subjected to Zone II lightning strikes at various locations were received for use in the test program. The laminate layup was $(45/135/0/90)_{4s}$. Details of the lightning strike tests are given in Reference 3. Compression test specimens were machined from both the undamaged and lightning strike areas and tested in compression to failure.

5.2 COMPRESSION TEST PROCEDURES

Three lightning damaged and three undamaged compression specimens were machined and instrumented per Figure 5-1 from two panels tested in Lightning Strike Test Series IV. Specimens 261-C, 261-D, and 263-A from Panels 261 and 263 were damaged by lightning strikes #6, #7, and #12, respectively. The original specimen locations on each panel are shown in Figures 5-2. Figures 5-3 and 5-4 show the specimen locations superimposed on standard ultrasonic c-scans of the panels to show the approximate extent of the damage following the lightning strikes. The specimens were tested in the simply supported composite compression test fixture shown in Figure 5-5. Tests were conducted in the 200 kip MTS machine shown in Figure 5-6 at a stroke rate of 0.05 in./min. at room temperature.

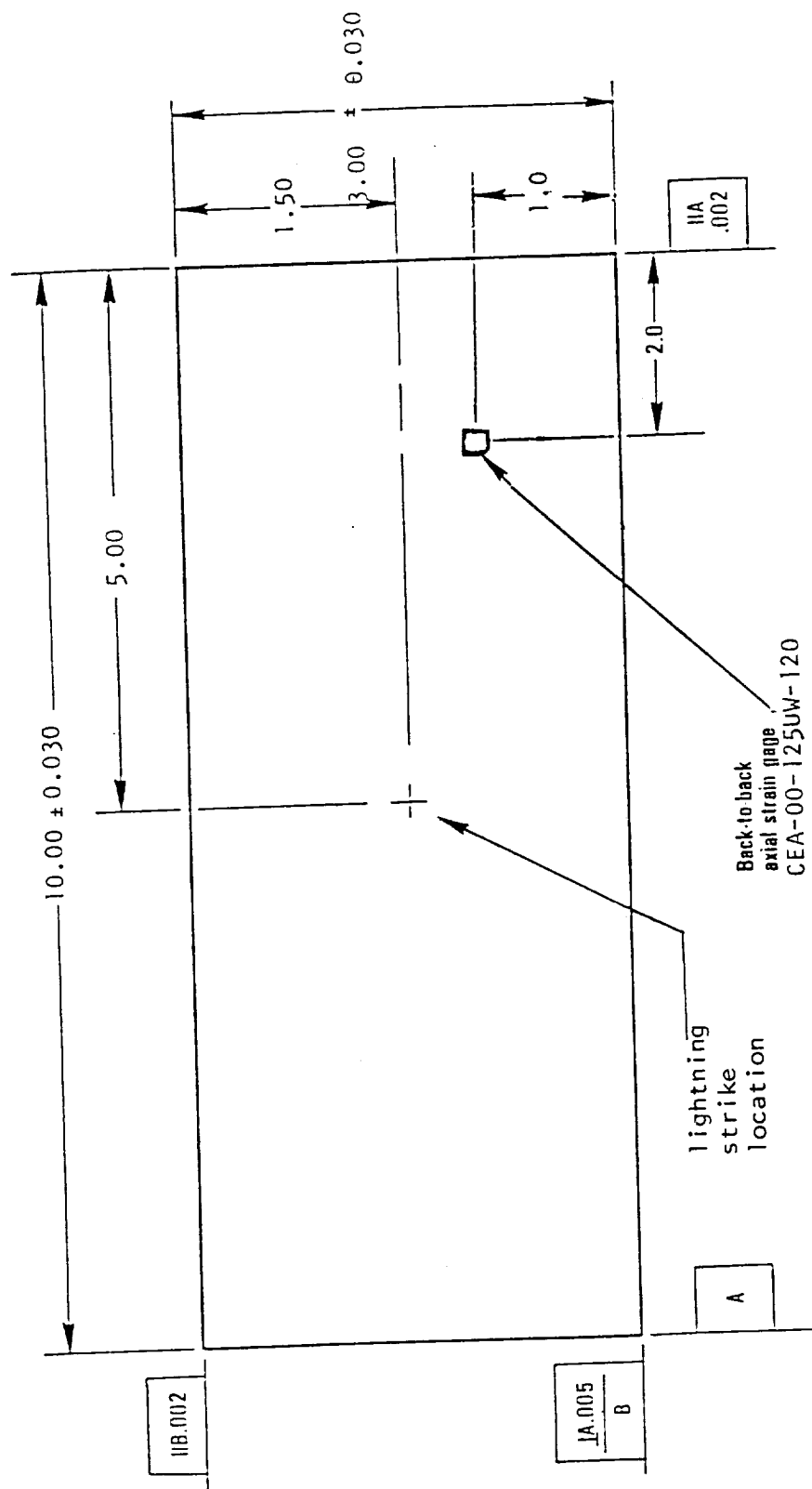


Figure 5-1: Compression coupon.

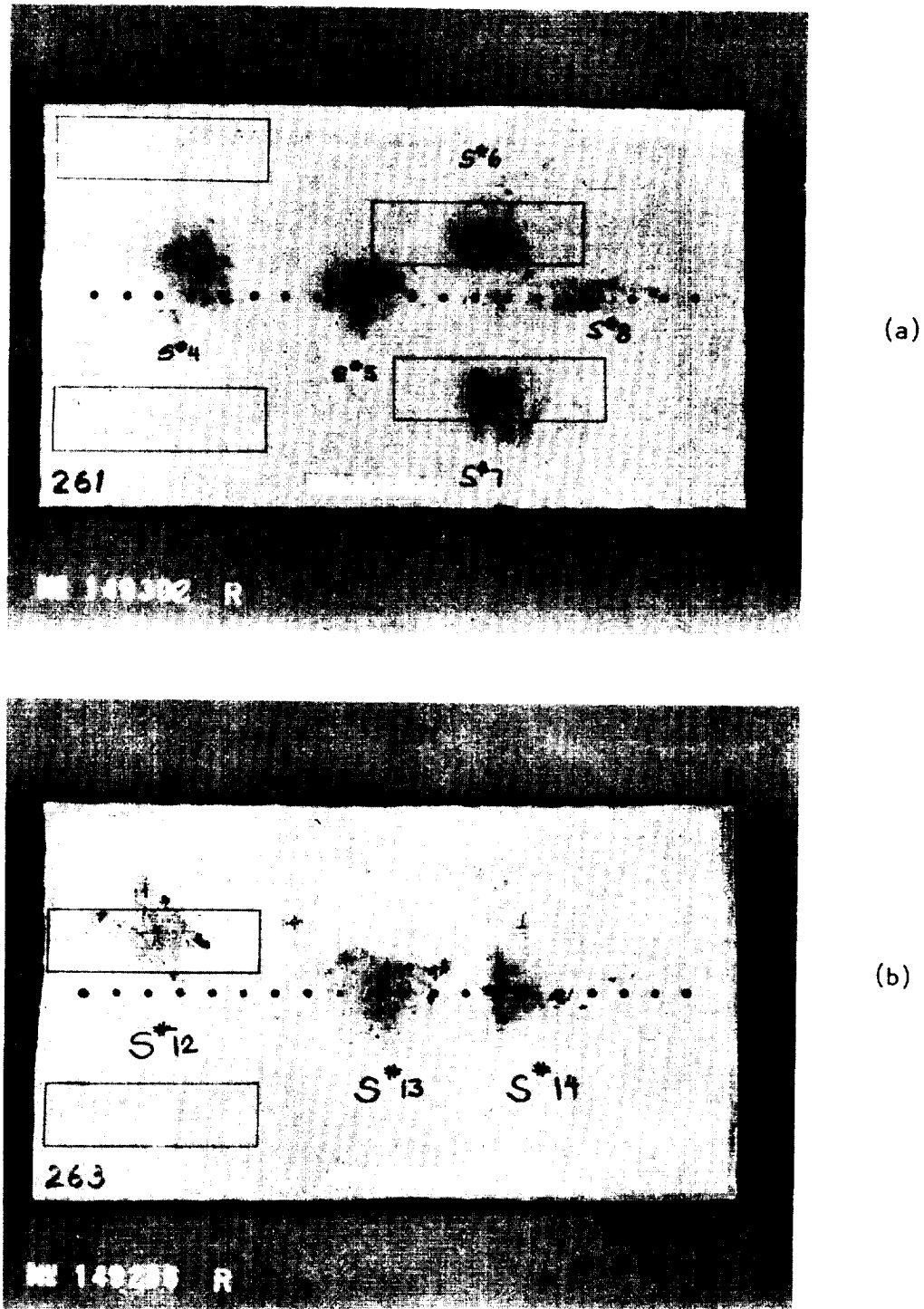


Figure 5-2: Compression test specimen locations on lightning strike panels: a) Panel 261, b) Panel 263.

ORIGINAL PANEL IS
OF POOR QUALITY

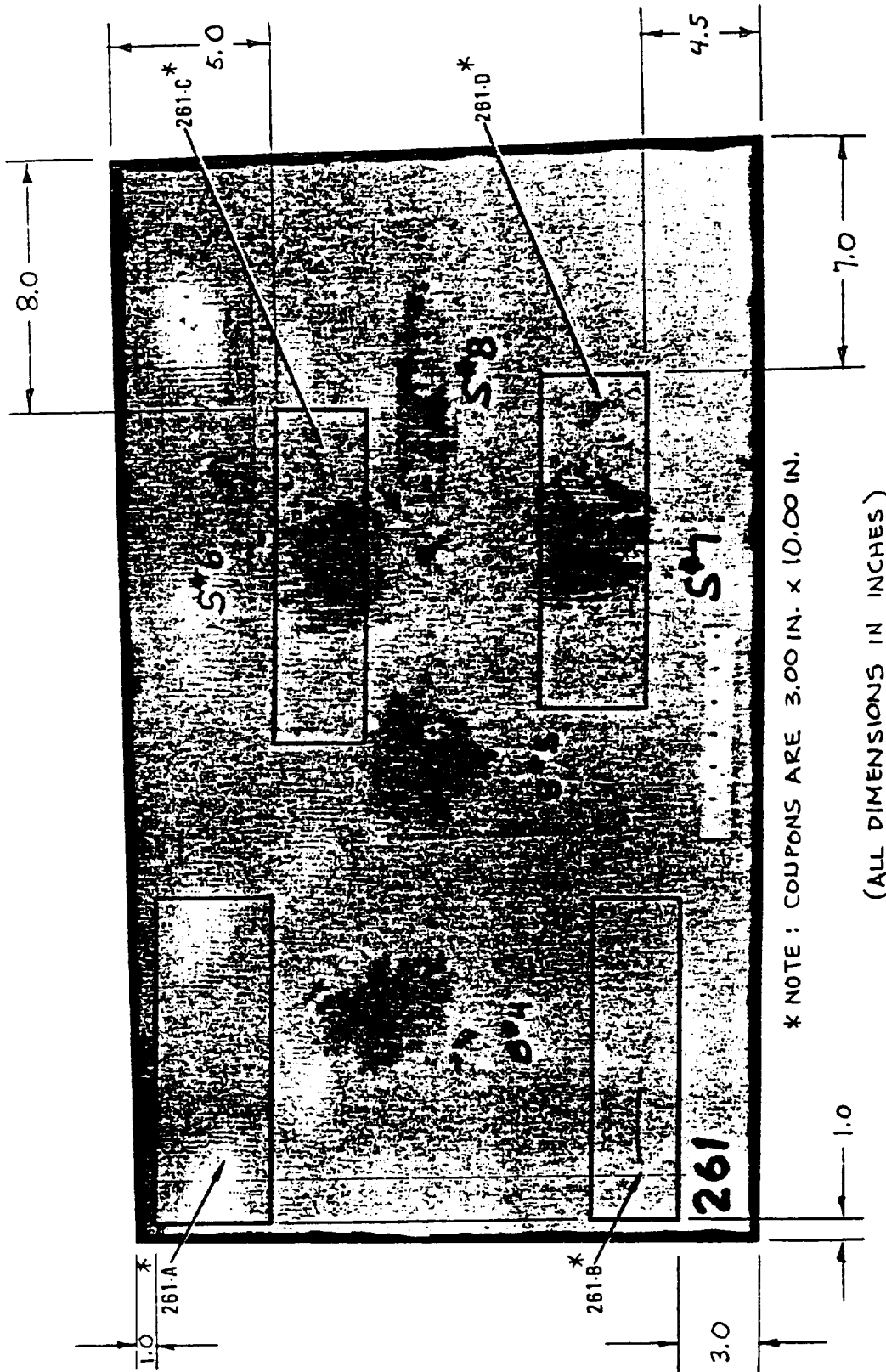


Figure 5-3: Damaged and Undamaged Compression Test Coupon Locations from Panel 261.

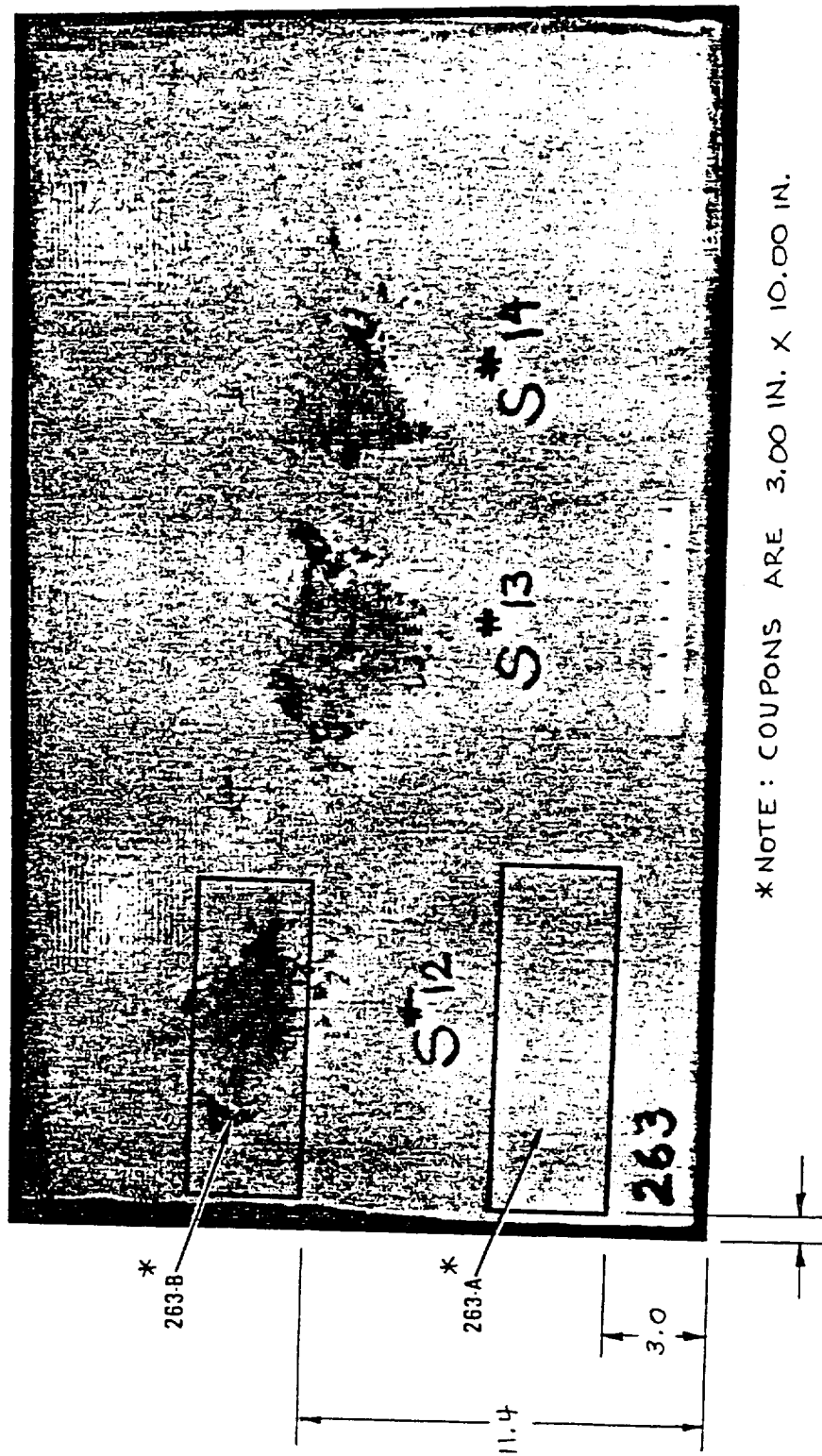


Figure 5-4: Damaged and Undamaged Compression Test Coupon Locations from Panel 263.

5.3 COMPRESSION TEST RESULTS

Load vs strain plots were obtained from back-to-back axial strain gages for each test. The failure stress, failure strain, and modulus values are summarized in Table 5.1. The reported strain and modulus values are averages from the back-to-back strain gages on each specimen. Photographs of the failed specimens are shown in Appendix L.

All specimens, both damaged and undamaged, failed in buckling. The divergence of the load/strain plots and the long delaminations within the laminate indicated buckling had occurred. The characteristic delamination occurred between the outermost 0° and 90° plies of the $(45/135/0/90)_{4s}$ layup closest to the lightning protection layer. Thus, it was not only the lightning protection layer that failed, but also the laminate itself. The lightning protection plating surface cracked as the specimen was loaded, often inducing strain gage failure on that side after buckling had initiated but prior to specimen failure.

As can be seen from Table 5.1, Zone II lightning strike damage does not change the compression load carrying capability nor the failure strain of the lightning strike panels. The failure locations for the control and lightning damage were similar.

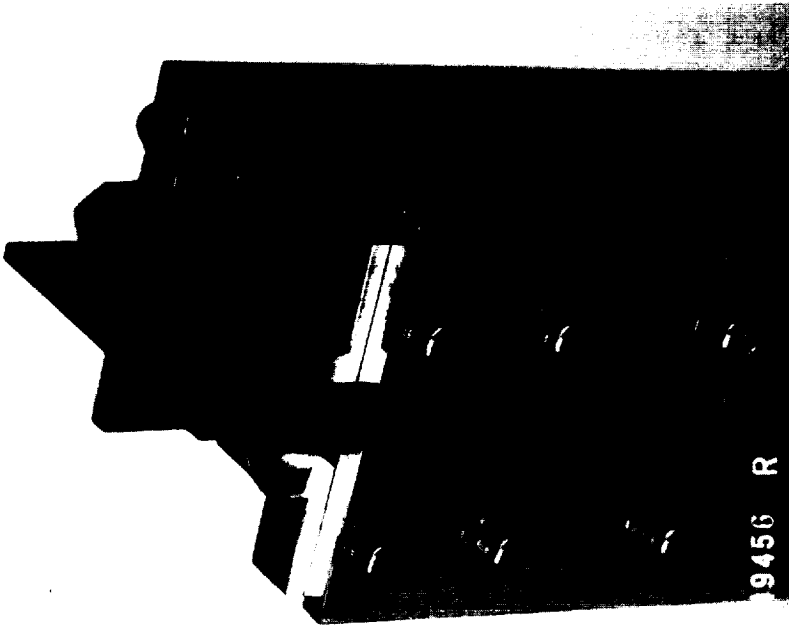
TABLE 5.1
COMPRESSION TEST RESULTS FOR LIGHTNING STRIKE
DAMAGED AND UNDAMAGED COMPRESSION TESTS

Coupon ID	Test Type and Condition	Thickness, in.	Width, in.	Area, in. ²	Buckling Failure Load, kip	Buckling Failure Stress, ksi	Buckling Failure Strain, in./in.	Final Failure Load, a kip	Final Failure Stress, a ksi	Modulus, b msi
261-A	Undamaged	0.184	3.001	0.552	-29.80	-54.0	-0.0083	-38.5	-69.7	6.8
261-B	Compression	0.183	3.001	0.550	-32.30	-58.7	-0.0091	-40.8	-74.2	7.1
263-A	75°F, Dry	0.187	3.001	0.562	-29.75	-52.9	-0.0081	-43.9	-78.1	6.7
Average					-30.62	-55.2	-0.0085	-41.1	-74.0	6.9
261-C	Damaged	0.186	3.000	0.559	-33.02	-59.1	-0.0097	-41.2	-73.8	7.3
261-D	Compression	0.186	3.001	0.557	-30.92	-55.5	-0.0084	-42.0	-75.5	7.4
263-B	75°F, Dry	0.189	3.001	0.567	-31.67	-55.9	-0.0085	-45.3	-79.9	7.1
Average					-31.87	-56.8	-0.0089	-42.8	-76.4	7.3

a) Final failure load/stress - maximum load/stress experienced by specimen.

b) Modulus calculated at 0.002.

ORIGINAL RECORD
OF POOR QUALITY



(b)

149456R

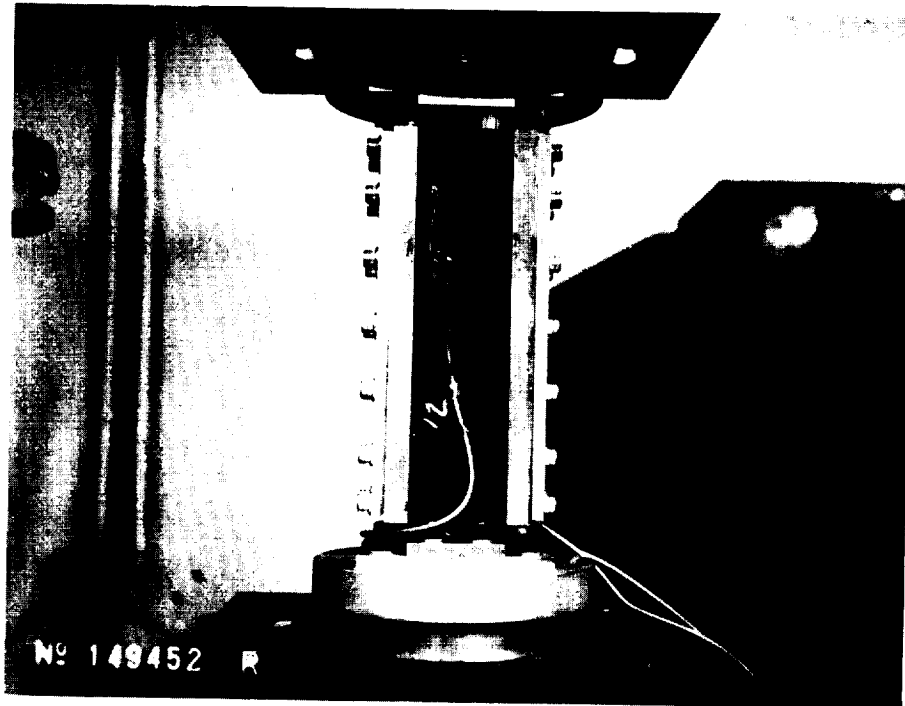


(a)

149454R

Figure 5-5: Simple supported composite compression test fixture #4 (Drawing No. 16963): a) full view, b) edge supports.

ORIGINAL PAGE IS
OF POOR QUALITY



149452R

Figure 5-6: Simple supported composite compression test fixture #4
(Drawing No. 16963) in MTS test machine.

SECTION 6

TECHNOLOGY DEMONSTRATION ARTICLE

6.1 INTRODUCTION

The objective in testing the demonstration article was to verify the structural technology that was developed for damage tolerance, lightning protection and fuel containment in a stiffened panel with attached substructure. The demonstration article was representative of a moderately loaded area of a transport aircraft wing.

The demonstration article was delivered to the Structures Laboratory at the Kelly Johnson Research and Development Center on July 12, 1984. The article had been subjected to a simulated lightning strike prior to receipt. A series of tests were conducted, the tests involving structural loading (fuel containment and pressure, fatigue, and residual static strength) interspersed with impact damage incidents and inspections. All testing was done in accordance with Reference 4.

6.2 SUMMARY OF RESULTS

The test article exhibited no fuel leakage through the skin during any of the fuel containment proof or ultimate pressure tests. No damage was detected due to the one lifetime of fatigue loading consisting of 36,000 cycles to 50% of the design limit compressive load and 36 cycles to 80% of the design limit load.

The article successfully withstood application of the design ultimate compressive load of -294,000 pounds after the fatigue testing had been completed. Failure subsequently occurred at 338,500 pounds during the residual static strength test. The failure occurred transversely near the

center of the test section, passing through previously inflicted impact damage representative of an impact energy of 30 ft-lbs. Strains of -6400 to -6500 μ in./in. were recorded immediately prior to failure.

6.3 TEST ARTICLE

The test article, Part Number CL2225-03-03-101, was a blade-stiffened graphite/epoxy panel with attached substructure, designed to be representative of a transport wing skin panel (Figures 6-1 through 6-3). The material system was AS4/2220-1. The panel had a 25-inch long test section of skin and stiffeners between aluminum simulated ribs. The panel was 18-inches wide with the two tee-sectioned stiffeners on a 6-inch center. The longitudinal edges were closed by angles (also graphite/epoxy) attached with mechanical fasteners. The interior surface was sealed for fuel containment using a 5-mil thick flexible polyurethane coating (Chemglaze by Lord Chemical). The exterior (skin) surface was painted using standard epoxy primer and two coats of urethane paint (white).

The skin, stiffeners, and edge-closure angles were extended beyond the ribs to provide for installation of the end fittings and doublers required for structural loading. Graphite/epoxy doublers (Figure 6-4) were bonded to the interior and exterior surfaces. Aluminum end doublers and fillers (Figures 6-5 and 6-6) were also installed.

The test article was subjected to the testing sequence below:

<u>ITEM</u>	<u>DESCRIPTION</u>
1	Lightning strike (prior to receipt by Structures Laboratory).
2	Fuel containment (10 psig) with fuel enclosure and simulated fuel.
3	Impact of skin exterior surface.

ORIGINAL PAGE IS
OF POOR QUALITY

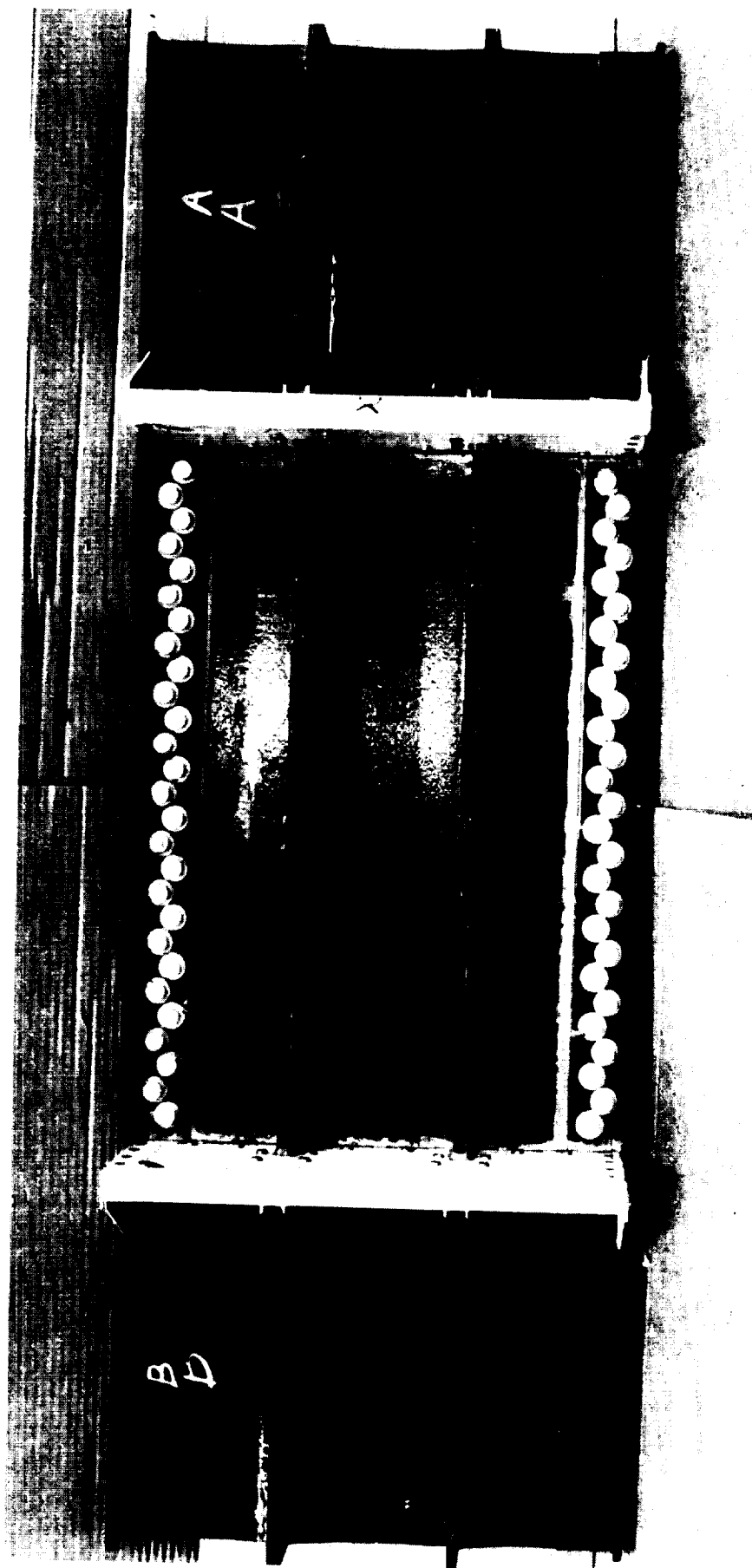


Figure 6-1: Interior surface of the test article, PN/CL2225-03-03-101, as received.

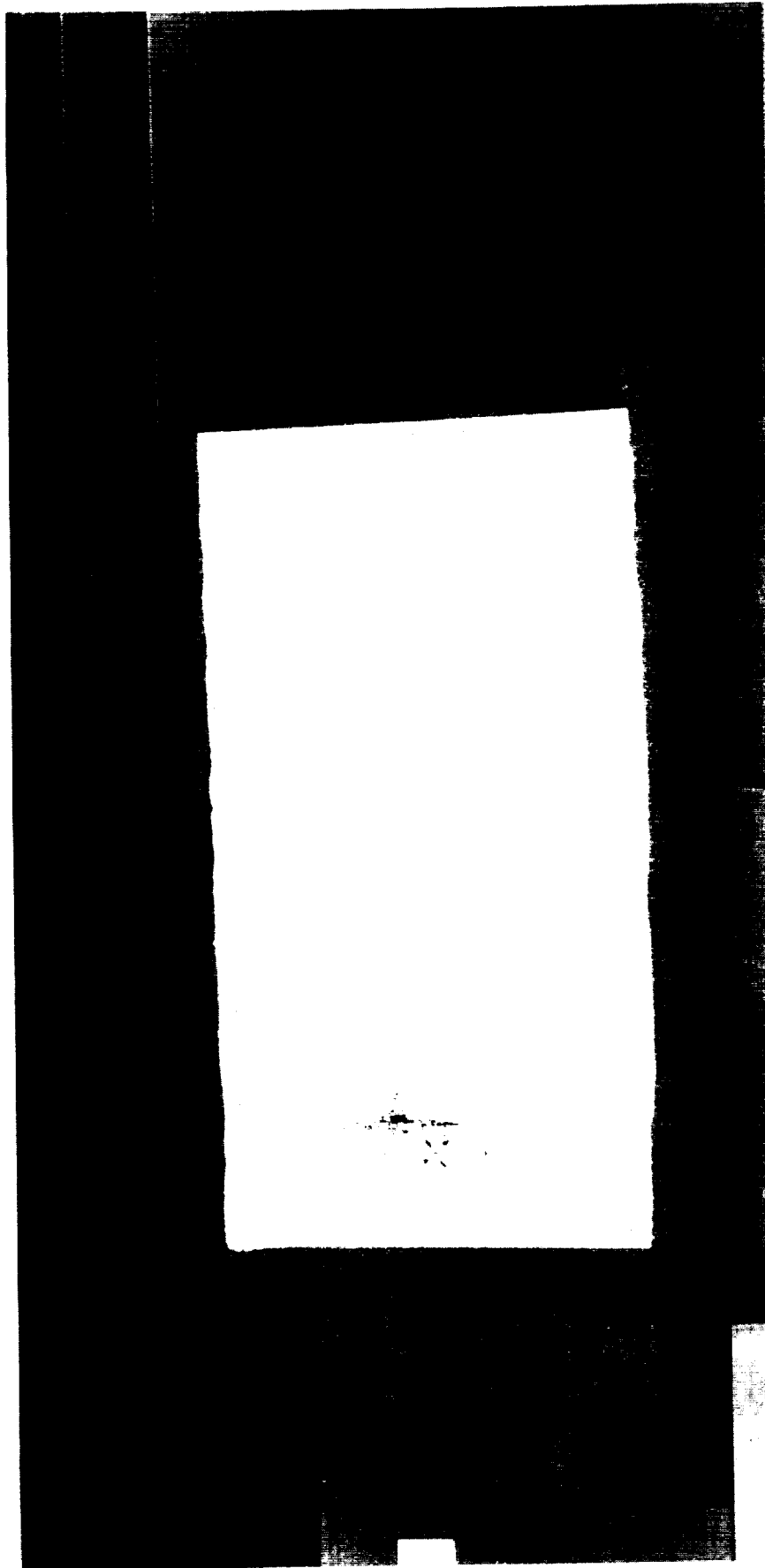


Figure 6-2: Exterior surface of the test article showing simulated lightning strike at "B" end of painted portion, as received.

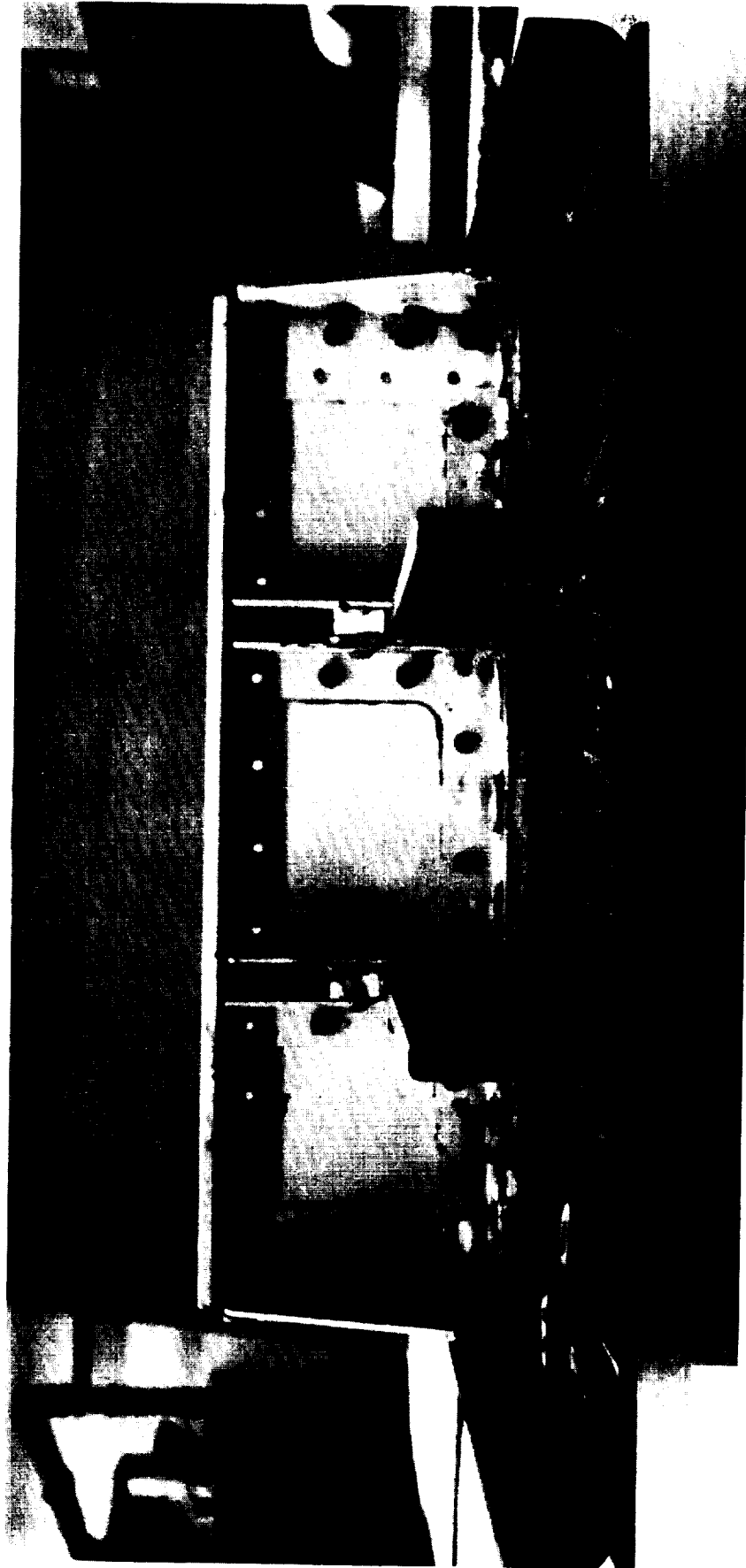
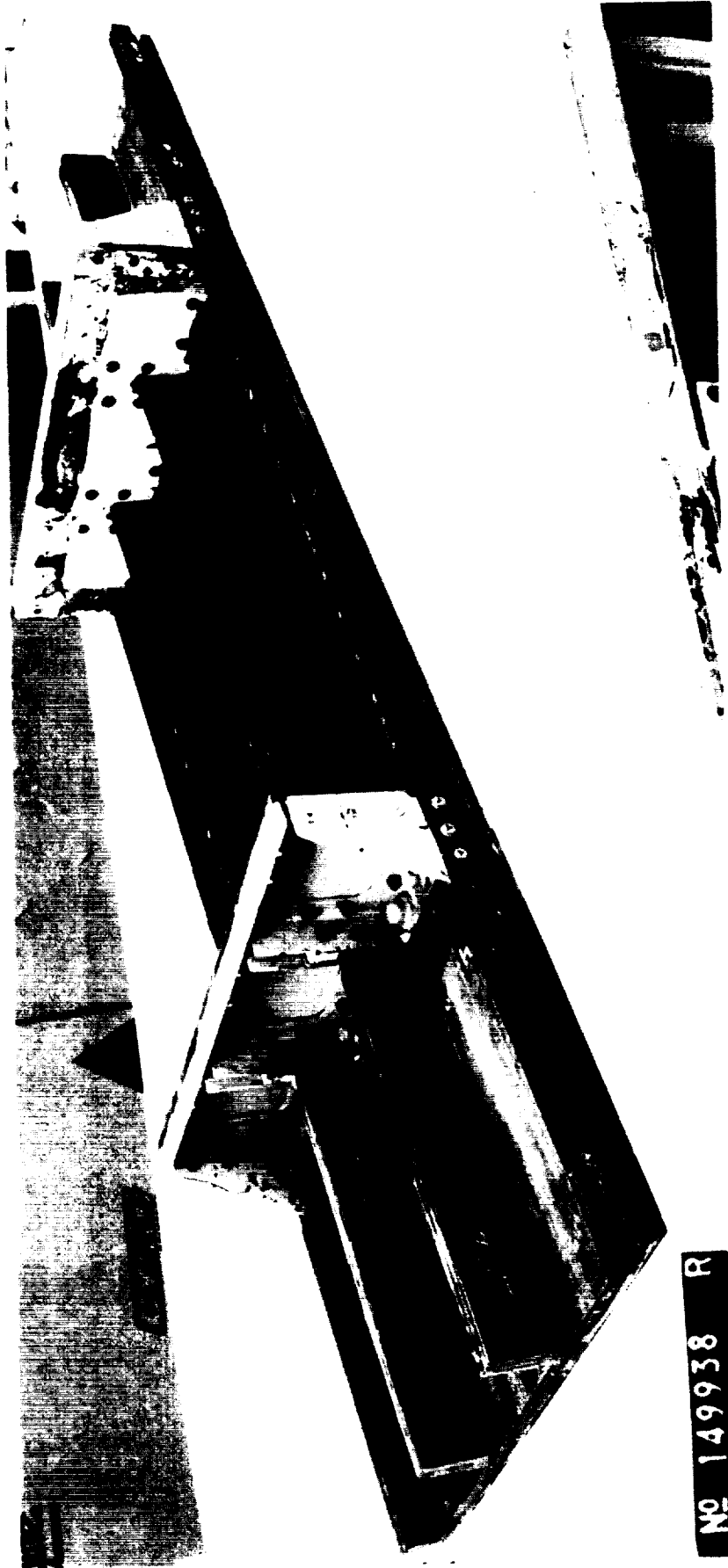


Figure 6-3: End view of test article showing typical cross section and simulated rib, as received.

ORIGINAL FILED IN
OF POOR QUALITY



NO 149938 R

Figure 6-4: Test article with graphite/epoxy and doublers installed.



Figure 6-5: Aluminum end doublers installed on interior surface of test article, typical.

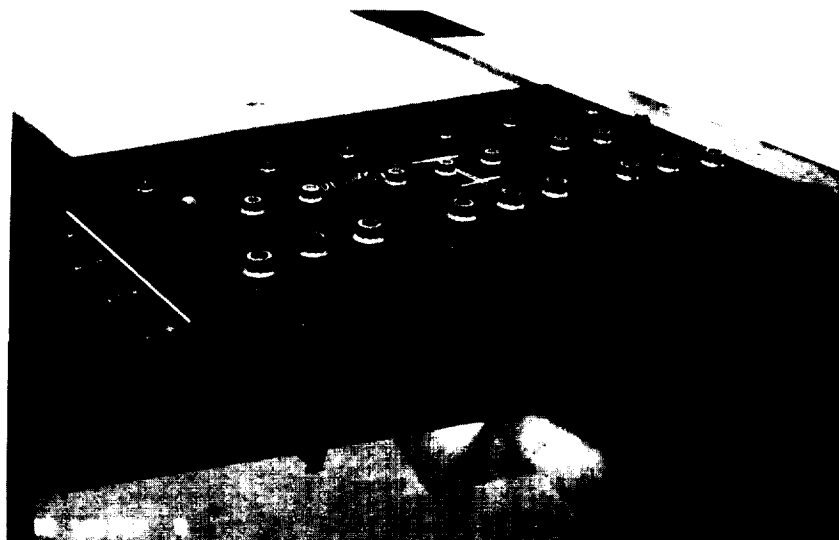


Figure 6-6: Appearance of test article exterior surface after doubler installation.

- 4 Non-destructive inspection of impact damage.
- 5 Fuel containment test (10.0 psig).
- 6 Fatigue loading to one lifetime, uniaxial load cycles.
- 7 Fuel containment test to ultimate pressure (15.0 psig).
- 8 Static loading to design ultimate load, uniaxial load.
- 9 Impact of skin exterior surface.
- 10 Static loading to failure, uniaxial load.

6.4 TEST PROCEDURE

Prior to receipt for testing, the test panel had been subjected to a simulated Zone II lightning strike (outside vendor, LTRI; strike shown in Figure 6-2) and post strike non-destructive inspection (CALAC Quality Assurance Laboratory). The first test was a fuel containment test. A fuel enclosure, was fabricated and mounted over the test article between the simulated ribs (Figure 6-7). It was secured by attachments through the ribs and the panel edge-closure angles. Openings were provided for filling and viewing of a fuel simulant, Shell Oil Company "Pella A". Ports were furnished for pressurization, pressure dump, and fuel simulant draining.

The enclosure was filled to capacity (20 gallons) with fuel simulant to which a fluorescent tracer dye (T-100/OS-31, Shannon Luminous Materials, Santa Ana, California) had been added in a ratio of 1 part to 200 parts. Nitrogen was used to pressurize the grounded enclosure to the proof pressure (10.0 psig) through an electrically-operated solenoid pressure regulator (Figure 6-8). Pressure was held for 30 minutes during which time an ultraviolet light was used to check for visible leaks of fuel simulant from the pressurized surfaces (skin and ribs) of the panel.

After completion of the pressure test, the simulant was drained and the panel cleaned with methylethylketone, (MEK). A support frame

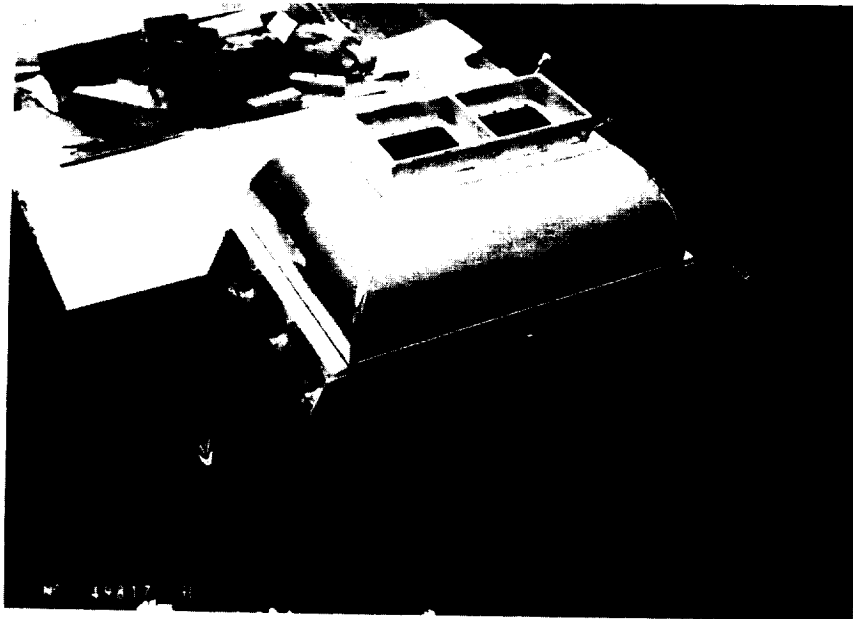


Figure 6-7: Fuel containment pressure enclosure mounted between ribs of test article, filling ports at top (cover not shown).

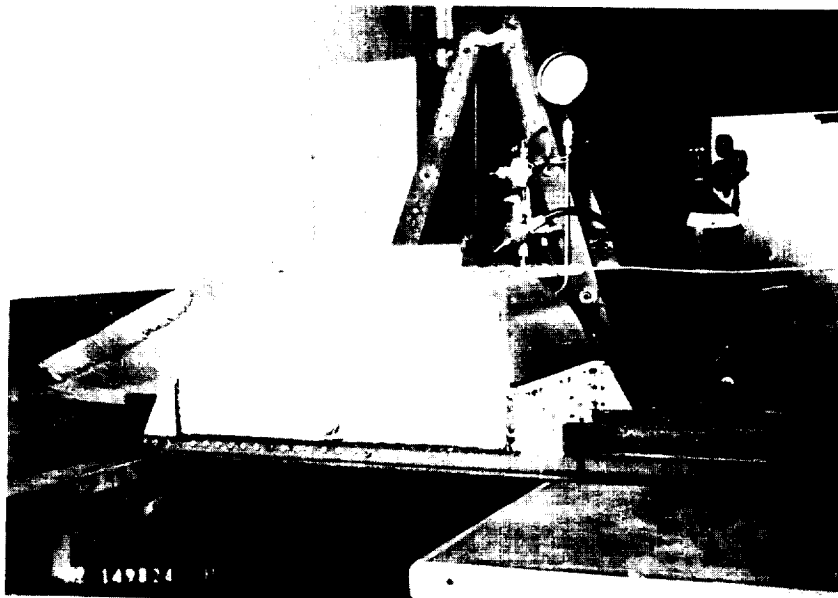


Figure 6-8: Fuel containment pressure test set-up with test article, nitrogen bottle pressure source, supply regulator, and pressure gauge.

(modified from the trial impact test) was installed over the test section (Figure 6-9). The exterior surface of the skin was impacted (Figure 6-10) using a 1/2-inch diameter hemispherical steel tip dropped to produce 30 ft-lbs of impact energy at the requested location (Figure 6-11, Impact 1). An ultrasonic A-scan inspection was performed on the impact area to determine the extent of damage (Figure 6-12).

A second fuel containment proof pressure test was run at 10.0 psig with the pressure held for 30 minutes. Upon completion, graphite/epoxy doublers were bonded to the ends of the panel using a film adhesive (see Figure 6-4). Aluminum doublers and fillers were added (Figures 6-5 and 6-6), maintaining the centroids of the panel test section.

A total of 18 (9 back-to-back) strain gages were installed (as shown in Figure 6-13). The polyurethane coating on the interior surface was removed locally for gage installation.

Fatigue testing was then performed in a uniaxial test machine (MTS 200,000 pound capacity machine) controlled by the Lockheed-developed direct digital control system. Loading, at approximately 2 HZ, was accomplished using a pair of sandwich end plates, bolted to each end of the article and pin loaded (Figure 6-14). The strain gages were monitored periodically throughout the one lifetime of fatigue loading. Refer to the test loading section for details of loading sequence and magnitudes. After completion of the loading cycles equivalent to one lifetime, another ultrasonic A-scan inspection was conducted on the impact location to determine any changes in the extent of internal damage.

A final fuel containment test was run to ultimate fuel pressure of 15.0 psig, with the pressure held for 30 minutes. The panel ends then were machined flat for the residual static strength test.

ORIGINAL IMAGE IS
OF POOR QUALITY

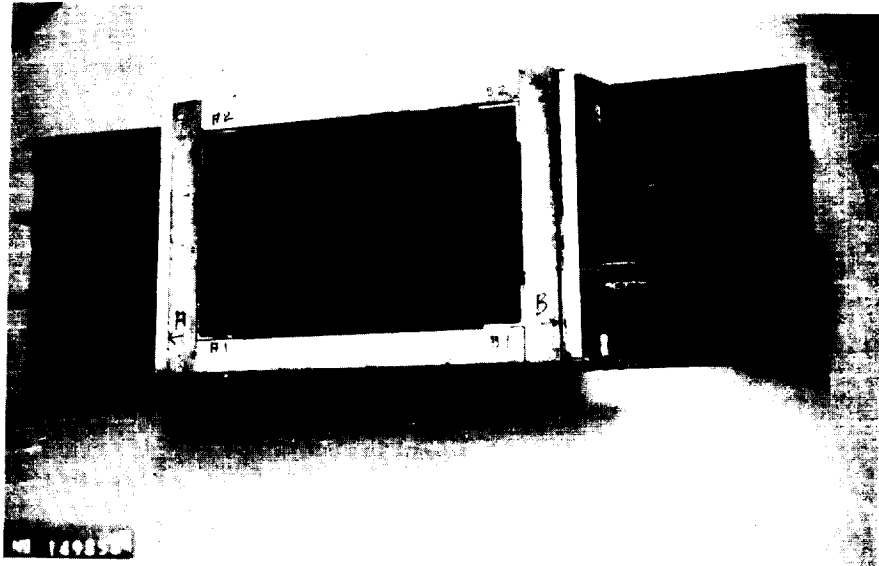


Figure 6-9: Impact support frame installed on test article.

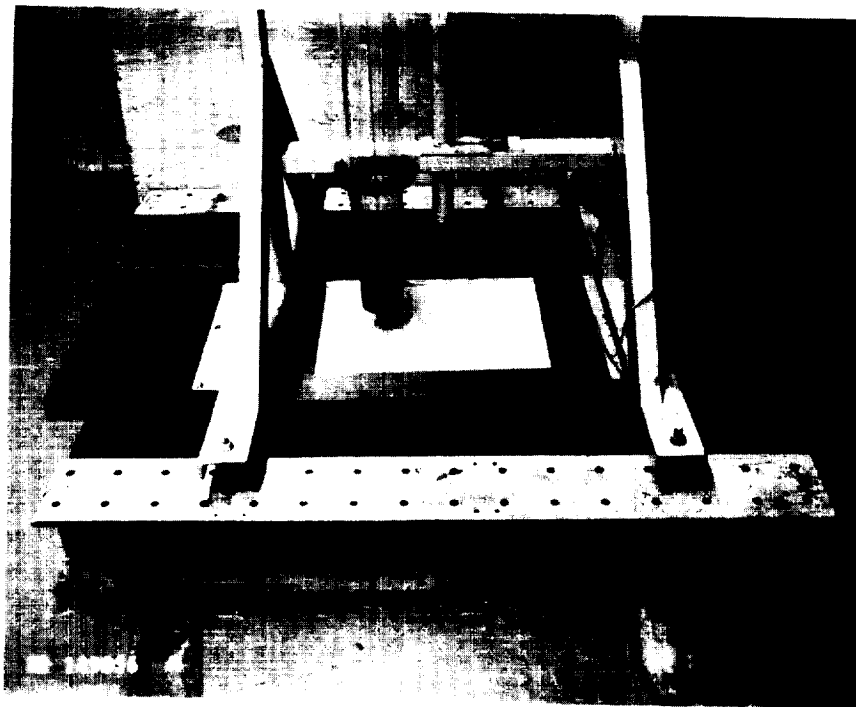


Figure 6-10: Impact test set-up showing panel with support frame, impact top and drop weight, and impact drop stand base.

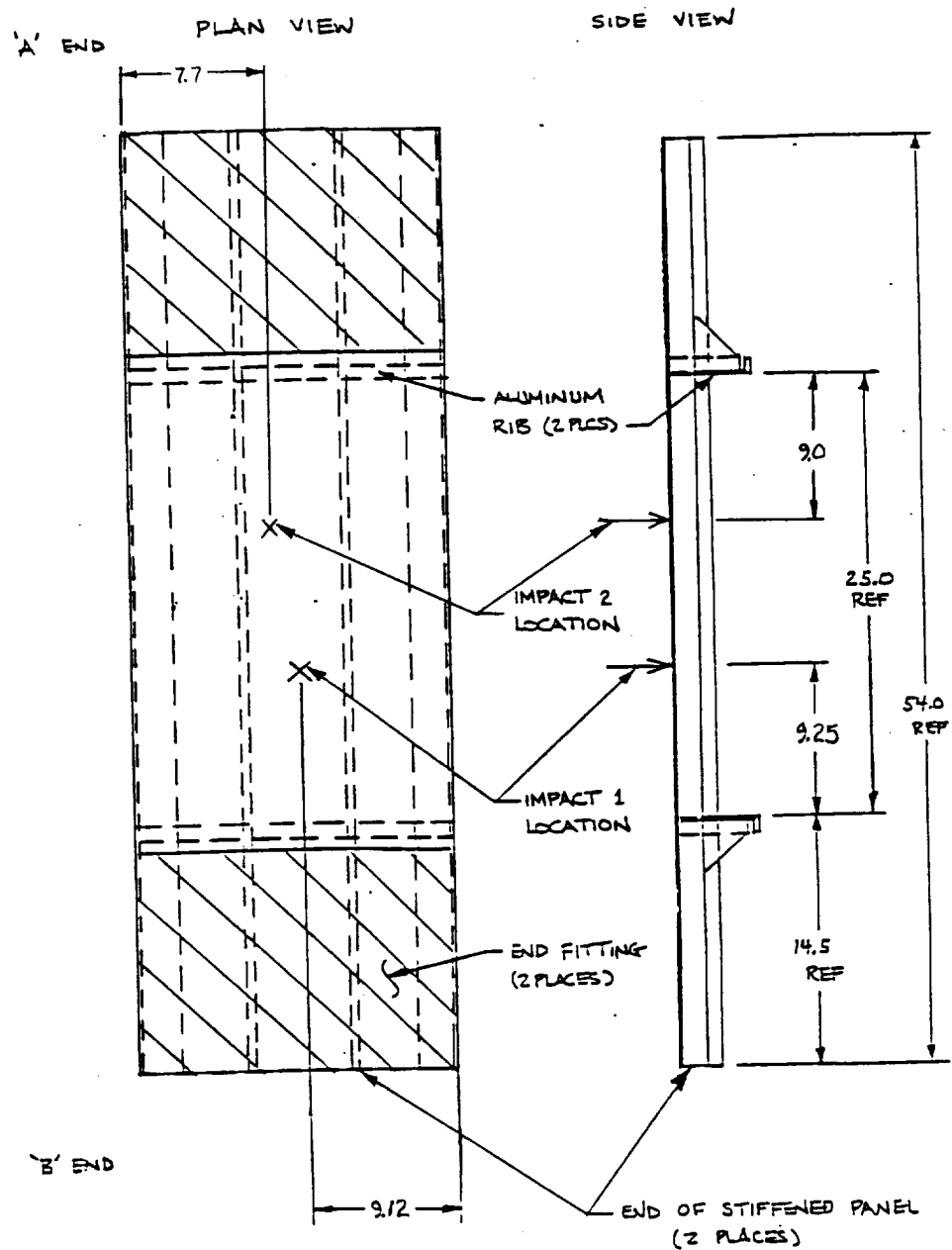


FIGURE 6-11 - Impact locations on test article; Location 1 impact done between pressure tests prior to fatigue test, Location 2 done during residual static strength testing

ORIGINAL PAGE IS
OF POOR QUALITY

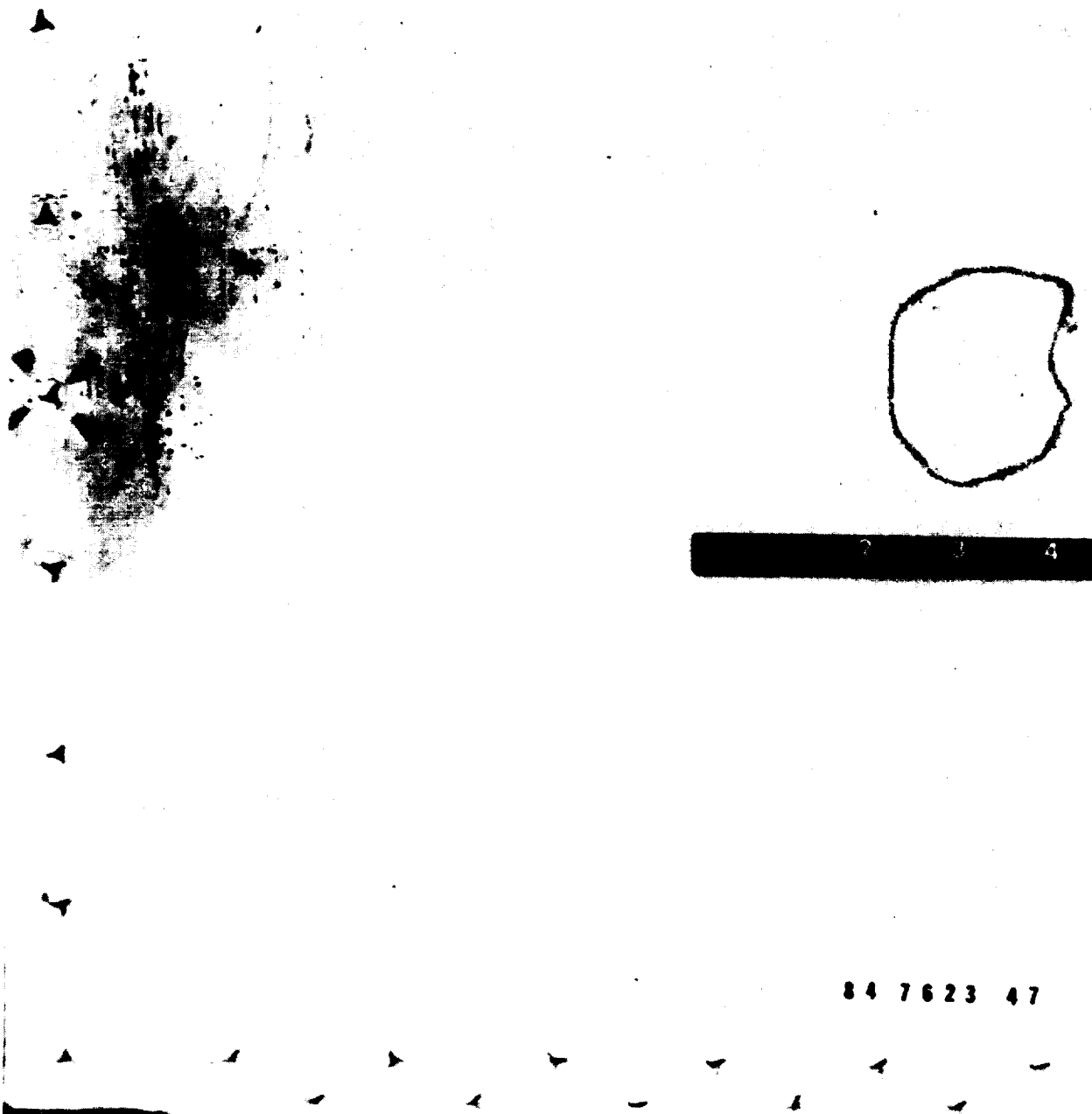


Figure 6-12: Extent of internal damage from impact (location 1, Figure 6-11), after first fuel containment test, as determined by nondestructive inspection.

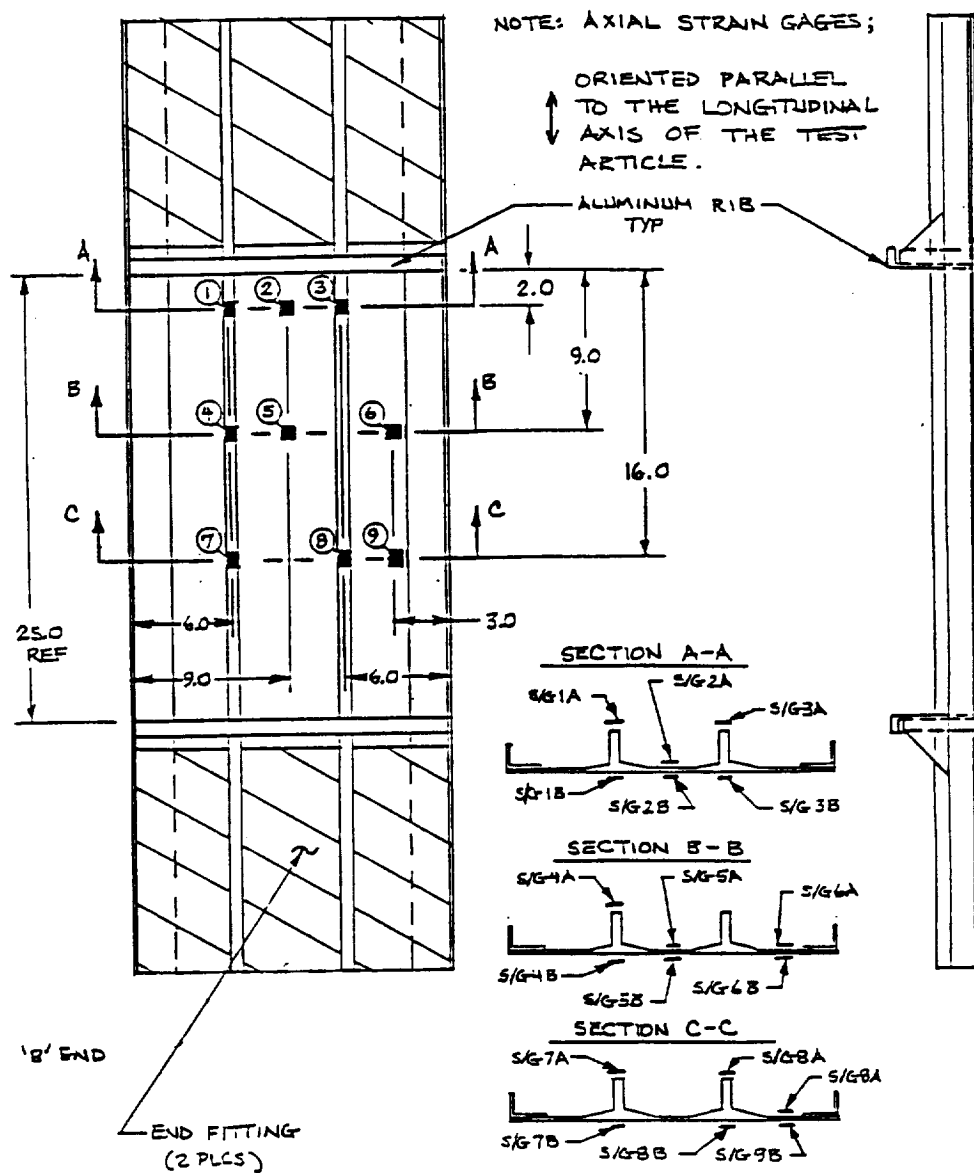


FIGURE 6-13 - Strain gage locations on test article, all gages axial



Figure 6-14: Fatigue test set-up showing test article with bending restraint flexure, loading plates, and test machine.

After installation in a Universal test machine (Figure 6-15) an LVDT was mounted to measure test machine head axial deflection. All residual strength loading was done at approximately .05 in./min. (machine head travel). All strain gages were operational and monitored during testing. At the request of the Advanced Structures Technology Department, a load equivalent to the design ultimate compressive load was applied and held for 30 seconds. After removal of load a second impact was made on the exterior surface of the skin (Figure 6-11, Impact 2). A 1.0-inch diameter hemispherical tip was used at 32 ft-lb energy level. Final loading to failure was then performed.

6.5 TEST LOADS, MONITORING, AND DATA ACQUISITION

6.5.1 Fuel Pressure Tests

The two fuel containment proof pressure tests were run at 10.0 psig. The ultimate fuel pressure test was run at 15.0 psig. All pressure monitoring was visual, a 0-15 psi calibrated pressure gauge being used. The calibration standard is traceable to the National Bureau of Standards. Leakage was monitored visually using an ultraviolet light to detect the dye in the fuel simulant.

6.5.2 Impact Tests

The impact damage inflicted at Impact Location 1 (Figure 6-11) was made using a dead-weight drop of a known mass (12 pounds) from a measured height to produce an impact energy of 30 ft-lbs. Previous experience had shown that this energy level would produce damage barely visible to the naked eye. The damage inflicted at Location 2 (also Figure 6-11) was made by a calibrated spring-loaded impact "gun". An energy level available from the gun device and most closely matching the desired 30 ft-lb level was 32-ft-lbs. This value was selected for use.

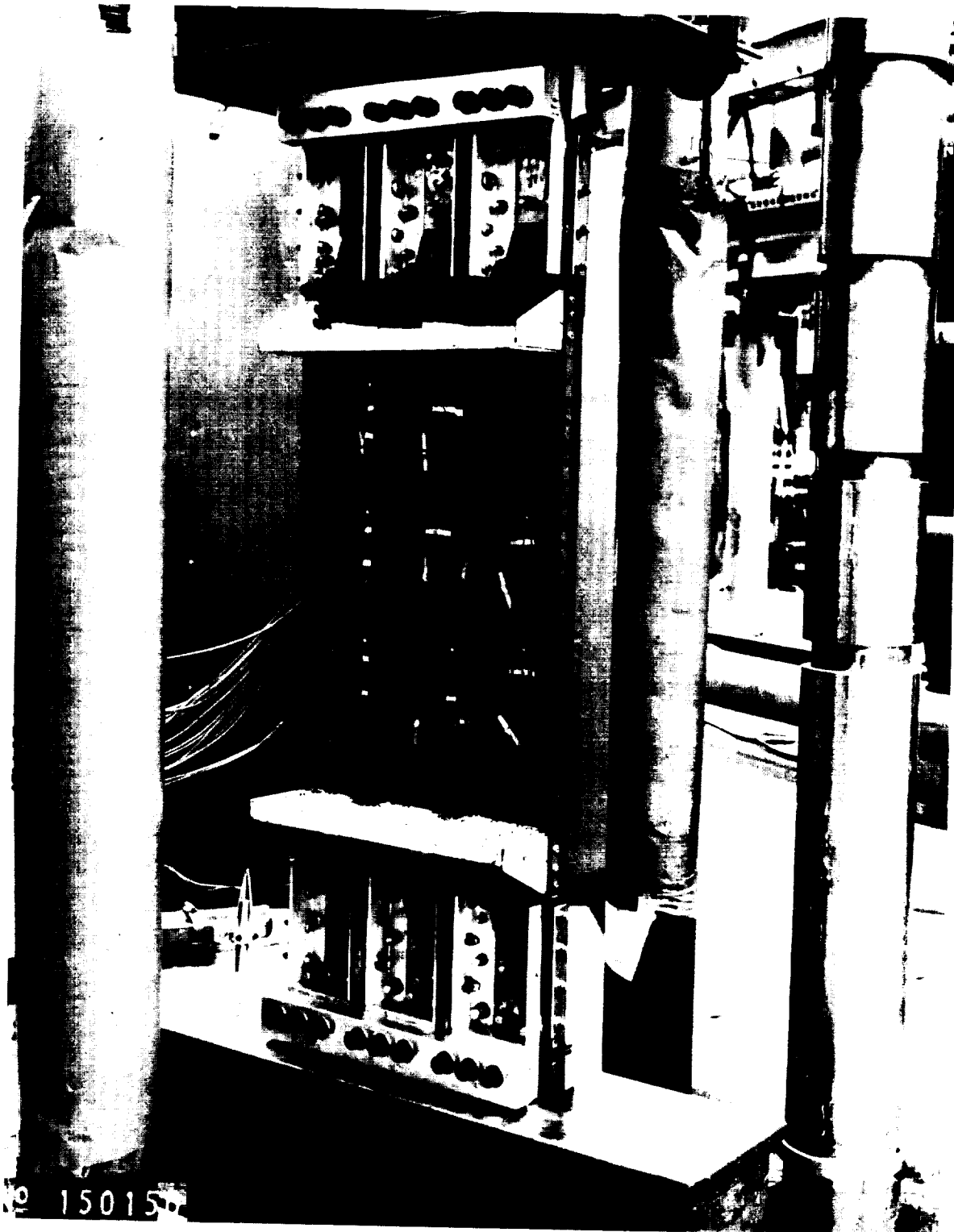


Figure 6-15: Residual static compressive strength test set-up, interior surface of test article shown.

6.5.3 Fatigue Loading Test

The fatigue test simulated one lifetime of loading and was comprised of 36,000 load cycles and 36 higher load cycles, applied one after each 1000 cycles. In all cycles, the minimum loads (compression) were twice the absolute magnitude of the maximum loads (tension), producing a range ratio of -2 (Figure 6-16). Load magnitudes are given below.

36,000 cycles -98,000/49,000 pounds
36 cycles -157,000/78,500 pounds

The load magnitudes during the 36,000 cycles represented 50% of the design limit compression load and during the 36 additional cycles represented 80% of design limit load.

Test load, test machine ram deflection, and test panel strains were continuously recorded during all 36 high load cycles and for loads verification at random times throughout the 36,000 cycles.

6.5.4 Residual Static Strength Test

Prior to the residual static compressive strength test to failure, a compression load of 294,000 pounds was applied and held for 30 seconds. This load represented the design ultimate compressive load for the panel. During both this preliminary test and the test to failure which followed, test load, test machine head deflection, and panel strains were continuously recorded.

6.6 TEST AND INSPECTION RESULTS

During the first fuel containment proof pressure test, the only leak noted from a location other than the fasteners associated with mounting of the pressure enclosure (Figure 6-8), occurred at the panel skin-to-rib faying surface at an edge-closure angle (Panel end "A"). The leak was

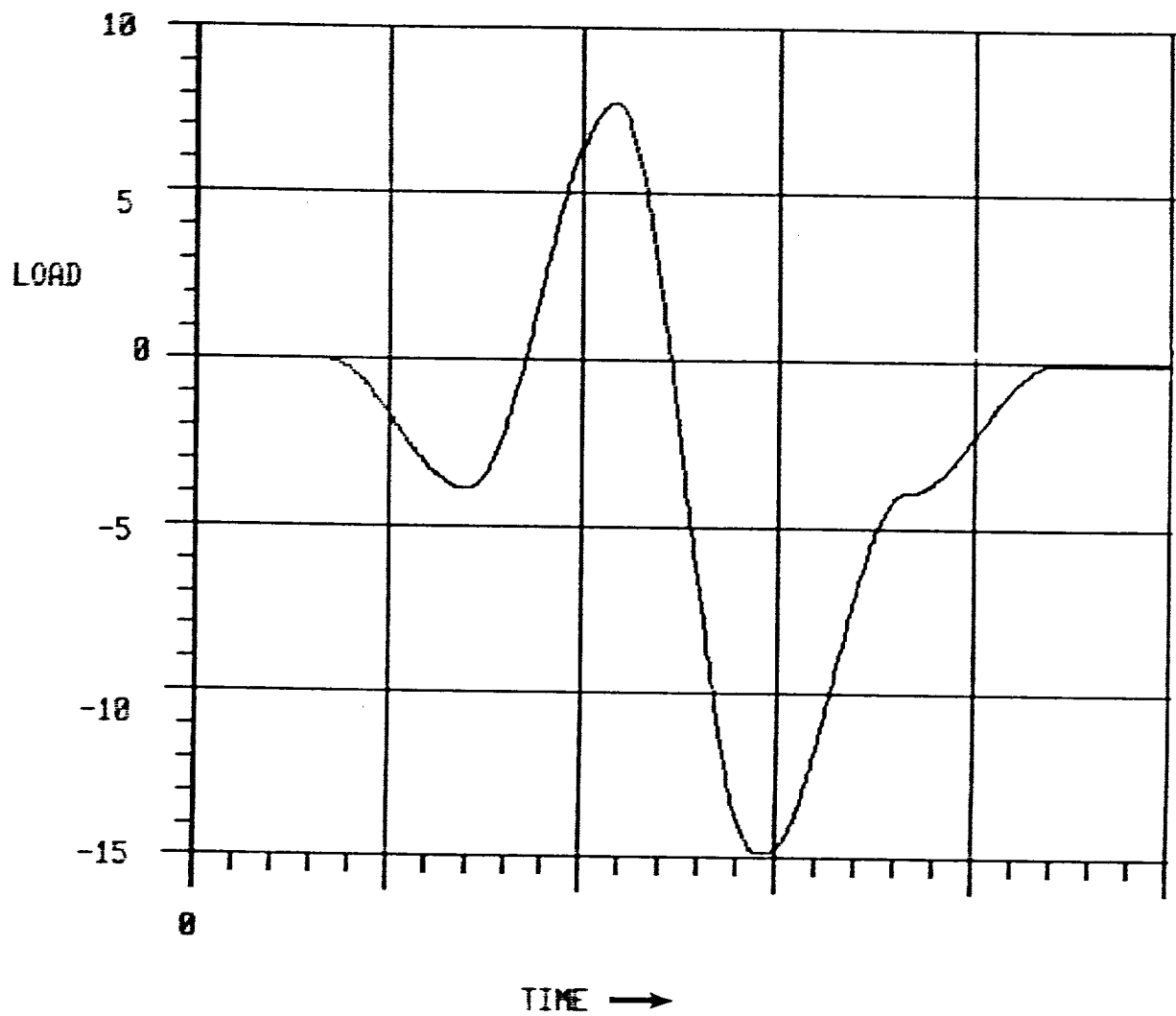


FIGURE 6-16 - Typical fatigue test loading cycle

characterized as a slight seeping and did not commence until eight minutes into the 30-minute pressure holding period.

The internal damage to the panel caused by the impact at Location 1 (Figure 6-11) was determined by nondestructive inspection techniques to be approximately 2 inches (longitudinally) by 2 1/2 inches (laterally) in extent (Figure 6-12, outlined on skin). The skin thickness in the impact area was 0.2585 inch. The impact created a spherical depression in the skin that measured 0.250 inch in diameter and 0.022 inch in depth.

In the second fuel proof pressure test, the two leaks noted were similar in magnitude to that seen during the first test, both being located at skin-to-rib faying surfaces at edge-closure angles. One was observed at each end of the panel, the one at the "A" end commencing before pressure was applied and the one at the "B" end starting after 3 minutes of the 30-minute pressure holding period. (The "A" end leak was observed at the opposite edge-closure angle from the leak noted during the first pressure test.)

Maximum and minimum strain gage readings taken over a typical 10-cycle interval of the fatigue test (specifically, during the thirty-first 1000-cycle interval) are presented in Table 6.1. As previously stated, one load cycle having a minimum load equal to 80% of the design limit load (range ratio -2) was applied at each 1000-cycle interval. The strain gage readings for the first and last such applications are presented in Table 6.2. Figures 6-17 and 6-18 show the deflections (test machine ram) during these same high load cycles.

The final fuel containment pressure test produced no new leaks. The only noted leak was at the same "A" end location as the leak noted during the second proof pressure test. At zero psig it was a slight seep; at 15.0 psig a small flow was noted.

The test panel successfully withstood the application of design ultimate compressive load of 294,000 pounds. The impact at Location 2 (Figure 6-11) produced no visible damage. As noted previously, a 1-inch diameter tip was used as opposed to the 1/2 inch diameter tip used at Location 1. Subsequent

TABLE 6.1
Strain Gage Readings during a Typical
Interval of Fatigue Loading

Gage No.	Maximum Strain $\mu\text{in./in.}$	Minimum Strain $\mu\text{in./in.}$
1A	718	-1365
1B	662	-1328
2A	684	-1418
2B	696	-1431
3A	671	-1333
3B	698	-1396
4A	691	-1243
4B	681	-1389
5A	718	-1401
5B	684	-1362
6A	701	-1426
6B	710	-1470
7A	608	-1294
7B	715	-1387
8A	669	-1313
8B	713	-1438
9A	701	-1409
9B	691	-1428

Note: Maximum and minimum test loads during the subject cycles were 49,300 pounds and -98,500 pounds respectively, and deflections were .051 inch and -.096 inch.

TABLE 6.2

Strain Gage Readings for the First and Last Application of the 80% Design Limit Compressive Load Cycle During Fatigue Testing

Gage No.	Strain, $\mu\text{in./in.}$			
	Maximum		Minimum	
	Cycle 1001	Cycle 36036	Cycle 1001	Cycle 36036
1A	963	1024	-1543	-2109
1B	1052	1100	-2247	-2070
2A	1094	1141	-2297	-2203
2B	1125	1168	-2368	-2227
3A	952	918	-1526	-1985
3C	1088	1162	-2314	-2186
4A	981	1030	-1416	-1893
4B	1069	1117	-2322	-2179
5A	1101	1152	-2275	-2207
5B	1061	1118	-2271	-2140
6A	1095	1144	-2280	-2239
6B	1105	1165	-2401	-2310
7A	961	991	-1544	-1923
7B	1078	1130	-2285	-2188
8A	978	1055	-1536	-1943
8B	1061	1091	-2327	-2239
9A	1088	1129	-2234	-2198
9B	1078	1113	-2355	-2249

Note: Maximum and minimum test loads during the subject cycles were as follows.

Cycle 1001 77,200/-148,500 pounds
 Cycle 36036 80,100/-151,400 pounds

Deflections are presented in Figures 6-17 and 6-18.

TABLE 6.3
Strain Gage Readings for the Static Tests to
Design Ultimate Compressive Load and Residual
Strength Failure Load

Gage No.	Strains, $\mu\text{in./in.}$	
	Design Ult. Load	Failure Load
1A	-4170	-4797
1B	-4084	-4827
2A	-4282	-5106
2B	-4242	-5082
3A	-4100	-4808
3B	-4261	-5029
4A	-4112	-5118
4B	-4365	-5051
5A	-4306	-5175
5B	-4134	-4865
6A	-4510	-5634
6B	-4772	-6499
7A	-4146	-5110
7B	-4170	-4753
8A	-3842	-3888
8B	-4501	-5855
9A	-4501	-5622
9B	-4666	-6372

Note: Design ultimate compressive load was -294,000 pounds. Failure load was -338,500 pounds; deflection is given in Figure 6-78.

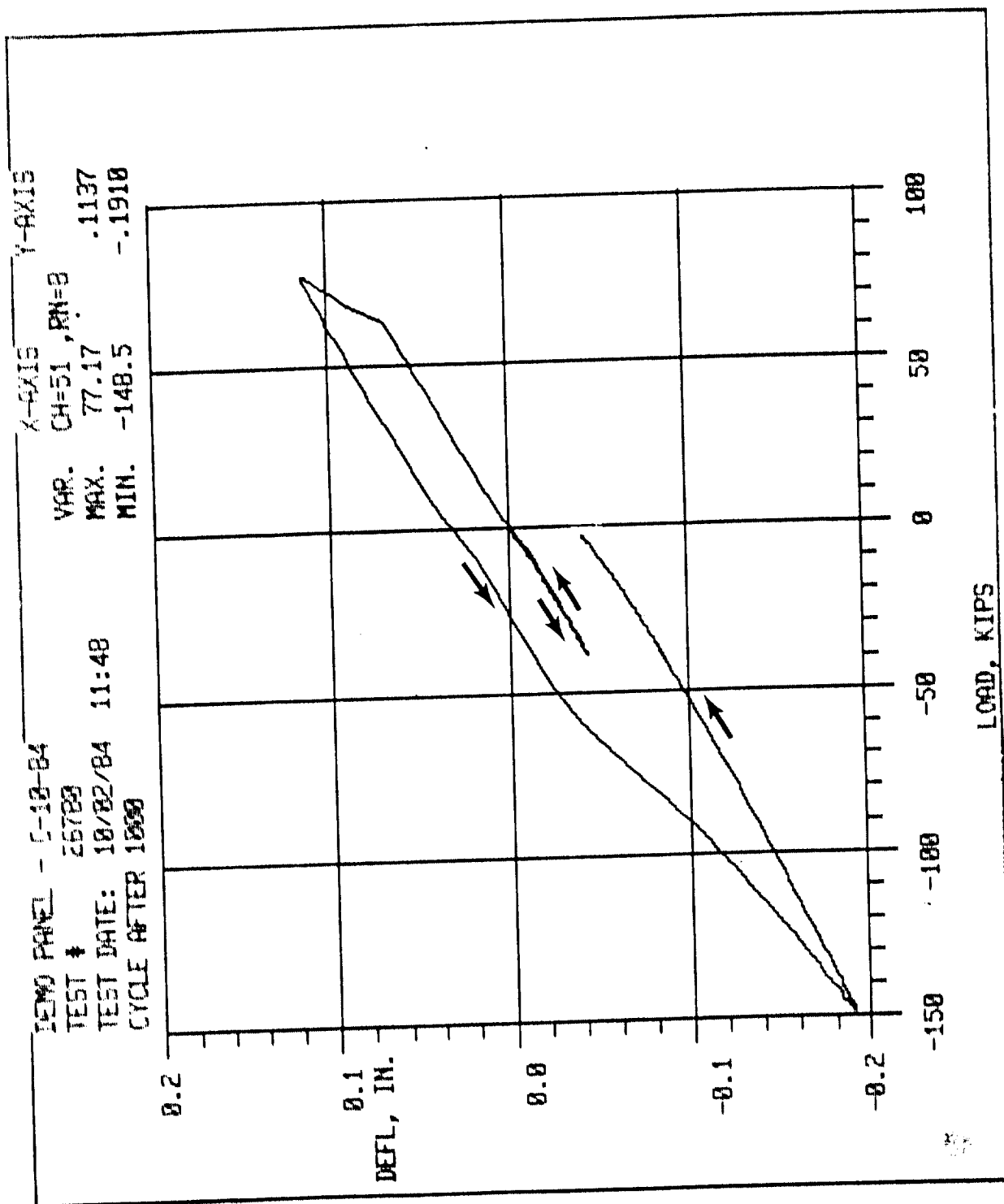


FIGURE 6-17 - Deflection during fatigue test application
 of the first load cycle equivalent to 80%
 of design limit compressive load

ORIGINAL PAGE IS
OF POOR QUALITY

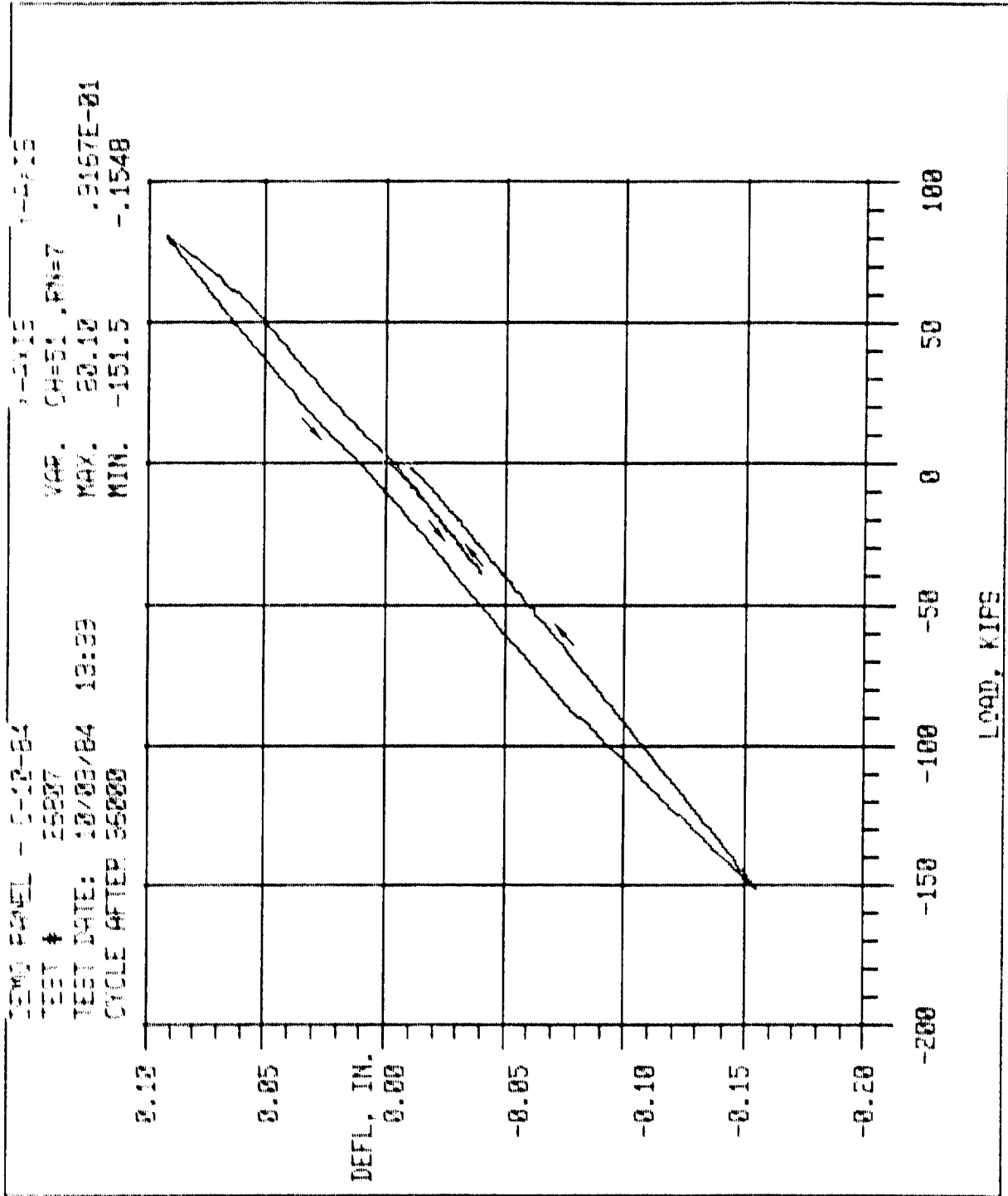


FIGURE 6-18 - Deflection during fatigue test application of the last load cycle equivalent to 80% of design limit compressive load

loading produced failure of the panel at 338,500 pounds with a deflection (test machine head) of 0.1987 inch.

Failure occurred transversely through the panel at Impact Location 1, approximately 3 to 5 inches from the center of the panel test section, involving failure of all test section components (Figures 6-19 through 6-22). Secondary damage was noted in one edge-closure angle near both simulated ribs (Figure 6-23). The compressive strains for the design ultimate and failure load runs are presented in Table 6.3. Figure 6-24 is a plot of deflection versus load during the run to failure. The strains, plotted against load, are shown in Figures 6-25 through 6-33. Each figure presents the data for one back-to-back gage pair. The compressive strains recorded for two gages near the failure location (Gages 7 and 9, A and B) ranged from approximately 5860 to 6370 μ in./in. Strains elsewhere on the panel were of similar magnitude. The readings for Gages 8A and 8B (a blade/skin pair) indicating significant local bending (Figure 6-86)

ORIGINAL PAGE IS
OF POOR QUALITY

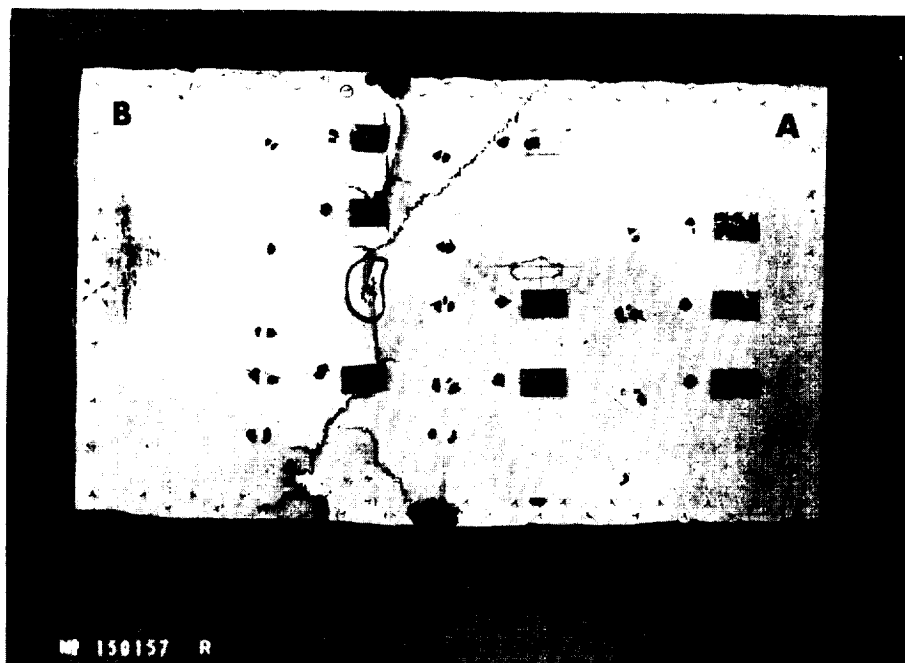
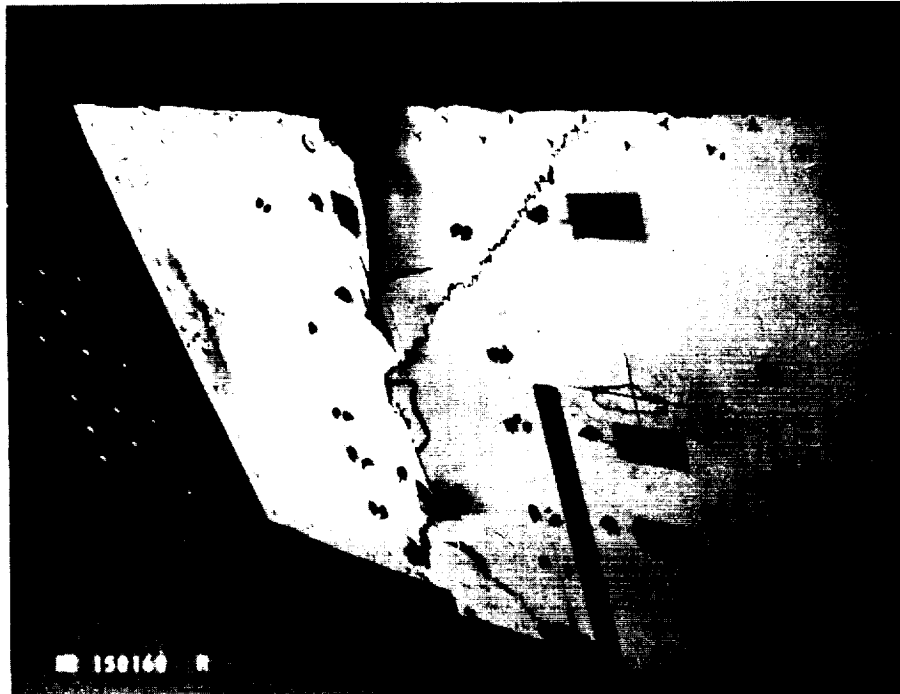


Figure 6-19: Exterior surface of the test article after failure in the residual static compressive strength test.



ORIGINAL PAGE IS
OF POOR QUALITY

Figure 6-20: Exterior surface damage in failed test article.

ORIGINAL PAGE IS
OF POOR QUALITY

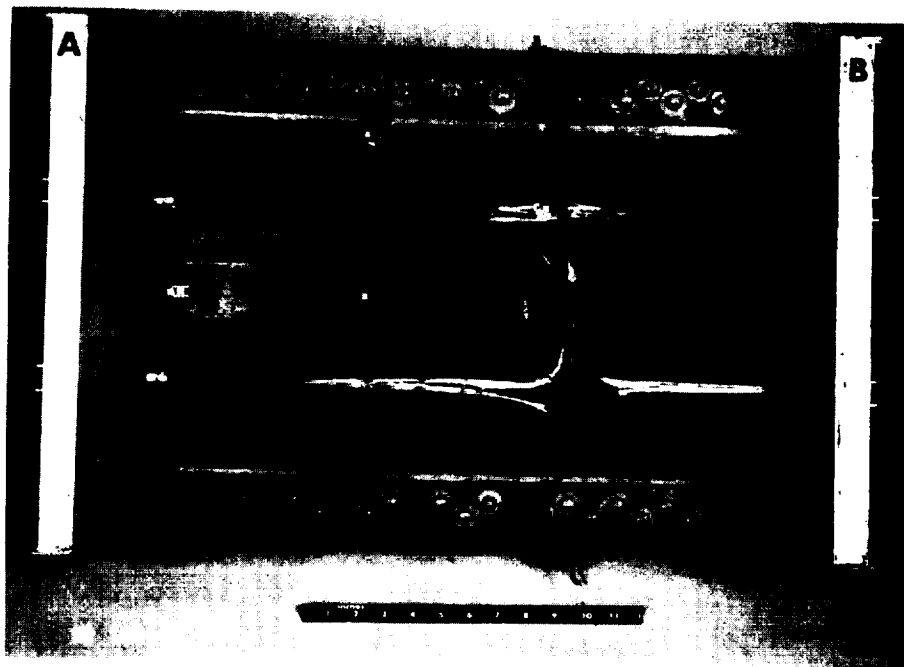


Figure 6-21: Interior surface of the test article after failure in the residual static compressive strength test.

ORIGINAL PHOTO
OF POOR QUALITY

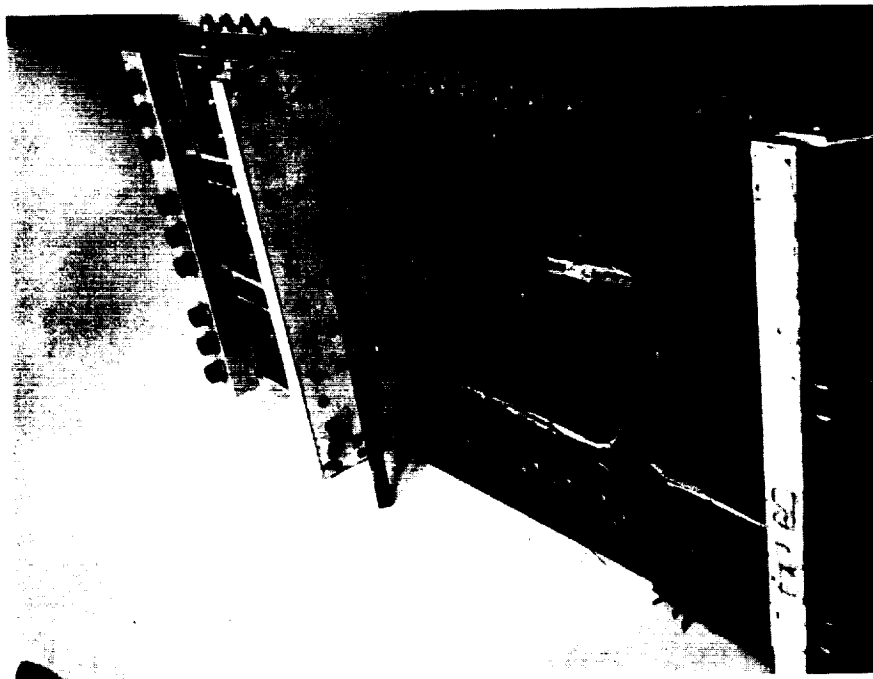


Figure 6-22: Interior damage in failed test article.

ORIGINAL FROM
OF POOR QUALITY

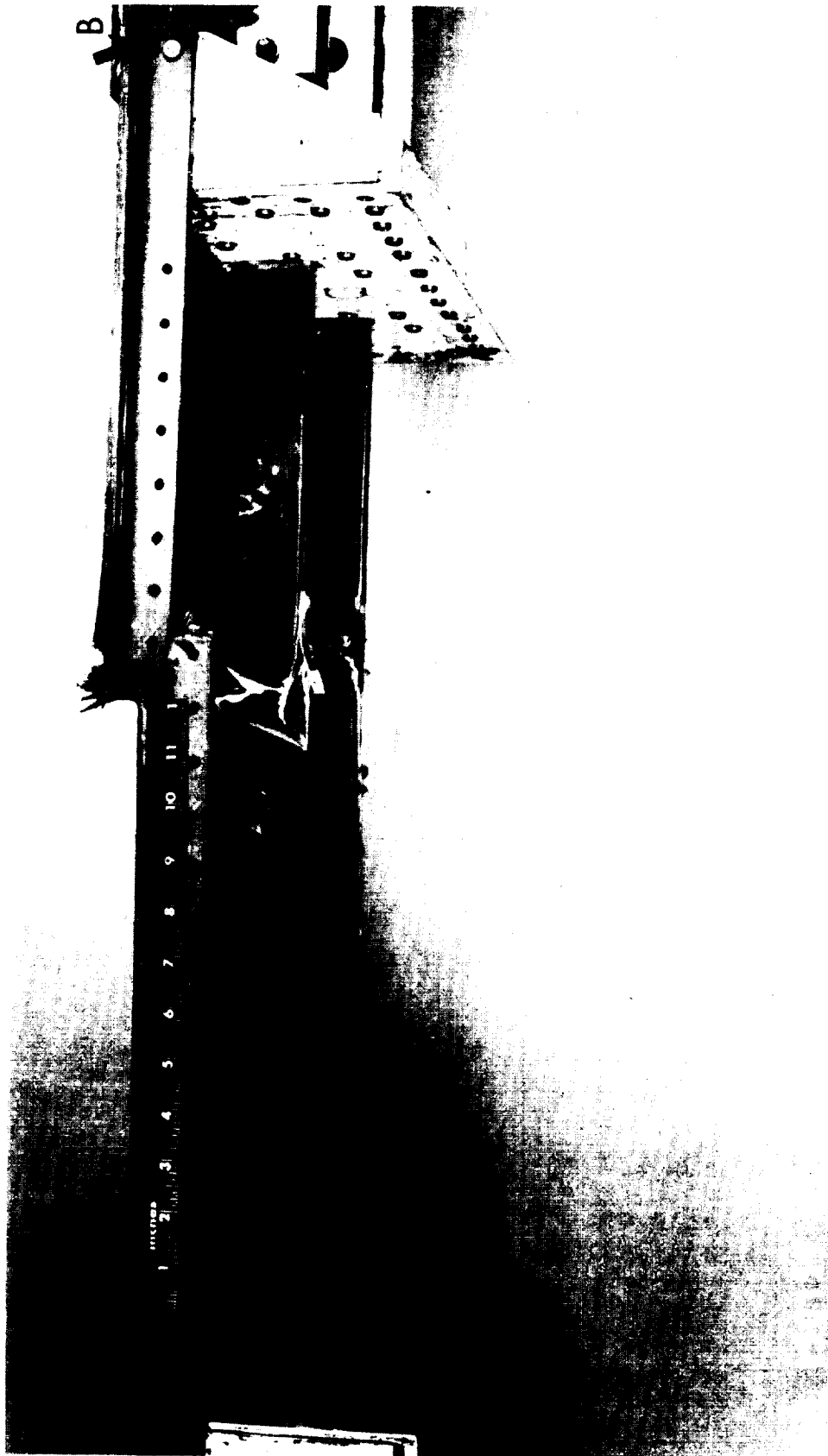


Figure 6-23: Edge view of failed test article with secondary damage to the edge-closure angle indicated by arrows.

ORIGINAL PAGE IS
OF POOR QUALITY

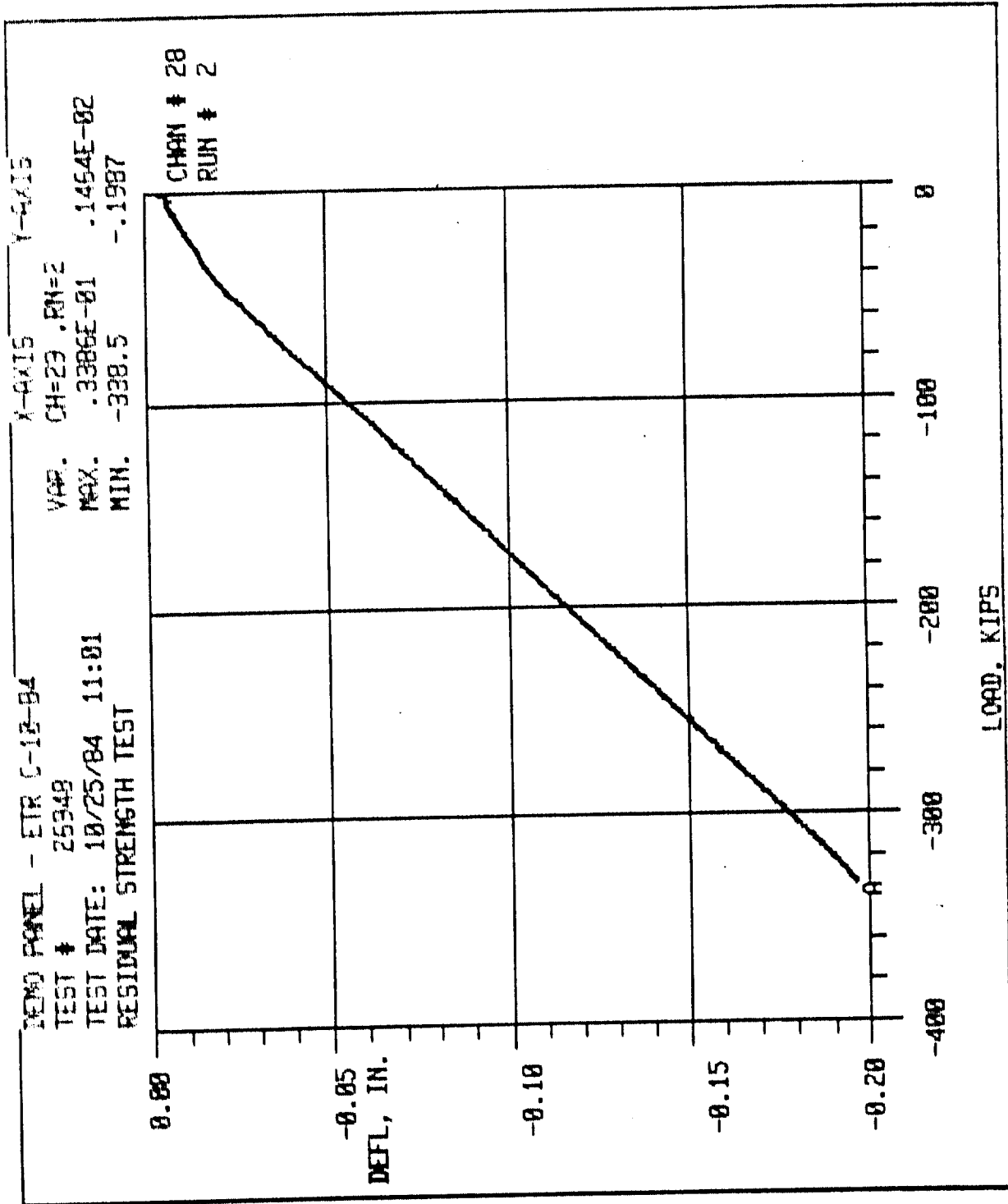


FIGURE 6-24 - Deflection during residual static compressive strength test

ORIGINAL PAGE IS
OF POOR QUALITY

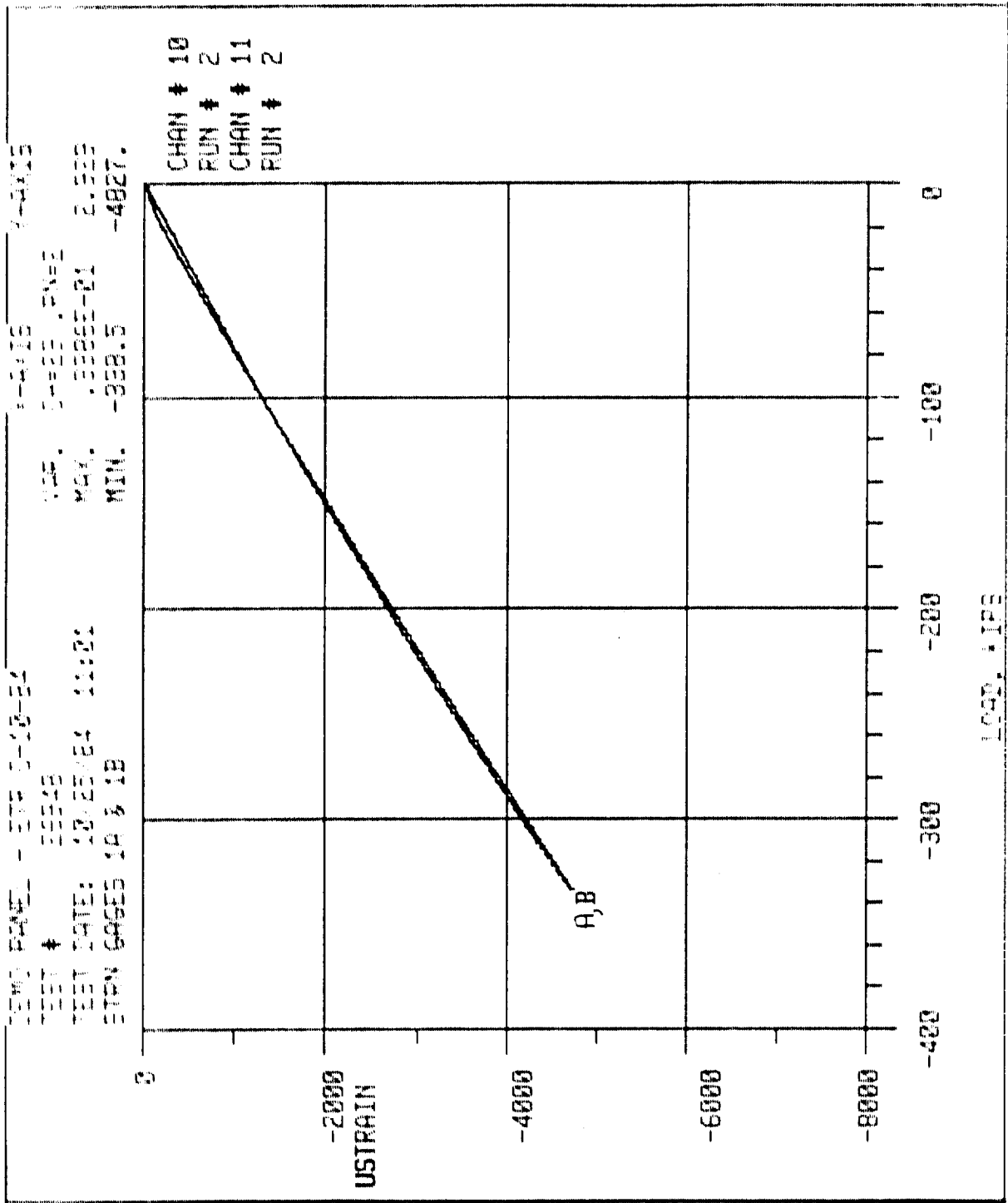


FIGURE 6-25 - Strains at gage locations 1A and 1B during residual static compressive strength test

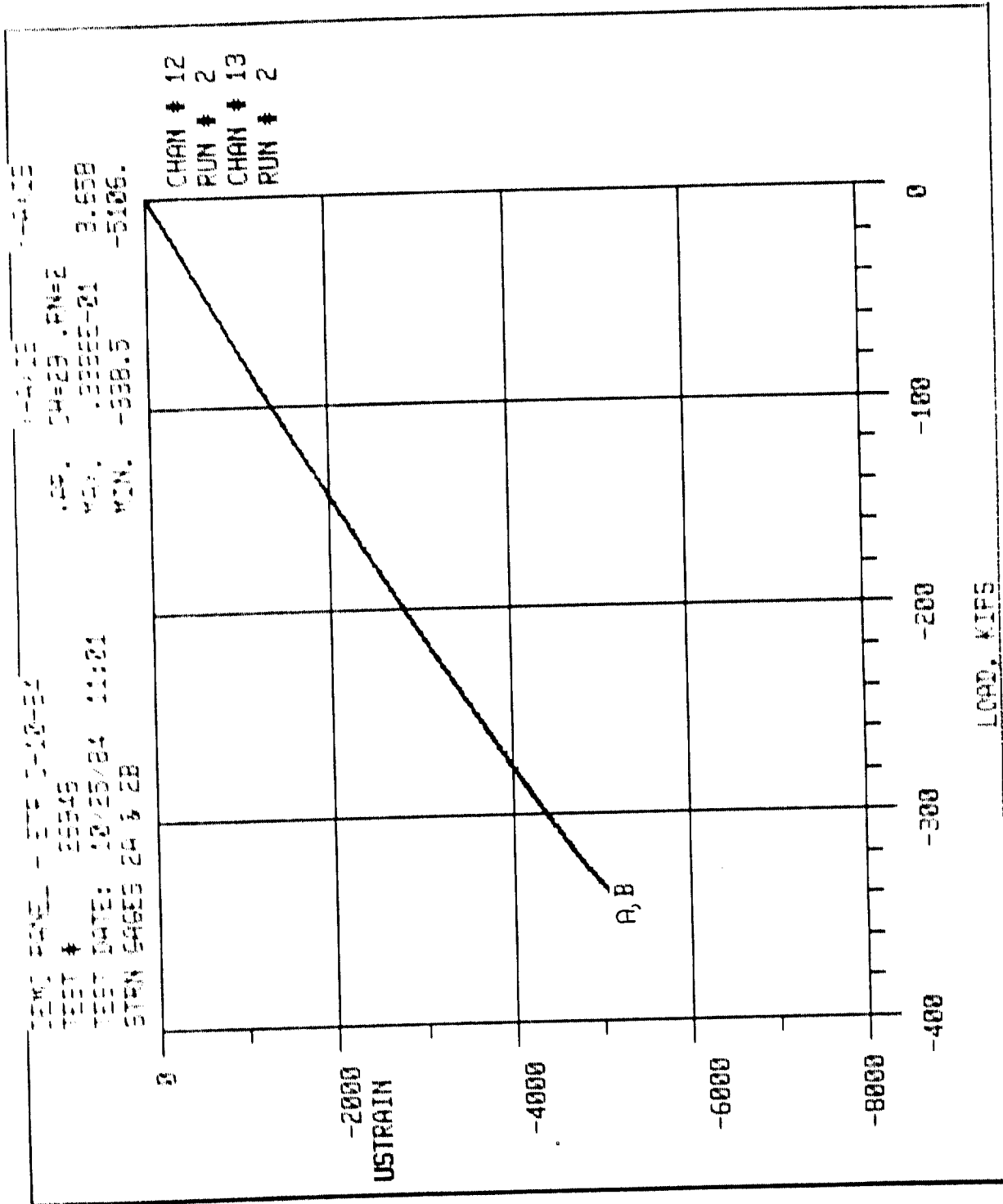


FIGURE 6-26 - Strains at gage locations 2A and 2B
during residual static compressive
strength test

ORIGINAL PAGE IS
OF POOR QUALITY

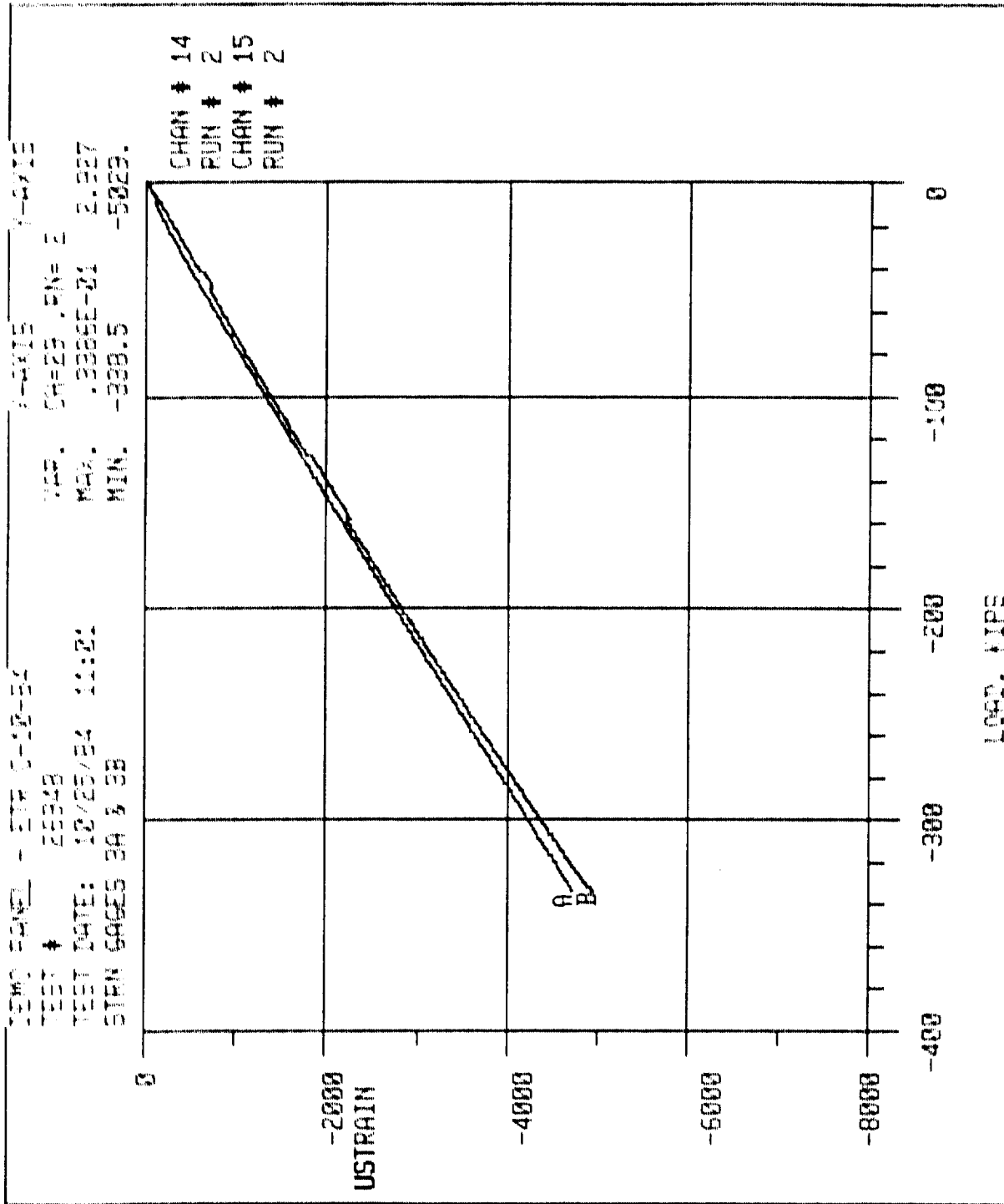


FIGURE 6-27 - Strains at gage locations 3A and 3B
during residual static compressive
strength test

ORIGINAL PAGE IS
OF POOR QUALITY

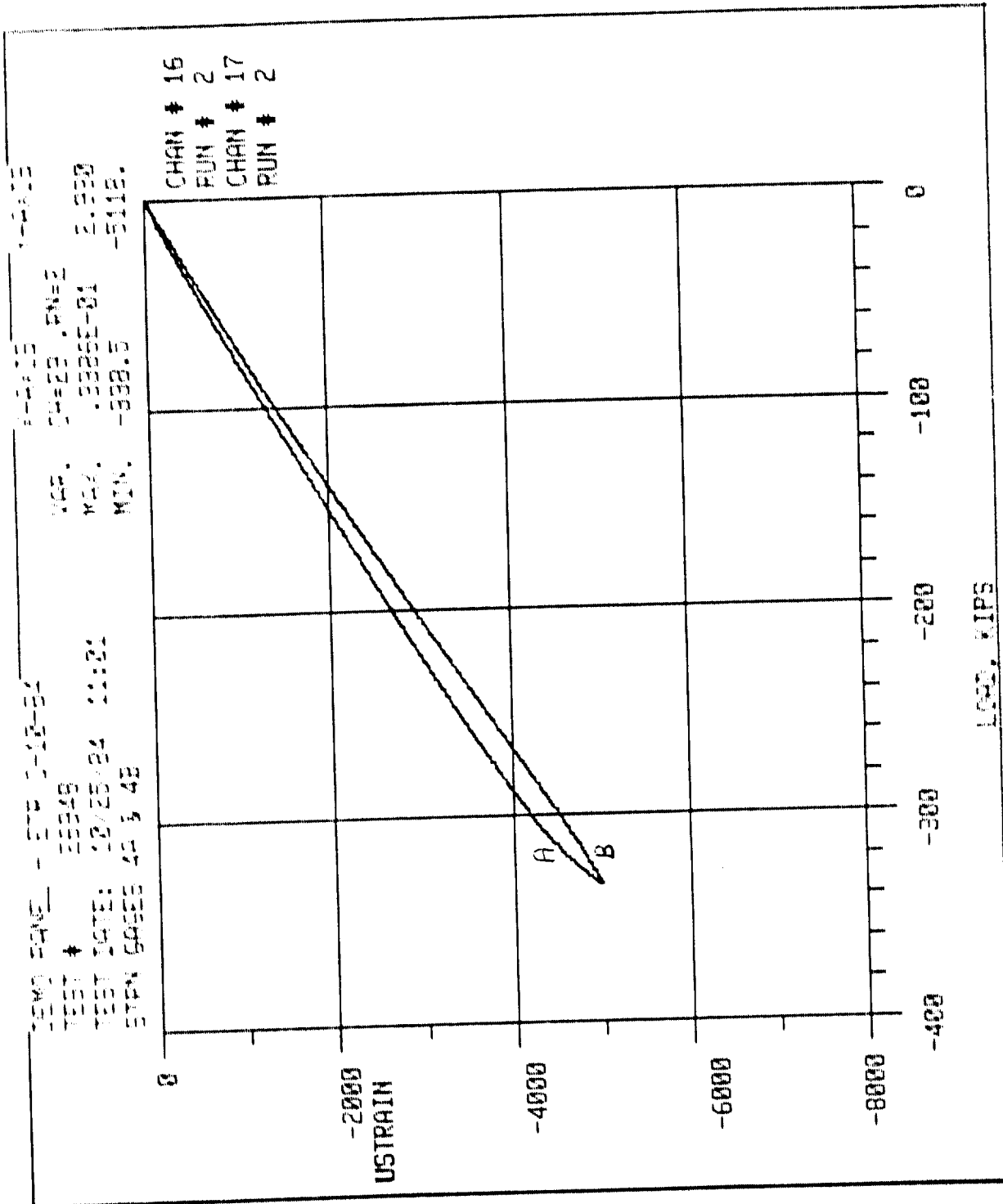


FIGURE 6-28 - Strains at gage locations 4A and 4B during residual static compressive strength test

ORIGINAL PAGE IS
OF POOR QUALITY

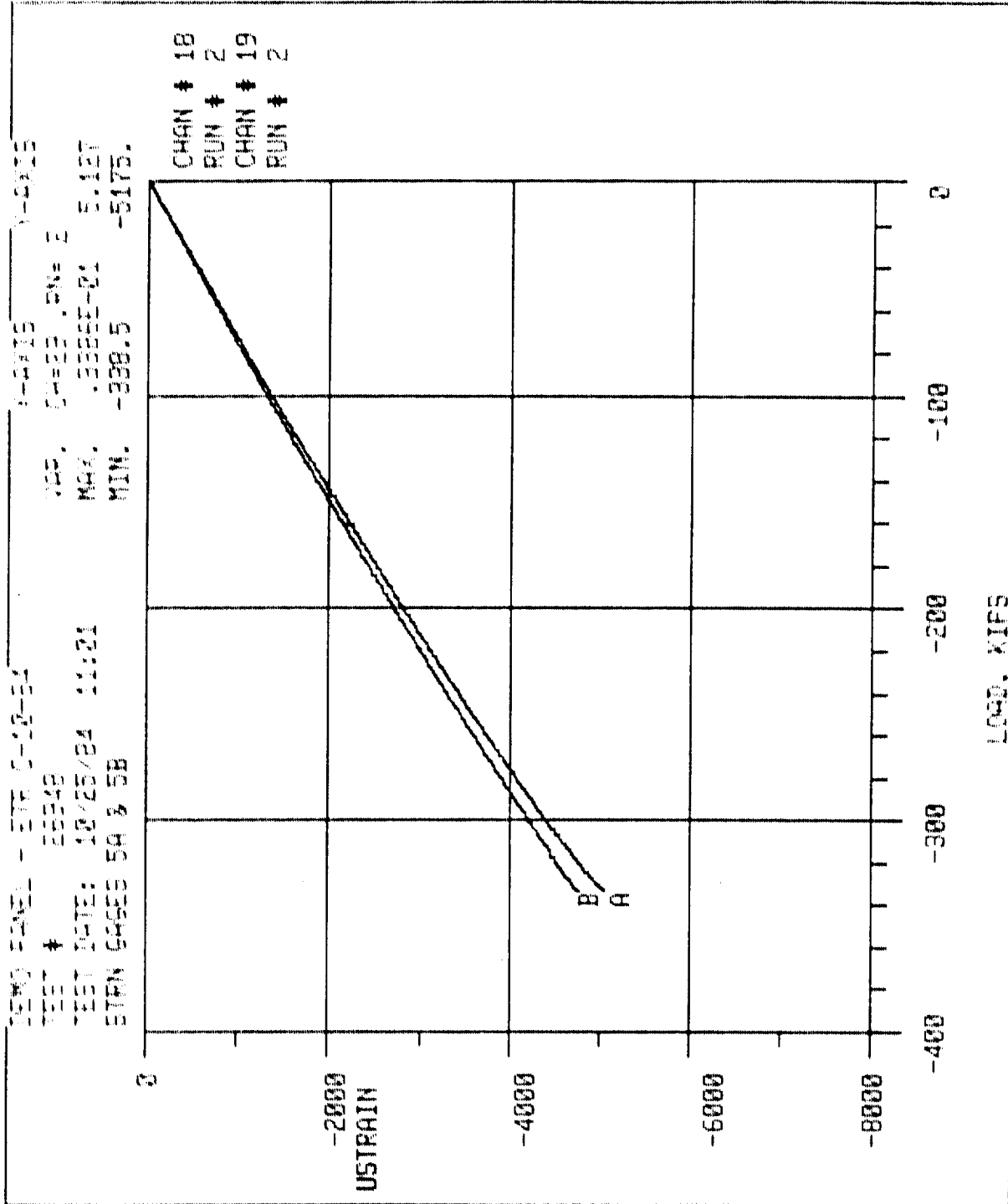


FIGURE 6-29 - Strains at gage locations 5A and 5B during residual static compressive strength test

ORIGINAL PAGE IS
OF POOR QUALITY

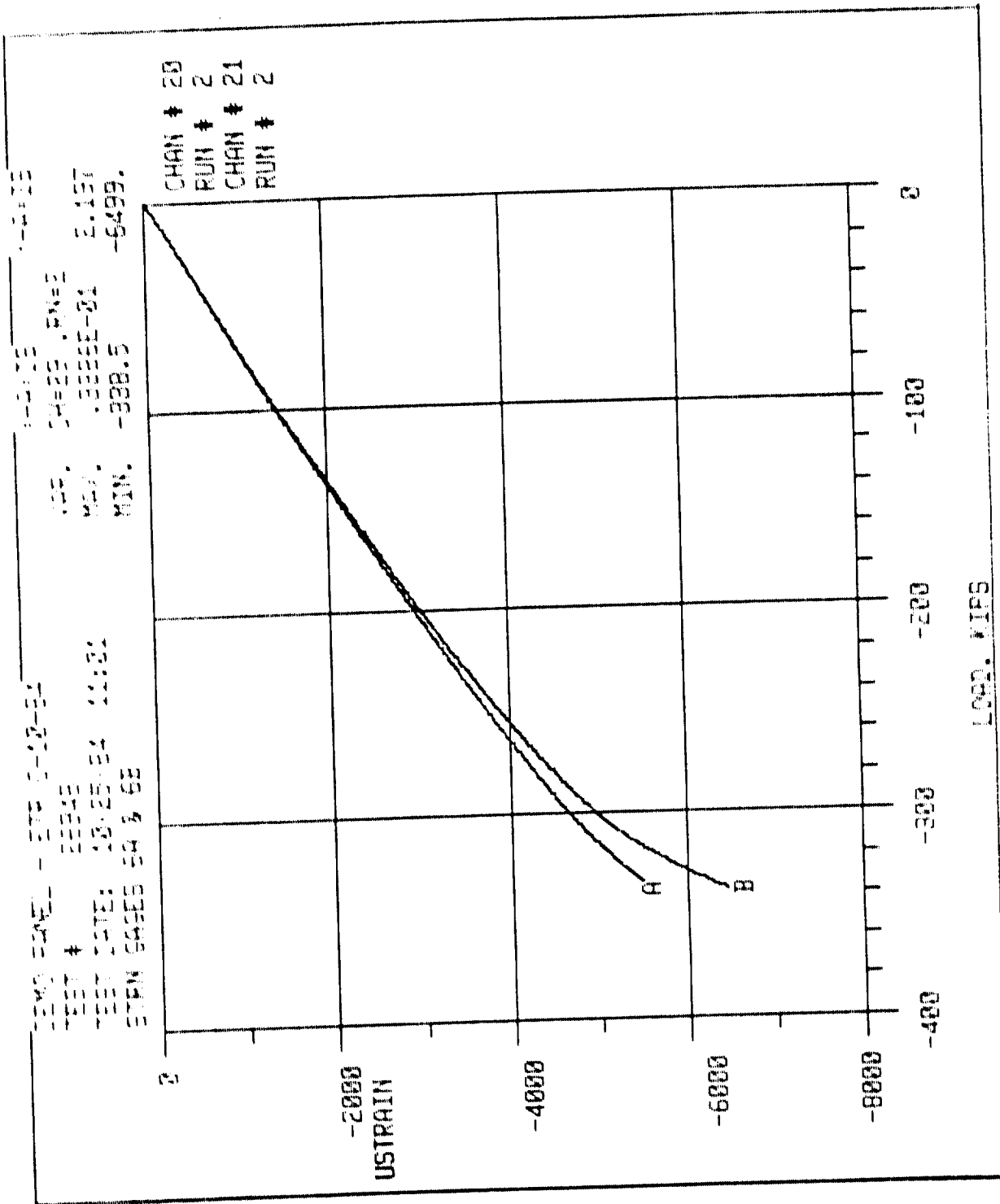


FIGURE 6-30 - Strains at gage locations 6A and 6B during residual static compressive strength test

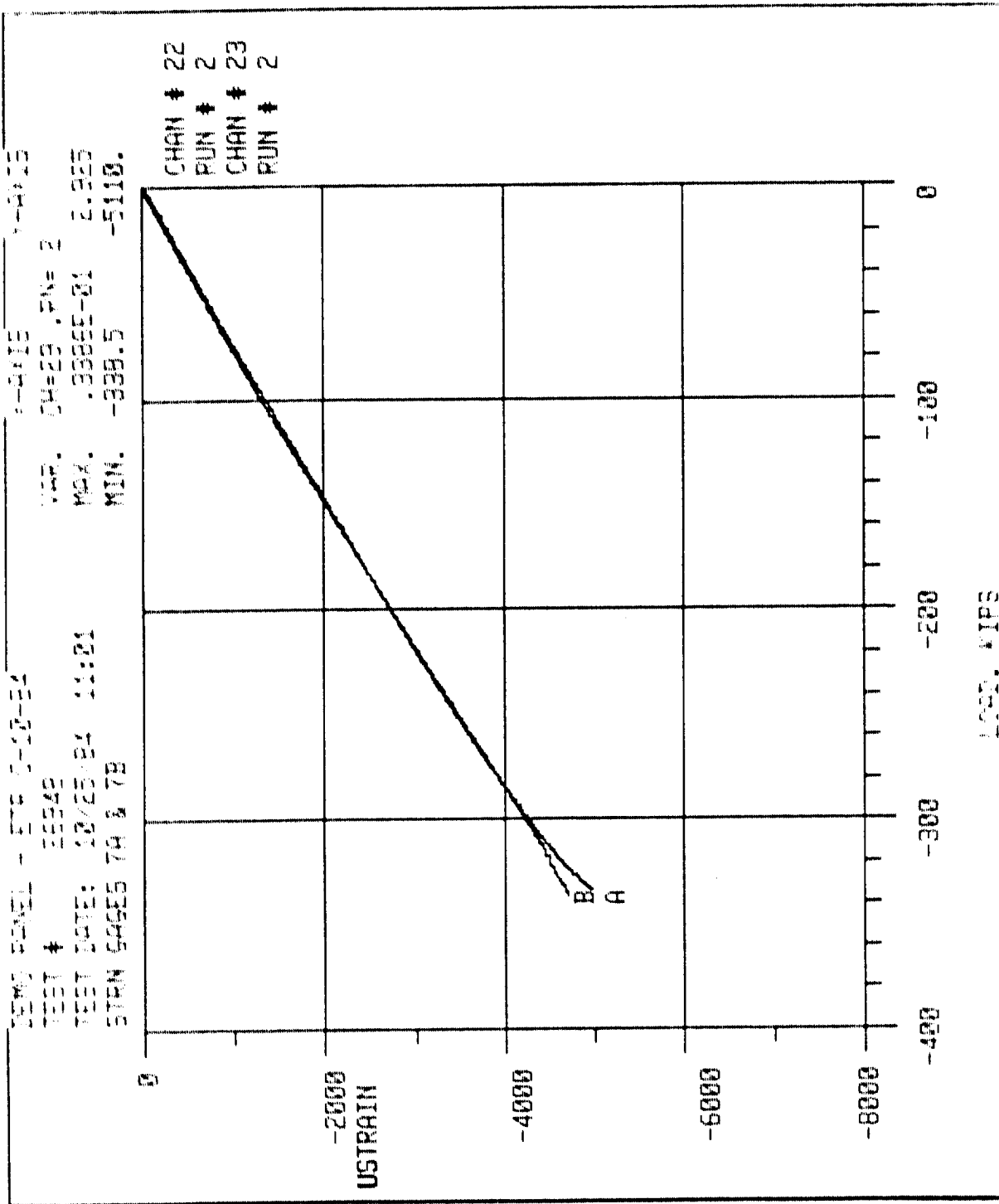


FIGURE 6-31 - Strains at gage locations 7A and 7B during residual static compressive strength test

ORIGINAL PAGE IS
OF POOR QUALITY

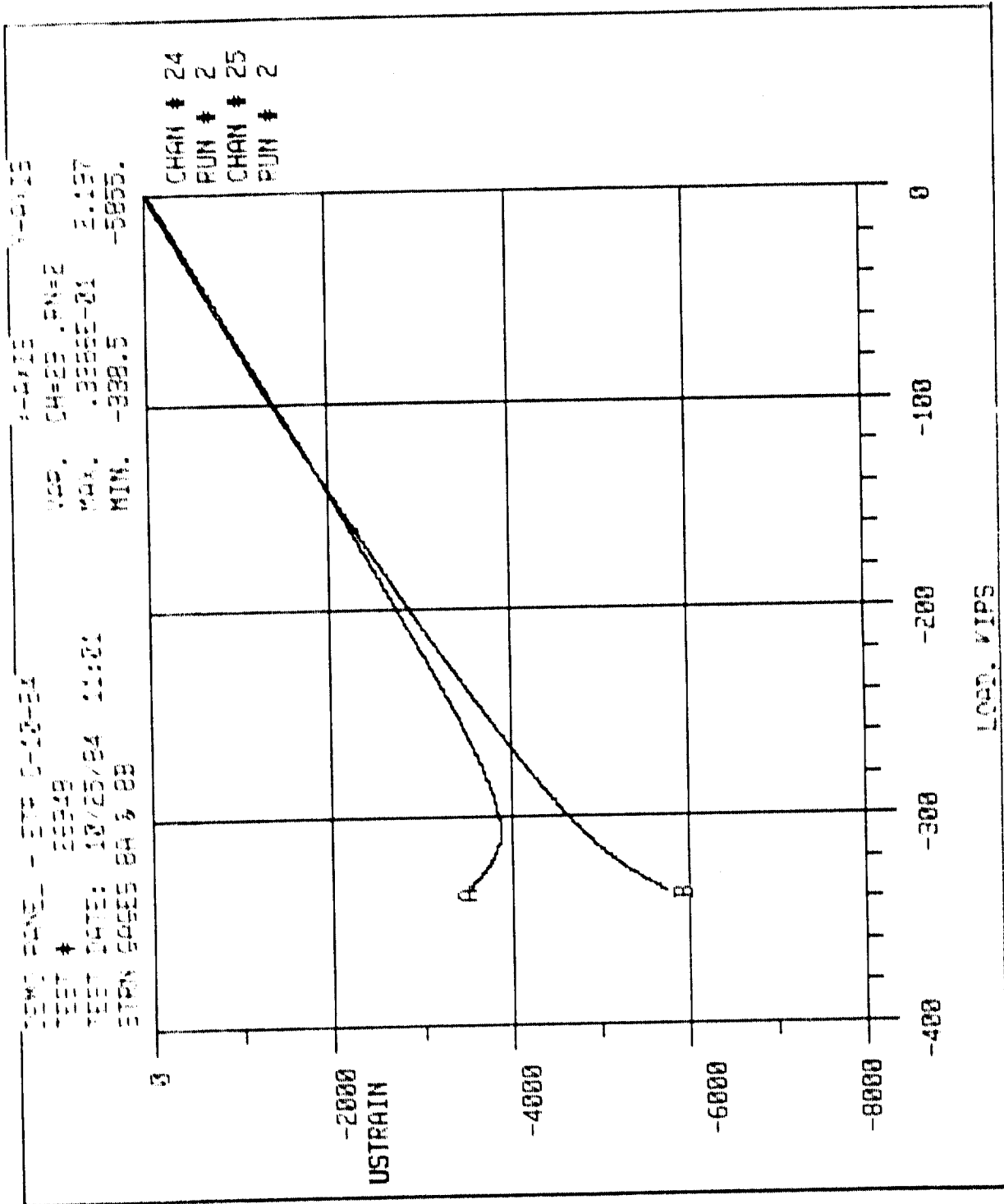


FIGURE 6-32 - Strains at gage locations 8A and 8B during residual static compressive strength test

ORIGINAL PAGE IS
OF POOR QUALITY

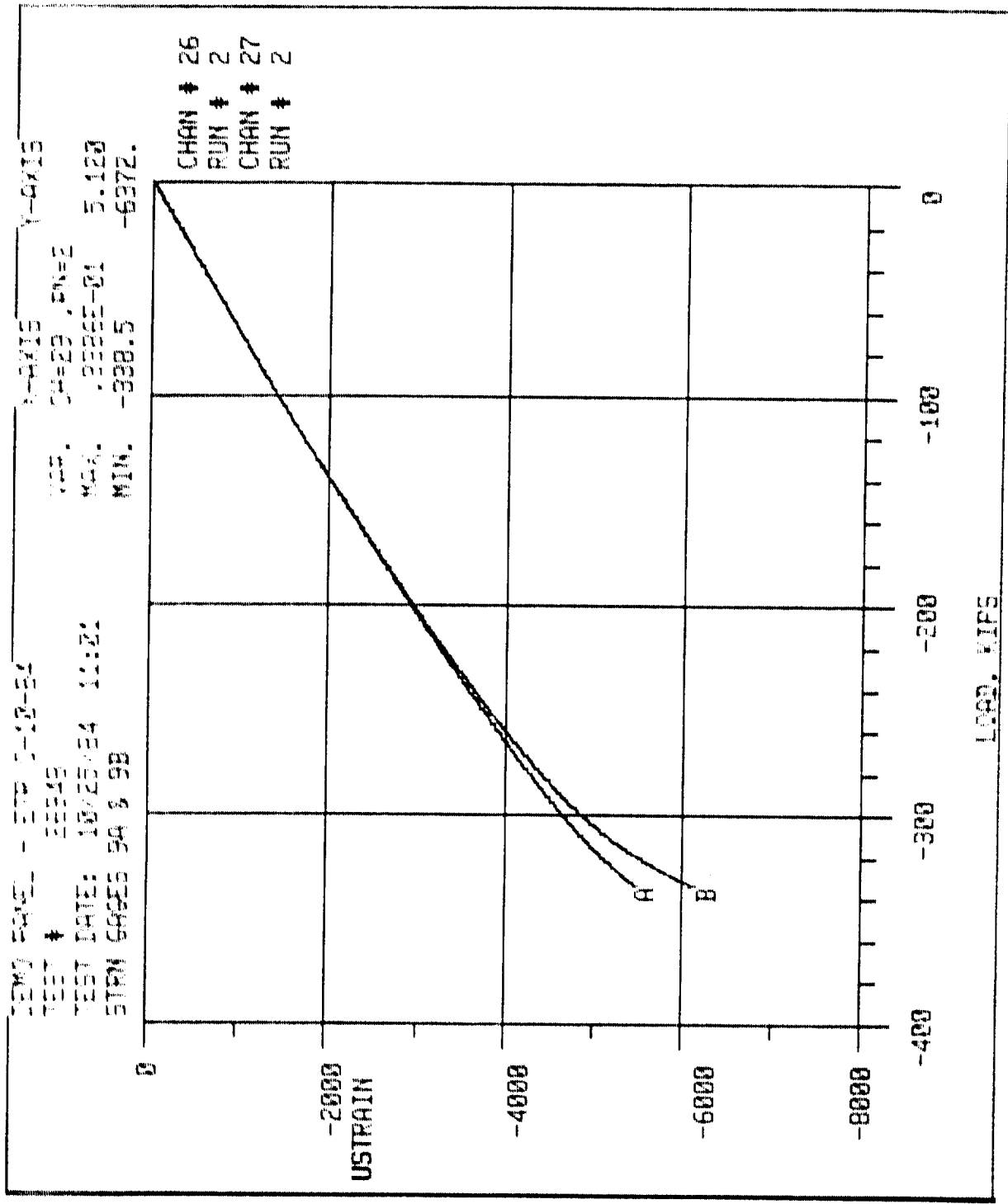



FIGURE 6-33 - Strains at gage locations 9A and 9B during residual static compressive strength test

REFERENCES

1. Sandifer, J.P., "Fuel Containment and Damage Tolerance in Large Composite Primary Aircraft Structures, Phase I - Testing", NASA-CR-166091, December, 1982.
2. Lockheed Interdepartmental Communication EL/74-71-173, "Fuel Containment Tests", written by D. Diggs to C. Griffin, October 21, 1983.
3. Contract No. NAS-1-16856, Periodic Technical Progress Reports 27 (December 1983) and 28 (January 1984).
4. Lockheed California-Company Engineering Test Request C-10-84, May 14, 1984.

1. Report No. NASA CR-172519		2. Government Accession No.		3. Recipient's Catalog No.	
4. Title and Subtitle FUEL CONTAINMENT AND DAMAGE TOLERANCE IN LARGE COMPOSITE PRIMARY AIRCRAFT STRUCTURES, PHASE II - TESTING				5. Report Date April 1985	
				6. Performing Organization Code	
7. Author(s) J.P. Sandifer, A. Denny, M.A. Wood				8. Performing Organization Report No.	
9. Performing Organization Name and Address Lockheed-California Company P.O. Box 551 Burbank, California 91520				10. Work Unit No.	
				11. Contract or Grant No. NAS1-16856	
12. Sponsoring Agency Name and Address National Aeronautics and Space Administration Washington, D.C. 20546				13. Type of Report and Period Covered Contractor Report	
				14. Sponsoring Agency Code	
15. Supplementary Notes Langley Technical Monitor: Marvin Dow Final Report					
16. Abstract A study was conducted to identify and resolve technical issues associated with fuel containment and damage tolerance of composite wing structure for transport aircraft. Material evaluation tests were conducted on two toughened resin composites: Celion/HX1504 and Celion/5245. These consisted of impact, tension, compression, edge delamination and double cantilever beam tests. Another test series were conducted on graphite/epoxy box beams simulating a wing cover to spar cap joint configuration of a pressurized fuel tank. These tests were to evaluate the effectiveness of sealing methods with various fastener types and spacings under fatigue loading and with pressurized fuel. Another test series evaluated the ability of selected coatings, films, and materials to prevent fuel leakage through 32-ply AS4/2220-1 laminates at various impact energy levels. To verify the structural integrity of the technology demonstration article structural details tests were conducted on blade stiffened panels and sections. Compression tests were performed on undamaged and impacted stiffened AS4/2220-1 panels and smaller element tests to evaluate stiffener pull-off, side load and failsafe properties. Compression tests were also performed on panels subjected to Zone II lightning strikes. All of these data were integrated into a demonstration article representing a moderately loaded area of a transport wing. This test combined lightning strike, pressurized fuel, impact, impact repair, fatigue and residual strength.					
17. Key Words (Suggested by Author(s)) Composites Damage Tolerance Fuel Containment			18. Distribution Statement 		
19. Security Classif. (of this report) UNCLASSIFIED		20. Security Classif. (of this page) UNCLASSIFIED		21. No. of Pages	
				22. Price	

████████████████████